Ross Large

AMIRA INTERNATIONAL

Sponsors Meeting - Presentations

Confidential

P544 - Proterozoic Sediment Hosted Copper Deposits

May 2002

Centre for Ore Deposit Research –
University of Tasmania
Colorado School of Mines

AMIRA International Limited ACN 004 448 266 ABN 60 176 687 975
9th Floor 128 Exhibition Street Melbourne 3000 Australia Phone: +61 3 9679 9999 Facsimile: +61 3 9679 9900
email: AMIRA@amira.com.au Website www.amira.com.au

CODES/CSM/AMIRA Project P544: Proterozoic Sediment-hosted Copper Deposits
Research Progress Meeting, Adelaide, 22–23 May 2002

AMF Building, Glenside

WEDNESDAY 22nd MAY

10:00 - 10:15am	Welcome and Introduction from AMIRA	***Allan Goode***
10:15 - 10:30am	P544 PROJECT OVERVIEW INTRODUCTION (Powerpoint presentation 01)	***Peter McGoldrick***
10:30 - 11:45am	Provisional Stratigraphic Comparison of Three Cu Mineralised Basins; the Zambian Copperbelt, the Polish Kupferschiefer and the Adelaide Fold Belt (Powerpoint presentation 02)	***Stuart Bull***
SOUTH AUSTRALIAN STUDIES		
11:45 - 12:30pm	STH AUSTRALIA INTRODUCTION AND OVERVIEW (incorp. Basin Architecture During Lower Umberatana Group Sedimentation) (Powerpoint presentation 03)	***David Selley***
12:30 - 1:30	LUNCH BREAK	
1:30 - 1:50 pm	Sedimentology and Structure of the Curdimurka Subgroup; Willouran Range, South Australia - An Introduction (Powerpoint presentation 04)	***Wallace MacKay***
1:50 - 2:30 pm	Stuart Shelf Geochemistry - Emmie Bluff (Powerpoint presentation 05)	***Peter McGoldrick***
2:30 - 2:40	SMOKO	
ZAMBIAN STUDIES (Pt 1)		
2:40 - 3:10pm	Zambia overview and recap of critical questions from Zambian Field Meeting, June 2001 (Powerpoint presentation 06)	***Peter McGoldrick***
Basin Architecture and Stratigraphy		
3:10 - 3:40pm	Chibuluma West (Powerpoint presentation 07)	***David Selley***
3:40 - 4:10pm	Basement - Roan Relationships: Mufulira (Powerpoint presentation 08)	***Robert Scott***
4:10 - 4:30	TEA BREAK	
4:30 - 4:50pm	Basement - Roan Relationships: Ndola West (Powerpoint presentation 09)	***Robert Scott***
4:50 - 5:10pm	Geology and Genesis of the Nkana - Mindola Deposits (Powerpoint presentation 10)	***Mawson Croaker***
5:10 - 5:30pm	Petrology of Lower Roan - Basement Contacts, Konkola East and Ndola East Areas (Powerpoint presentation 11)	***David Broughton***

THURSDAY 23rd MAY

AMF Building, Glenside

ZAMBIAN STUDIES (Pt 2)

8.00 - 8.30am	Mineral Zonation and Controls on Fluid Pathways at Chibuluma West (Powerpoint presentation 12)	***David Selley***
8.30 – 9.00am	Sulfur Isotope Systematics of the Chibuluma West Cu - Co Deposit (Powerpoint presentation 13)	***David Cooke***
9.00 – 9.20am	Sedimentology, Mineral Paragenesis and Geochemistry of the Konkola North Copper Deposit (Powerpoint presentation 14)	***Nicky Pollington***
9.30 – 10.00am	Timing, Character and Paragenesis of Konkola Copper Ores (Powerpoint presentation 15)	***Robert Scott, Nicky Pollington***
10:00 - 10:20am	TEA BREAK	
10:20 - 10:50am	Comparative Study of Drill Cores from the Konkola North Orebody and Barren Gap (Powerpoint presentation 16)	***David Broughton***
10:50 - 11:20am	Character, Distribution, Timing and Origin of Copper Mineralisation at Mufulira (Powerpoint presentation 17)	***Robert Scott***
11:20 - 11:50pm	Style and Stratigraphic Context of Copper Mineralisation: Ndola West (Powerpoint presentation 18)	***Robert Scott***
11:50 - 12:00pm	Zambian Lithogeochemistry Update (Powerpoint presentation 19)	***Peter McGoldrick***

ZAMBIAN SHRIMP GEOCHRONOLOGY

12.00 - 12:30pm	In Situ Xenotime and Monozite U-Th-Pb Geochronology (Powerpoint presentation 20)	***Galvin Dawson, Neil McNaughton***

SUMMARY, DISCUSSION AND FUTURE DIRECTIONS

12:30 - 1:30pm	Discussion and future directions	***All***
1.30-2.30	LUNCH BREAK	

THURSDAY 23rd **PIRSA Core Library, Glenside**

2.00-4.30 Emmie Bluff core & Tapley Hill Formation core

ARC/AMIRA P544

Proterozoic sediment-hosted copper deposits

- Aims to compare and contrast Proterozoic sediment-hosted copper deposits in Australia and Zambia
  - Study Areas: Zambian Copperbelt, South Australian Neoproterozoic sequences, Paterson Orogen in WA
  - formal Research Collaboration CODES, CSM (AMIRA & ARC funding - SPIRT/Linkage Scheme)
  - complementary UWA CGM geochronology (separate ARC funding to P544)

AMIRA P544 May 2002 ppt01.mcgoldrick

ARC/AMIRA P544

Personnel

- David Selley, Peter McGoldrick, Stuart Bull, Rob Scott, David Cooke, Ross Large, Wallace Mackay, Nicky Pollington, Mawson Croaker
- Murray Hitzman, David Broughton
- (Galvin Dawson, Neal McNaughton)

AMIRA P544 May 2002 ppt01.mcgoldrick

ARC/AMIRA P544

Timing & progress to date

- July 2000 to December 2000 start-up with AMIRA funding only
- First progress meeting and report in Perth, December 2000
- 2001 first full year at full funding (ARC & AMIRA)
- Field meeting in Zambia, June 2001
- Major progress report dated Dec 2001 covering CODES work in 2001 was circulated to sponsors in March 2002
- Second sponsors meeting planned for early December or early February was postponed to May for various reasons

AMIRA P544 May 2002 ppt01.mcgoldrick

ARC/AMIRA P544

Timing & progress to date (con)

- Broughton PhD (CSM) commenced August 2000
- Mackay PhD (CODES) commenced February 2001
- Pollington PhD (CODES) commenced June 2001
- Croaker PhD (CODES) commenced August 2001

AMIRA P544 May 2002 ppt01.mcgoldrick

South Australia

Focus on two key stratigraphic associations:

- **Umberatana Group hosted Cu mineralisation e.g., Stuart Shelf deposits and widespread minor Cu elsewhere in the AFB**
- **Callanna Group basal level of the AFB sequence and tectonostratigraphic equivalent of Roan sequences**

Western Australia

Paterson Orogen/ Yeneena Basin

Aims

- **use potential field and EM data sets to develop a better structural/stratigraphic framework**
- **place recent deposit-related PhD studies into this context**

Zambia

Copperbelt stratigraphy/ basin architecture
- regional - Kafue Anticline (DB, MH)
- Chambishi Basin
  - basement topography (DS, SB)
- Chambishi Basin
  - growth faults (SB, DS, PMcG)

Orebody geometry/geology
- Nkana (MC, DS, HC)
- Konkola North (NP, RS, PMcG, SB)
- Chambishi (DS,MH)

Copperbelt deformation history
- thrust at top of Mwashia (DB, MH)
- structural history of Katangan cf Muva & Lufubu (DS)

Katangan chemistry, isotopes & mineralogy
- orebody specific studies (MC, NP, PMcG)
- stratigraphic studies (DB, PMcG, DS, SB, GD)
- alteration (DB, MH, PMcG, DS, MC, NP)
- fluid sources, fluid chemistry (MH, DC, RL)

Zambia

Copperbelt stratigraphy/ basin architecture
- regional - Kafue Anticline (DB, MH)
- Chambishi Basin
  - basement topography (DS, SB)
- Chambishi Basin
  - growth faults (SB, DS, PMcG)

Orebody geometry/geology
- Nkana (MC, DS, HC)
- Konkola North (NP, RS, PMcG, SB)
- Chambishi (DS,MH)

Copperbelt deformation history
- thrust at top of Mwashia (DB, MH)
- structural history of Katangan cf Muva & Lufubu (DS)

Katangan chemistry, isotopes & mineralogy
- orebody specific studies (MC, NP, PMcG)
- stratigraphic studies (DB, PMcG, DS, SB, GD)
- alteration (DB, MH, PMcG, DS, MC, NP)
- fluid sources, fluid chemistry (MH, DC, RL)

AMIRA P544 May 2002 ppt01.mcgoldrick

Meeting Format

- **Basin comparisons: KFS, Zambia, SA**
- **South Australia**
  - **Umberatana Group time basin architecture**
  - **Curdimurka Subgroup sedimentology & structure**
- **Zambia**
  - **Basin architecture & stratigraphy**
  - **Deposit studies**

Provisional stratigraphic comparison of three Cu mineralised basins; the Zambian Copperbelt, the Polish Kupferschiefer and the Adelaide Fold Belt

Stuart Bull, David Selley, Murray Hitzman, David Cooke, Wallace Mackay, Ross Large & Peter McGoldrick

AMIRA P544

Introduction

Timely now that we are up and running in both the ZCB and AFB to begin to make broad comparisons

Also prompted by;

- A visit to the Polish Kupferschiefer (SB, RL, WM)
- Navel gazing in concentrating effort in interpreting individual Roan holes - needed to take a broader view

AMIRA P544

Introduction

Fundamental constraints on basin analysis in the ZCB

- Preserved fragment of a much larger basin system dismembered in the Lufilian Orogeny
- Lack of outcrop around the Kafue Anticline to provide detailed geometrical and kinematic data
- Lack of access to regional geophysical datasets

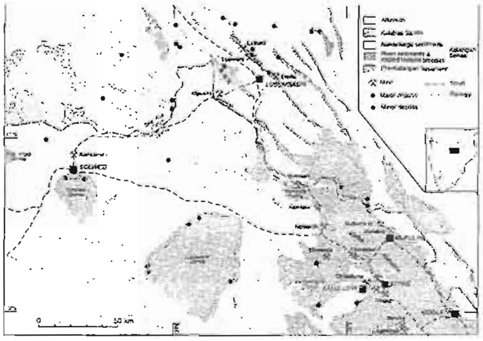

Progress is being made so what do we know?

AMIRA P544

Zambian Copperbelt

Stratigraphy

Overlain by a diverse hanging wall succession of coarse- and fine-grained clastics and carbonates (upper Roan, Mwashia and lower Kundelungu)

Abruptly overlain by thin but laterally persistent fine-grained deposits (Ore Shale or correlative carbonates)

Basal arkosic/quartzitic & locally conglomeratic succession of variable thickness (lower Roan)

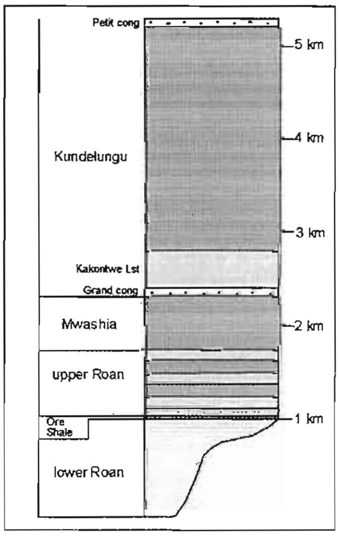

AMIRA P544

Zambian Copperbelt

Stratigraphy

Facies association and lateral facies and thickness variability of lower Roan = tectonically controlled sedimentation

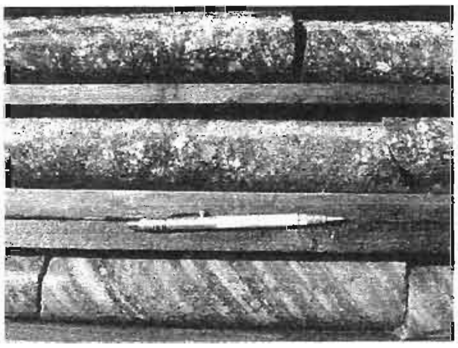

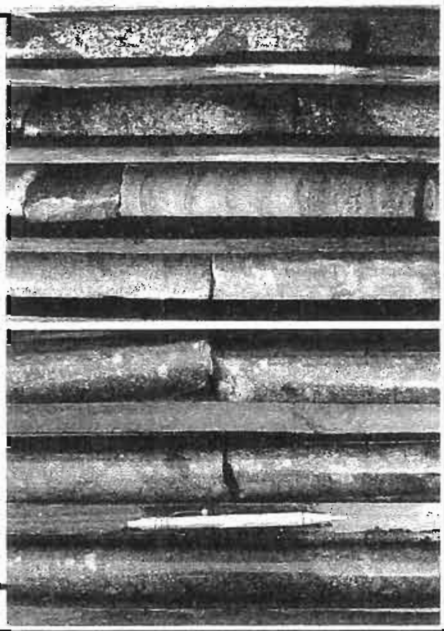

AMIRA P544

Zambian Copperbelt

Evaporites

Primary evaporite textures in the form of nodular anhydrite are preserved from around the level of the ore shale

Anhydrite is most abundant in the hanging wall sequence as cements, vughs and veins

Presumably represent evaporitic material remobilised on various scales (S and Sr? isotopes)

No evidence of halite recognised

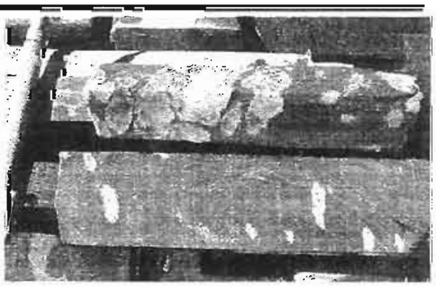

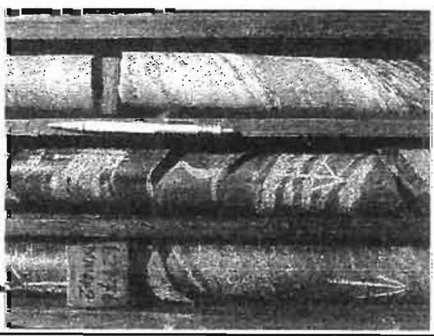

AMIRA P544

Zambian Copperbelt

Mineralisation

- Bulk of the economic Cu-Co is stratabound at around the lower Roan - Ore Shale contact
- A substantial proportion of the ores are hosted in the footwall sandstones
- Much of the economic ore now resides in structurally controlled sites eg. Nkana SOB MC
- Some ore occurs as disseminations within fine-grained, reduced ore shale that are not obviously structurally controlled eg. the Konkola system NP & RS

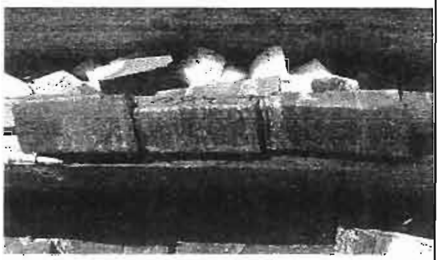

AMIRA P544

Polish Kupferschiefer

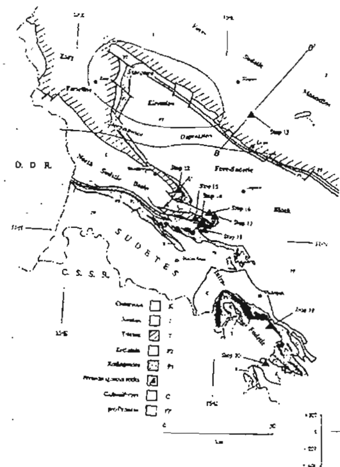

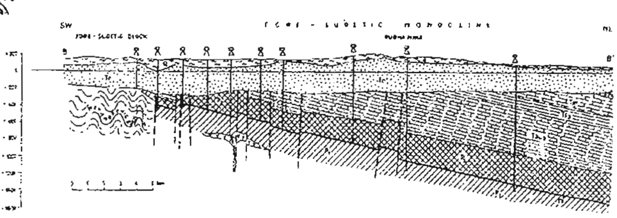

Figure 45. Geologic cross-section of the Fore-Sudetic Monocline in the area of the Rudna Mine (location in

AMIRA P544

Polish Kupferschiefer

Stratigraphy broadly similar to the ZCB

- Basal clastic sequence of variable thickness (Rotligendes) - in this case includes bimodal volcanics
- Abruptly overlain by a thin organic rich shale with carbonate correlates (Kupferschiefer)

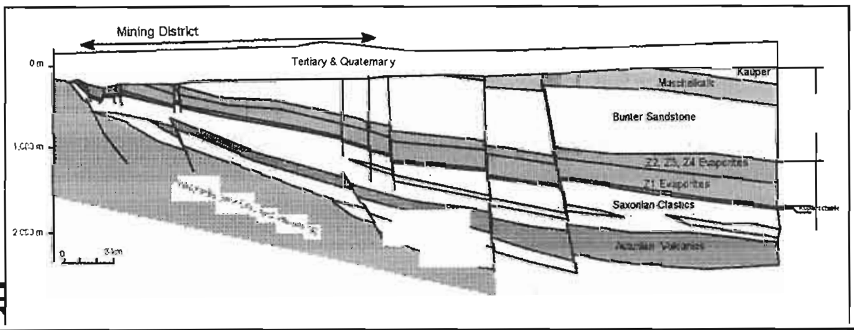

AMIR

Polish Kupferschiefer

- Overlain by a carbonate and evaporitic succession (Zechstein) that includes in situ thick massive anhydrite and halite units

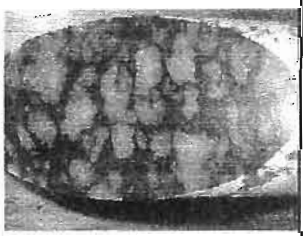

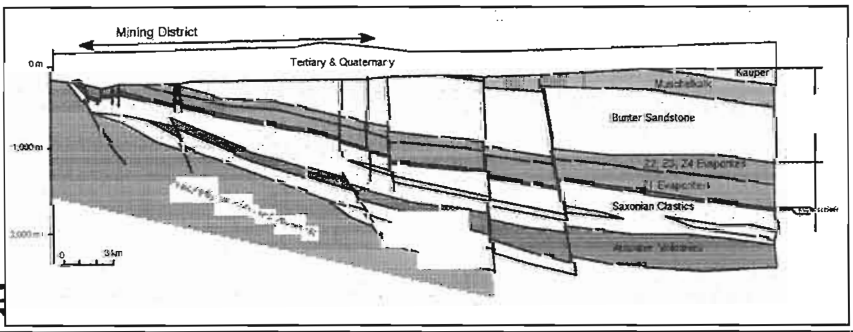

AMIR

Polish Kupferschiefer

Mineralisation broadly analogous to the □ZCB

- Stratabound and concentrated around the base of the Kupferschiefer
- Substantial deposits mined entirely in the footwall sandstones (eg. Lubin Mine)

Significance of the Polish system - low structural and metamorhpic grade allows the Cu mineralisation to be placed firmly in its basin context

AMIRA P544

Polish Kupferschiefer

Genetic models (eg. Jowett, 1986)

- Leaching of metals during diagenetic convection of oxidised brines through the basal rift phase
- Reduction induced metal precipitation around the base of the regional seal, the organic-rich Kupferschiefer

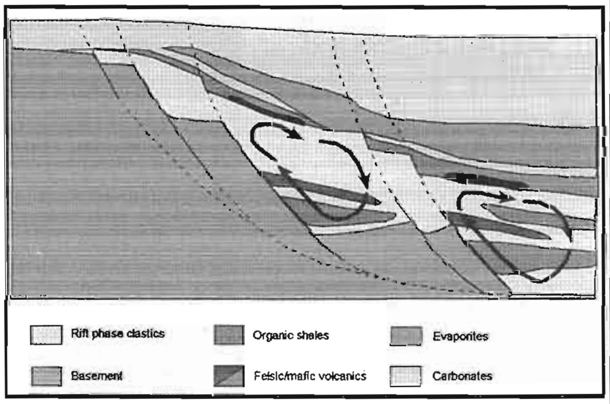

AMIRA P544

Polish Kupferschiefer

- Significance of evaporites
- Position of shale-hosted vs sandstone hosted deposits

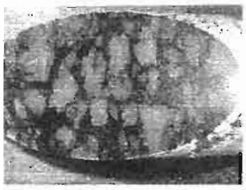

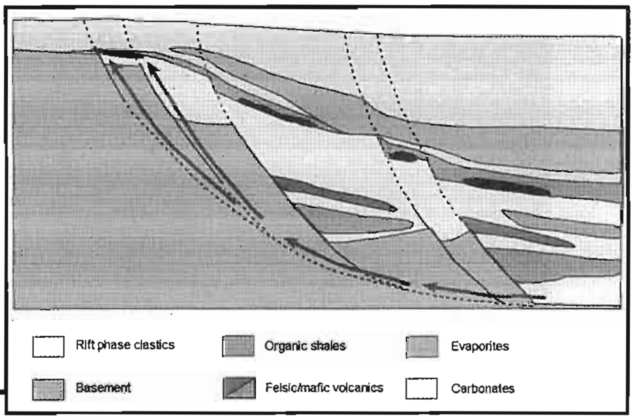

AMIRA P544

Polish Kupferschiefer

Stratiform syn-diagenetic Cu (Kupferschiefer-style) - no reason can't have occurred in ZCB

- Need a substantial clastic succession retains primary porosity & permeability - the initial rift phase
- Only trap Cu during this phase if there is a suitable reductant developed
- The initial rift phase is the only time when the trap is in hydrological contact with basement

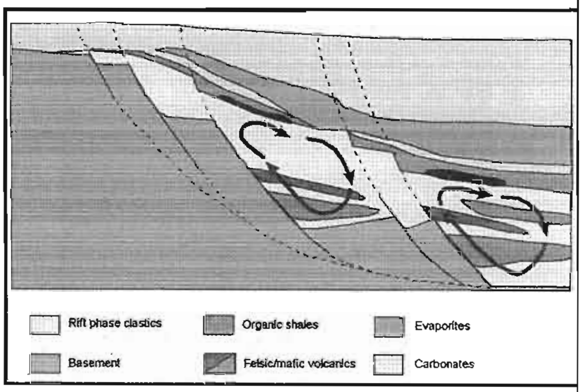

AMIRA P544

CODES SRC

Adelaide Fold Belt

AMIRA P544

CODES SRC

Adelaide Fold Belt

Stratigraphy

- Relatively thick - complex multi-phase basin history
- Glacial deposits are in third main basin cycle ~ Kundelungu in ZCB
- Callanna and Burra Groups are potential Roan correlates (WM)

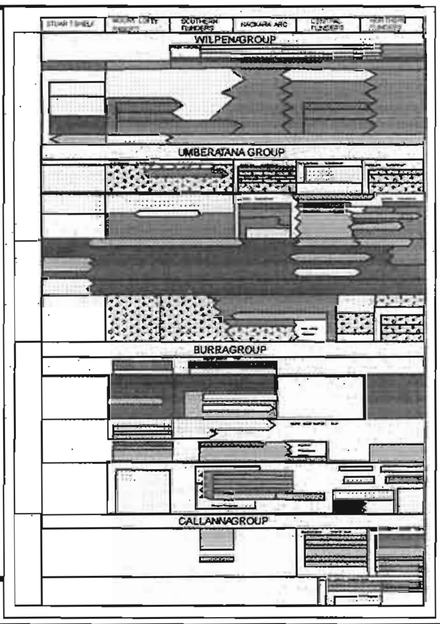

AMIRA P544

Adelaide Fold Belt

Evaporites

- Abundant in the Callana & Burra Gps
- Extensive salt tectonics - wholesale mobilisation of evaporitic stratigraphy (Callana Group) into diapiric breccias

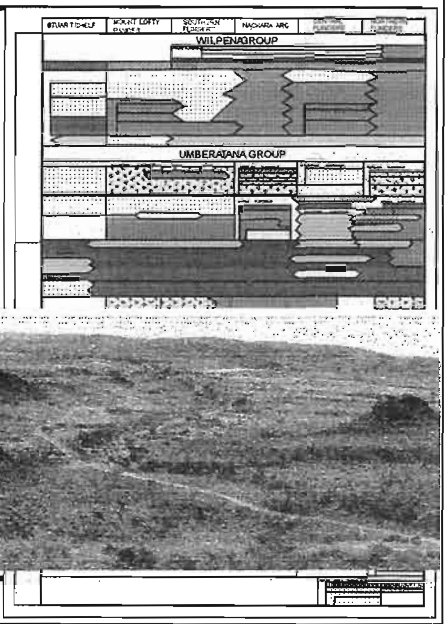

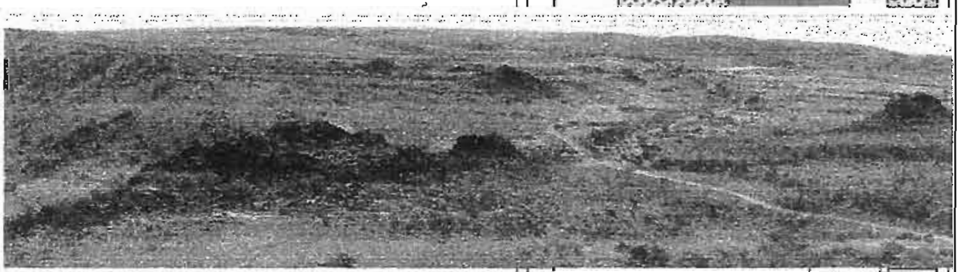

AMIRA P544

Adelaide Fold Belt

Mineralisation

- Tapley hill Formation Cu deposits of the Stuart Shelf have been interpreted as Kupferschiefer-style
- Reduced trap rocks in the Umberatana Group occur higher in the basin stratigraphy than the ore hosts in the Polish system or the ZCB
- On the Stuart Shelf there is no significant footwall rift-phase
- Difficult to see how Kupferschiefer-style syn-diagenetic Cu episode could have operated at Umberatana time

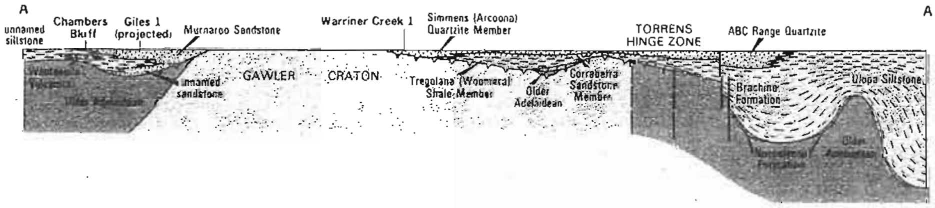

Adelaide Fold Belt

Mineralisation

- Purely stratigraphic model predicts the Callana Group as the site of Kupferschiefer-style Cu
- Not present to a significant extent on the Stuart Shelf
- Within the depocentre largely covered by younger basin phases
- Where Cu is hosted in the Umberatana Gp in the basin proper - spatial association with diapiric breccias of dismembered Callanna stratigraphy (DS, SB & WM)

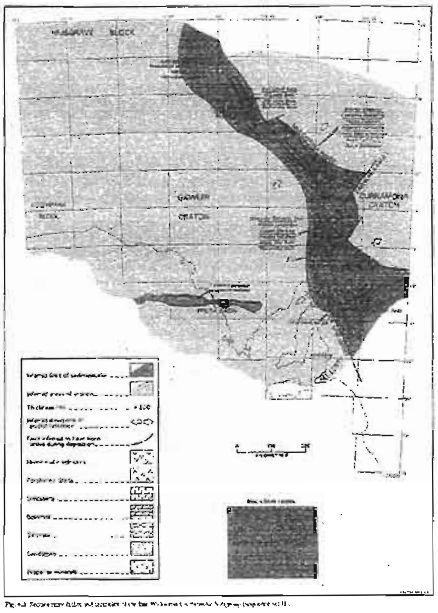

AMIRA P544

Zambian Copperbelt

ZCB preserved remnant of a much larger basin

- Polish stratigraphic analogue? Relatively simple one cycle system

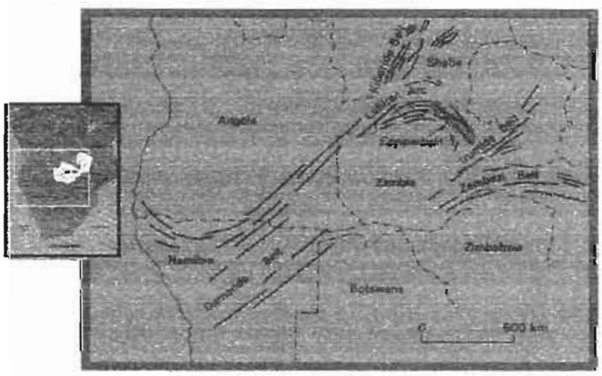

AMIRA P544

Zambian Copperbelt

Polish stratigraphic analogue? Relatively simple one cycle basin system

- Thickness and distribution of lower Roan/ore shale
- Distribution of mineralisation
- Carbonates & evaporites in the hanging wall

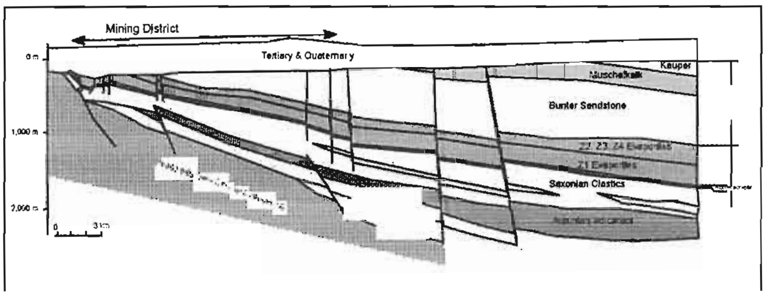

AMIRA P544

Zambian Copperbelt

AFB stratigraphic analogue? More complex multi-phase basin
If so where are we in this system?

- Facies of lower Roan suggest active tectonism = not in a shelf position
- Ore shale (first fine reduced rocks) locally in contact with basement = not in thick basin center

= Torrens Hinge Zone type position?

- Model predicts major basin phase boundaries within ZCB stratigraphy- manifest as unconformities and/or abrupt provenance changes (DB, DS, SB)

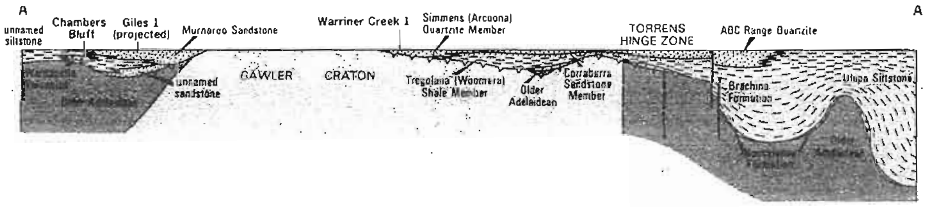

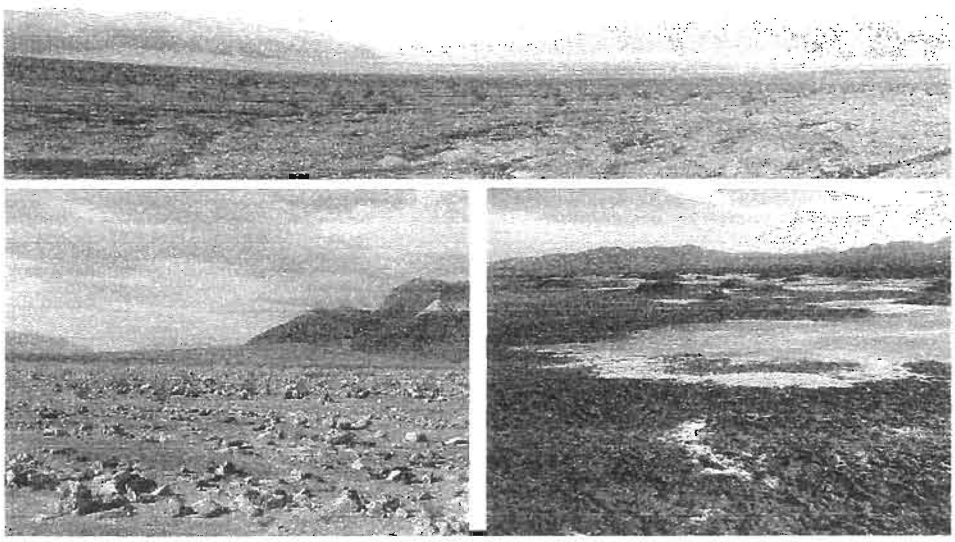

AMIRA P544

Kupferschiefer District,

Central and Eastern Europe

Kupferschiefer District

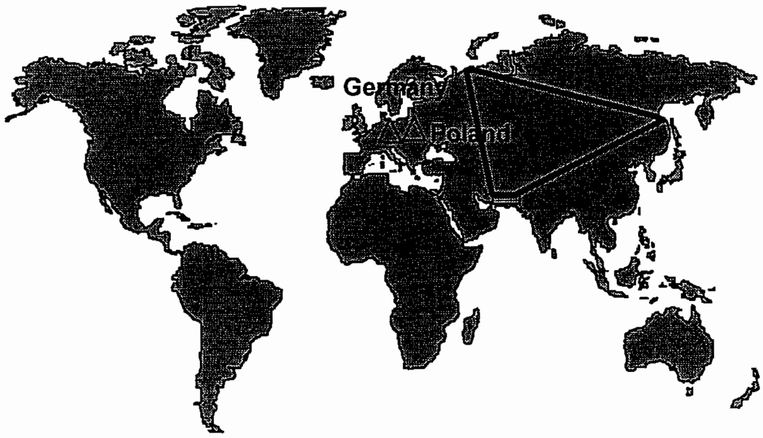

Kupferschiefer - Tonnage & Grade

Deposit	Cu%	Ag(g/t)	Size (Mt)
Mansfield, Germany	2.9	150	75
Lubin, Poland	2.0	50	2600

Deposits also contain significant Zn-Pb with minor Co, Ni, Au, and PGE

Kupferschiefer District - Stratigraphic Framework: Rotliegendes

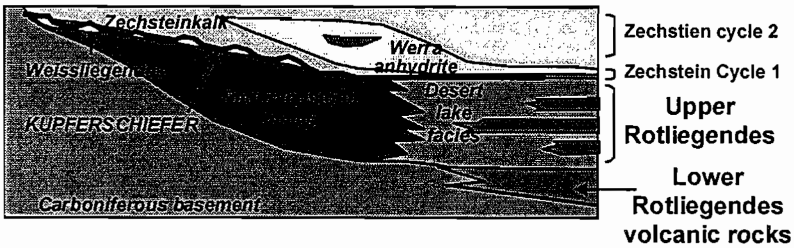

Lower Permian Rotliegendes red beds (250 - 900m which are composed of coarse-grained, locally derived clastic rocks deposited in a fluvial-eolian desert environment that was tectonically similar to the Basin and Range. In the North Sudetic Basin and Lubin Basin the Rotliegendes contains basal bimodal volcanic rocks.

Kupferschiefer District - Stratigraphic Framework: Rotliegendes

Lower Permian Rotliegendes red beds (250 - 900m thick are composed of coarse-grained, locally derived clastic rocks deposited in a fluvial-eolian desert environment that was tectonically similar to the Basin and Range. In the North Sudetic Basin and Lubin Basin the Rotliegendes contains basal bimodal volcanic rocks.

Lowermost Upper Rotliegendes (Freisener Beds - Nahe Group) near Waldbokelhein, Germany. Red claystones and shales interbedded with medium-grained, red conglomerates. Claystones with many green reduction spots.

Kupferschiefer District- Stratigraphic Framework: Weissliegendes

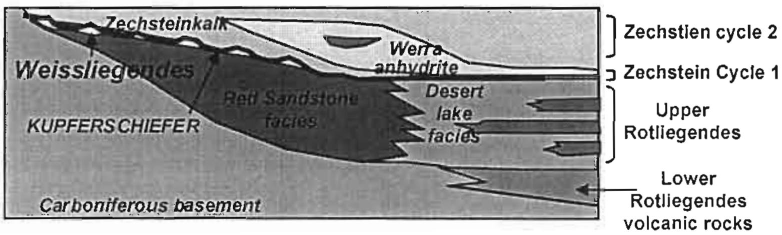

The top of the Upper Rotliegendes contains the Weissliegendes (white sand) on the margins of the basins. In the basin interiors this unit is called the Grauliegendes (grey sand). These sandstone are interpreted to have formed as eolian dunes. The initial Zechstein transgression has often eroded and reworked the top several meters of the Weissliegendes and given it a marine character. The Weissliegendes is locally economically mineralized.

Kupferschiefer District- Stratigraphic Framework: Weissliegendes

The top of the Upper Rotliegendes contains the Weissliegendes (white sand) on the margins of the basins. In the basin interiors this unit is called the Grauliegendes (grey sand). These sandstones are interpreted to have formed as eolian dunes. The intial Zechstein transgression has often eroded and reworked the top several meters of the Weissliegendes and given it a marine character. The Weissliegendes is locally economically mineralized.

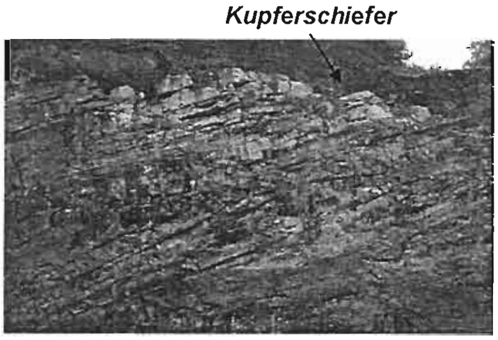

Cross bedding in Cornberg Sandstone (Weissliegendes); Sontra, Germany

Kupferschiefer District- Stratigraphic Framework: Kupferschiefer (Zechstein 1 Cycle)

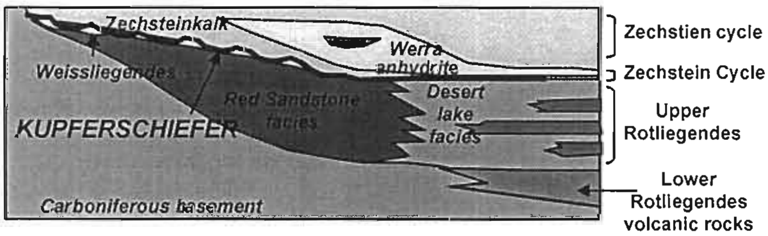

The Kupferschiefer (copper shale) represents the basal layer of the Zechstein 1 Cycle marine transgression.

In Germany and Poland the Kupferschiefer is commonly underlain by a thin (0.15m on basin margin to 7 m in basin interior) fossiliferous to massive dolostone to limestone termed the Border Dolomite (Poland) or the Productus-Kalk (Germany).

The Kupferschiefer is typically a laminated, black, pyritic, coaly, carbonate-rich shale. It is generally thin (<80 cm) on the basin margin and up to 6 m thick in the basin interior. Undulating topography on Weissliegendes sand bodies caused the Kupferschiefer to thin and thicken.

Kupferschiefer District- Stratigraphic Framework: Kupferschiefer (Zechstein 1 Cycle)

The Kupferschiefer is typically a laminated, black, pyritic, coaly, carbonate-rich shale. It is generally thin (<80 cm) on the basin margin and up to 6 m thick in the basin interior. The Kupferschiefer represents a transgressive sequence in a peri-marine coal swamp into a shallow intertidal-subtidal environment.

Thin (20 cm) Kupferschiefer. Here it is a carbon-rich (1.8 - 6.7 TOC), saprolitic shale with:

0.5 - 8 % Cu,
153-260 ppm Pb — 120 - 600 ppm Zn
200 - 440 ppm Ni — 150 - 380 ppm Co

Cornberg Quarry, Sontra, Germany

Kupferschiefer District- Stratigraphic Framework: Kupferschiefer (Zechstein 1 Cycle)

Drill core from upper Roteliegendes (L) through reduced (black) conglomerate into grey-green Weissliegendes into black Kupferschiefer (very low Cu here). Cornberg, Germany.

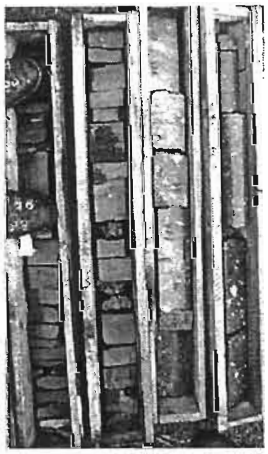

Drill core (DDH Koscielna Weis 184; 961 - 964m) from upper Roteliegendes (R) into Zechsteinkalk basal conglomerate and into basal limestone. Note limestone is reddened at its base. North Sudetic Trough, Poland.

Kupferschiefer District- Stratigraphic Framework: Kechsteinkalk (Zechstein 1 Cycle)

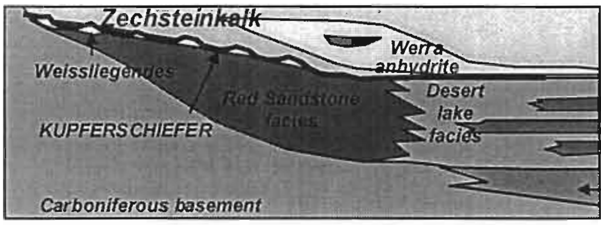

The Zechsteinkalk directly overlies the Kupferschiefer. It forms a shallow lacustrine to marine sequence (30 - 100 m thick). It contains shallow-water carbonate grainstones in near-shore environments and carbonate mudstones in deeper zones. The near-shore facies are well zoned from a landward shaley and sandy lime mudstone with oncolites and oolites to a discontinuous algal-bryozoan boundstone barrier to carbonate mudstones and wackestones farther seaward.

Kupferschiefer District- Stratigraphic Framework: Kechsteinkalk (Zechstein 1 Cycle)

The Zechsteinkalk forms a shallow lacustrine to marine sequence (30 - 100 m thick). The near-shore facies are well zoned from a landward shaley and sandy lime mudstone with oncolites and oolites to a discontinuous algal-bryozoan boundstone barrier to carbonate mudstones and wackestones further seaward.

Zechsteinkalk. Bedded micrite and algal grainstones, immediately adjacent (landward) from boundstone barrier. Minor hematization (weak Rote Faule alteration). Bauch Kupfermergel Quarry, Korbach, Germany.

Kupferschiefer District- Stratigraphic Framework: Werra Anhydrite (Zechstein 1 Cycle)

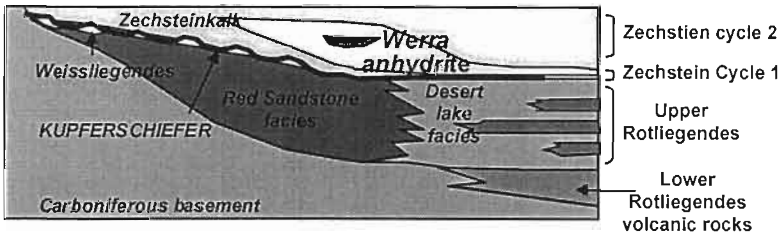

- With time, water depths shallowed leading to local exposure of the Zechsteinkalk. It is conformably overlain by marine evaporites dominated by anhydrite on the basin margins and anhydrite + halite in the basin interior.
- The Werra Anhydrite is overlain by carbonates (and later evaporites) of Zechstein cycle 2.

Kupferschiefer District- Stratigraphic Framework: Werra Anhydrite (Zechstein 1 Cycle)

The Werra Anhydrite forms the top of the Zechstein 1 cycle. It consists of marine evaporites dominated by anhydrite on the basin margins and anhydrite + halite in the basin interior.

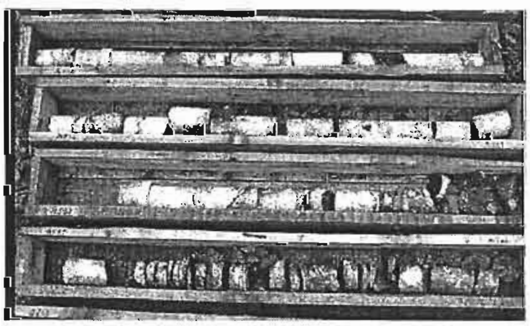

Drill core (Koscielna Wies 184; 880m) of Zechstein 1 anhydrite with red clay zone. This is from near base of anhydrite layer. North Sudetic Trough, Poland.

Kupferschiefer Mineral Zonation
Sectional View - Lubin Orefield, Poland

- Mineral and metal zonation transgresses stratigraphy at a very low angle from the Weissligiendes up through the Kupferschiefer and into the Zechsteinkalk.
- Rote Faule (hematitic) alteration locally extends into the Werra Anhydrite.
- Rote Faule - copper transitions commonly occur over or beside basement highs.

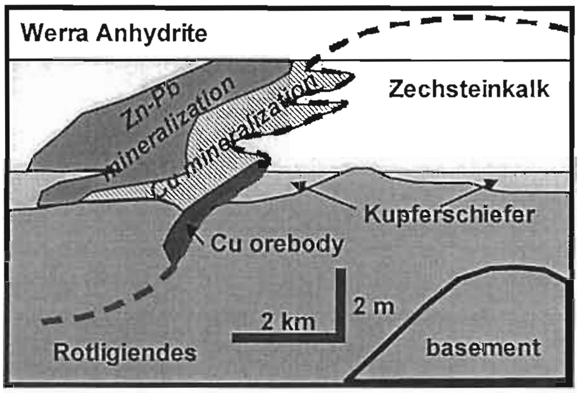

Kupferschiefer Mineral Zonation
Plan View - Lubin Orefield, Poland

- Mineral zones in plan view are arranged from hematite (Rote Faule) to chalcocite to bornite to chalcopyrite (all with Ag and locally Au + PGE). Then out to galena, then sphalerite and finally diagenetic pyrite.
- At any one location, the three major base metals (Cu, Pb, Zn) occur together in various proportion.
- In detail, contacts between mineral zones are quite irregular.

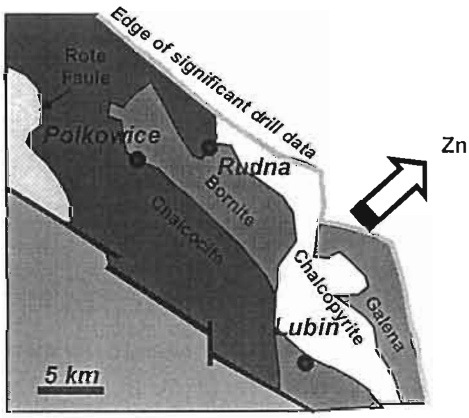

Kupferschiefer Mineralization

Mineralization occurs in the Weissligiendes, Kupferschiefer, and in the lower portions of the Zechsteinkalk.

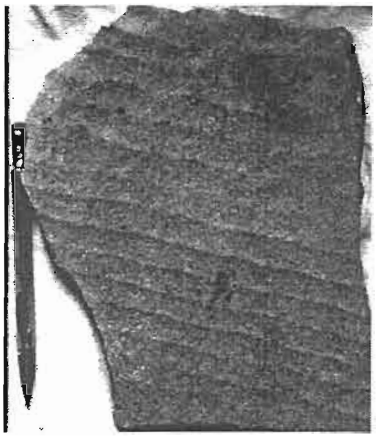

In the Weissligiendes, mineralization occurs as intergranular cement. Grades range up to 15% Cu.

Here chalcocite occurs along individual cross beds. Rudna Mine, Poland

Kupferschiefer Mineralization

Mineralization occurs in the Weissligiendes, Kupferschiefer, and in the lower portions of the Zechsteinkalk.

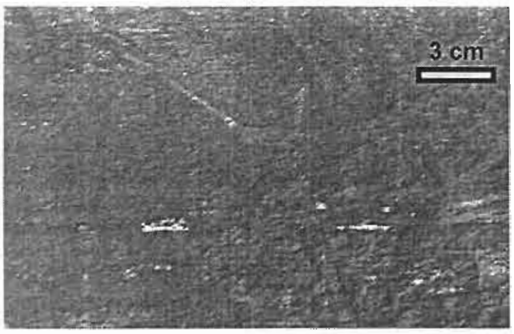

In the Kupferschiefer, mineralization occurs as disseminations (directly replacing diagenetic pyrite) and as veins (most bedding parallel).

Sample contains 11% Cu. Rudna Mine, Poland

Kupferschiefer Mineralization

Mineralization occurs in the Weissligiendes, Kupferschiefer, and in the lower portions of the Zechsteinkalk.

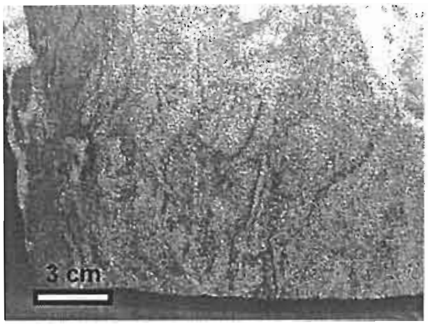

In the Zechsteinkalk, mineralization occurs as disseminations and irregular bedding plane replacements.

Sample contains 10.9% Cu, 500 ppm Ag

Rudna Mine, Poland

Kupferschiefer - Rote Faule Alteration

The Rote Faule is an irregular zone of reddish oxidation (hematite) which extends upward from the Rotligiendes into the Zechstein and locally as high as the Werra Anhydrite.

Rote Faule alteration cuts diagenetic cements in the Weissligiendes.

Rote Faule alteration of basal Zechsteinkalk. Rote Faule zone here contains 50 - 250 ppm Cu. Immediately adjacent to Rote Faule, unoxidized limestone contains 1.4% Cu.

Bauch Kupfermergel Quarry, Korbach, Germany

Kupferschiefer - Sulfide Textures

- Disseminated sulfides (occur as small disseminated grains or agglomerates of grains):
  - Sequential mineral replacement is common.
  - Chalcocite and bornite commonly replaced by hematite.
  - Bornite and chalcopyrite commonly replaced by chalcocite.
  - Chalcopyrite, galena, and sphalerite replace diagenetic pyrite.
  - Copper sulfides also replace carbonate grains and cements and organic fragments.
  - In sandstone ore, copper sulfides replace detrital quartz, feldspar, rutile, and magnetite grains as well as clay and carbonate minerals.
- Veinlet sulfides
  - Form as long streaks or veins parallel to bedding.
  - Veins may be monomineralic or contain several minerals
  - Generally sulfides in veins matches those in adjacent disseminations.

Kupferschiefer - Mineralization Model

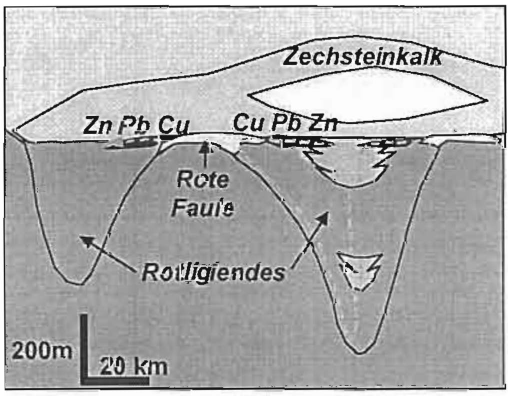

Rapid subsidence during the early Triassic marks extension associated with Tethys opening. A thermal anomaly accompanying extension caused heating of formational brines in Rotligiendes, leaching of metals and movement of fluids up along basement highs to Kupferschiefer. Reaction of these oxidized fluids with the more reduced sediments produced the observed mineral zonation. Fluids moved along the Rotligiendes - Kupferschiefer boundary toward the basin center and eventually sank back down into the basin (convection cell).

Basin Architecture During Lower Umberatana Group Sedimentation

David Selley
&
Stuart Bull

Introduction

- Tapley Hill Fm (THF) is host to numerous small, stratiform, disseminated and vein hosted Cu deposits

- In terms of sedimentary facies, THF superficially resembles carbonaceous "ore shale" facies

  Similarities
  - dark, organic rich, fine-grained facies = chemical trap
  - major transgression of rift shoulders
  - historical focus of exploration

  Differences
  - occurs considerably higher in the basin history
  - within rift axis, THF is separated from basal siliciclastic package by up to 6km

Introduction (cont.)

- Within Northern Adelaide Fold Belt, mineralised THF occurs in two distinct basin positions (stratigraphic associations):

<u>Stuart Shelf</u>

- basal Adelaidean is either highly condensed or missing
- spatial association with Mesoproterozoic Fe-oxide Cu-Au deposits

<u>Rift Axis</u>

- mineralised THF overlies a substrate of thick, dismembered lower Adelaidean strata
- mineralisation is lacking where lower basin cycles are intact
- strong spatial association with breccia units, historically considered to represent diapirically emplaced, basal evaporitic strata
- thus, although THF is temporally displaced from the "engine room", a distinct spatial relationship remains

Stratigraphic Architecture

Warrina SGp

- restricted depocentres at fringes of axial rift
- stacked rift-sag phases with cyclical internal structure
  - prograding clastic wedges
  - finer clastic and carbonate deposits
  - Callanna Gp records more restricted basin environment: evaporitic strata

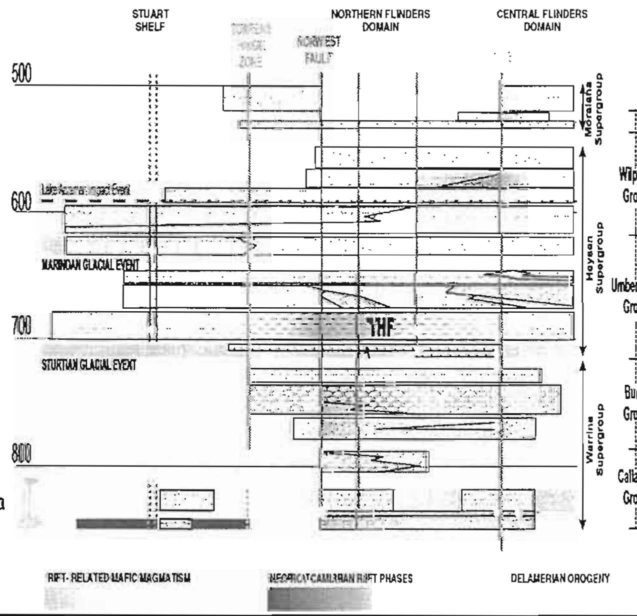

Stratigraphic Architecture

Umberatana Gp

- spans 2 main glacial episodes
- transgression of rift shoulders
- abrupt basin reconfiguration
  - compartments
  - stacked unconformities
  - marine sedimentation
  - sedimentary breccia units
  - diapiric breccias
- Rodinean breakup

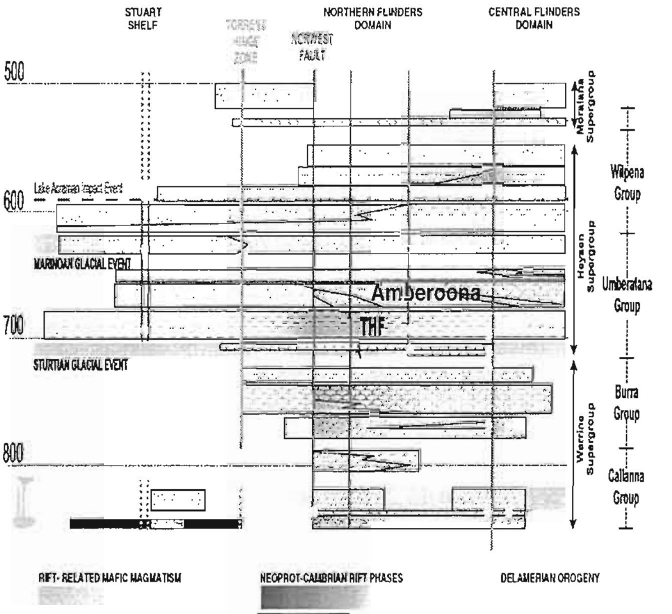

Northern AFB

- Main basin elements:
  - Norwest Fault
  - Paralana "transfer system"
- Willouran Ranges coincide with gravity trough
- Comparison of stratiform Cu on Stuart Shelf with rift axis

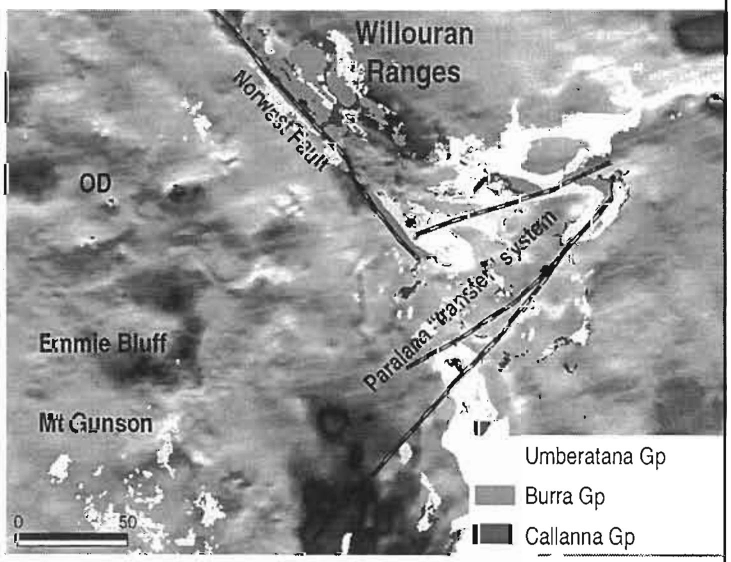

Umberatana Depocentres

- 3 Umberatana depocentres
- broadly NW trend
- straddle complex fault zones
  - record both growth and inversion histories
- facies architecture provides constraints on original basin geometry

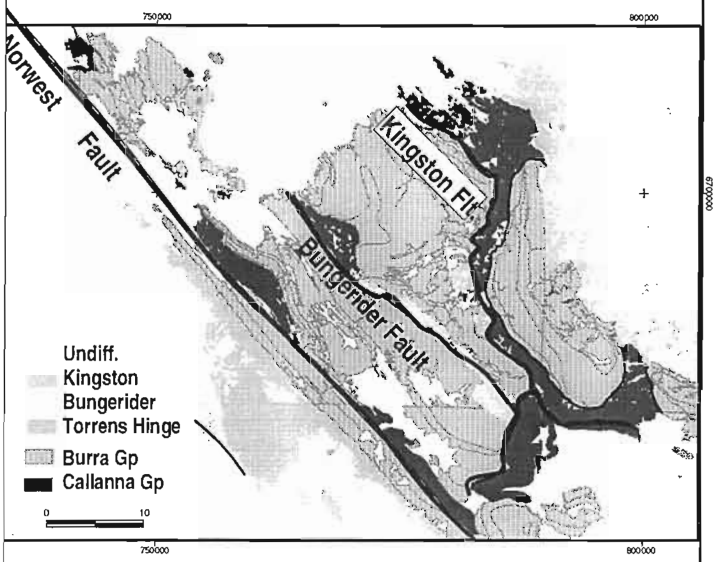

Bungerider Depocentre

- Narrow NW trending synclinal trough
  - bisected by Bungerider Fault Zone
- Complex internal architecture contrasts with "tram-track" geometry unconformably underlying Burra Gp
  - high angle unconformities occur both at the base and internally
  - second unconformity occurs within the THF

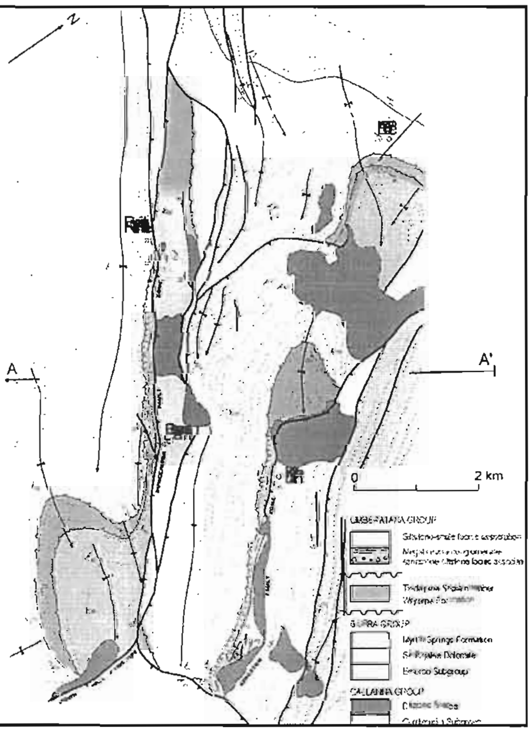

Bungerider Depocentre

- Variation in facies architecture occurs both longitudinally and laterally
  - lower stratigraphic levels are preserved within a non-cylindrical embayment to the SE
  - unconformity within THF cuts down-section to NW
  - high angle unconformities on SW limb
  - low angle unconformities on NE limb
  - thickness and facies variation across hinge

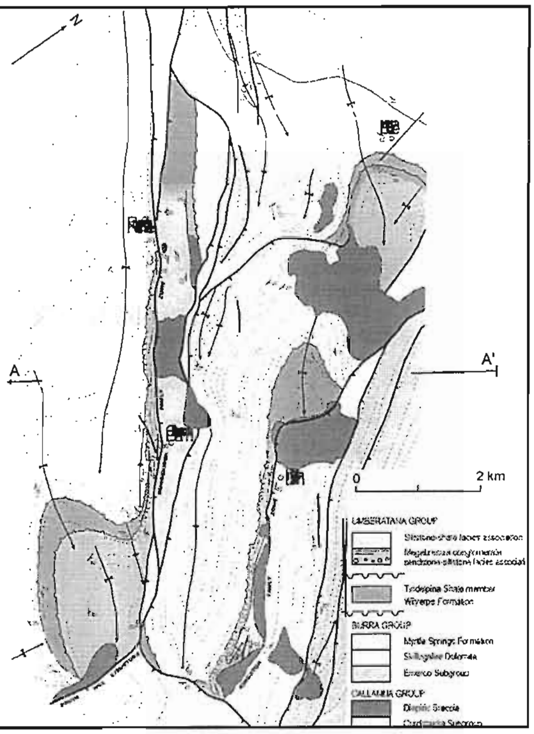

Lower Umberatana

- Glacial deposits (Wilyerpa Fm) & Tindelpina Shale Member of THF
- package wedges out along both limbs of the synform between upper and lower U/Cs
- basal unconformity increases from a few degrees to >25^0 at the northern pinch out
- variation in restored Burra dips indicate broad SW-plunging trough to SE at Umberatana time

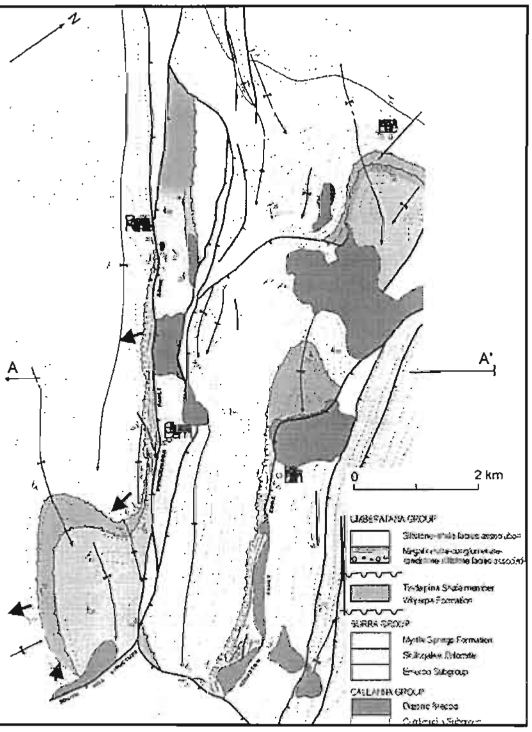

Middle Umberatana

- Upper THF & Amberoona Formation
  - broadly upward fining succession
- basal member cuts down-section within canyon system on SW flank
  - megabreccia
  - tabular to channelised dolomitic sandstone
  - channel geometry indicates ENE palaeoflow (ie. transverse drainage system)
  - basal U/C >40^{0}, locally approaching 90^{0}

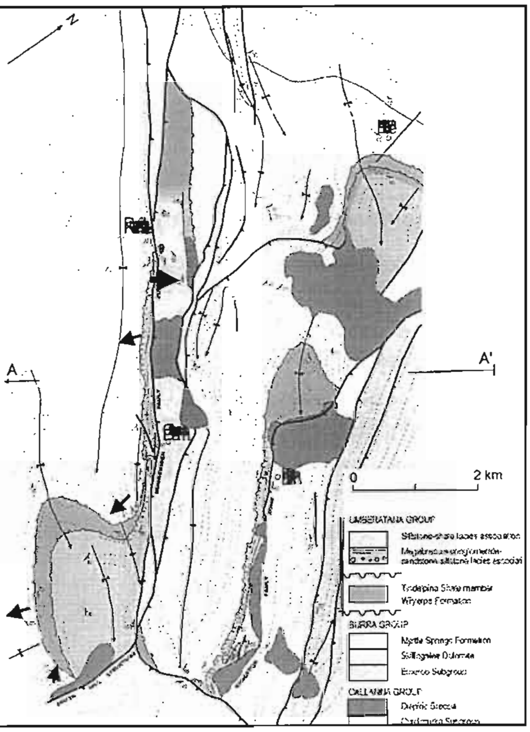

Middle Umberatana

- Upper THF transgresses canyon margins
  - intercalated dolomitic siltstone & shale, dolarenite and breccia deposits
- thickens & coarsens towards SE (ie. to South Hill Structure)
- abundant syn-depositional structures indicate SE-dipping palaeoslope
- transitional contact with Amberoona Fm on NE flank

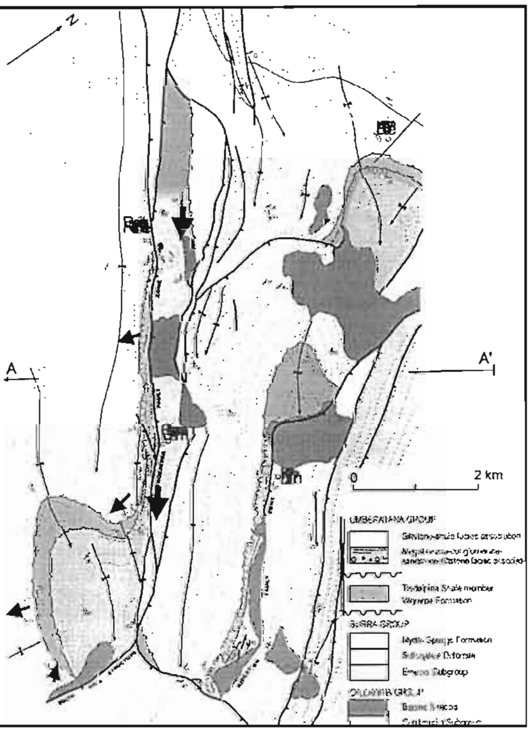

Implications for Basin Growth

Elements of facies architecture

- amalgamated high angle U/Cs
  - rapid, significant rotation of substrate
- asymmetric accommodation space
  - asymmetric facies architecture
  - chaotic facies contained within deeply incisive transverse drainage systems
- longitudinal variation in facies architecture and palaeoslope

Similarities to supra-detachment basins

- high rates of extension
- low angle, corrugated extensional fault systems
- significant tilt-block rotation
- pronounced topographic relief within the footwall block

Basin Geometry

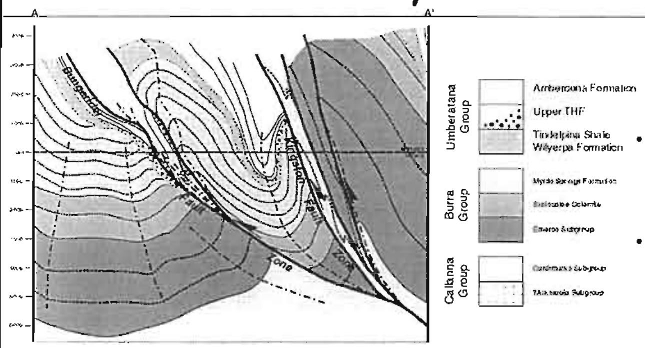

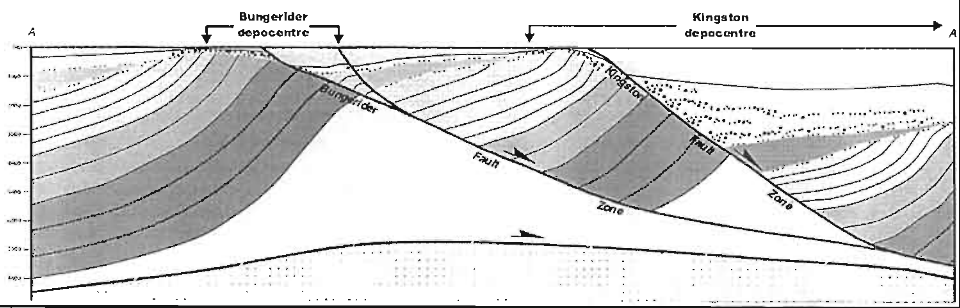

- SW & NE flanks of the syncline = respective footwall & hangingwall of shallow growth fault
- soles into detachment within evaporitic Callanna Gp
- megabreccias shed from highly rotated footwall

Kingston Depocentre

- extreme thickness/facies contrast across depocentre
- complex, corrugated fault system
- widespread diapirism

- Footwall Succession
  - Sturtian glacials removed
  - condensed THF with thick basal megabreccia
  - <300m thickness
  - punctuated by diapiric breccias

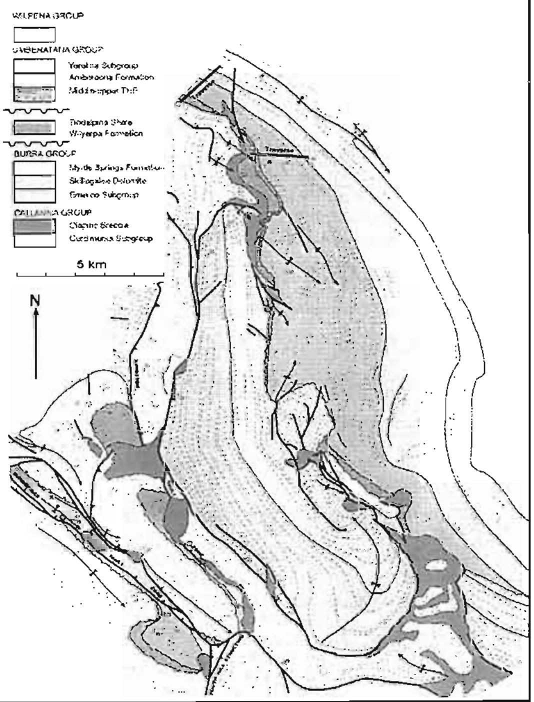

Diapiric Breccias

- THF megabreccias contains clasts with superficial compositional and textural similarities to diapiric breccias
- diapirs emergent by THF time?

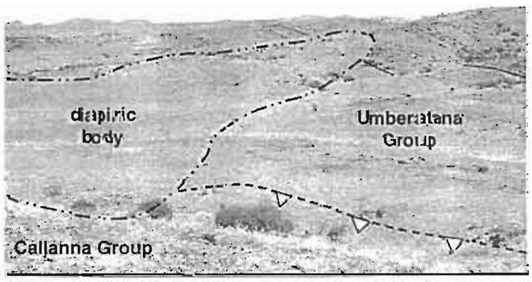

Kingston Depocentre

- Hangingwall Succession
  - thickest preserved glacial sequence
  - THF 2000m
  - longitudinal thickness changes
  - complex basal contact, transgressing deeply eroded Burra Gp & Upper Callanna Gp
  - diapiric breccias emplaced near base of the Umberatana Gp at peripheries of Burra Gp
  - fragments of breccia matrix within Sturtian glacials

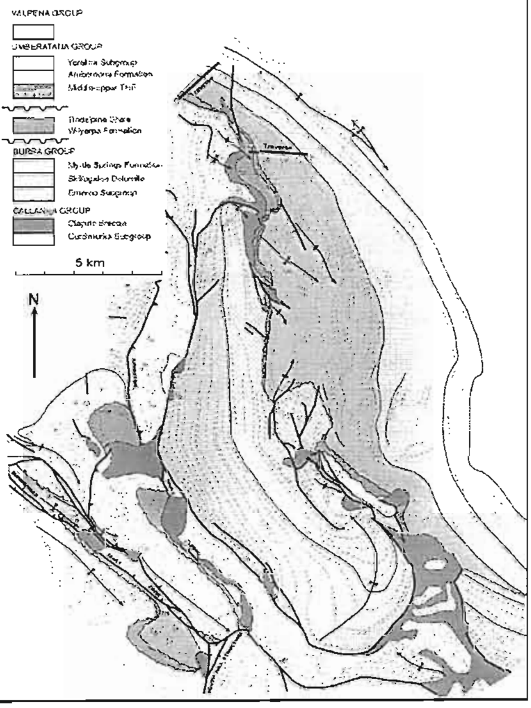

THF

- unconformity above the Tindelpina Shale Member
- facies association:
  - dark grey siltstone & shale
  - fine parallel- & ripple-laminated sandstone
  - tabular to channelised dolomitic sandstone, coarse lithic sandstone, granule conglomerate
  - megabreccia containing granitic fragments
- thicker, with increased fines component, but analogous to footwall sequences

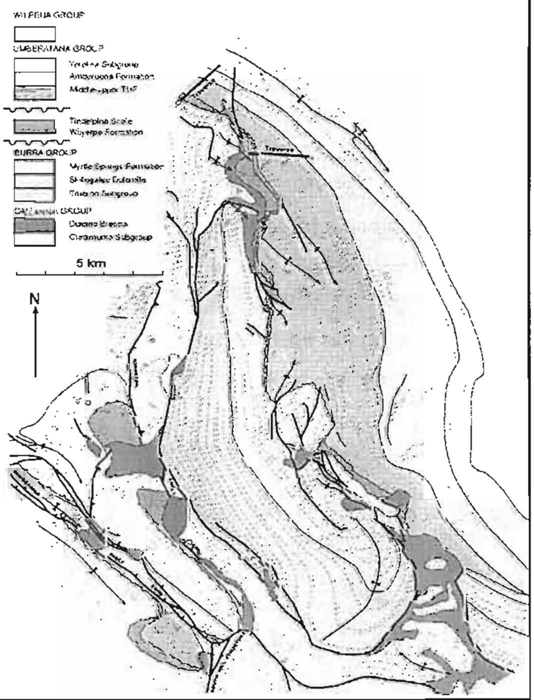

Mechanism of Basin Growth

- Substantial dismemberment of Warrina Supergroup prior to and during deposition of Umberatana Group
  - high angle, amalgamated unconformities within an at the base of the Umberatana Group
  - unconformities transgress major structures which juxtapose markedly different levels of Warrina Sgp stratigraphy
- Compartmentalisation of basin framework
- Substantial transverse and longitudinal thickness and facies variation

Mechanism of Basin Growth

- Accelerated extension at 700Ma was potentially accommodated by lateral "spreading" above evaporitic decollement surface within the Callanna Gp
  - collapse & fragmentation of thick Burra Gp packages above corrugated, listric normal faults
  - high degrees of footwall block rotation
  - evidence that diapiric breccias were emergent by early Umberatana times

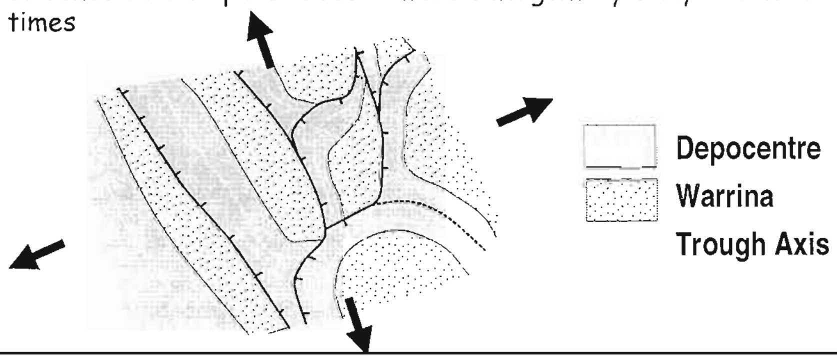

Experimental Salt Tectonics

- Experimental studies (Guglielmo et al. 1998) demonstrate that gravitational spreading can generate within sloping salt sheets overlain by considerable stratigraphic thicknesses.
- Overburden progressively fragments, rotates and subsides into the salt substrate.
- Depocentres generate above downthrown hangingwall blocks.
- Diapirs rise at block sutures (ie. depocentre maxima) and ultimately pierce newly deposited strata.

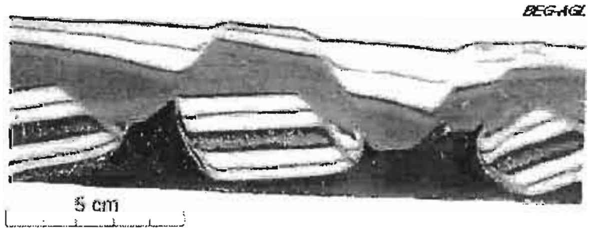

Cu Distribution: Willouran Ranges

- Cu distribution strongly linked Callanna Gp inliers (particularly where in diapiric form)
- Breaden Centre
  - stratiform Cu occurs where diapiric breccias pierce basal THF black shales

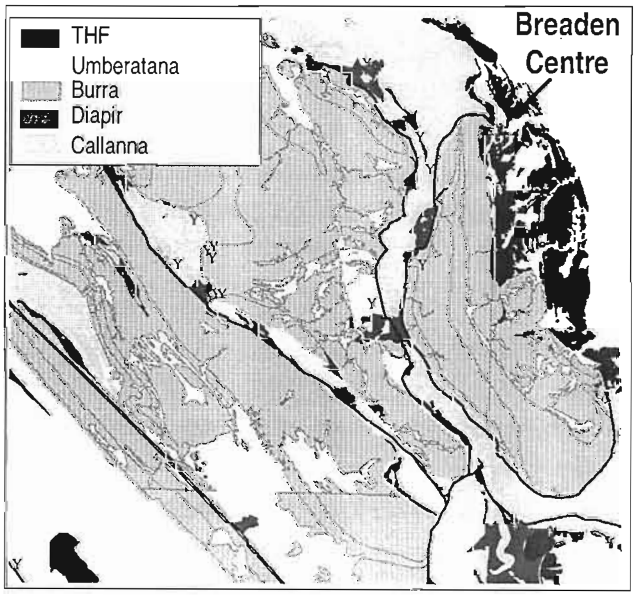

Cu Distribution: Northern AFB

- Regional Cu distribution shows spatial association with diapirs and "reduced" strata of THF and Bunyeroo Fm
- Cu is rare within Burra Gp and upper levels of Adelaidean stratigraphy
- THF is barren where it conformably overlies Burra Gp (ie. W of Leigh Ck)

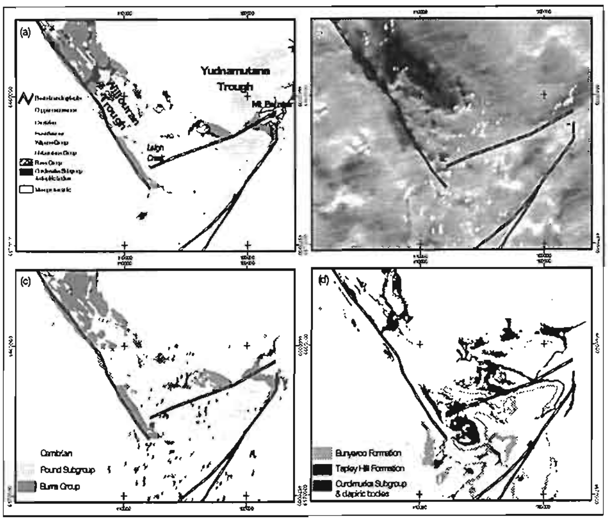

Summary

Working Hypothesis

- abrupt change in facies and basin architecture across the Warrina Supergroup - Umberatana Group boundary reflects coupled extension and salt mobility
- diapirism is focussed within depocentre maxima, providing a mechanism by which potentially Cu-bearing fluids can interact with chemically suitable trap rocks

Implications

- reactivation of the proposed decollement surface during inversion may have resulted in decoupling of the Callanna Gp from Burra Gp and higher levels
- significant thickness of presently unexposed, intact Callanna Gp may be preserved below the decollement

Summary (cont.)

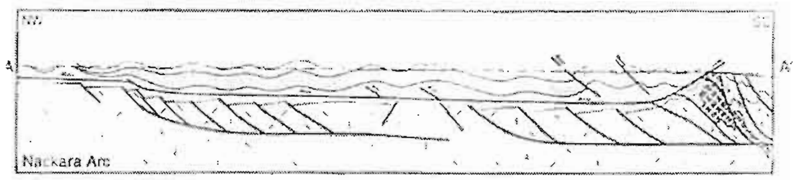

Marshak & Flottmann, 1996

Cross section through the Nackara Arc, southern Adelaide Fold Belt, demonstrating detachment at the base of the Burra Group.

Sedimentology and Structure of the Curdimurka Subgroup; Willouran Range, South Australia – An Introduction

Wallace Mackay

Study Aims

- to identify the depositional setting of the Curdimurka Subgroup in the Willouran Range

- to identify the overall structure of the Willouran Range
- to determine the origin of breccias within the Willouran Range
- from the identification of evaporite mineralogy, determine the influence of that mineralogy on basinal fluids.

CODES SRC

The Adelaide Foldbelt and sediment-hosted copper

- Adelaide Foldbelt similar age to Katangan
- Similar tectonic setting?
- Curdimurka Subgroup has a similar stratigraphy to that of the Roan Group
- Known copper mineralisation
- Presence of evaporites

CODES SRC

Constituent Studies

- structural evolution
- environment of deposition
- provenance and nature of the Dome Sandstone
- fluid chemistry as seen in the quartz and carbonate veins

Study Area – the type locality for the Curdimurka Subgroup

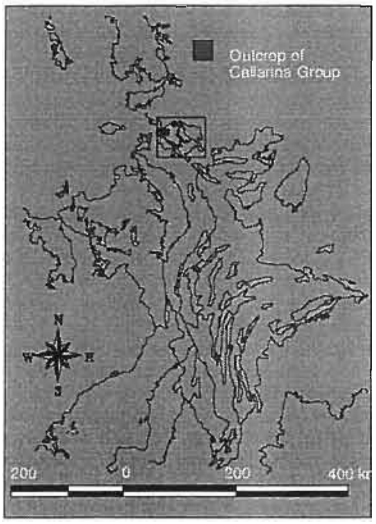

4 Proterozoic sediment-hosted Cu deposits

Stratigraphy of the Curdimurka Subgroup

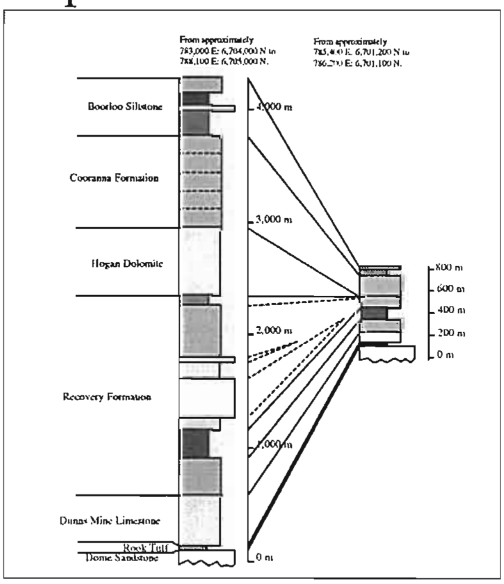

4 Proterozoic sediment-hosted Cu deposits

CODES SRC

Regional Structure

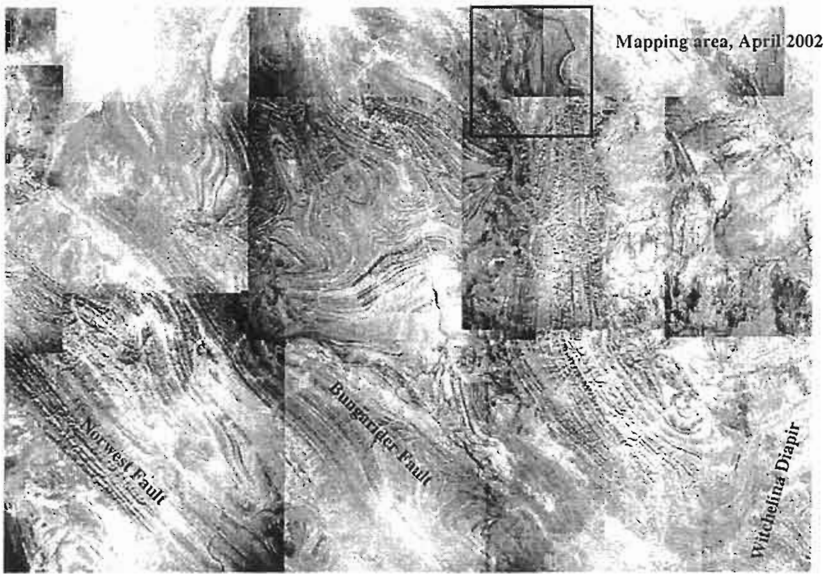

4 Proterozoic sediment-hosted Cu deposits

CODES SRC

Regional Structure

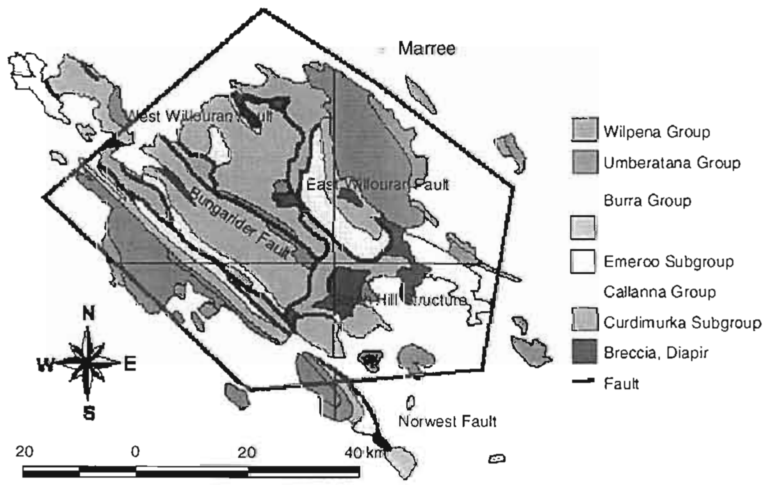

4 Proterozoic sediment-hosted Cu deposits

The Norwest Fault

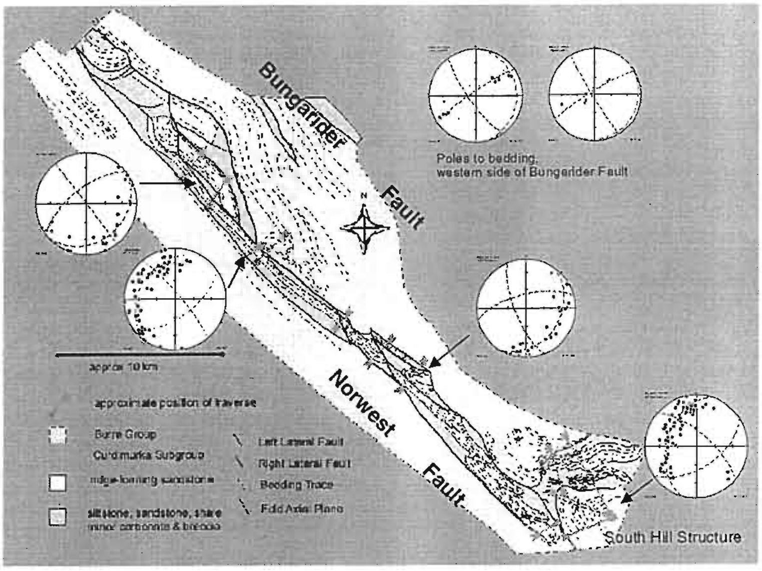

44 Proterozoic sediment-hosted Cu deposits

April 2002 Mapping

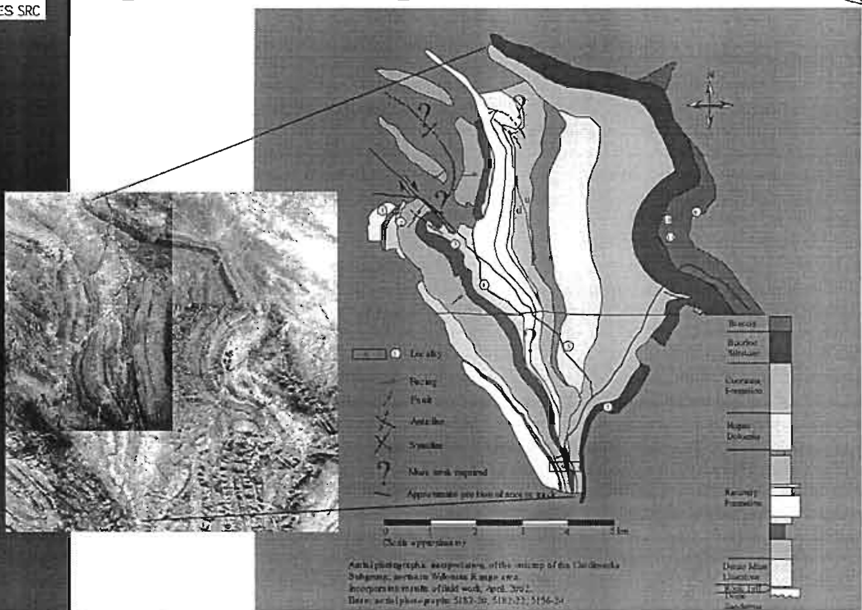

44 Proterozoic sediment-hosted Cu deposits

Sediment-hosted copper and evaporites

- Davidson, 1967
- Renfro, 1974
- Eugster, 1985
- Warren, 1999
  - (Basinal) Brine and ion source
  - Seal and trap to basinal fluids
  - Focus for fluid flow

Evaporite Textures

Sample 574 - microcline after gypsum

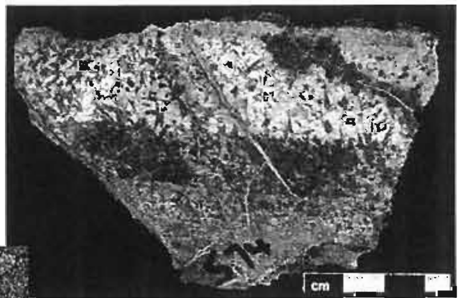

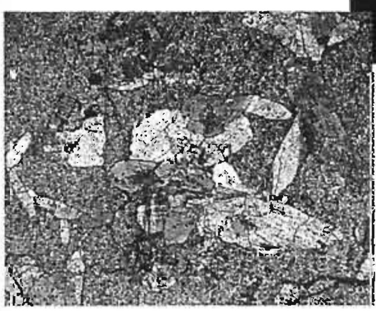

Sample 574, xpl, f.o.v., 6 mm

How common is Kfeld after gypsum?

Evaporite Textures

Sample 570b - quartz and dolomite after gypsum

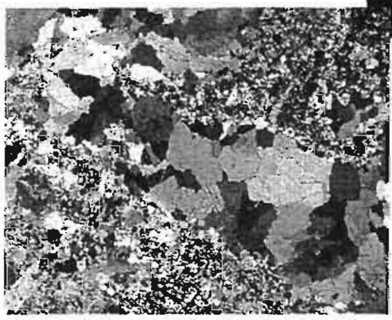

Sample 570b, xpl, f.o.v. 6 mm

Evaporite Textures

Sample 603c, rod-like pseudomorphs in limestone

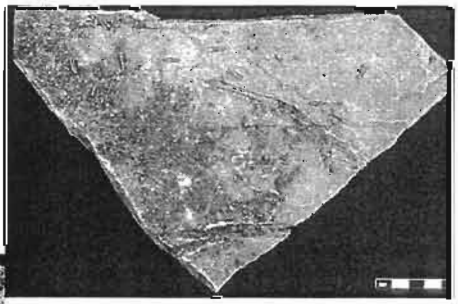

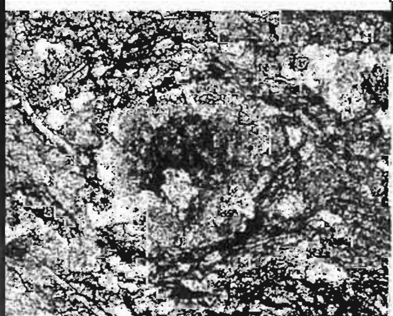

Sample 603b, ppl, f.o.v., 1.25 mm
Quartz rims around a chlorite core

The Dome Sandstone

Sample439a - rhombohedral casts after halite in quartz - feldspar sandstone

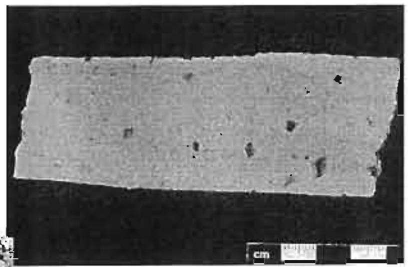

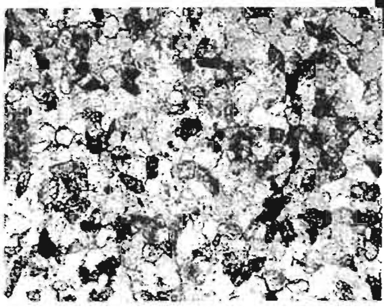

Sample439a - ppl, f.o.v., 2 mm - Feldspathic arenite

Is the feldspar detrital or diagenetic?

Conclusions

- There remains a lot of work to be done.

Stuart Shelf Geochemistry 1

Emmie Bluff

Peter McGoldrick

Two types of copper mineralisation

- Olympic Dam style Cu in Fe-stones at abt. 1000m
- Stratabound Cu in and near Tapley Hill Formation at abt. 400m

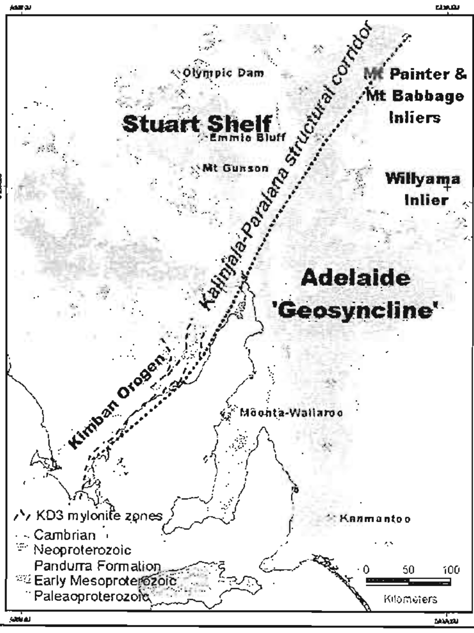

Fundamental Question

- Is there are genetic as well as a spatial link between the two types of mineralisation?

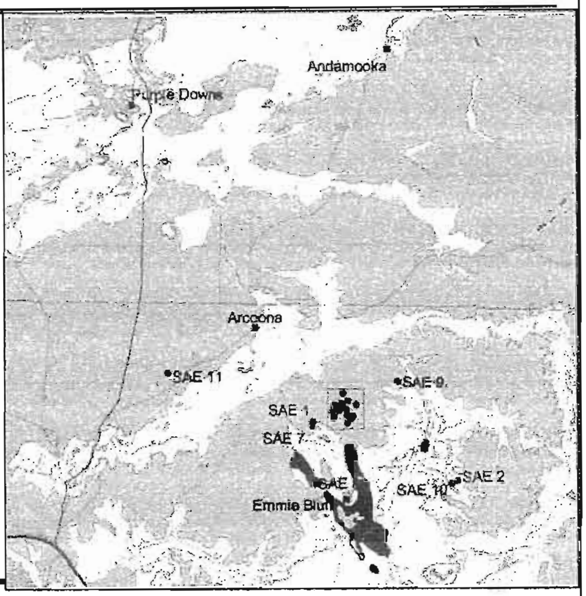

Andamooka Limestone
Corraberra Formation
Simmens Quartzite Member
Pandura Formation
SAE Series Drill Hole
Locality

10 0 10 20 Kilometers

Talk Outline

- describe the Fe-stone hosted mineralisation
- describe stratabound mineralisation in the cover rocks
- present selected major and trace element data for Fe-stones and cover rocks
- discuss implications for genesis and chemical vectors

Fe-stone Cu

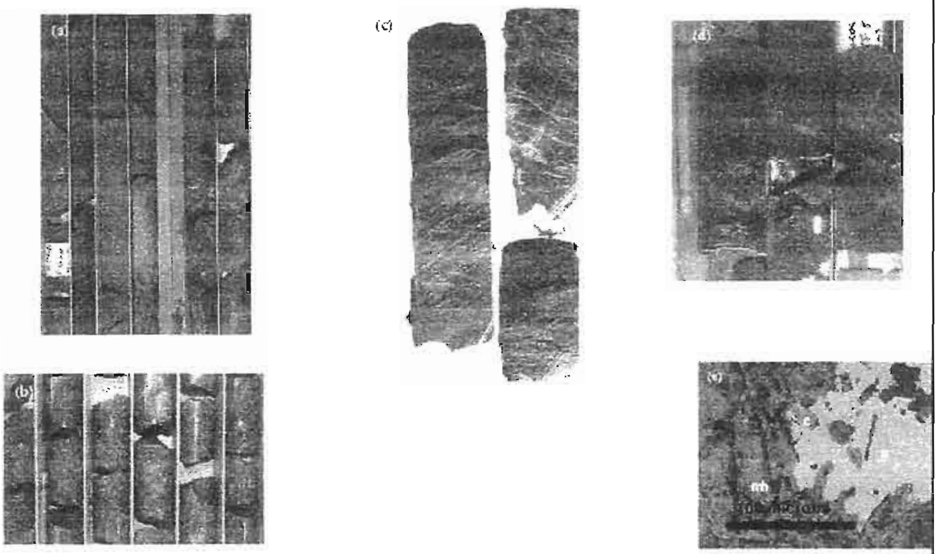

Fe-stone chemistry

- Six samples
- Two low Cu
- Four with Cu > 0.1%

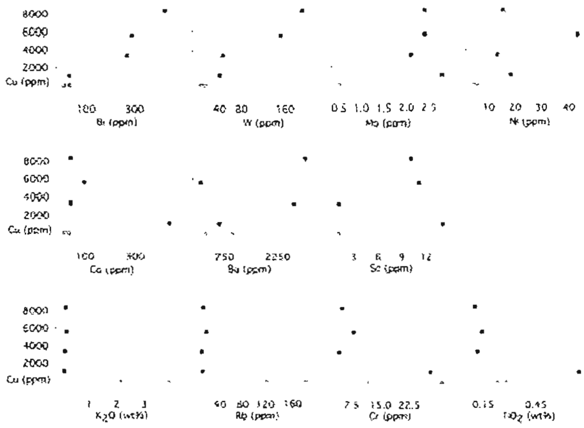

- **Elevated Bi, W, Mo & Ni associated with Cu**
- **Absolute Mo low**
- **3 samples with measurable Au (0.02 to 0.1 ppm**
- **One sample with > 200 ppm U, but others low**
- **Low K, Rb, & ?Ti, ?Cr associated with Cu**

Cu in the Cover Rocks

- Cu sulfides almost ex… s,
  dolomitic siltstones of … n
- Little bit Cu in Whyalla … F
- Neoproterozoic THF r … eeply
  weathered Mesoprote … on
- At EB 5 DDHs were s…
- The THF varies from (… thick
- 24 Mt @ 1.3% Cu

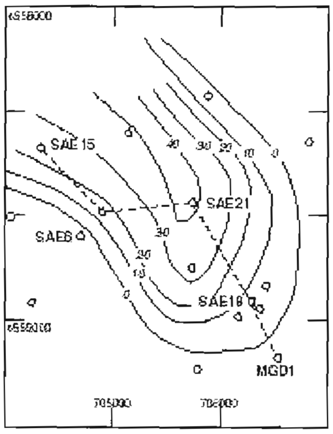

Cover Rocks

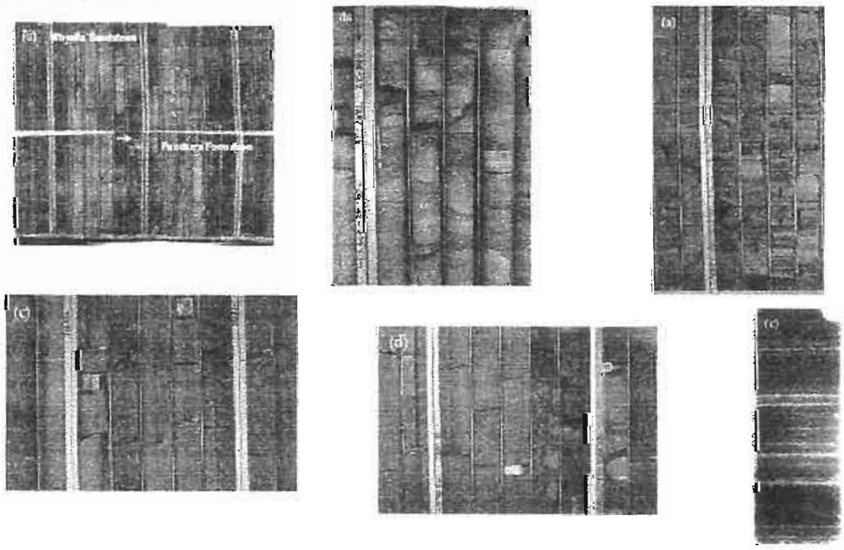

CODES SRC

Cu mineralisation in Cover Rocks

- Both Fe and Cu sulfides (py, cpy, bn, cc, dg)
- Fine grained in seams/beds
- Fine and coarse grained clots, patches and veins in siltstones & intraclasts bxs
- More visible Cu at upper and lower contacts of THF (confirmed by assays)

CODES SRC

Cu in Cover (con)

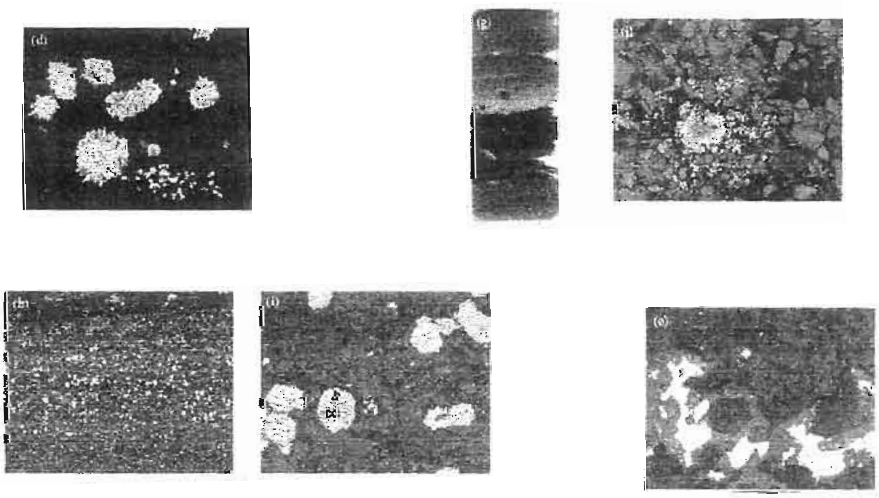

AMIRA P544 May 2002 ppt05.mcgoldrick

CODES SRC

Geochemistry of Cover Rocks

- 119 samples analysed for major & trace elements by XRF
- 5 holes 0 m to 40 m of THF
- Most samples were THF, but some WS and few PF
- Report contains series of downhole plots & box plots summarising the data

CODES SRC

Major Elements

- Some simple observations

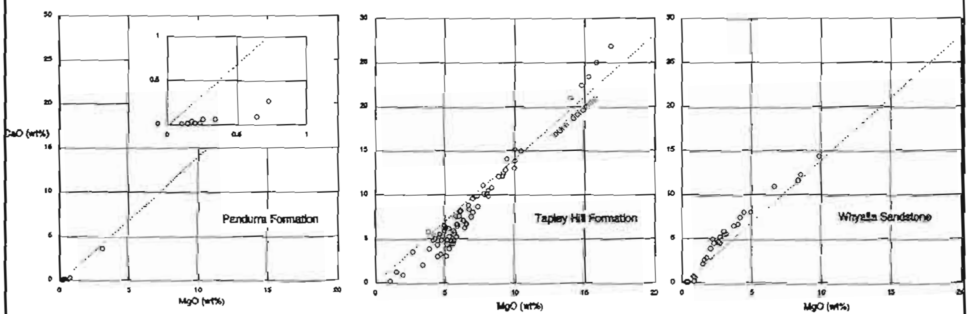

e.g., no carbonate in the PF cf THF & WS

Major Elements (con)

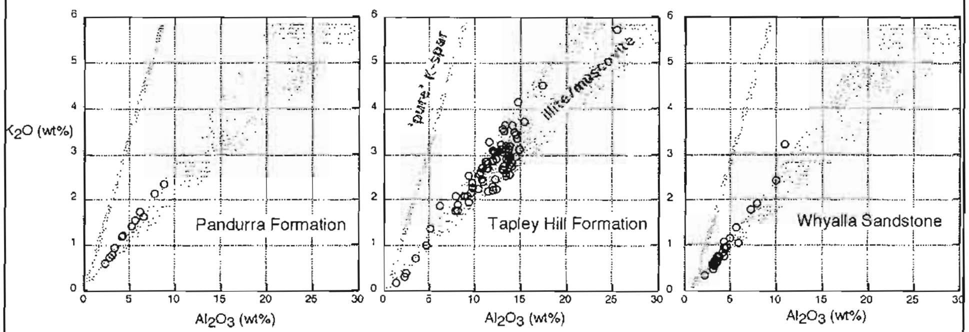

e.g., the sandy units are not arkoses & the THF contains more clay/muscovite than the PF & WS

Trace Elements

- The THF samples have elevated Cu, Co, Zn & Pb cf average black shale
- However, Ni, As, Bi, Mo & Tl are not elevated
- Cu appears decoupled from Zn & Pb (esp. in holes with the two thick THF intersections)

Trace Elements (con)

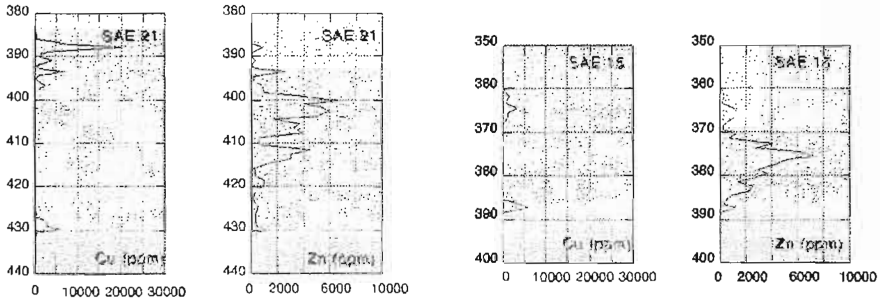

AMIRA P544 May 2002 ppt05.mcgoldrick

Trace Elements in Cover cf Fe-stones

- Cover rocks contain more Zn, Pb & Ag (possibly more Ni & V)
- Fe-stones are richer in Bi & W (& possibly U & Au)
- Other chalcophile elements (As, Tl & Mo) are similar in both

AMIRA P544 May 2002 ppt05.mcgoldrick

Trace Elements Differences: Genetic Implications

- consistent with a separate origin for each style of Cu mineralisation

BUT

- physico-chemical changes in an ore fluid ascending 600 m vertically might explain the differences e.g., cooling, boiling, mixing etc
- differences in metal trapping mechanisms might also be an explanation e.g., reaction with mte-py skarn cf carbonaceous siltstone

Formation of Emmie Bluff Cu deposits

3 possibilities

- Coincidence
- Fe-stone Cu is earlier, but remobilised to form cover Cu
- Both styles of Cu mineralisation formed during the same Neoproterozoic fluid flow event

What about isotopes — S
C/O
Pb ?
Sr ?

Coincidence

- Unlikely because of the association of both cover and basement mineralisation to regional scale features (e.g., lineaments, gravity highs) on the Stuart Shelf

AMIRA P544 May 2002 ppt05.mcgoldrick

Coincidence

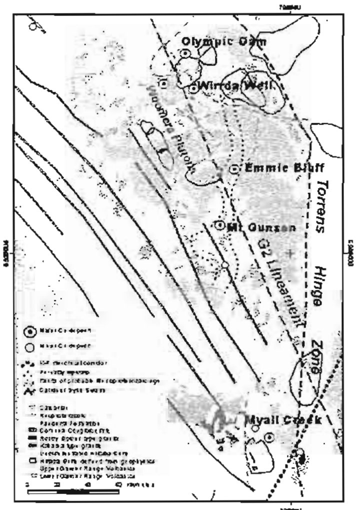

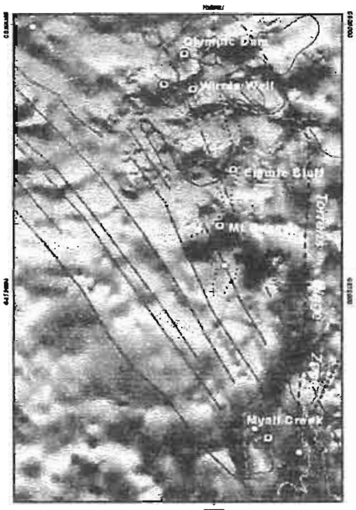

AMIRA P544 May 2002 ppt05.mcgoldrick

Remobilisation

- Gow et al. (1994) argued that the Emmie Bluff Fe-stone Cu had a similar origin to Olympic Dam

BUT

- EB Fe-stone Cu timing is not constrained (cf 1590 Ma for OD - Johnson & Cross, 1995)

Remobilisation

- In a remobilisation model fluids move through the old Fe-stone Cu mineralisation & dissolve Cu which later precipitates new Cu sulfides at the next reducing trap (e.g., THF carbonaceous siltstones)
- ? circulating groundwaters
- other fluid possibilities

Remobilisation

PROBLEMS

- where is the evidence that an oxidised fluid has affected the Fe-stone Cu (e.g., secondary Cu minerals) ?
- the Fe-stone Cu has low Zn&Pb; where does the Zn&Pb in the THF come from?
- could the deep Cu have been sheltered from deep circulating fluids for 1000 Ma ?

Single Fluid Model

- Both styles of Cu mineralisation form when a fluid flow (circulation) is established post-Whyalla sandstone times
- Warm to hot (up to a few hundred degrees) oxidised fluids flow through the Fe-stones and through (or around) the THF (for the THF Cu this is essentially the model of Knutson et al., 1983)
- This model is OK chemically for sulfate-dominant metal carrying fluids
- Both mte-py skarn and carbonaceous units will trap Cu
- Hotter fluids at depth explain Bi, W (&Au) in Fe-stone Cu ?

Single Fluid Model

Fluid Source

- **Intrabasinal ?**
- **Extrabasinal ?**

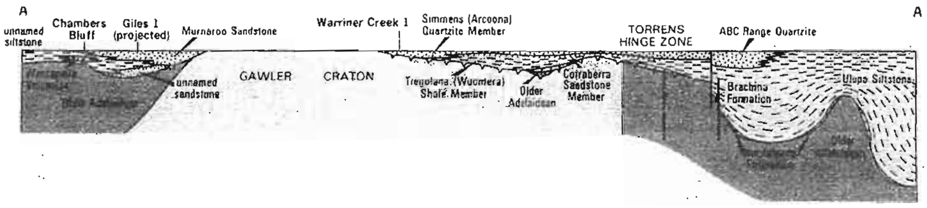

AMIRA P544 May 2002 ppt05.mcgoldrick

Single Fluid Model

Fluid Source (con)

- **If the Adelaide Fold Belt is an important fluid source, then hydraulic connectivity must be maintained onto the Stuart Shelf**
- **Only possible during highstands**
- **Hence the maximum age of Emmie Bluff Cu would be younger than the Marinoan glaciation (abt. 600 Ma)**

AMIRA P544 May 2002 ppt05.mcgoldrick

Single Fluid Model

Fluid Source (con)

- Recent Sr isotope work by Foden et al., (2001) shows that the AFB experienced a major fluid flow event at 586±30 Ma
- The same radiogenic Sr is recored in samples of THF from the Stuart Shelf (Lambert et al., 1984)
- Hence the Stuart Shelf may have experienced the same fluid flushing at abt. 600 Ma as the AFB

Implications for Vectors to Cu Ores

SPECULATION !

- If a major lateral fluid flow event out of the thick AFB sequences does form the Stuart Shelf Cu deposits, then basement structure and grain will exert a strong control on flow flow paths (& maybe chemistry); this would explain the empirical association between basement structures and Cu deposits

CODES SRC

Implications for Vectors to Cu Ores

SPECULATION (con.)

- **This type of non-focused fluid flow may produce cryptic pervasive alteration effects that are very difficult to recognise cf 'point source' type deposits**

WILD SPECULATION !!

- **Can Olympic Dam be explained this way?**

CODES SRC

Further Work

- Some additional analyses of THF carbonaceous siltstones from thicker sequences (AFB)
- Reconnaissance search for monazite and xenotime for direct dating mineralization or fluid flow event(s)
- Fluid flow modelling of one or two key transects through the AFB

Isotopes – S

Sr ← Should follow up with Sr isotopes on the carbonate-rich samples.

Zambia: Key Questions

Stratigraphy/Host Rocks

•What lithological/facies/provenance changes are present regionally - laterally & vertically?

•What is the sedimentary environment for the different sedimentary packages? (Can we develop facies models to help guide exploration?)

•What is the basement/Roan relationship?

•Were there thick evaporites (lacustrine and/or marine) in sequence? If so, where were they and did they move?

•Why are different lithologies (shale, siltstone, arkose, and carbonate) ore host?

Zambia: Key Questions (con)

Structure

- What is the broad structural framework of the Copperbelt?
- How much of the observed deformation is pre-lithification vs tectonic?
- Are there multiple deformation events or a single progressive deformation?
- Why is strain partitioned and what controls this?
- What is the style of deformation - flattening vs rotational?

Zambia: Key Questions (con)

Alteration

- What are the different alteration types (albitic, biotitic, carbonate) - what are their relative age relationships and stratigraphic distribution (including basement?)
- What is the age (and spatial) relationship of different alteration types to mineralisation? (Can alteration point to ore?)
- What is the difference between metasomatic alteration (eg. "grit") and metamorphism? (ie. the "biotite problem")
- Are some of the ore-hosting quartzites /arkoses (TFQ-Nchanga, Mufilira, and Chibuluma) intensely altered rocks?

Zambia: Key Questions (con)

Mineralisation

- What precipitates copper sulfides? (why is mineralisation in different lithologies?).
- What is (are) the age(s) of mineralisation? (pre- and post/syn-deformation?)
- What are the controls on barren gaps?
- What controls the distribution of cobalt?
- Where is the zinc?
- What is/are source(s) of Cu and S?
- Is the chalocite primary, secondary or both? If both, which is dominant?
- Fluids involved in mineralisation - T,P, salinity

Basin Architecture

- Basin evolution at the onset of Katangan sedimentation
  - basement-Roan relationships
  - architecture of the mineralised package
  - regional stress patterns
- Relationship of basin geometry to mineralisation
  - association of mineralisation with syn-rift faults/basement highs?
  - association of mineralisation with basin re-configuration?
  - implications of basin geometry for size and shape of fluid cells
- Expression of syn-rift architecture in Lufilian geometry
  - can variation in style and geometry of Lufilian folds aid in defining syn-rift structures?
  - do abrupt changes in metamorphic grade coincide with fundamental breaks between basin compartments?
  - does the Kafue Anticline separate major basin compartments?

Presentations

- Deposit-scale studies at Chibuluma West, Mufulira, Ndola West, Nkana & Konkola
  - shapes of the containers
  - evolution of basement highs
  - facies architecture
  - basin re-configuration
  - distribution of mineralisation

Chibuluma West

- Deposits at periphery of "basin"
- Chibuluma system within condensed southern margin
- "footwall" hosted system
- Does fold interference pattern reflect superposition of Lufilian shortening on rift architecture?

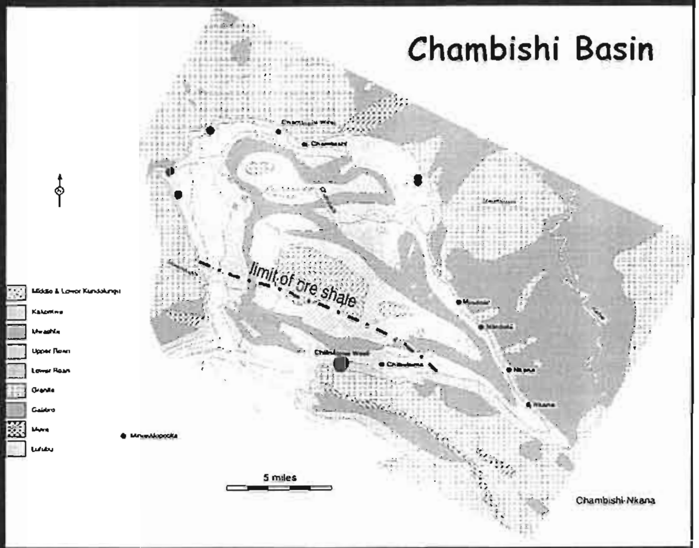

Why Chibuluma West?

- Anomalous in terms of Cu-belt deposits
  - relatively small + high grade
  - coarse-grained sulfide textures
- Clear basement topography
  - pronounced basement highs
  - marked thickness variation in the host sequence
- Tectonic folds appear locally oblique to overall structural grain
  - is it possible to separate structures related to rifting from those formed during inversion?

Methods

- Data derived largely from surface collared and underground drill logs
  - constrain thickness and facies variation in the Lower Roan
  - re-interpret drill sections to build "3-D" geometry of structural architecture
  - sections restored to the level of the hangingwall
  - plans produced at 200, 400 & 600m levels
- Logged 8 surface collared holes from the western end of the deposit
  - thickness and facies variation was pronounced
- Minor underground mapping

Stratigraphy of the Lower Roan

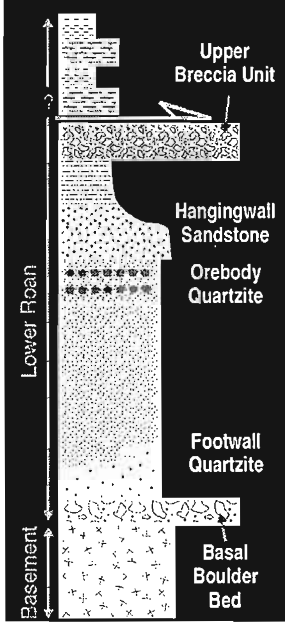

Basement

- biotite granite
  - generally weakly deformed
  - local mylonitic shear zones (mineralised)

Lower Roan

- basal unconformity generally well preserved: minor strain/alteration
- Basal siliciclastic package
  - = Nkana Footwall Sequence
- Upper mixed argillite-carbonate succession
- ubiquitous strain at contact of upper and low packages
  - shear fabrics
  - asymmetric folds

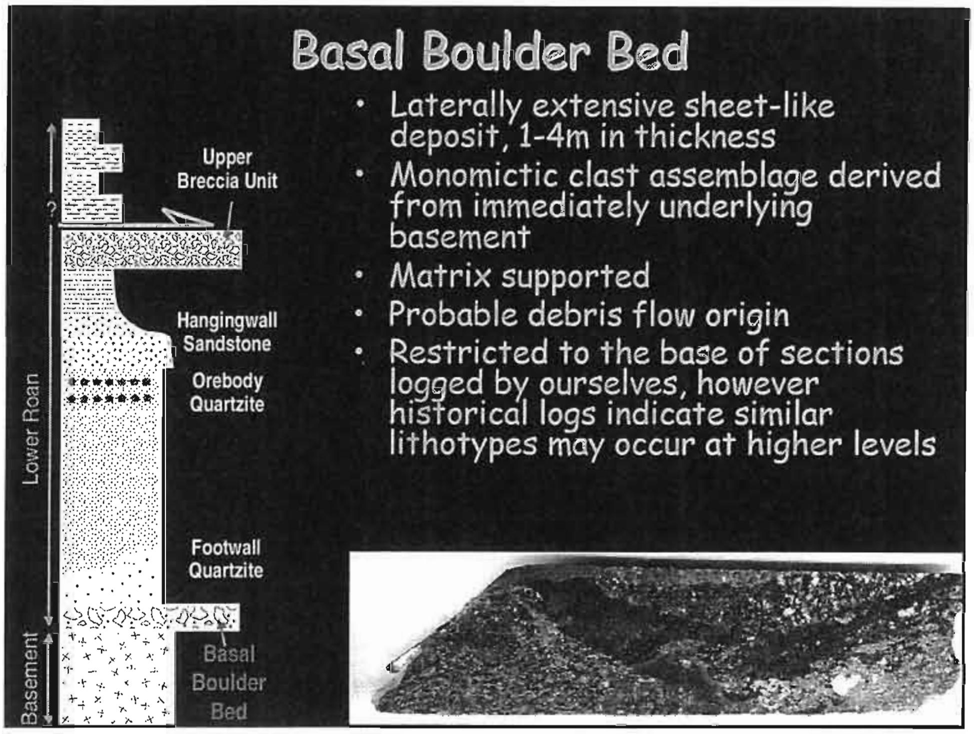
Basal Boulder Bed
• Laterally extensive sheet-like deposit, 1-4m in thickness
• Monomictic clast assemblage derived from immediately underlying basement
• Matrix supported
• Probable debris flow origin
• Restricted to the base of sections logged by ourselves, however historical logs indicate similar lithotypes may occur at higher levels
Upper Breccia Unit
Hangingwall Sandstone
Orebody Quartzite
Footwall Quartzite
Basal Boulder Bed
Lower Roan
Basement

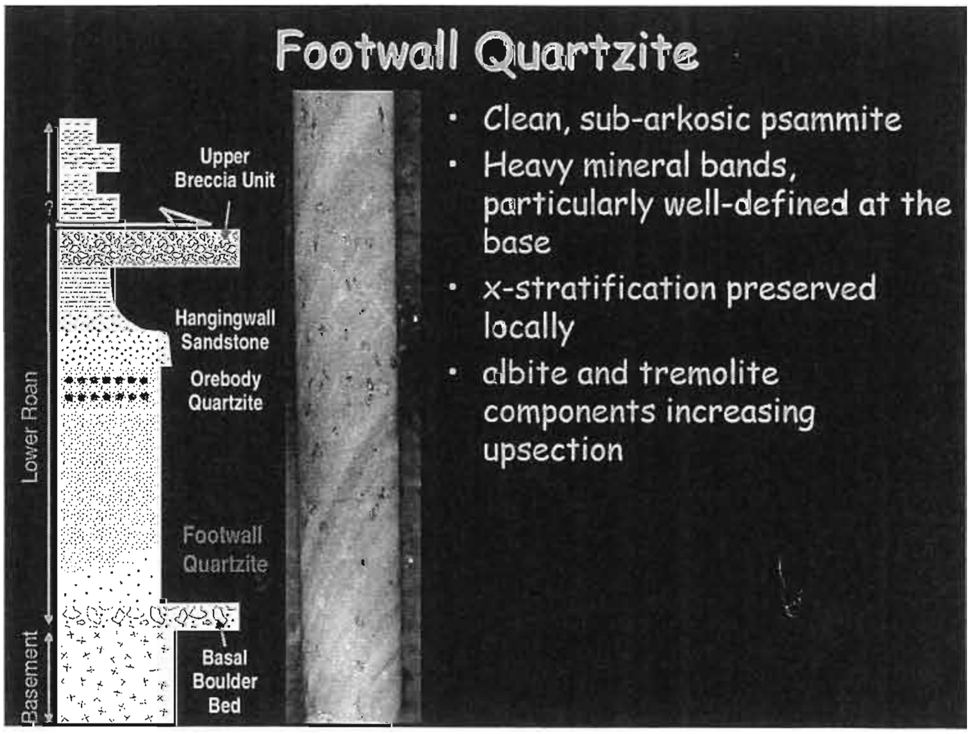
Footwall Quartzite
• Clean, sub-arkosic psammite
• Heavy mineral bands, particularly well-defined at the base
• x-stratification preserved locally
• albite and tremolite components increasing upsection
Upper Breccia Unit
Hangingwall Sandstone
Orebody Quartzite
Footwall Quartzite
Basal Boulder Bed
Lower Roan
Basement

Footwall Quartzite (cont.)

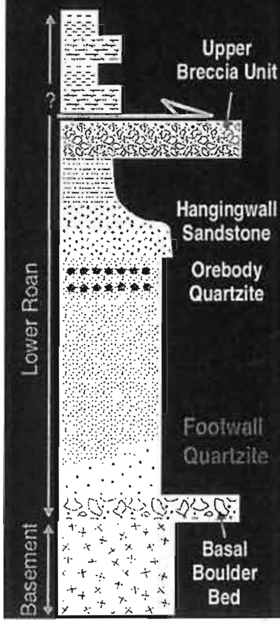

- intensely recrystallised
  - "glassy" appearance in core
  - interlocking grain margins in thin section
- basal few metres characterised by interstitial calcite-tourmaline

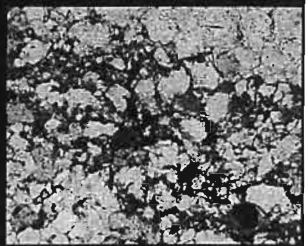

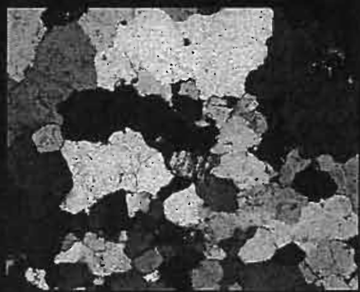

Orebody Quartzite

- No obvious primary compositional or facies distinction from the Footwall Quartzite
- Defined by the presence of sulfides
- Increased albite and tremolite component
- Textural destruction at the core-scale
- Primary layering defined by relict heavy mineral bands, stratiform sulfide & albite accumulations

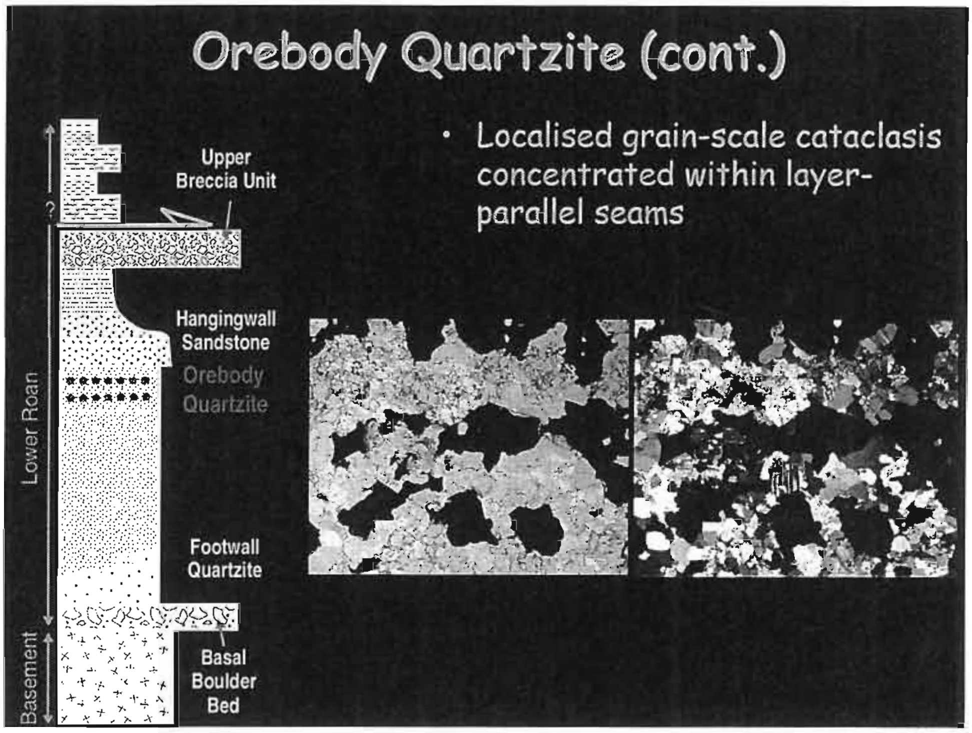
Orebody Quartzite (cont.)
• Localised grain-scale cataclasis concentrated within layer-parallel seams
Upper Breccia Unit
Hangingwall Sandstone
Orebody Quartzite
Footwall Quartzite
Basal Boulder Bed
Lower Roan
Basement
?

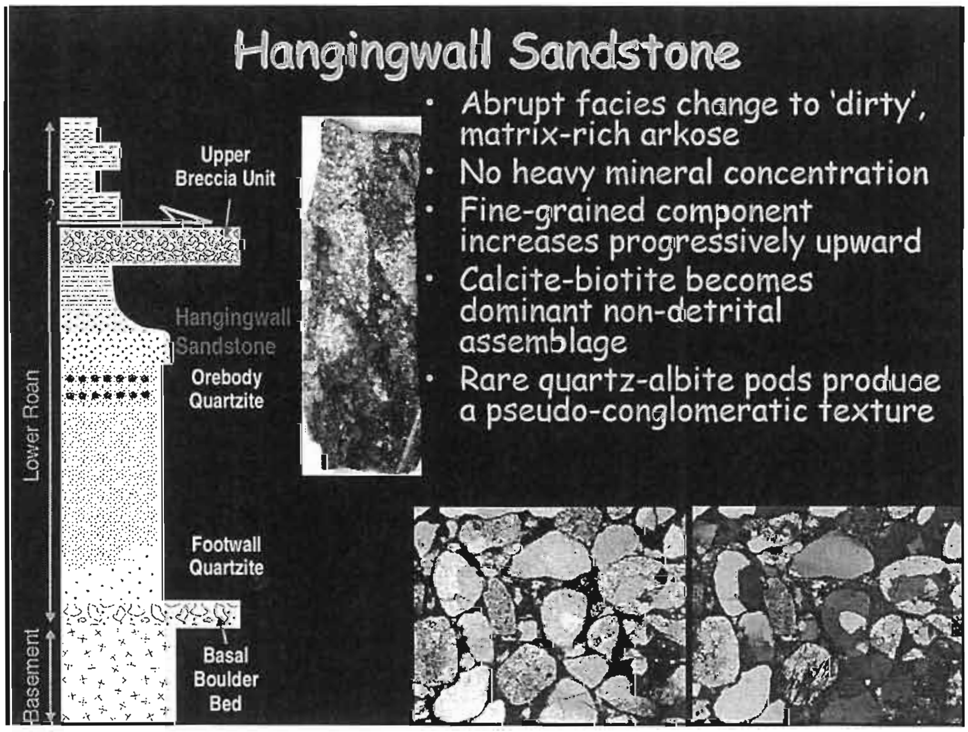
Hangingwall Sandstone
• Abrupt facies change to 'dirty', matrix-rich arkose
• No heavy mineral concentration
• Fine-grained component increases progressively upward
• Calcite-biotite becomes dominant non-detrital assemblage
• Rare quartz-albite pods produce a pseudo-conglomeratic texture
Upper Breccia Unit
Hangingwall Sandstone
Orebody Quartzite
Footwall Quartzite
Basal Boulder Bed
Lower Roan
Basement
?

Upper Breccia Unit

- Thicker than Basal Boulder Bed (>75m), but very restricted in distribution
- Pervasive textural destruction via talc-phlogopite-albite + retrograde chlorite-calcite alteration
- Shear bands common
- Rare preservation of convincing clastic texture
- Similar to breccia unit at base of Mwashia

Upper Breccia Unit (cont.)

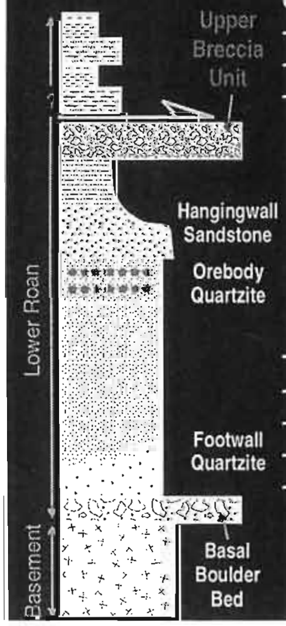

Clast Types
- heavy minaral rich sandstone
- no obvious granitic input
- enigmatic igneous textures

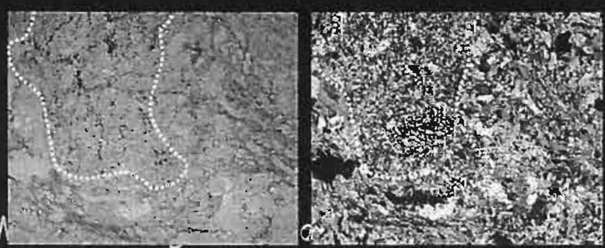

- M [illegible]
- minor evidence for *in situ* fragmentation
- clast types are inconsistent with enclosing lithotypes
- well-rounded habit of some clasts
- sedimentary fragmentation most likely - reworking of lower stratigraphic levals

Upper Mixed Dolomite-Argillite

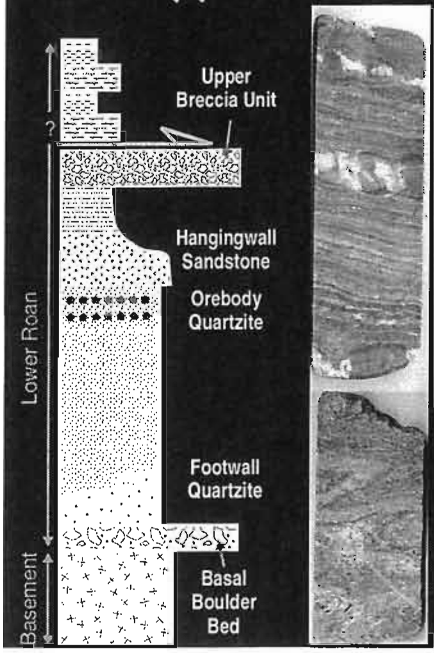

- abrupt cessation of coarse clastic input
- possibly reflecting a change in basin configuration
- chloritised, dolomitic shales and siltstones
- increased strain relative to underlying siliciclastic package
  - ubiquitous shearing at lower contact
  - significant layer-parallel shear/attenuation
  - decollement surface between upper and lower packages

Basin Architecture

- Lower siliciclastic package is contained within the cores of three WNW-trending synclines
- basement inliers separate synclinal closures
- fold wavelength decreases progressively WNW, where structures die out against a NNW-trending basement ridge

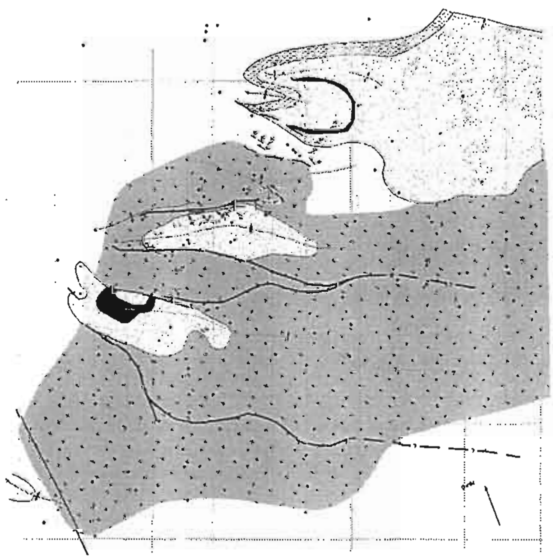

Basin Architecture

- Lower siliciclastic package is contained within the cores of three WNW-trending synclines
- basement inliers separate synclinal closures
- fold wavelength decreases progressively WNW, where structures die out against a NNW-trending basement ridge

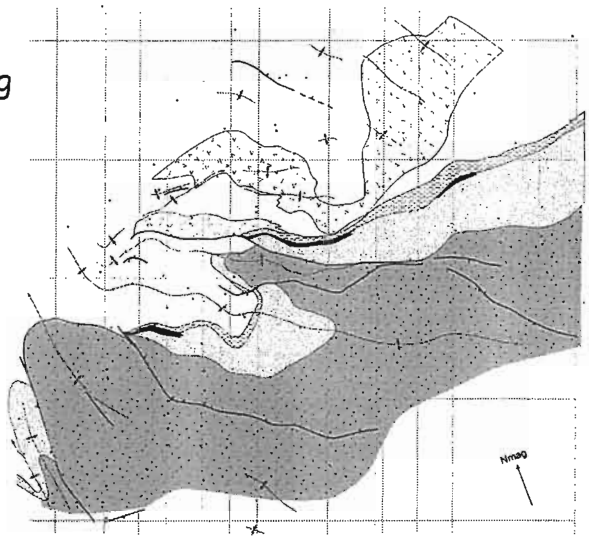

Basin Architecture

- Lower siliciclastic package is contained within the cores of three WNW-trending synclines
- basement inliers separate synclinal closures
- fold wavelength decreases progressively WNW, where structures die out against a NNW-trending basement ridge

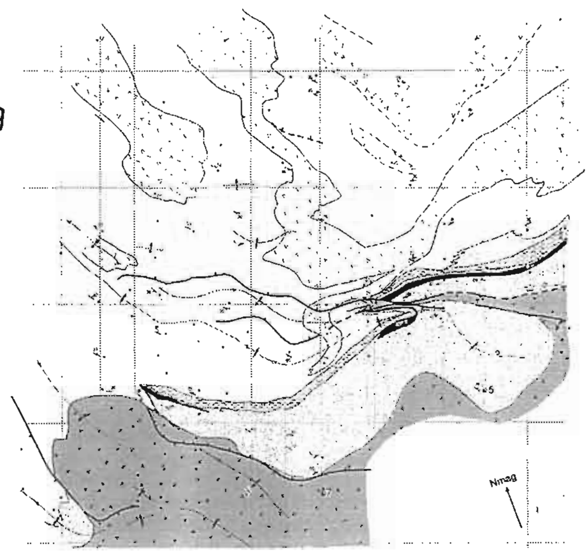

Isopachs of Lower Siliciclastics

- Thickness variation reveals a series of discrete sub-basins:
  - N thickening ramp to NE
  - pinch outs onto WNW-trending basement highs in central zone
  - pinch out onto NNW-trending basement ridge to W

Isopachs vs Fold Geometry

- Isopach trends mirror fold geometry
  - thickness maxima displaced from fold axial traces
- Structural geometry is inherited from basin topography

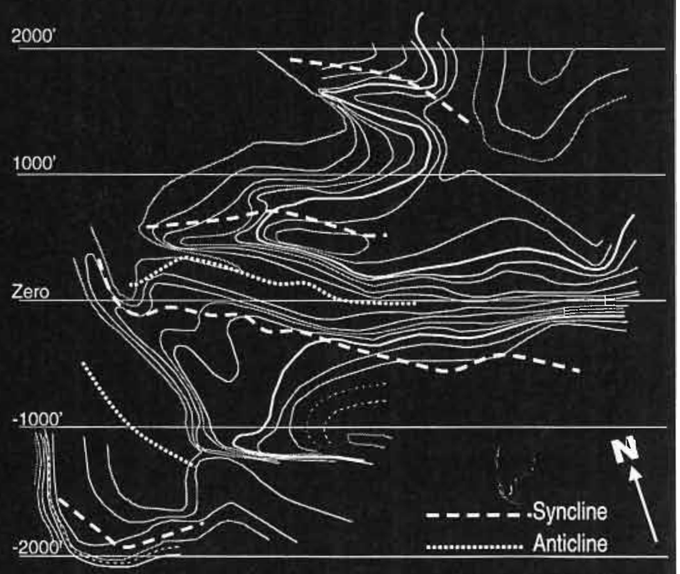

Isopachs vs Fold Geometry (cont.)

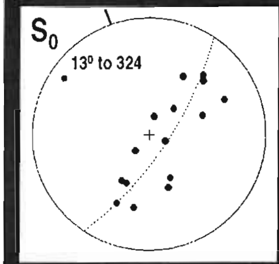

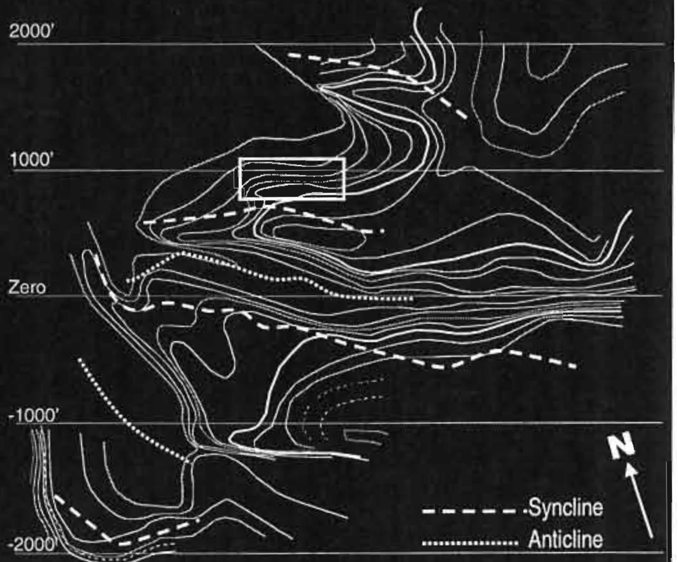

- Minor low wavelength folds trend obliquely to main synclines
- do these reflect far field stresses?

Basin Growth

- How is accommodation space generated?
- Two end-member scenarios:
  1) incision of emergent granitic terrain
    - canyon systems cut into basement at uplifted basin periphery
    - no direct structural control on accommodation space
    - depocentres generated at the onset of sedimentation

  2) active basin subsidence and adjacent basement uplift
    - fault-controlled architecture
    - basin geometry evolved with sedimentation

Canyonised System

- Although geologically viable, internal facies architecture of the lower siliciclastic package indicates that basement "highs" amplified during sedimentation
  - sequences draping basement "highs" are *condensed*, yet *complete*

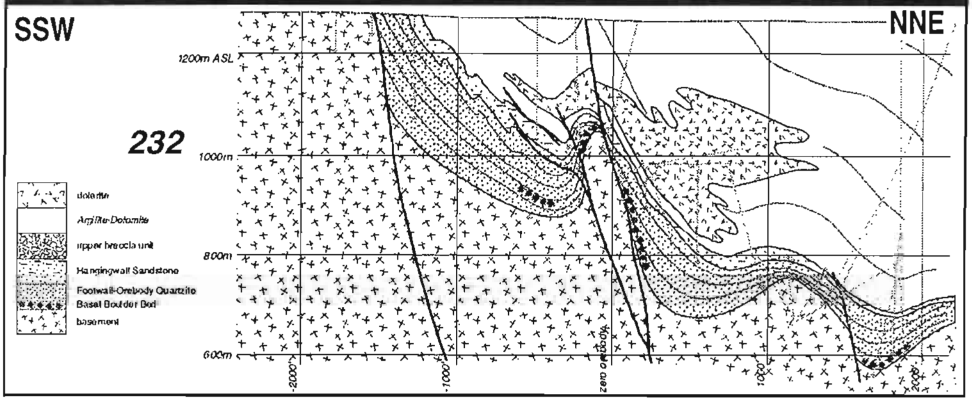

Rift Architecture

- Constraining fault architecture
  - obscured by inversion
  - fault architecture inferred largely from facies architecture
  - limited control on fault geometry at depth
- Preferred model = NNE-dipping half-graben system

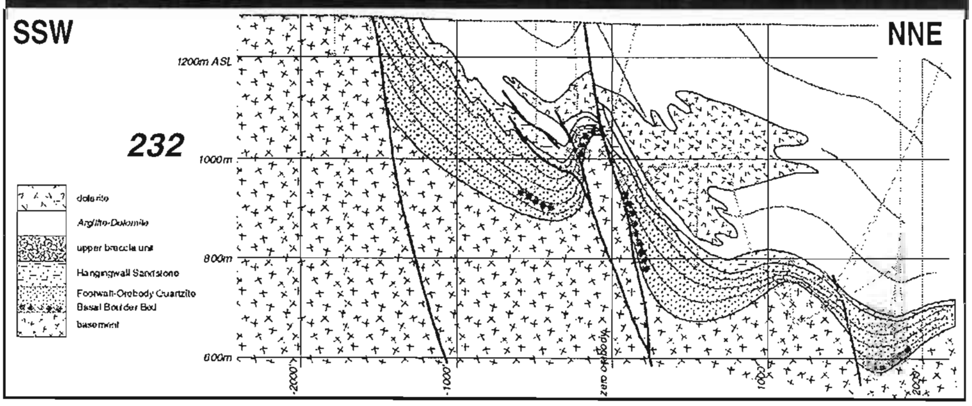

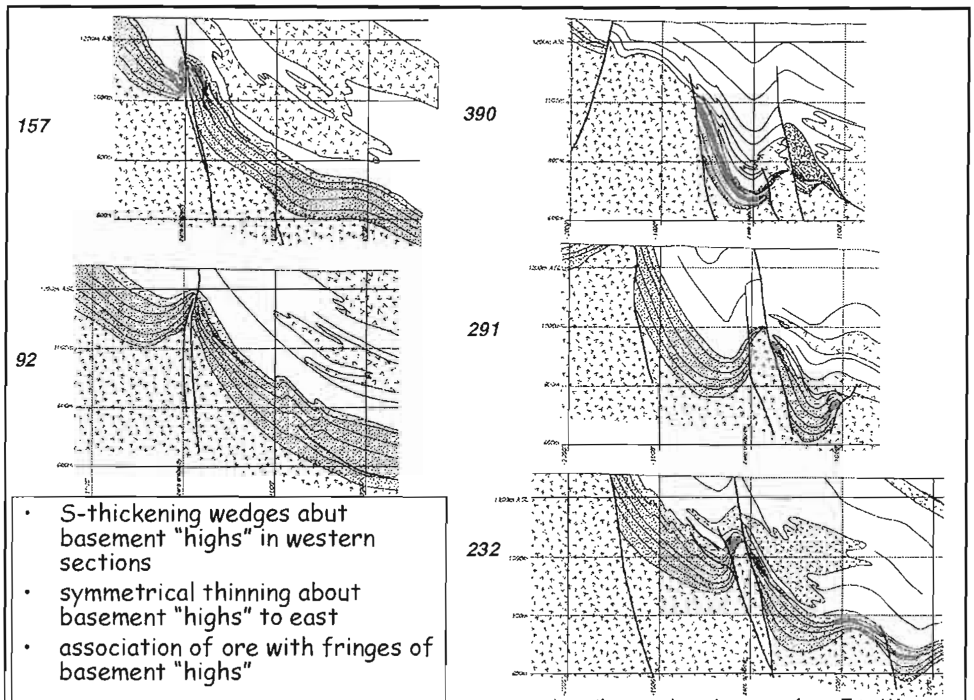

- S-thickening wedges abut basement "highs" in western sections
- symmetrical thinning about basement "highs" to east
- association of ore with fringes of basement "highs"

* section numbers increase from E to W

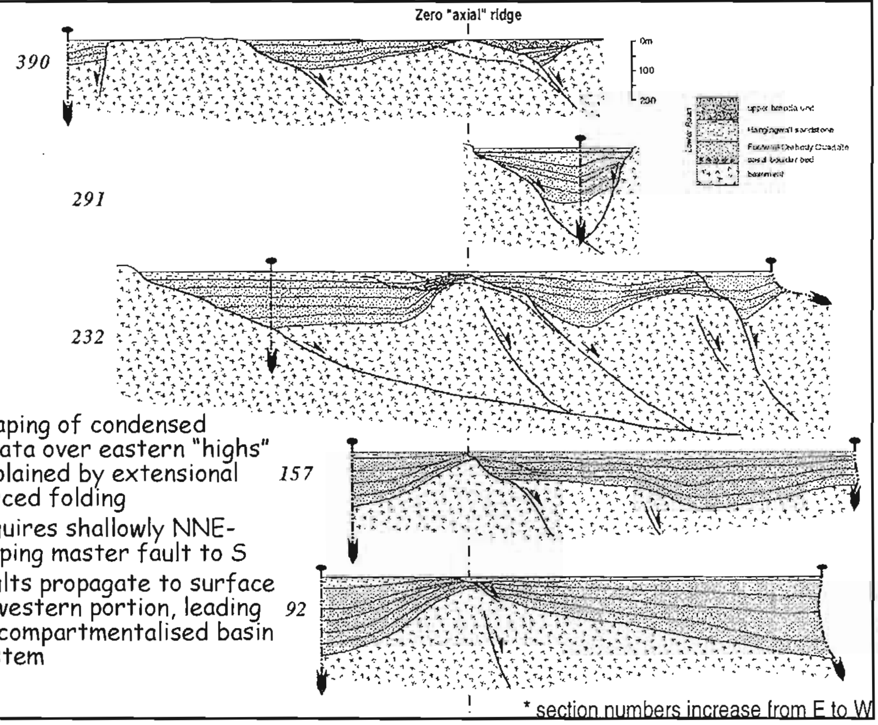

- Draping of condensed strata over eastern "highs" explained by extensional forced folding
- requires shallowly NNE-dipping master fault to S
- faults propagate to surface in western portion, leading to compartmentalised basin system

* section numbers increase from E to W

Upper Breccia Unit

- Largely restricted to the western end of the basin system
- Late-stage emergence of the NNW trending ridge
  - reworking of lower stratigraphic levels
- Possible transfer system, linking discontinuous growth fault arrays

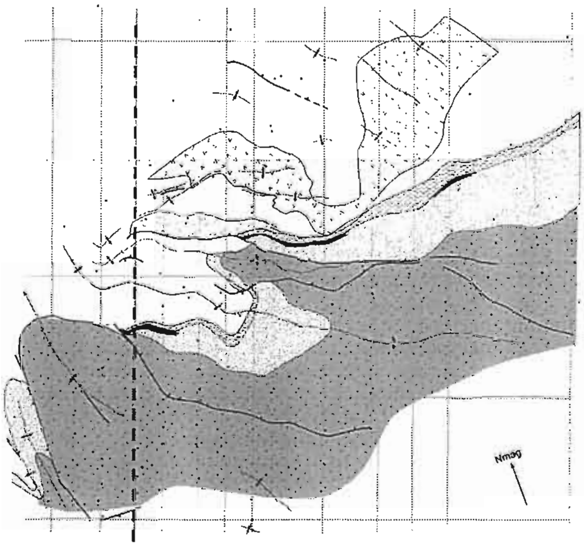

Conclusions

- Basal Roan sedimentation is recorded by a broadly upward fining siliciclastic cycle
  - compartmentalised basin system
- Vertical facies architecture reflects probable transition to shallow marine conditions and flooding of local source areas
- Cessation of coarse clastic input occurs a short distance above the host sequence - Upper mixed argillite-dolomite package
  - transgresses intra-basinal basement "highs"
  - increased shear strains & decollement surface at the base of the package
  - records a fundamental basin reconfiguration
  - possibly coeval with typical ore shale deposition at a regional scale

Conclusions (cont.)

- Basin configuration is best explained in terms of an evolving ESE-trending half graben system

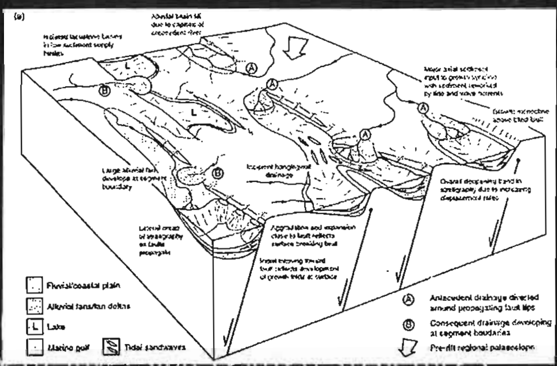

- Original ... the geometry
  - fold traces mimic trends of depocentres
  - regional fold geometry (deduced from geophysics) may be used to delineate major basin-bounding structures

Pre OR stale

Basement - Roan Relations at Mufulira

Robert Scott
Centre for Ore Deposit Research
University of Tasmania

Introduction

- Mufulira largest Copperbelt deposit NE of Kafue anticline
- mine sequence generally dips ~45°NE
- 30—80m thick Ore Formation within the Lower Roan Group consists of variably argillaceous quartzite and arkose, interbedded with lesser shale and dolomite
- thickness of the Lower Roan below the Ore Formation is highly variable (0—180m) reflecting basement topography during initial stages of basin development (Brandt et al., 1961)

Location

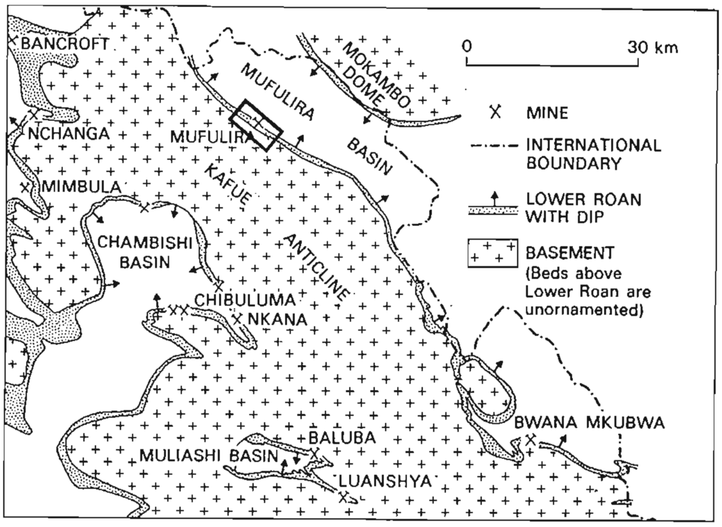

Basement - Roan Relations at Mufulira

- nature of the basement — Roan contact at Mufulira
- origin and evolution of basement topography
  - controls on basin development
  - significance w.r.t. timing and distribution of copper mineralisation
  - localisation of post-Katangan deformation
- extent and significance of internal deformation within basement and Lower Roan and implications for timing and distribution of copper mineralisation

Approach

- underground mapping and sampling (petrological and microstructural examination) along basement contact on 1140' and 1240' Levels
- restored isopach maps of the Footwall and C-Orebody (Ore Formation) constructed from mine sections

Mufulira long-section

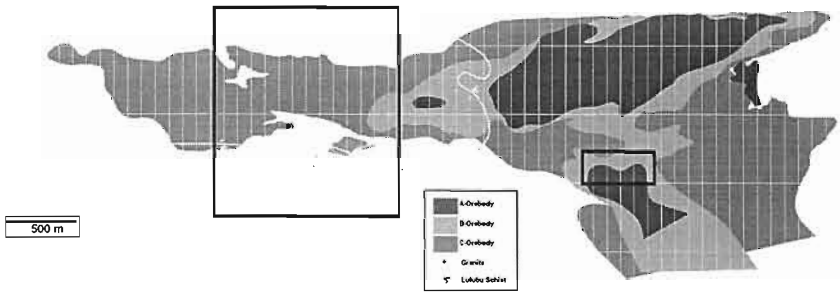

Basement highs (not shown) define 3 sub-basins
Areas of isopach map and underground mapping outlined

Mufulira: cross-section & stratigraphy

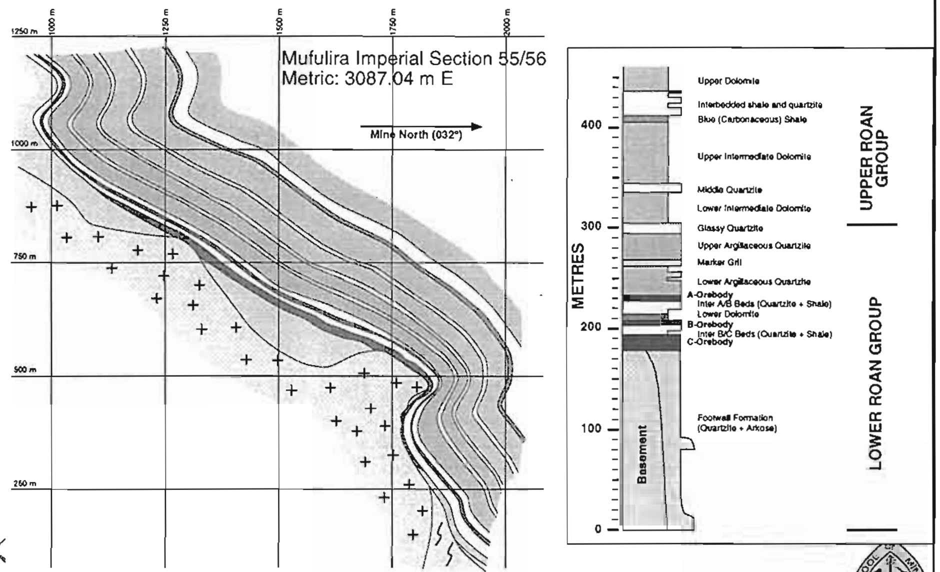

CODES SRC

SCHOOL OF MINES 1874 COLORADO

Basement contact

- despite representing a break of ~1000 m.y., the basement-Roan contact is subtle in areas where the Lufubu Schist forms basement and
  - a basal conglomerate is not present in the Lower Roan
  - Footwall (or Ore) formations are massive (unstratified) where they abut basement

CODES SRC

SCHOOL OF MINES 1874 COLORADO

Basement contact

- subtle nature of the contact in areas of Lufubu Schist reflects
  - lack of true schistosity in the basement (predominantly felted mass of fine to medium grained white mica, with lesser interstitial quartz and biotite)
  - the "schist" has a similar grainsize to the overlying quartzite and arkose
  - recrystallisation of basal Roan successions, obscuring evidence of stratification and clastic character

Basement contact

Basement Contact

- characteristic cross-hatch pattern of muscovite in Lufubu Schist (decussate texture) interpreted to reflect static growth of micas originally aligned parallel to S2 and (crenulated) S1 foliations in basement
- relict foliations in Lufubu Schist are truncated at the basement contact and pre-date Katangan sedimentation
- however, static growth of basement micas (forming decussate texture) post-dates deposition of Lower Roan

Nature of the basal Roan contact

- Exact angular relationship between Lower Roan strata and the basement contact is uncertain. However:
  - no intensification of brittle or ductile fabrics towards the contact (in areas visited) ⇒ sedimentary contact
  - except for minor clasts of Lufubu Schist in the Lower Roan, immediately adjacent to the basal contact, Footwall Formation derived from granitic source, not underlying Lufubu Schist
  - although masked by later metamorphism, the apparent preservation of tectonic fabrics in the Lufubu Schist within cms of the Roan contact, suggests basement was not deeply weathered, and may have been exhumed shortly before Katangan sedimentation began

Origin and evolution of basement topography: Isopach Maps

- remove effects of post-Katangan deformation ⇒ basement topography at Ore Formation time
- use "original" basement topography to assess possible structural controls basin development
- determine extent and thickness of C-Orebody in relation to "original" basin topography

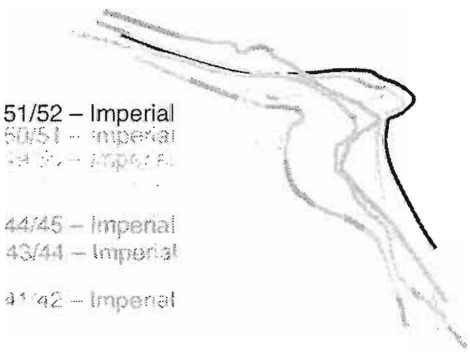

Geometry of basal contact across "basement high"

CODES / CSM AMIRA PROJECT P544 — MAY MEETING, 2002

Unfolding mine sections

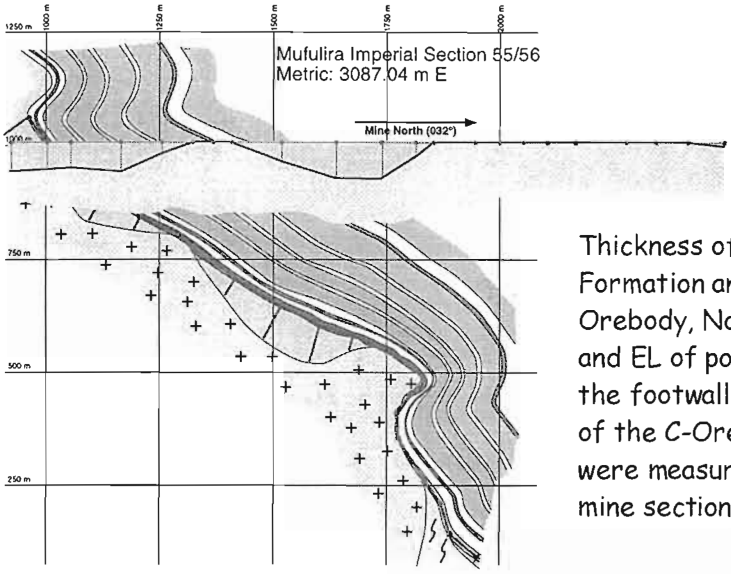

Thickness of Footwall Formation and C-Orebody, Northing and EL of points along the footwall contact of the C-Orebody were measured from mine sections

CODES SRC

CODES / CSM AMIRA PROJECT P544 — MAY MEETING, 2002

Construction of isopach maps

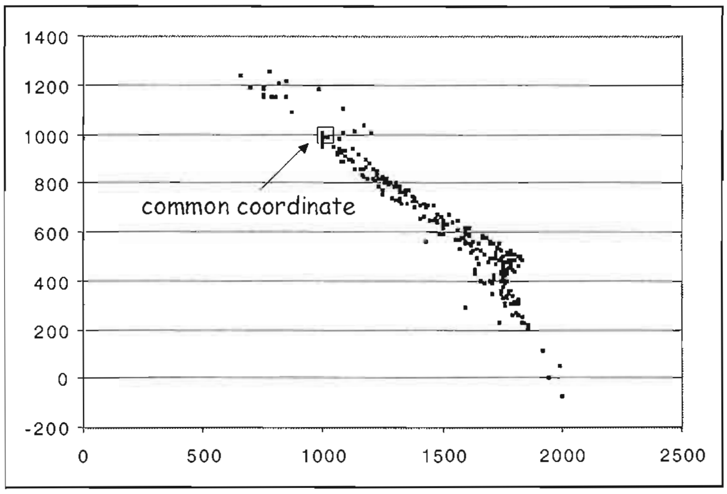

CODES SRC

CODES / CSM AMIRA PROJECT P544 — MAY MEETING, 2002

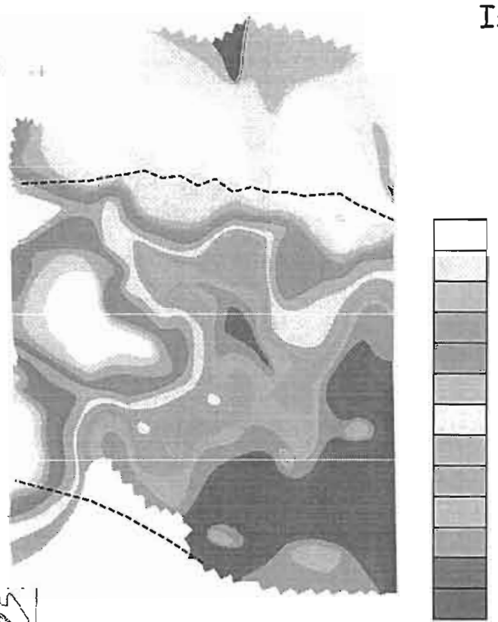

Isopach map: Footwall Fmn (Central Sub-basin)

- no systematic basin asymmetry indicated
- E- and SE-trending structural grain suggested by basement topography
- "ridge crest" localised along southern margin of SE-trending basement high

CODES SRC

CODES / CSM AMIRA PROJECT P544 — MAY MEETING, 2002

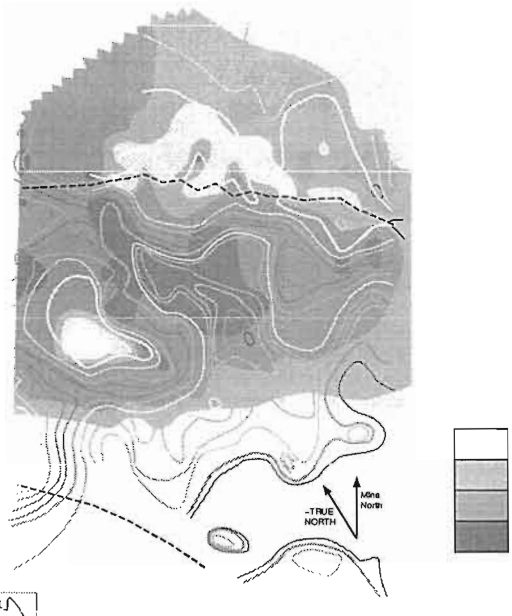

Isopach maps: Footwall Fmn & C-OB

- thickness variations in C-Orebody reflect original basin topography, but horizon is continuous across irreg. basement topography

CODES SRC

CODES / CSM AMIRA PROJECT P544 — MAY MEETING, 2002

Models for basement topography

- Three end-member models for development of basement topography at Mufulira

  (1) entirely predates deposition of Lower Roan

  (2) development roughly synchronous with deposition of Footwall Formation

  (3) basement topography due to domino-style rotational normal faulting following deposition of Footwall Formation and peneplanation prior to deposition of Ore Formation

Timing and origin of basement topography

- Individual units within Footwall Formation not correlated from one sub-basin to the next
- Ore Formation (and stratigraphically higher units) conformably overlie Footwall Formation and continuous across the tops of the palaeohighs
- Deposition of Ore Formation:
  - followed burial of original basin topography by Footwall Fmn.
  - coincided with change from series of small restricted basins, to more extensive basin with limits outside the Mufulira area

Development of basement topography

- Development of basement topography *entirely* predates deposition of the Footwall Formation:
  - basal contact should be unconformity everywhere (although margins of some palaeohighs may be eroded fault scarps)
- Development of basement topography synchronous with deposition of Footwall Fmn
  - stratigraphic relations / facies distribution depend on relative rates of faulting and sedimentation
  - expect some basement-Roan contacts to be faulted
  - strong structural control to sub-basin geometry

Evidence for structural control on sub-basin geometry?

- No faulted margins to basement highs identified in u'ground mapping *support* prior development of basement topography, but not conclusive due to limited study area
- Annels (1979): locally shear zones in basement granite parallel dominant NE-SW topographic trend, and continue into the Lower Roan, extending as far as C-Orebody
- Localisation of contractional strain along apparently steeper margins of basement highs consistent with reactivation of syn-depositional faults

Timing and origin of basement topography

- Although C-Orebody continuous across underlying irregular basement topography, thickness variations in part reflect those in the Footwall Fmn, suggesting continued minor subsidence across steeper margins of basement highs
- Overall relations interpreted to reflect deposition of Footwall Fmn. in series of actively-forming, NW-trending half-graben.
- However, evidence is less conclusive than Chibuluma West. *Initial* development of basement topography at Mufulira predates deposition of the Lower Roan Group.

Basin evolution & copper mineralisation

- If deposition of the host sequence followed a major change in internal basin geometry, did evolution of basin topography control/influence the development and distribution of copper mineralisation, and if so how?

CODES SRC

CODES / CSM AMIRA PROJECT P544 — MAY MEETING, 2002

SCHOOL OF MINES 1874 COLORADO

Basement-Roan relations: Ndola West

Robert Scott

Centre for Ore Deposit Research
University of Tasmania

Introduction

- Ndola West Prospect 3-6 km WNW of Ndola township
- NE flank of the Kafue anticline
- Study based on logging and sampling of four diamond holes, drilled by ZamAnglo in 2000 to test copper mineralisation in the Lower Roan

Location & Regional Geology

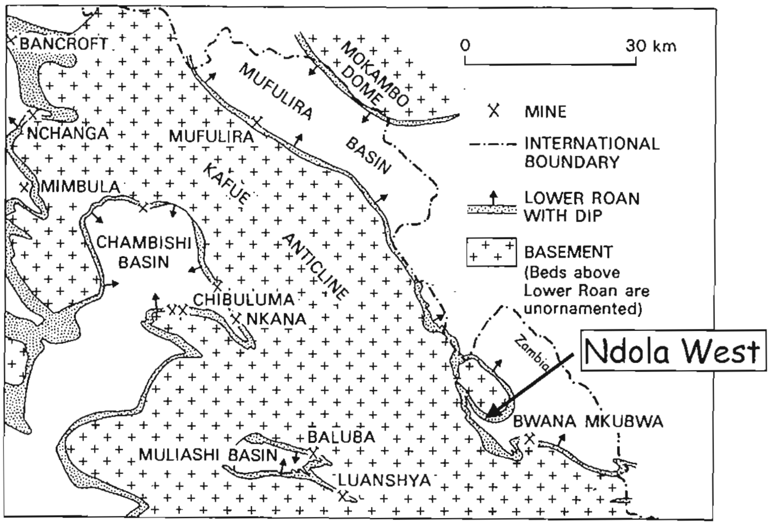

CODES / CSM AMIRA PROJECT P544 — MAY MEETING, 2002

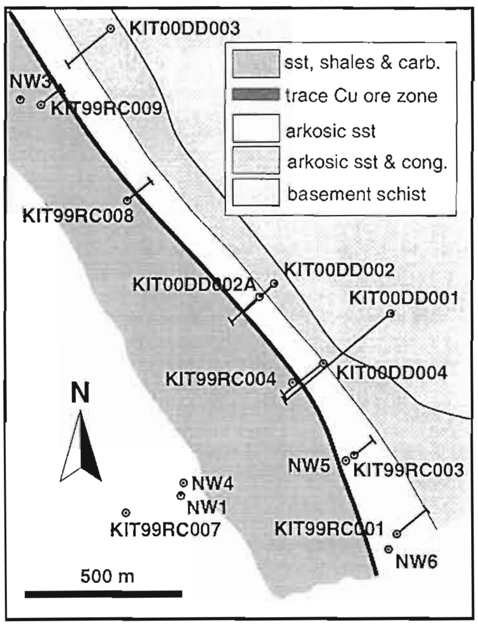

Location of drill holes - surface geology

Detailed stratigraphic and structural logging of Ndola West drillholes:

KIT00DD001 (730 m)
KIT00DD004 (300 m)
DD004 Def 1 (56 m)
DD004 Def 2 (58.5 m)

CODES / CSM AMIRA PROJECT P544 — MAY MEETING, 2002

Basement-Roan Relations: Ndola West

- Aim of presentation:
  - document structural relations across Basement-Roan contact in drill hole KIT00DD001

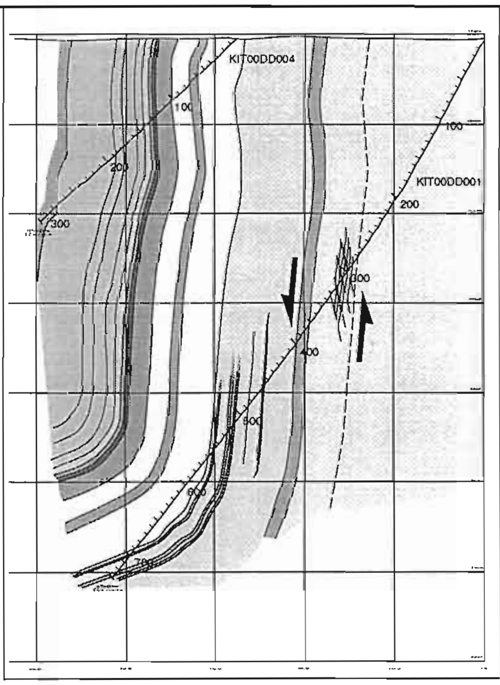

Geological section

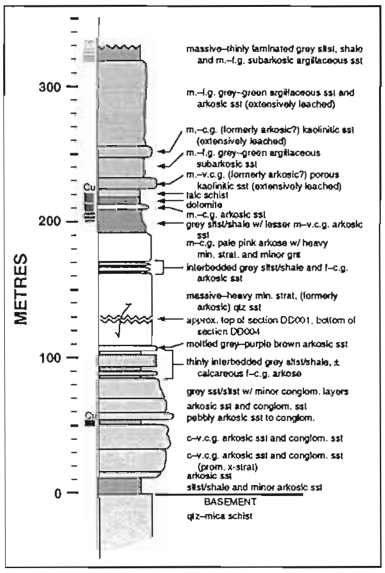

Basement: Ndola West

- qtz-mica schist (psammitic to psammopelitic precursor):
  - qtz+fsp (ksp+plag)+musc (ser) ± chl, bio, carb
  - accessory: FeTi-oxides (magn.), tourm., zircon

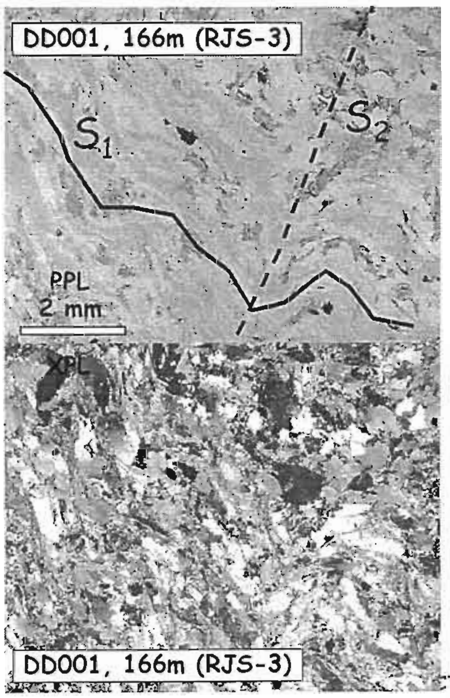

foliation development in the basement

- 2 widely developed fabrics
  - S_1, poorly preserved differentiated schistosity
  - S_2, poorly developed crenulation to strongly developed schistosity

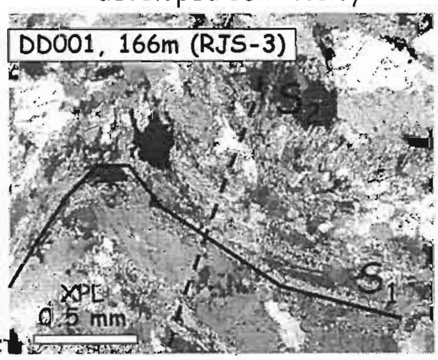

S_2 fabric development

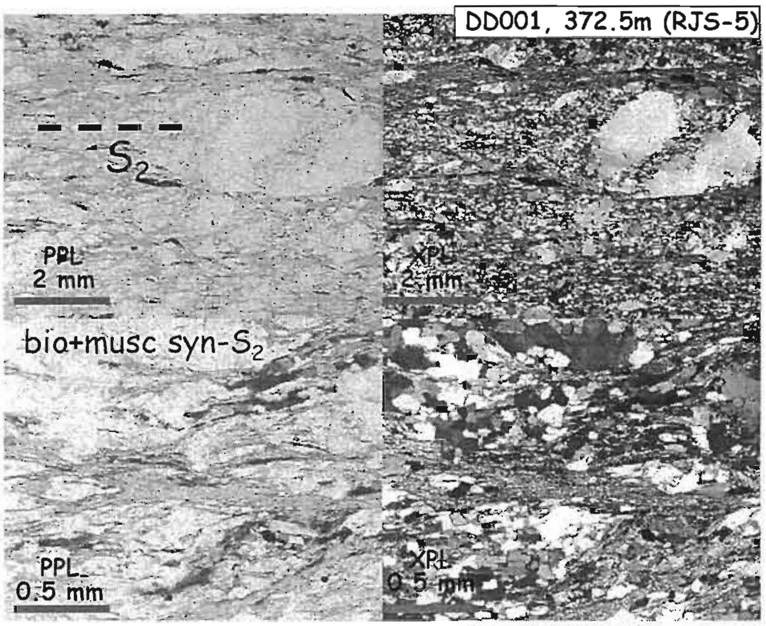

Basement high-strain zone

S2 intensifies towards the basal contact of the Lower Roan

E-block (basement) up

within 50 m of the basal contact shear fabrics are well developed

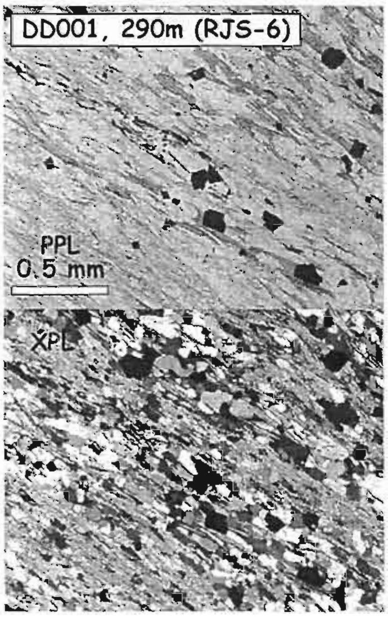

Structural relations: basal Roan

DD001, 396m (RJS-15)

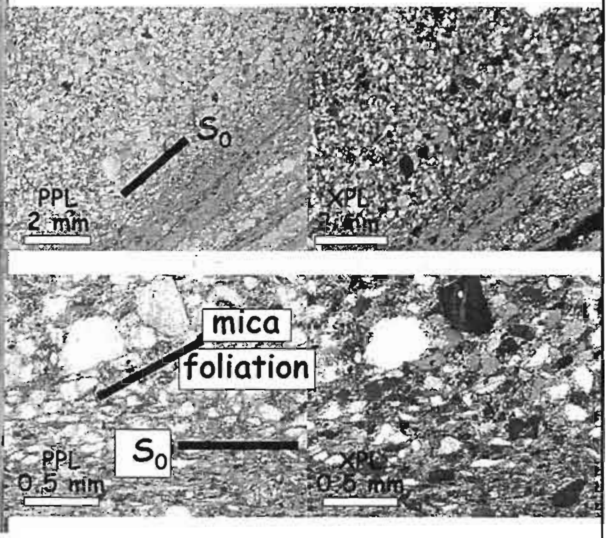

Layer parallel fabric (S_1) in Lower Roan

- variably developed throughout lower Roan
- generally pervasively developed in pelites
- weak to strong alignment of interstitial micas (±carbonate) in psammites

DD004 Def2, 124.5m

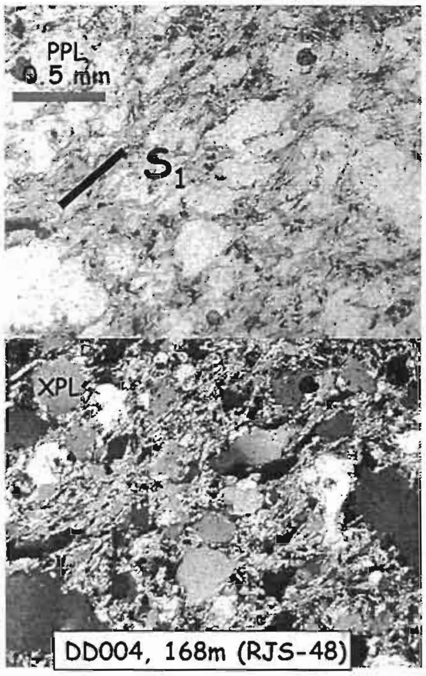

DD004, 168m (RJS-48)

Crenulation (S_2) in Lower Roan

- locally bedding and S_1 folded around asymmetric folds and microfolds
- folds rarely associated with development of a discrete cleavage
- asymmetry of folds consistent with large-scale synform, and interpreted to be same generation

Fabric relations in the Lower Roan

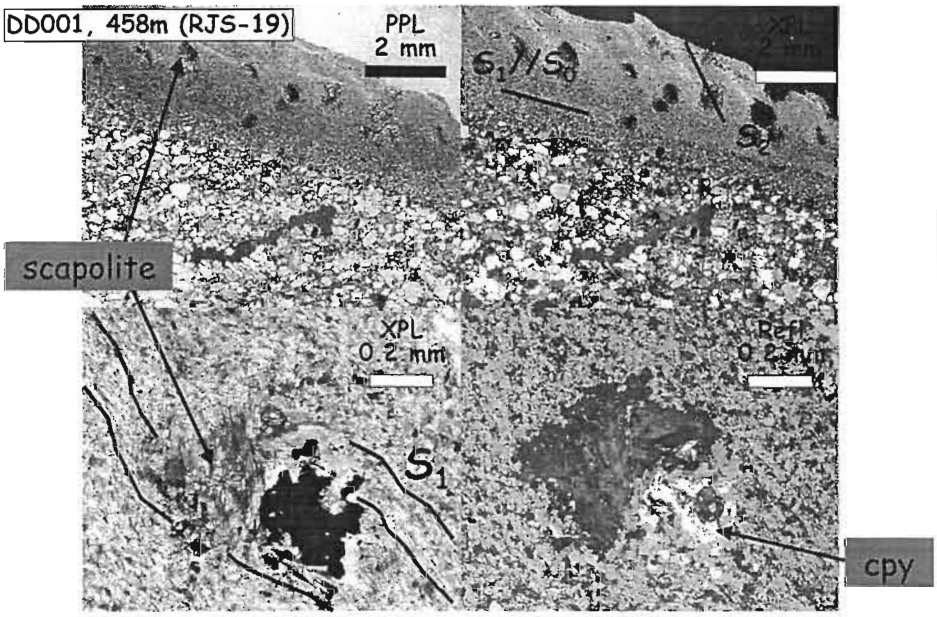

Summary

- Two widely developed fabrics in basement rocks
  - earlier fabric (S_{1B}) poorly preserved greenschist facies differentiated foliation ⇒ pre-Katangan
  - later fabric (S_{2B}), also greenschist facies, intensifies toward ~50m wide shear zone below the contact with Roan
- Shear fabric (S_{2B}) continuous into the Lower Roan, and correlated with layer parallel greenschist facies fabric developed throughout much of the Lower Roan (S_{1R}) ⇒ Lufilian?
- S_{1R} (S_{2B}) folded by NW-trending regional-scale folds associated with the development of weak crenulation cleavage (S_{2R}) at Ndola West

Summary cont……

- Although basement-Roan contact at Ndola West is sheared, the locus of highest strain appears to be well within basement
  - basal contact of the Roan could either be faulted or an unconformity (attenuated in the margin of shear zone)
  - apparent localisation of strain within "crystalline" basement probably reflects sense of movement across zone with uplift of deeper levels of the shear zone on the eastern (basement) side

GEOLOGY AND GENSIS OF THE NKANA-MINDOLA DEPOSITS, ZAMBIA

'A 16KM STRIKE LENGTH Cu-Co OREBODY'

MAWSON CROAKER

AMIRA P544 NKANA-MINDOLA PhD

PRESENTATION OUTLINE

- OUTLINE THE MAIN STRATIGRAPHIC RELATIONSHIPS IDENTIFED SO FAR FOR NKANA AND MINDOLA.
- LITHOLOGICAL CHARACTERISITCS – DIFFERENCES OF THE 'ORE SHALE' ALONG STRIKE.
- OVERVIEW OF THE DEFORMATION HISTORY OF NKANA (SOB) SYNCLINORIUM AREA.
- FOOTWALL SS AND 'ORE SHALE' ALTERATION AT THE NKANA (SOB) SYNCLINORIUM AREA.

5. FUTURE WORK PLAN AND IDEAS.

AMIRA P544 NKANA-MINDOLA PhD

ACKNOWLEDGEMENTS

- HUGH CARRUTHERS AND MIKE STUART OF FIRST QUANTUM MINERALS, ZAMBIA.
- GIDDY MWALE AND ALL THE GEOLOGICAL STAFF AND HELPERS AT MOPANI COPPER MINES.
- PETER MANN AND STAFF, ESPECIALLY 'SPIDER' AND THE MECHANICS AT ZAMANGLO FOR KEEPING THE 'LOVE BUS' ON THE ROAD.
- AMIRA SPONSORS, CODES STAFF AND CSM.
- JUNE PONGRATZ.

AMIRA P544 NKANA-MINDOLA PhD

WHY NKANA-MINDOLA?

Integral part of the 'Chambishi Basin Study' as it provides access to:

- Stratigraphic record of the Lower Roan and differences along strike.
- Deformation characterization for the SE portion of the basin.

3. Several mineralisation styles – both of significant economic importance.

WORK TO DATE:

- Project began in August 2001.
- Field season completed August-September 2001, second field season underway since March 2002.
- Preliminary petrography work, sedimentological and structural characterization, detailed stratigraphic-structural interpretation of Nkana Synclinorium. Assessment of different types of 'Barren Gaps'.

AMIRA P544 NKANA-MINDOLA PhD

PROJECT AIM AND SPECIFIC OBJECTIVES

Constrain the genesis of copper mineralisation at NM by investigating stratigraphic, sedimentological, structural, petrological and geochemical aspects of the Neoproterozoic mineralised system.

Achieved by:

1. Document the local stratigraphy and establish the sedimentary architecture.
2. Determine the local deformation history of the NM system .
3. Assess the spatial and temporal relationships of the copper assemblages to stratigraphy, alteration and structure.
4. Document the nature and timing of metamorphic and hydrothermal processes

STRATIGRAPHY OF NKANA-MINDOLA

BASEMENT
- Biotite Schist, Quartz Biotite Gneiss, K-Feldpsar granite, quartz-muscovite schist.
- Unconformity and tectonic contact with the overlying Lower Roan Formation.
- No contact relationship with K-feldspar granite identified so far.

LOWER ROAN – (Mine Terminology)

- Basal Debris / Talus breccia. (ca. 0 to 20m thick).
- Basal Quartzite and sandstone, widely distributed. (ca. 0 to 60m thick).
- Lower Conglomerate, widely distributed. (ca. 0 to 8m thick).
- Footwall Sandstone, widely distributed (ca. 0 to 30m thick).
- Footwall Conglomerate – limited distribution (ca. 0 to 4m thick).
- Ore Formation – continuous along 16km strike length. (ca. 4m to 15m)
- Interbedded Argillites / Dolomites / Quartzites.

AMIRA P544 NKANA-MINDOLA PhD

CHARACTERISTICS OF MINERALISED 'HORIZON'

SOUTH OREBODY

- Upper portion of Footwall Sandstone and Lower section of the Ore Formation.
- All lithologies metamorphosed to greenschist facies grade.

- FWS – dolomitic ss, complex alteration, distinct negative relationship to anhydrite, extensively shearing along base.
- chalcopyrite, carrolite, bornite and minor pyrite and pyyrohite.
- Close relationship of dolomite and a lesser extent calcite alteratio

- ORE FORMATION - Grey to black interbedded carbonaceous silt-shale.
- Dolomitic basal horizon ca. 3m thick and basal portion often altered.
- Chalcopyrite and pyrite.
- Aligned along main structural fabric and associated with qtz-cal vns.

- Late shear related chalopyrite and bornite hosted within Basal Quartzite and Lower Conglomerate.

AMIRA P544 NKANA-MINDOLA PhD

CHARACTERISTICS OF MINERALISED 'HORIZON'

CENTRAL SHAFT

- Upper Footwall Sandstone – Conglomerate and Lower portion of Ore Formation.

- Footwall SS and conglomerate, slightly higher proportion of carbonate.
- Sulphides disseminated in matrix, limited alteration.
- Chalcopyrite, minor bornite grading into pyrite.

- Ore Formation – lower grey to black 'schistose ore', tremolite rich horizon, interbedded argillite-dolomite-dolomitic ss (bedding paraell Carbonate veining) grey argillite.
- chalcopyrite, pyrite, bornite (commonly associated with late veins and breccias.

- Increase in disseminated proportion of bornite towards the northern end of the deposit, decrease in pyrite.

AMIRA P544 NKANA-MINDOLA PhD

CHARACTERISTICS OF MINERALISED 'HORIZON'

MINDOLA OREBODY

- Upper portion of the Footwall Conglomerate and lower portion of the Ore Formation.
- Orebody dips steeply to the NW – no evidence of macroscopic folding on higher levels.

- Footwall Conglomerate – matrix supported, pebbly conglomerate, laterally variable.
- Lower gradational contact, sharp upper contact.
- Disseminated chalcopyrite, minor bornite

- Ore Formation dolomitic – argillite sequence.
- Mineralisation is chalcopyrite-bornite grading upward to pyrite.
- Bedding parallel movement.
- Enriched mineralisation (mainly bornite) associated with cataclastic bedding parallel veins and small (10-20cm) breccias.

AMIRA P544 NKANA-MINDOLA PhD

STRUCTURE OF THE NKANA SYNCLINORIUM

- Main NE-SW directed compression resulted in tight to isoclinal folding and axial plane shearing – early phase of SSW directed progressive thrust event?

- Later thrusting and low angle normal faults (striking ~ 310) - relatively small scale within the Synclinorium Area.

- Fold axis, shear and thrust / normal fault orientation controlled by geographic position relative to basement.

- Strain is partioned differently in each stratigraphic unit – NO large scale decollement on any one particular stratigraphic boundary of the Lower Roan at SOB.

- Late stage chalcopyrite, bornite and carrolite syn alteration, overprinting 'altered' FWS and SOB and associated with late stage veins.

AMIRA P544 NKANA-MINDOLA PhD

ALTERATION OF FWS AND ORE SHALE

- Alteration affects both the FWS and carbonaceous argillite.
- Several phases-transition – variation in quantity of dolomite, calcite, tremolite and scapolite.
- Stratigraphic and structural control on the alteration.
- Main 'dolomite' alteration predominantly within the FWS.
- Close correlation of high cobalt (plus 0.2%) and dolomite rich zones, not always correlated with high Cu.
- Principle sulphides are chalcopyrite, bornite and carrolite – minor pyrite, pyrrhotite, molybendite.
- Lack of structural fabric within certain alteration zones of FWS, however fine biotite defined fabric recognised within other intervals.

AMIRA P544 NKANA-MINDOLA PhD

PRELIMINARY IDEAS

- BASEMENT TOPOGRAPHY INFLUENCES THE DEPOSITION OF FOOTWALL SEQUENCE.
- TOP OF THE ORE 'SHALE' FORMATION REPRESENTS A 'MAXIMUM FLOODING SURFACE' HOWEVER ACCURATE RECOGNITION OF THE POSITION IS OFTEN DIFFICULT.
- DEEPENING OF THE BASINS TOWARDS THE WEST AND SOUTH AT TIME OF 'ORE SHALE' DEPOSITION.
- FLUVIAL- SHALLOW MARINE ENVIRONMENT AT TIME OF DEPOSITION OF FWS AND ORE SHALE – COMPLEX SEDIMENTATION ENVIRONMENT PARTLY DUE BASEMENT CONTROLS ON SUB-BASINS.
- PRELIMINARY INVESTIGAGTIONS INDICATE THE UPPER ROAN SEQUENCE TO BE WIDESPREAD WITH NO 'LOCAL' SEDIMENTATION CONTROLS.
- AT LOCAL SCALE DIFFERENT LITHOLOGIES DO CONTROL MINERALISATION WHILE ACROSS THE N-M SYSTEM IT IS A STRATIGRAPHIC CONTROL.

AMIRA P544 NKANA-MINDOLA PhD

PRELIMINARY IDEAS-QUESTIONS

- BASEMENT 'TOPOGRAPHY' LOCALLY INFLUENCES THE STRUCTURAL GRAIN OF EARLY LUFILIAN DEFORMATION – CAN 'EARLIER' EVENTS BE SEEN AT NKANA?

- AT LEAST TWO PRINCIPLE PHASES OF SULPHIDE MINERALISATION ACROSS THE NKANA-MINDOLA DEPOSITS – DOES THIS REPRESENT a DIAGENETIC TIMING MINERALISATION PHASE AND A LATER METAMORPHISM RELATED REMOBILISATION / INTRODUCTION MINERALISATION PHASE?

- THREE OR FOUR DIFFERENT 'BARREN GAPS' – THE 'GAPS' ARE UNECONOMIC PORTIONS OF ORE HORIZON ONLY RARELY TOTALLY UNMINERALISED – SEDIMENTARY RELATED AND/OR STRUCTURAL-METAMORPHISM CONTROL?

AT LEAST TWO TYPES OF DOLOMITE – THERE IS A POSITIVE AND NEGATIVE CORRELATION OF DOLOMITE TO Cu AND Co MINERALISATION. – IS DOLOMITE IS SEDIMENTARY AND/OR ALTERATION-METAMORPHISM?

AMIRA P544 NKANA-MINDOLA PhD

FUTURE DIRECTION

- West Limb of Nkana Synclinorium (why no economic mineralisation).
- Understand the role and age? of 'Dolomite' – sedimentary vs alteration.
- Relationship of 'Dolomite Barren Gaps' and basement high 'Barren Gaps' sub-basins? to stratigraphy, basin architecture and mineralisation.
- Phases of biotite and relationship to structure and metamorphism – Ar-Ar biotite dates.
- Differentiate primary (diagenetic?) and remobilised sulphides characteristics, and stratigraphic-alteration-structural relationship.
- 'Anhydrite' primary vs secondary – both appear to have very poor correlation with sulphides.
- Dating different phases of sulphides directly and/or by using relationship to Xenotime? and structural fabric defined by micas.

AMIRA P544 NKANA-MINDOLA PhD

Petrology of Lower Roan — Basement contacts, Konkola East and Ndola East areas

David Broughton, Colorado School of Mines

Introduction

This report describes samples of two drill cores selected to examine the nature of the basement — Katangan relationships, from holes drilled east of the Konkola mine and in the Ndola East area (Figure 1). The nature of the basement contact has been contentious since the earliest geological investigations in the Copperbelt, and remains poorly documented. The Copperbelt is underlain by basement of middle to late Proterozoic age, which consists predominantly of granites, schists/gneisses and quartzites. Of interest are the granites, most of which are of Ubendian age (1800 to 2000 Ma), and are locally termed the old or grey granites. Also present are red granites, including the Nchanga Red Granite, dated at 880 Ma, the youngest basement age obtained in the Copperbelt. The samples from hole KW26 in the Konkola East (Kawiri) area come from the Muliashi Porphyry, which has some petrological similarities to the Nchanga granite but has not been dated. Basement in the Ndola East hole IT28 consists of quartz-feldspathic gneiss of uncertain age.

This study used petrographic, cathodoluminescence and SEM studies of nine thin sections to document the original mineralogy and diagenetic/metamorphic/hydrothermal overprints of the basement and cover rocks, in order to place constraints on provenance, timing of diagenetic and hydrothermal events.

In both cores a zone of residual, weathered — but now metamorphosed — basement is interpreted to occur at the contact. In hole KW26, approximately 2.5 metres of residual Muliashi Porphyry is preserved, at a down-hole depth of 536.0 to 538.5 metres (thin sections 82, 83). In hole IT28, the depth of preserved basement weathering is at least 3 metres.

Konkola East (Kawiri) Area, Drill Hole KW26

Basement-Muliashi Porphyry (thin section 81)

The Muliashi porphyry forms the basement in the Konkola area, and is overlain by sandstones and conglomerates of the basal Lower Roan. There is considerable vertical relief on the basement topography: east of Konkola on the Kawiri (KW) property the Ore Shale is interpreted as missing (not deposited) against a local basement high, whereas in the area between Konkola and Musoshi a basal Lower Roan thicknesses of at least a kilometre are known from drilling.

In hand specimen, the Muliashi Porphyry consists of about 40% cm-sized pink phenocrysts of k-feldspar with conspicuous pale greenish sericitized plagioclase rims, in a groundmass of mm- to cm-sized bluish quartz (25%), greenish sericitized plagioclase (25%), and dark biotite (10%) (Figure 2). The phenocryst morphology is similar to a Rapakivi texture. Accessory sphene and magnetite can also be seen.

In thin section, the phenocrysts are seen to consist of perthitic microcline and orthoclase overgrown by plagioclase (Fig 3a, b). The k-feldspar typically forms multiple, optically continuous crystals that together comprise the phenocryst, separated by thin zones of interstitial quartz. The plagioclase is zoned, with epidote-biotite-(clinozoisite, calcite) altered cores and clear, unaltered rims. SEM/EDS examination confirms that the plagioclase cores are sodic-calcic, whereas the rims are sodic (albite). Under CL the k-feldspar is characteristically bluish, and the unaltered plagioclase and perthitic intergrowths brownish. The calcite has a red to golden yellow luminescence, indicating probable Fe and Mn substitution.

The groundmass blue quartz varies from polycrystalline and fine-grained, to monocrystalline and strained (undulose extinction, Figure 3c). The quartz typically has smooth, rounded contacts with the feldspars, and forms oval to subcircular grains. The polycrystalline quartz has grain boundary textures that range from sutured (unstable, Figure 3d) to metamorphic triple-point (stable). The sutured boundaries appear very similar to textures in Lower Roan arenites in drill hole IT28, and are probably related to Lufilian deformation. There is little consistent indication of the origin of its blue colour, either under the petrographic or the CL microscope, except that colour zoning in some grains is related to the internal distribution of polycrystalline versus monocrystalline quartz. This quartz is a common detrital component throughout the Lower and Upper Roan.

Biotite forms mm-sized to fine-grained flakes, some with inclusions of rutile that have optically darkened haloes, and is difficult to determine whether it is igneous or metamorphic/hydrothermal in origin: both grain sizes may be associated with epidote-clinozoisite.

Euhedral sphene is a common accessory in the groundmass, and shows no indication of alteration. Apatite forms euhdral to rounded tabular grains, and is very common in zones of clotted biotite-epidote, but rare within the feldspar phenocrysts. The apatite has a moderately strong greenish yellow luminescence, possibly indicative of Mn, and some grains are zoned. Magnetite is euhedral and occurs only within the altered plagioclase that mantles the phenocrysts. Minute grains of chalcopyrite also occur only within the altered plagioclase, where they are associated and locally enclosed within epidote (Figure 3e).

The phenocrysts are cut by minor veinlets of calcite, epidote, biotite, and rare chalcopyrite, that are locally continuous with the more pervasive alteration zones. This alteration-mineralization event is interpreted as Katangan or Lufilian in age.

Residual Basement (thin sections 82, 83)

The porphyry is separated from bedded, clearly sedimentary rocks by approximately 2.5 metres of dark, biotitic rock containing about 15% scattered pink feldspar phenocrysts and 15% blue-grey quartz grains, floating in a brownish-green matrix (Figure 4). The impression is one of a sedimentary rock derived very proximally from the porphyry.

In thin section, the feldspar phenocrysts and blue quartz grains are effectively indistinguishable from those in the underlying sample. The perthitic k-feldspar phenocrysts are unaltered and shows no signs of (incipient) weathering, possibly because of its inherent stability (Figure 5a). In both thin sections the phenocrysts have a discontinuous halo of calcite-hematite-muscovite 1-2 mm thick, not seen in the unweathered porphyry. These same minerals occur locally in the groundmass, as irregular clots. Plagioclase phenocrysts are intensely altered to muscovite-epidote-clinozoisite-biotite (Figure 5b).

The brownish groundmass consists in thin section of 10 to 20% fine-grained biotite intergrown with 5 to 15% epidote-clinozoisite-muscovite, all overgrowing granitic-textured plagioclase and k-feldspar (Figure 5c). In most places the abundance of the secondary minerals prevents recognition of grain boundaries, and it is difficult to be certain whether the groundmass comprises large, eroded and transported porphyry fragments, or metamorphism of an in-situ residual porphyry. On the basis of the preserved igneous texture of the groundmass, the intact phenocrysts, the knowledge that phenocryst abundances vary widely within the Muliashi Porphyry (ie. 15% is not an unacceptably low abundance), and a comparison with the textures in the overlying bedded sediments, it is reasonable to interpret this as a metamorphosed residual porphyry.

The groundmass also contains sphene, ilmenite and hematite. Sphene forms subspherical detrital grains cored by ilmenite and locally apatite. The grains have a characteristic irregular, bumpy outline that is morphologically similar to the ubiquitous hematite grains in the Lower Roan sediments. Ilmenite occurs as bladed angular grains that are the likely precursor for the bladed, Ti-bearing hematite in the Lower Roan. Specular hematite forms pseudomorphs (martite) after euhedral magnetite, and lacks Ti.

The features of the residual zone suggest that weathering of the porphyry was accomplished by clay alteration of the feldspars, and oxidation of magnetite. The general lack of carbonate, silica or other infilling in the feldspars suggests that the secondary porosity created by clay weathering was not cemented, but preserved until later metamorphism to micas. Calcite, epidote-clinozoisite and biotite are common replacement products of the plagioclase, and also formed during metamorphism.

Lower Roan meta-sandstones and conglomerates (thin sections 84, 85)

Thin sections 84 and 85 are taken from bedded sandstone and conglomerate 10 to 20 cm above the weathered zone. In hand specimen the conglomerate contains obvious mm to cm-sized fragments of pink k-feldspar phenocrysts and blue quartz, within a sand matrix similar in composition to the sandstones (Figure 6). Graded bedding is absent or poorly developed and quite abrupt, and sorting is minimal. Outsized grains are commonly visible in the sandstones.

In thin section, the conglomerates are framework-supported with coarse sand to granule-sized grains of porphyry, feldspar and quartz, commonly with a moderate rounding (Figure 7a). In most cases this can be ascribed to the original texture of the porphyries (rounded feldspar phenocrysts and blue quartz), but other grains appear to have undergone significant transport. In particular, well-rounded quartz grains may be derived from other basement sources, most likely the Muva quartzites. Accessory grains of detrital muscovite are typically acicular and up to 1 cm in length, were not seen in the granites and also appear to have a different, unknown basement source (Figure 7b). The larger detrital grains occur within a framework of fine to medium-sized sand grains of angular to subangular quartz and feldspar, of clearly local origin. Also present are subspherical to broken, sand-sized grains of hematite, some of which show incomplete alteration from magnetite (Figure 7d-f). These are interpreted to have been derived from the primary magnetite and the zoned sphene-ilmenite grains in the granites. Rutile occurs as rare pseudomorphs after sphene, and more commonly as silt to clay-sized grains within the groundmass and coating detrital grains.

The estimated detrital composition of the conglomerates is 30 to 50% lithics, (including porphyry, polycrystalline quartz), 25% quartz, 15% k-feldspar, 5 to 10% plagioclase, and accessory muscovite, and hematite. The conglomerate contains 5 to locally 10% silty matrix that under crossed polars has a fine mosaic texture and very low birefringence (Figure 7e,f), and is variably replaced by metamorphic biotite, muscovite or calcite. The SEM/EDS indicates that this matrix material consists largely of k-feldspar.

The sandstones contain a similar compositional range of detrital components, but intact porphyry rock fragments are rare. Framework grains are subangular to subrounded, the greater textural maturity due to elimination of the large lithic grains with roundness inherited from the porphyry. On average, the sandstones contain 40% quartz (monocrystalline), 30% feldspar (including 10% plagioclase), 5 to 10% lithics (porphyry, polycrystalline quartz), 1 to 2% detrital muscovite, 2 to 4% hematite, and about 1% rutile. The matrix comprises 5 to 20% of the rock, and is locally replaced by biotite, or calcite. The composition of the sandstone can be irregularly domainal on an intra-bed scale, such that they range in classification from lithic wacke to lithic arkose to feldspathic sandstone. This immaturity also occurs on an inter-bed scale.

Grain boundaries in both the sandstones and conglomerates are typically straight, smooth or curved, rather than sutured. Grains in the sandstone are most commonly floating or in contact with one or two other grains, and overgrowths occur on where grains are in contact (Figure 7c). A few of the detrital muscovite flakes are bent around quartz or feldspar grains, but there is otherwise little evidence of significant compactional deformation.

Overall, the sandstones show remarkably little evidence for cementation, dissolution and other diagenetic processes. In this regard it is noteworthy that the feldspar grains in the sandstone and conglomerate are no more altered to muscovite/biotite than in the samples of porphyry, possibly because the more weathered grains were destroyed during transport. More puzzling is the lack of either detrital or in-situ (ie. within plagioclase) epidote-clinozoisite in the sedimentary rocks, given their ubiquitous presence in the footwall granites. If these minerals represented a pre-Katangan metamorphic event, one would expect them to form part of the detrital record, particularly within large, intact granitic rocks fragments. If they represent a Lufilian hydrothermal/metamorphic event, which is suspected on the basis of their association with veining and chalcopyrite mineralization, their absence in the metasediments suggests a strongly localized control.

SEM/EDS work on the micas indicates that there are two end-member compositions present in the KW26 section. A pale, weakly to non-pleochroic, stubby lath-shaped mica with high birefringence is present in the plagioclase alteration, in calcite veinlets, and in mantled zones around feldspar phenocrysts in the residual zone. It contains little or no Ti, no Cl and is low in Mg, but has significant Fe. It is likely an Fe-bearing muscovite. The second mica is a brown, pleochroic, biotite that also occurs in the plagioclase alteration and veinlets, as well as in the residual granite groundmass, in nodules or clumps of coarser biotite, and as a mantle to the hematite and detrital muscovite. It contains considerably more Fe than the pale mica, as well as significant amounts of Ti and Cl. Coarse-grained biotite associated with mineralization in the Konkola drill hole KLB145 also tends to be elevated in Fe, Ti and Cl. More work needs to be done to confirm this association, and may help constrain the type and pathways of mineralizing fluid.

Ndola East Area, Drill Hole IT28

A series of drill holes some thirty years ago tested the area around the present-day Ndola Lime operation, several of which passed into a gneissic basement. Unlike the Konkola area, the thickness of the Lower Roan beneath the Ore Shale is remarkably consistent between holes, such that individual beds immediately above the basement contact can be correlated over several kilometres. The depositional setting appears to have been tectonically much quieter from that at Konkola. Although all of the holes contain copper mineralization, its grade is consistently sub-ore (<2%). The contact is also interesting because the gneissic basement appears to contain windows of Lower Roan sandstone and it is not obvious that an erosional contact exists.

In hand specimen the contact between the gneiss and the sandstone parallels the orientation of poorly defined layering within the sandstone, as well as the orientation of a hematite-bearing vein in the gneiss (Figure 8). The gneissic layering lies almost perpendicular to these features, and is abruptly cut by the contact with the sandstone. Unlike the basal sandstones described from Konkola, the sandstones here are even-grained, dark, and contain no material obviously derived from their immediate footwall.

The sandstone consists in thin section of more than 90% quartz with less than 10% feldspar (microcline and accessory plagioclase), accessory biotite and hematite, and rare zircon, and hence is a quartz arenite (Figure 9a). The framework grains are well-sorted, and mud or silt-sized matrix is absent. The rock has a striking sutured texture, which along with a moderately developed preferred orientation of grains indicates strong pressure solution parallel to bedding (the basement contact). This is supported by the rarity of preserved dust rims of Fe-Ti oxide and mica (clay) dust rims (Figure 9a). However, their presence indicates a period of early diagenetic oxidation similar to that at Konkola.

The arenite gradually decreases in average grain size and sorting towards the contact with the gneiss, coincident with a gradual increase in the abundance of suture-lining fine-grained biotite, and of sutured, and in many instances stylolitic grain boundaries (Figure 9 b). These changes may reflect a change in the original sediment toward a more poorly-sorted, feldspathic arenite, with slightly higher clay content expressed as grain coatings.

The sutured texture could be interpreted as related to diagenetic pressure solution during burial. However, the texture occurs locally within the underlying gneiss (Figure 9d), and in the hematite-bearing plagioclase-calcite-quartz-biotite vein. Together these suggest that the sutured texture developed, or was at least modified, during metamorphism-deformation.

The contact with the gneiss is indistinct to irregular on the thin section scale. The uppermost part of the gneiss consists of large quartz, feldspar and quartz-feldspar intergrowths that define the steep gneissic texture, separated by zones of fine-grained sandstone similar to that above the contact (Figure 9c). Hematite is much more abundant below the contact, and forms large, mm to cm-sized irregular grains within the sandstone. The texture could be interpreted as being due to sandstone deposited within steep cracks penetrating the basement, or, alternatively, as a metasomatic overprint upon the sandstone. However, dark, mosaic-textured, k-feldspar-quartz matrix occurs locally within the gneiss, supporting a framework of detrital grains, and indicates a sedimentary origin (Figure 9e).

Two types of biotite occur, a fine-grained biotite that overgrows the matrix and detrital feldspar and contains rutile, and a younger, coarse-grained biotite that lacks rutile and mantles late, clear plagioclase (Figure 9f). The younger biotite is texturally similar to the coarse biotite found in mineralized nodules. Further SEM work is required to characterize the different generations of biotite.

Vein hematite appears to have formed (or remobilized) late in the paragenetic sequence, because it truncates and brecciates sutured quartz and the vein infilling minerals, albite, k-feldspar, and calcite. Vein minerals show evidence of deformation prior to truncation by hematite, such as kink bands in albite, undulose extinction and suture development in quartz. The timing and morphology of the vein hematite is similar to that of the vein-associated sulfides, and they may be temporally related. Clear, twinned albite occurs in the veins and locally around their margins, and in one instance demonstrably overgrows an earlier detrital k-feldspar grain (Figure 9f). Sodic alteration is apparently absent at Konkola, but is here seen to be associated with hematite mineralization.

Summary and Conclusions

The basement — Lower Roan contacts in the Konkola East (Kawiri) and Ndola East areas contain transitional zones where igneous textures are partially preserved yet sedimentary features are also present. These zones are interpreted as metamorphosed regoliths. At Kawiri, the transition is characterized by intense biotite-epidote alteration of the feldspars, taken to reflect original weathering of the granite. At Ndola, the transition is marked by high-angle fractures filled with sediment from the overlying sandstone.

Plagioclase in the Muliashi porphyry is altered to epidote-biotite-(muscovite-calcite), which also forms thin veinlets and carries minor chalcopyrite. This mineralization is interpreted to be associated with Lufilian deformation, on the basis of its similarities with late Ore Shale mineralization. Significant zones of basement-hosted mineralization such as at Samba may well be Lufilian, rather than pre-Katangan, and would not provide a copper source for the Lower Roan ore bodies.

The early diagenetic features of the Lower Roan rocks are remarkably consistent between these widely spaced locations, specifically the presence of oxides and clays coating detrital grains. Pressure solution is strongly developed in the Ndola basal sandstones, but is also present in the gneiss, and is likely related to deformation rather than burial diagenesis. Weathering of the basement rocks may locally be preserved as a regolith, but feldspars in the overlying sandstones are no more visibly weathered than in the basement.

The granites contain sphene that is a source for the detrital/authigenic rutile and ilmenite in the Lower Roan. Magnetite occurs in the granites but is associated with the epidote-biotite alteration, and so may be secondary. Hematite in the Lower Roan is likely derived from replacement of ilmenite, and the metamorphism of amorphous iron oxides. The peculiar blue quartz characteristic of the Roan sedimentary rocks is granitic in origin.

Biotite in both the basement and sedimentary rocks has two forms, small, groundmass biotite that is locally associated with or encloses rutile, and coarse biotite flakes that are paragenetically late. Similar coarse biotite is elsewhere associated with mineralization. Albite is mantled by the coarse biotite and formed at an earlier stage, and also occurs in calcite-hematite veins. Sodic alteration is important at a few Katangan deposits, but is not consistently developed in the Copperbelt ore bodies.

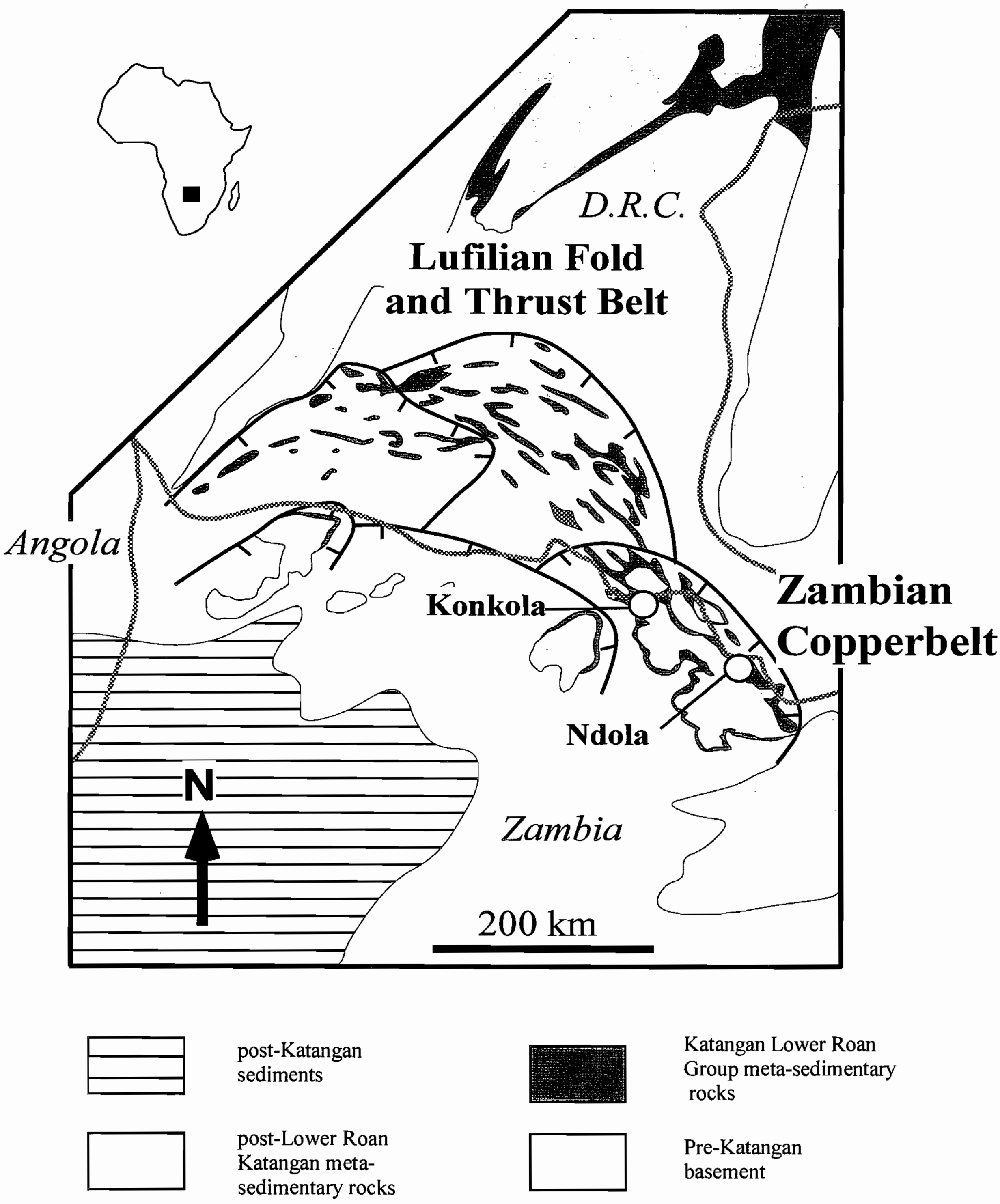

Figure 1. Location of Konkola mine (drill hole KW26) and Ndola property (drill hole IT28) within the Zambian Copperbelt.

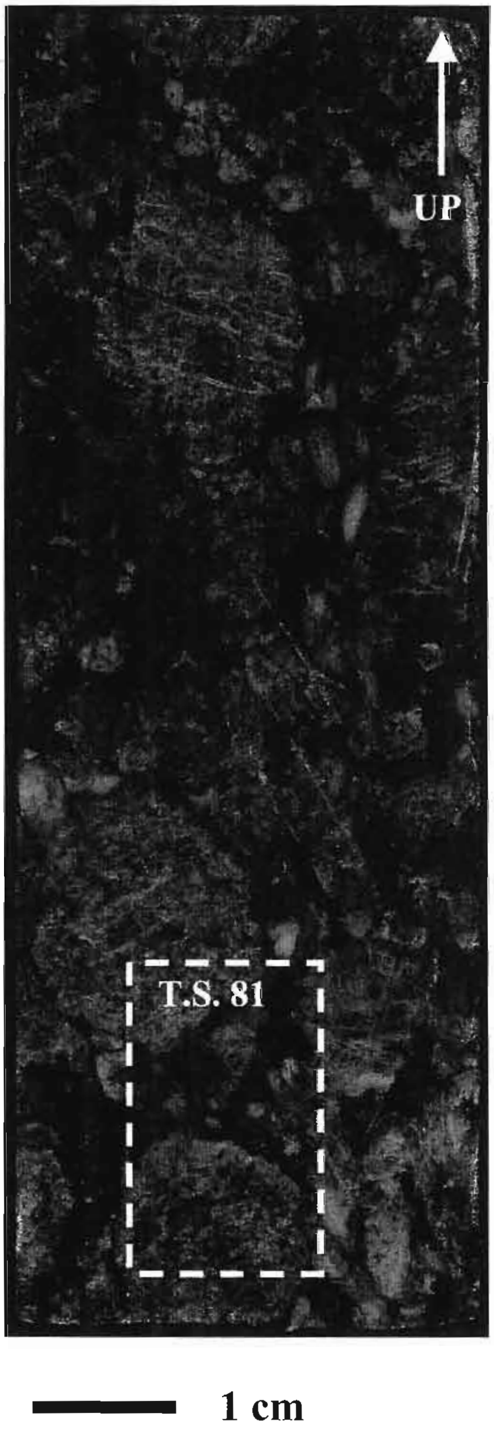

Figure 2. KW-26, 553.3 m, Muliashi Porphyry. Note large k-feldspar phenocrysts mantled by greenish altered plagioclase, blue quartz, and dark biotite.

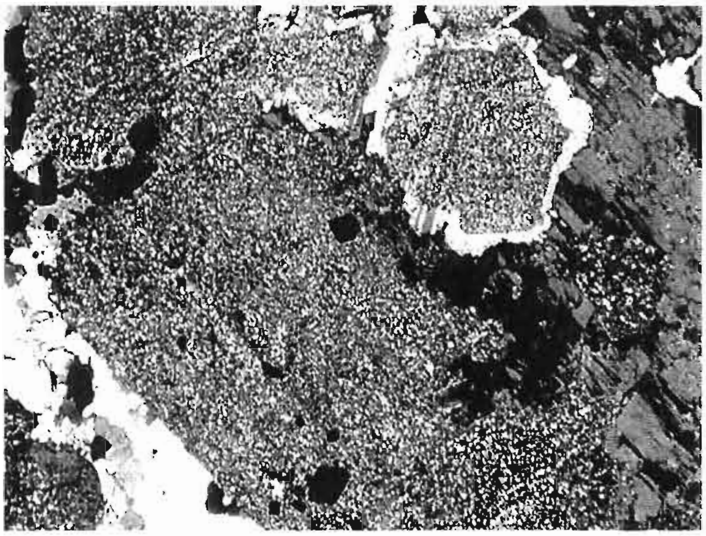

Figure 3a. TS81, cpl. View of edge of feldspar phenocryst, against polycrystalline quartz. Grey microcline overgrown by plagioclase, which is zoned from epidote-biotite altered, calcic cores to clear, unaltered, albitic rims. The phenocryst is mantled by altered plagioclase, which contains euhedral magnetite.

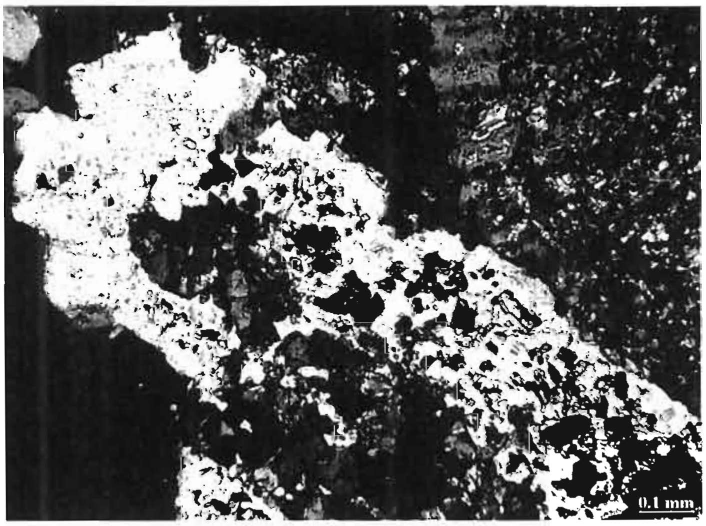

Figure 3b. TS81, cpl. Relatively coarse-grained epidote and clinozoisite, with associated biotite, replacing plagioclase.

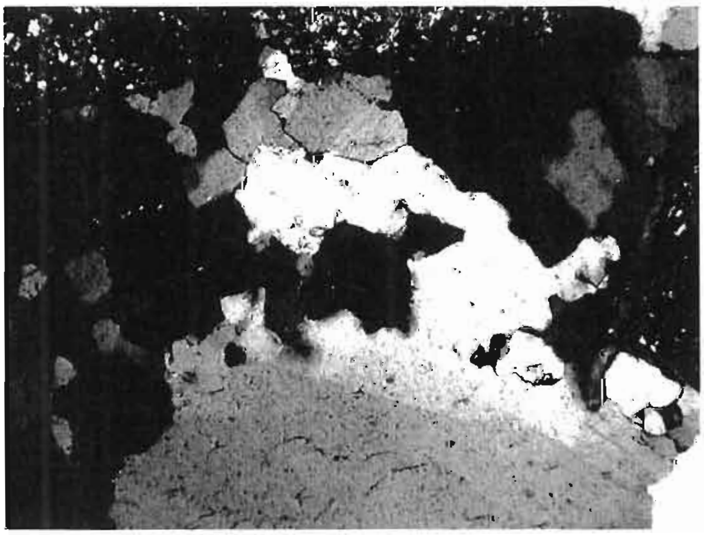

Figure 3c. TS81, cpl. Typical texture of polycrystalline quartz, on margin of large, 3-5mm blue quartz grain. Some grains show metamorphic triple-point boundaries, others are sutured, all show straight to almost-straight extinction. Core of grain is monocrystalline, with undulose extinction.

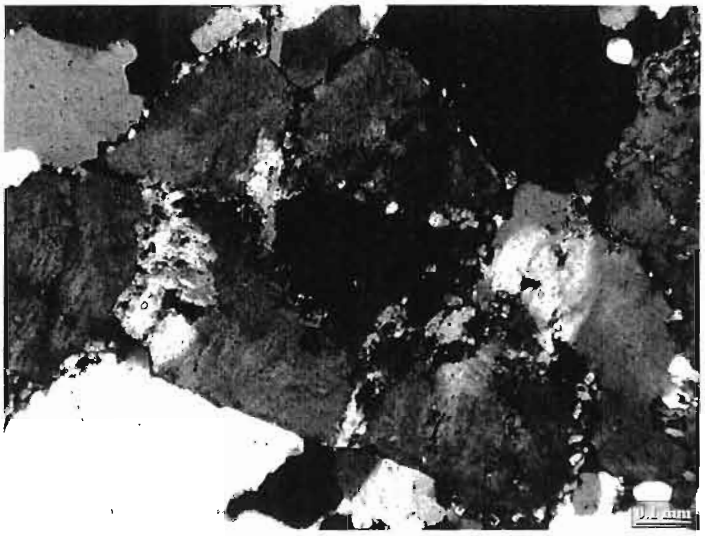

Figure 3d. TS81, cpl. Polygonal texture in microcline and quartz. The microcline is optically continuous, and dissected by thin seams of minute quartz-plagioclase-muscovite-biotite.

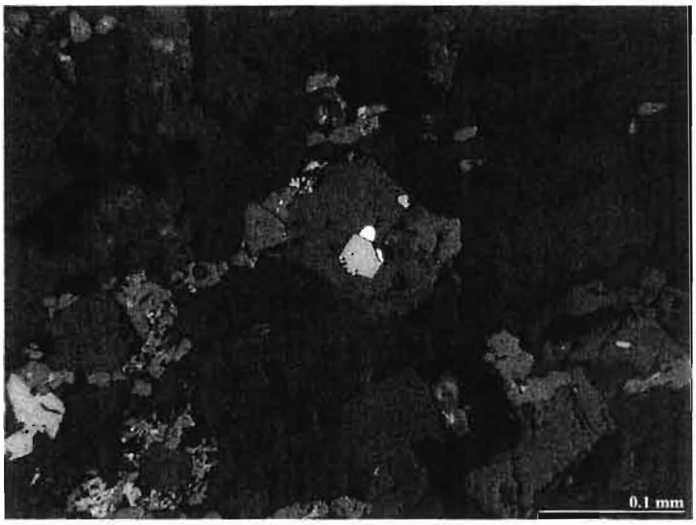

Figure 3e. TS81, reflected light. Chalcopyrite rimming rutile, within grain of epidote. Minor chalcopyrite is typically associated with epidote-biotite-(muscovite) alteration of plagioclase.

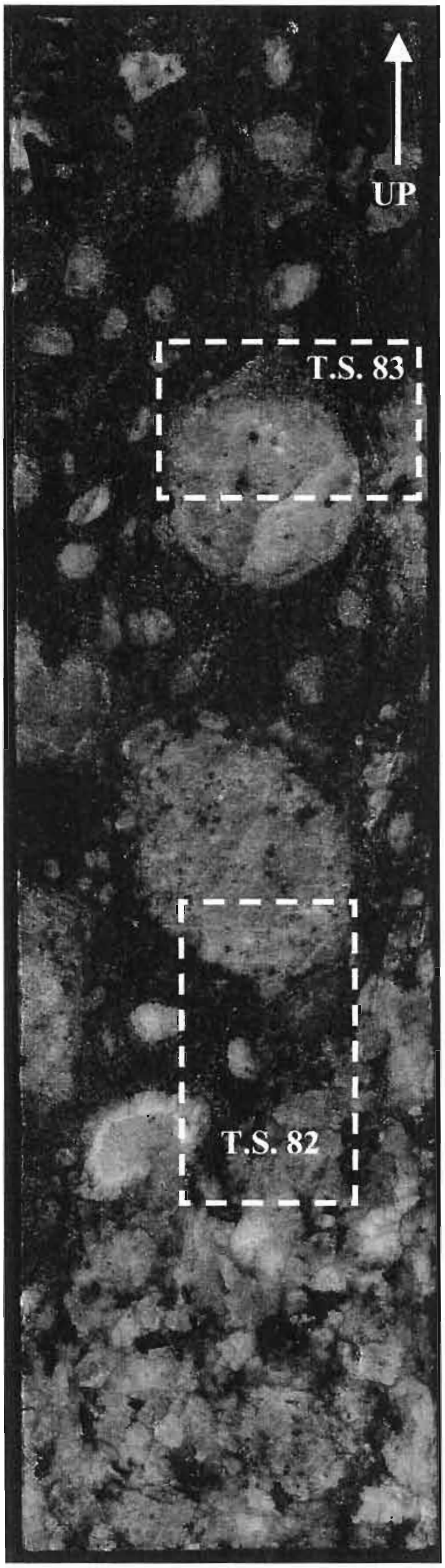

1 cm

Figure 4. KW-26, 538.3 m, Regolith, Muliashi Porphyry. Intensely altered brownish matrix contains phenocrysts of k-feldspar, plagioclase and blue quartz.

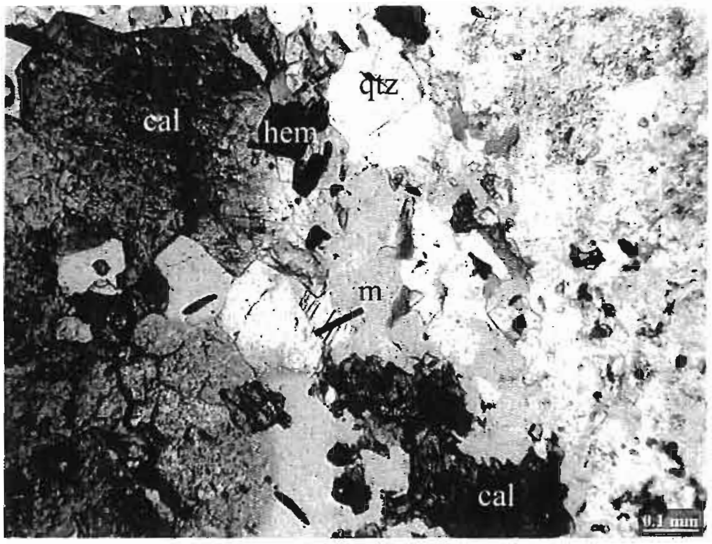

Figure 5a. TS82, ppl. Margin of large feldspar phenocryst (to right), with selvege of quartz, calcite, muscovite, hematite.

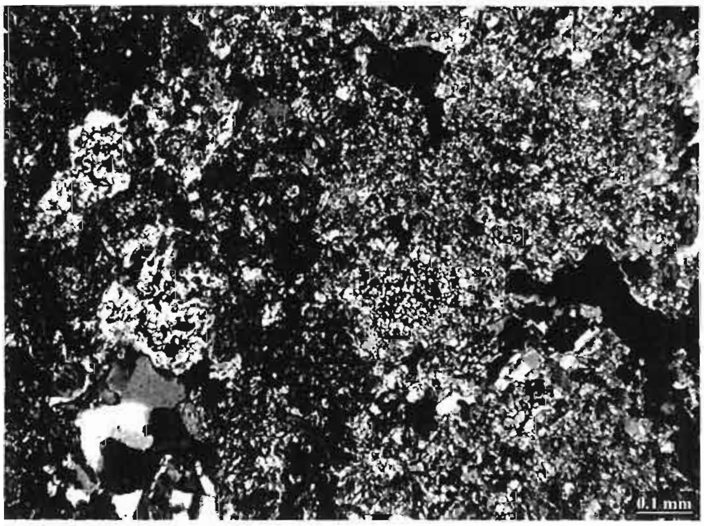

Figure 5b. TS83, cpl. Intensely altered plagioclase phenocryst, almost completely replaced by biotite-epidote-(muscovite). Dark grey interstitial quartz preserves original texture of phenocryst.

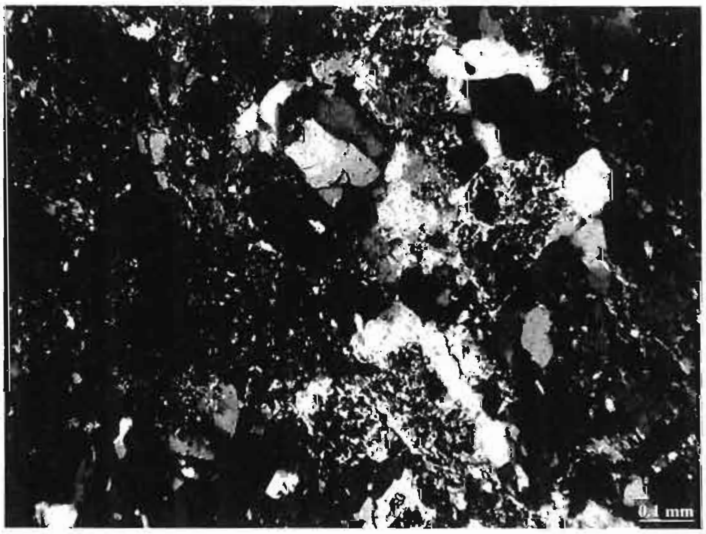

Figure 5c. TS83, cpl. View of groundmass to large feldspar phenocrysts. Groundmass has dark colour due to abundance of fine grained metamorphic biotite and epidote, but igneous texture is preserved. Interpreted as a metamorphosed residual granite.

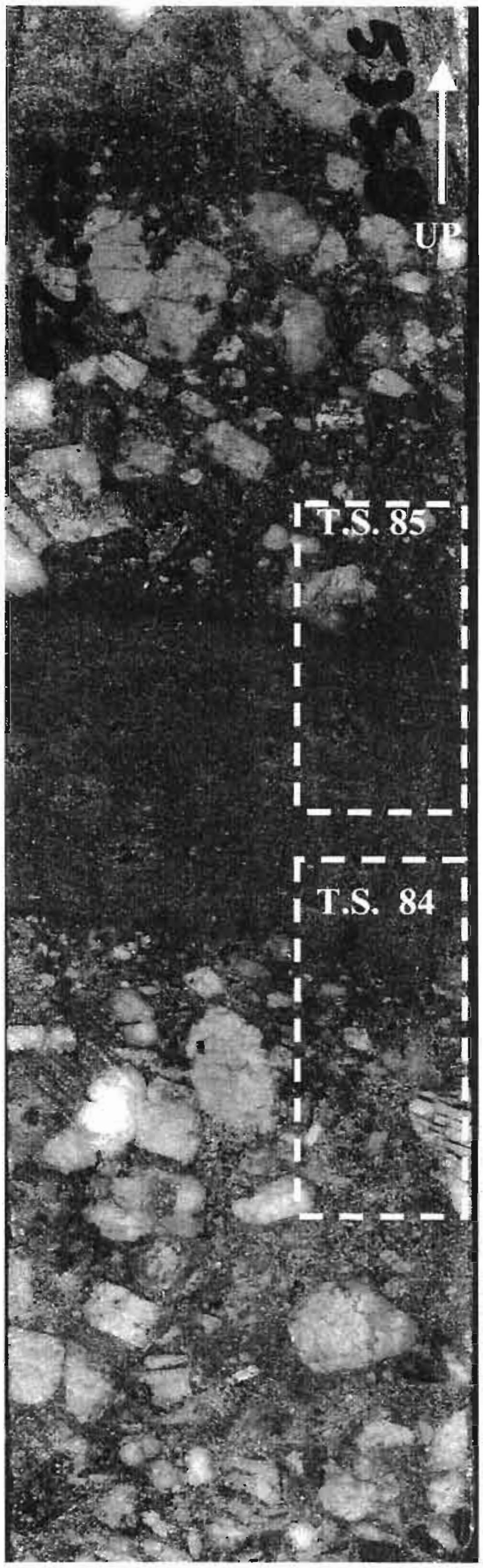

1 cm

Figure 6. KW-26, 535.8 m, Lower Roan conglomerate and sandstone, 10cm above contact with porphyry. Note large angular granitic rock fragments, blue quartz and k-feldspar, poor sorting and lack of compaction textures.

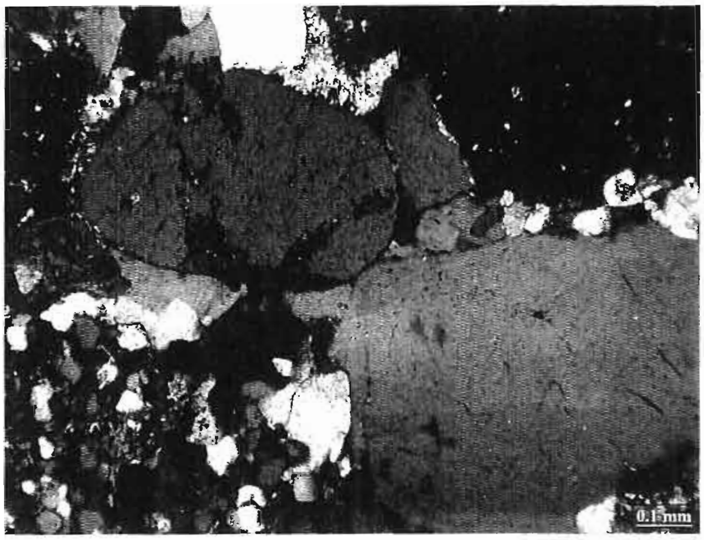

Figure 7a. TS84, cpl. View of framework grains in conglomeratic sandstone. Detrital k-feldspar (upper left) and quartz with biotite and Fe-Ti oxide dust rims, cemented by quartz.

Figure 7b. TS85, cpl. Compacted arkosic sandstone, with bent detrital muscovite and well-aligned framework grains of quartz and feldspar. The matrix appears undeformed (although partly replaced by metamorphic biotite), there are no quartz or feldspar overgrowths, and the framework grains are unaffected by pressure solution.

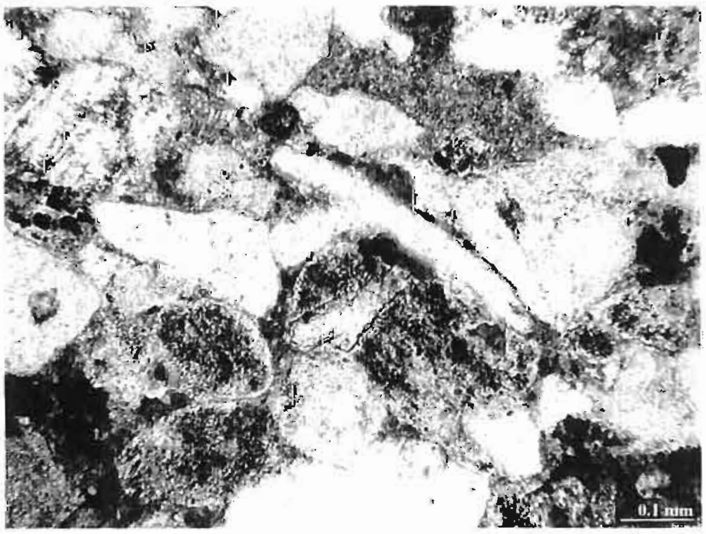

Figure 7c. TS84, ppl. Fine-grained arkosic sandstone, subrounded and well-sorted framework grains. Bent detrital muscovite, partly mantled by metamorphic biotite, which also partly replaces the matrix. The cloudy k-feldspar grains have thin overgrowths of clear feldspar.

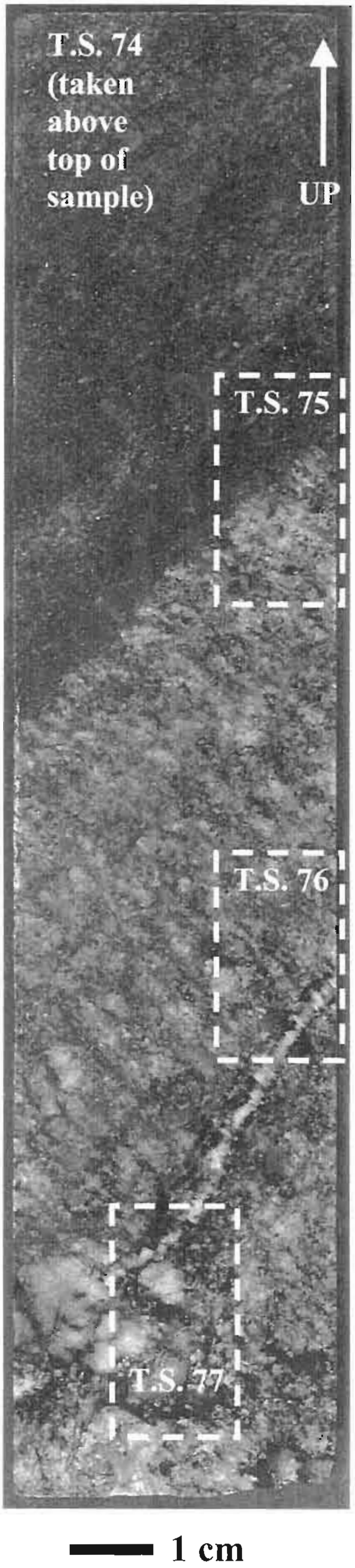

Figure 8. IT28, 5098 ft, contact between Lower Roan quartz arenite and basement gneiss. Note faint layering in arenite parallel to the contact and to the hematite vein, high angle gneissic banding in basement.

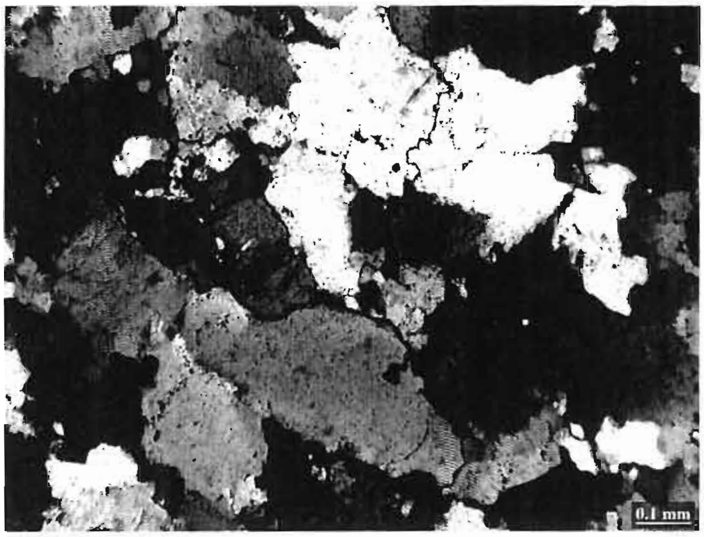

Figure 9a. TS74, cpl. View of part of thi section furthest above the basement contact. Quartz arenite, with locally preserved dust rims showing original detrital texture, largely obliterated by extensive pressure solution. Preferred orientation of grains subparallels the basement contact. Note lack of matrix — originally a clean sand.

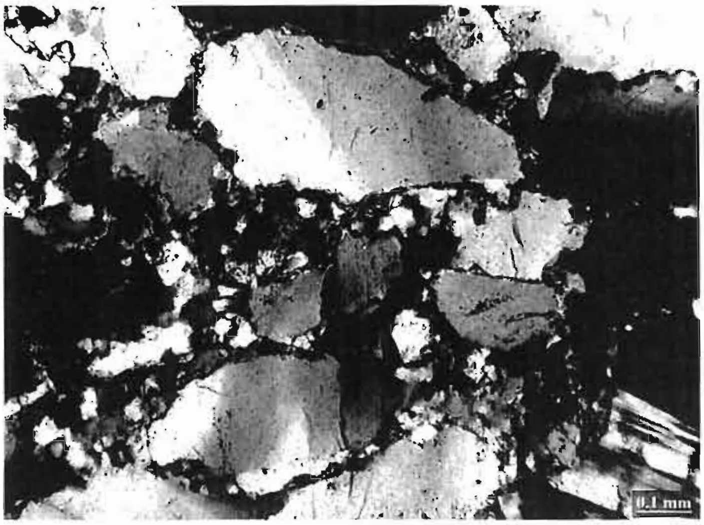

Figure 9b. TS74, cpl. Sample closer to the basement contact than (a), with more intense suture development associated with higher biotite content.

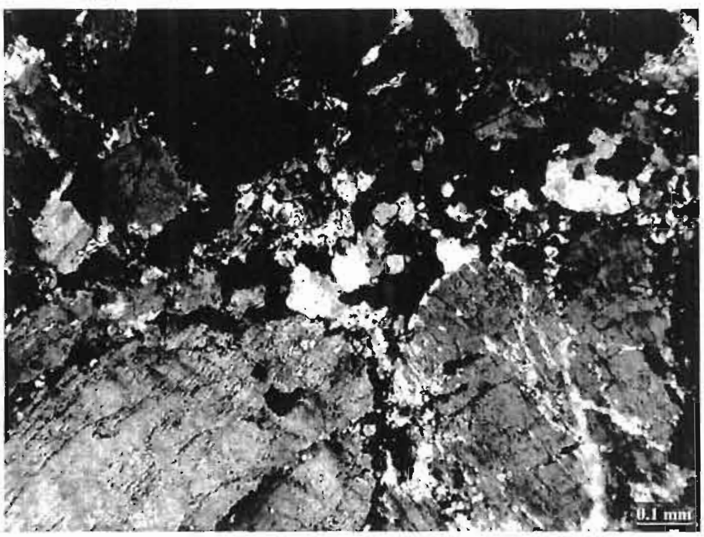

Figure 9c, TS75, cpl. View immediately inside basement contact (trends NW-SE immediately left of slide), long dimension of large feldspar grains perpendicular to contact. Basement consists of large granitic fragments with intervening zones of sand-sized detrital grains, and interstitial biotite.

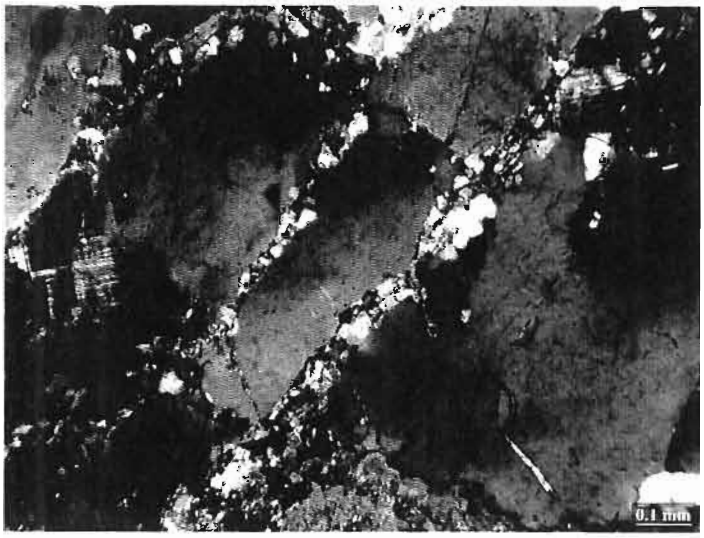

Figure 9d. TS76, cpl. Large quartz grain cut by quartz-plagioclase-biotite veinlets, compositionally similar and parallel to pressure solution seams and sutured texture in overlying sandstones. Also parallel to large veinlet of albite-quartz-biotite-carbonate-hematite.

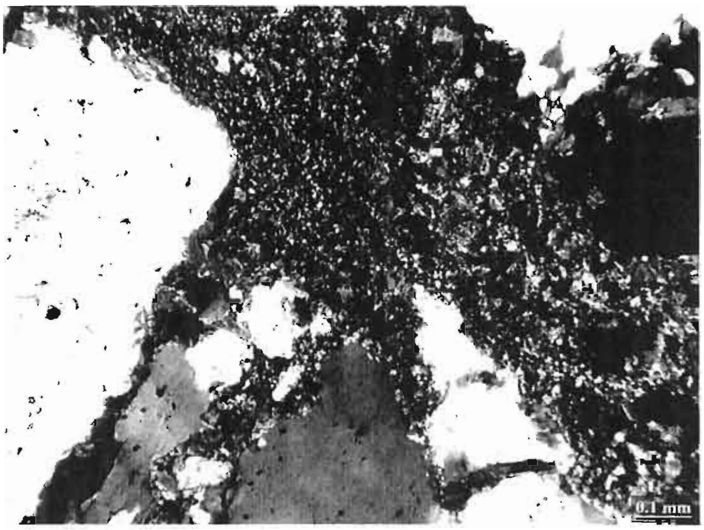

Figure 9e. TS76, cpl. Dark cherty matrix partly overgrown by biotite, surrounding large and locally broken grains of quartz, feldspar.

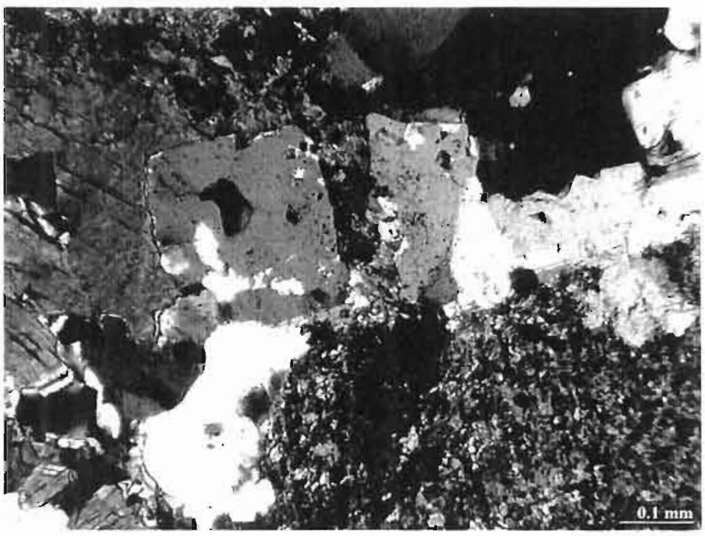

Figure 9f. TS78, cpl. Detrital/residual granitic fragment of dark k-feldspar partly overgrown by biotite, mantled and replaced by clear subhedral plagioclase. Two generations of biotite are present — fine-grained biotite with dark rutile, and a coarse-grained biotite that lacks rutile and mantles the euhedral plagioclase.

Mineral Zonation & Controls on Fluid Pathways at Chibuluma West

David Selley

Presentation Outline

- Distinct vertical zonation or partitioning of:
  - silicate minerals
  - sulphide phases
  - strain
- Zonation from sub-cm (delicately banded, stratiform ore textures) to metric scales (broad, systematic variation in sulphide composition)
- Zonation is largely controlled by primary layering
  - certain sulphide & silicate phases are strongly partitioned into discrete layer-parallel seams
  - heavy mineral bands
  - same domains are loci for post-mineralisation deformation and fluid influx

Structurally-controlled mineralisation?

- Textural relationships: ambiguous - metamorphic overprint - low strains
  - isochemical metamorphism/alteration?
  - sulphide bands and associated mineral assemblage cross-cut primary layering
  - highest grade intervals coincide with enhanced grain-scale fracturing and/or veining
  - deformation textures generally post-date mineralisation
  - collectively, textures are most consistent with fluid infiltration along zones of fracture-induced permeability
- Indirect dating methods
  - monazite recrystallisation related to hydrothermal fluids
  - intensely mineralised heavy mineral bands
- Sulphur Isotopes
  - is variation in Cu-grade and sulphide composition reflected in isotopic composition?

Lower Roan basin geometry

- "pinch out" onto W basement ridge
- WNW-trending basement ridges
- inverted tilt blocks
- NNE-dipping growth fault array

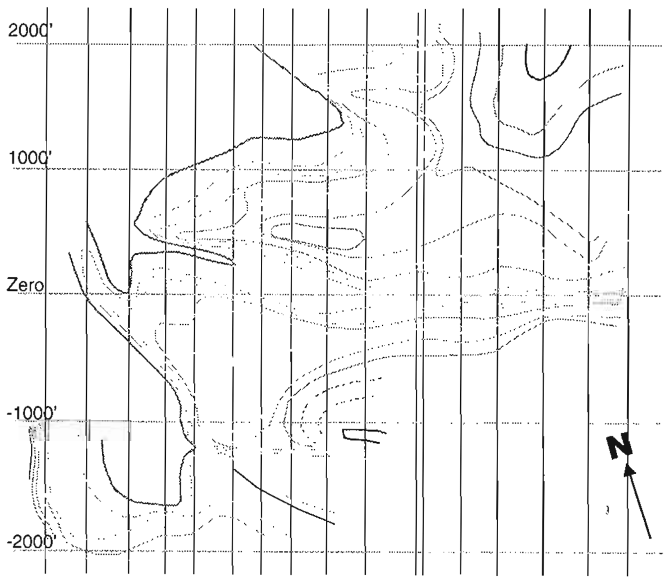

Cu ore body thickness

- Ore located at periphery of basement ridges
- Central zone symmetrically distributed about basement 'tilt block'

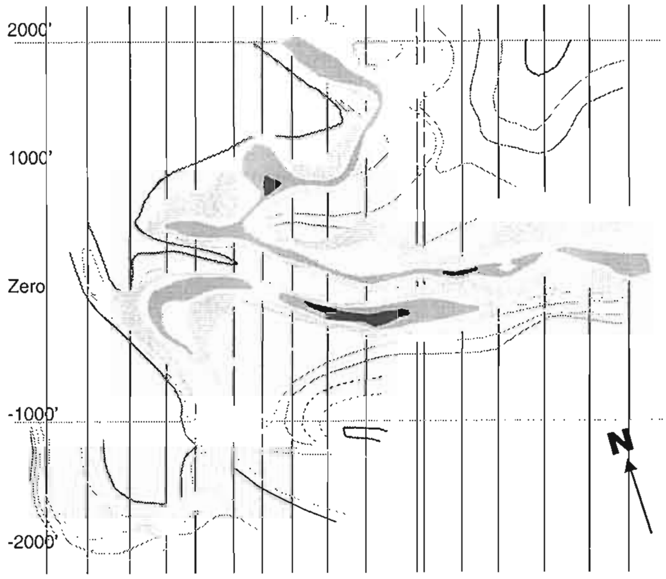

Cu ore body thickness - Fault Geometry

- Close association of thickness maxima and major fault zones
- Position of faults defined in part by abrupt thickness changes

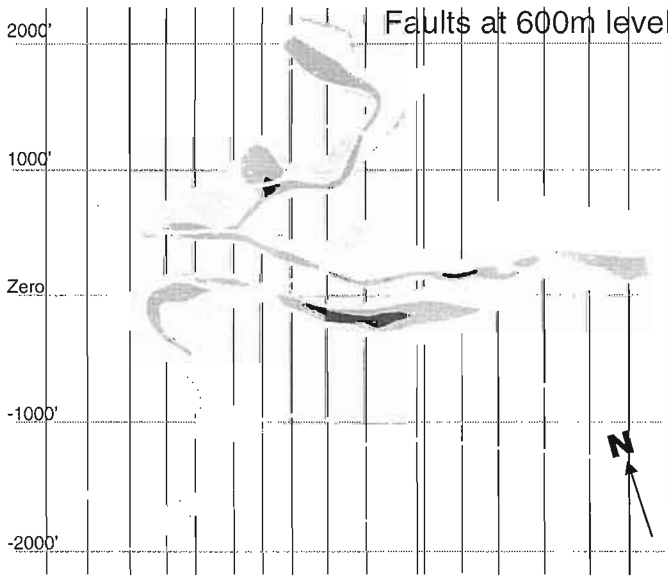

Cu ore body thickness - Fault Geometry

- Thickness maxima on southern side of 'Zero Ridge' coincides with footwall cut-out thrust

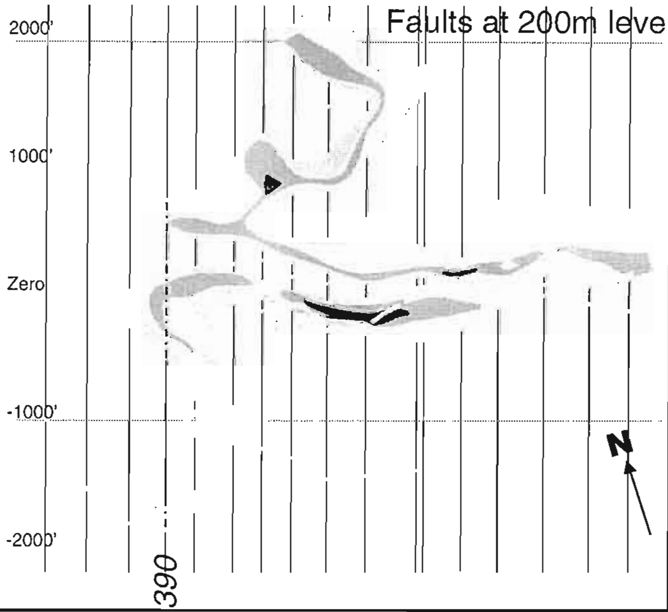

390 Section

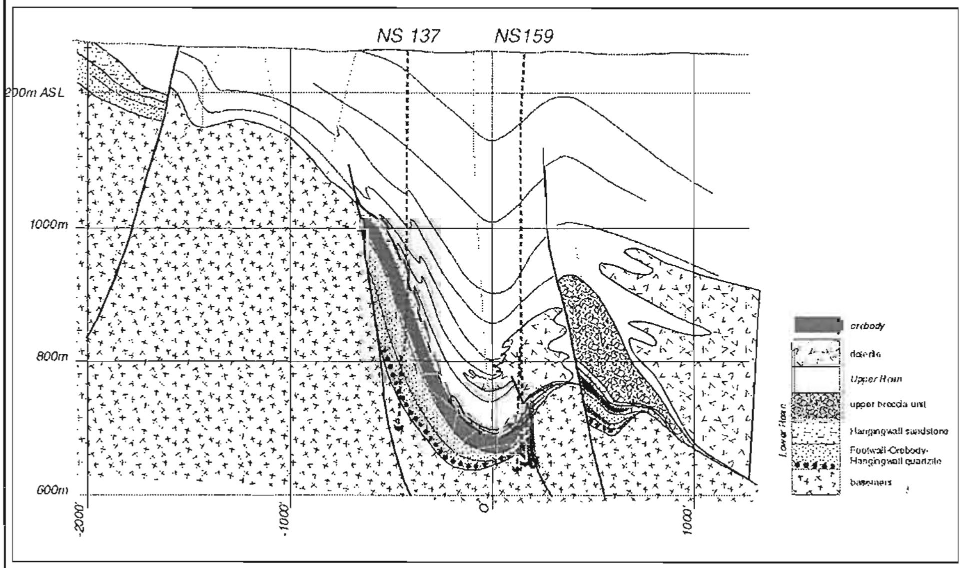

NS137 Cu-Co distribution

- 157' down hole intersection
  = 66' true thickness
- sampling interval 2'-4'
- lower Cu-rich orebody (45' true thick)
- upper Co-rich orebody (6' true thick)

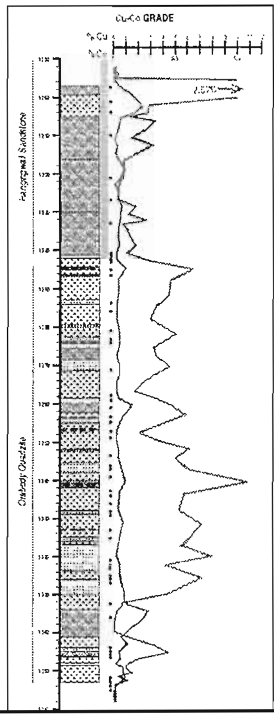

NS137 Cu-Co distribution

Cu orebody

- matrix-poor sub-arkosic sandstone
- heavy mineral bands
- top coincides with abrupt facies change to matrix rich arkose
- no obvious lithological contrast at base
- stratiform (banded), massive & disseminated
- Cu grade symmetrically disposed about 3' @ 10.8% peak at 1300'
- additional peaks coincide with layer-parallel, cm-scale massive sulphide intervals
- broad coincidence of Cu and Co peaks (exception 1333'-1341')

Hangingwall Sandstone

Orebody Quartzite

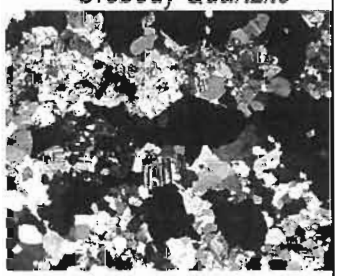

NS137 Cu-Co distribution

Cu orebody

- matrix-poor sub-arkosic sandstone
- heavy mineral bands
- top coincides with abrupt facies change to matrix rich arkose
- no obvious lithological contrast at base
- stratiform (banded), massive & disseminated
- Cu grade symmetrically disposed about 3' @ 10.8% peak at 1300'
- additional peaks coincide with layer-parallel, cm-scale massive sulphide intervals
- broad coincidence of Cu and Co peaks (exception 1333'-1341')

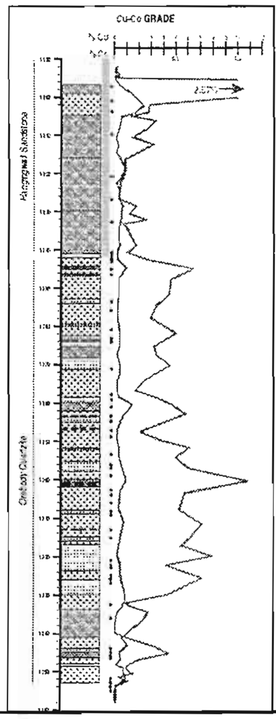

NS137 Cu-Co distribution

Co orebody

- typically concentrated within the upper parts of ore zones
- strong association with quartz-carbonate veining (chalcopyrite locally within veins)

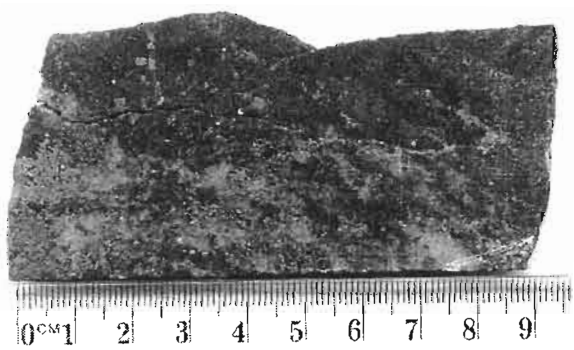

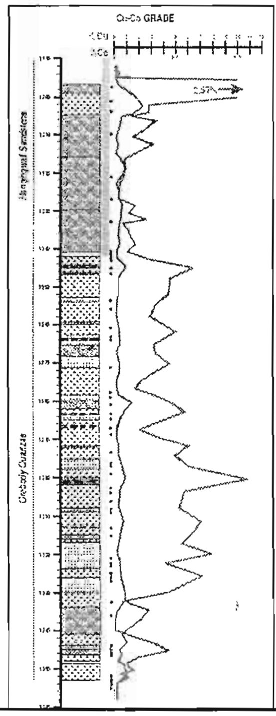

Can we analyse samples for Zn, Pb.

Vertical distribution of sulfide phases

Chalcopyrite

- dominant phase
- only Cu sulfide within upper ore body

Bornite

- erratic pattern
- broad correlation with Cu grade
- exception at high grade core

Pyrite

- very spiky
- good correlation with Cu grade peaks
- dominant sulfide within upper ore body

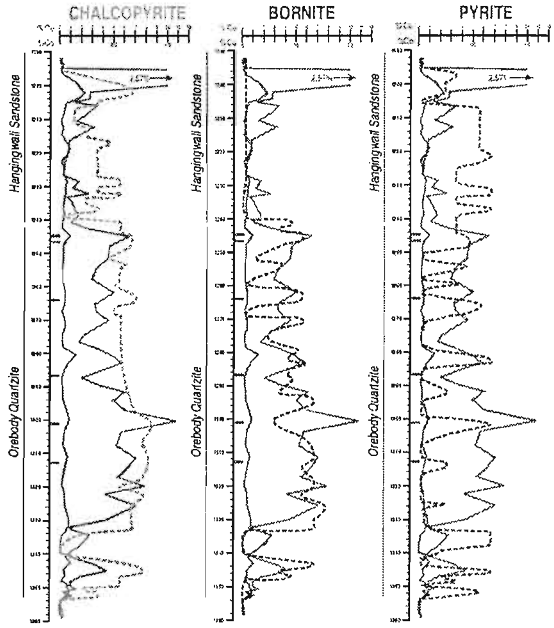

Distribution of non-detrital silicate phases

First Order

- albite-quartz-tremolite dominant phases within Cu orebody
- biotite-calcite prominent in Hangingwall Sandstone

Second Order

- antithetic relationship between albite and tremolite within Cu orebody
- strong correlation of albite with Cu, Co and pyrite peaks

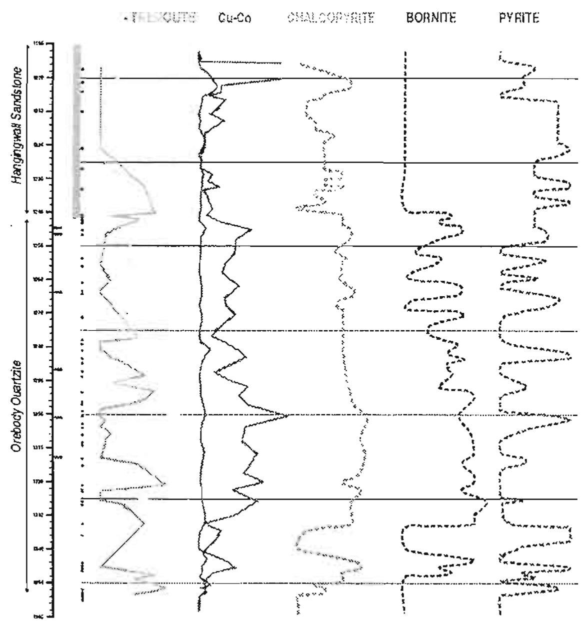

Vertical Sulphide Zonation

- Broad scale zonation from cpy-py-carr-alb within core to bn bearing assemblages at periphery
- second order zonation at periphery
- true thickness 5'

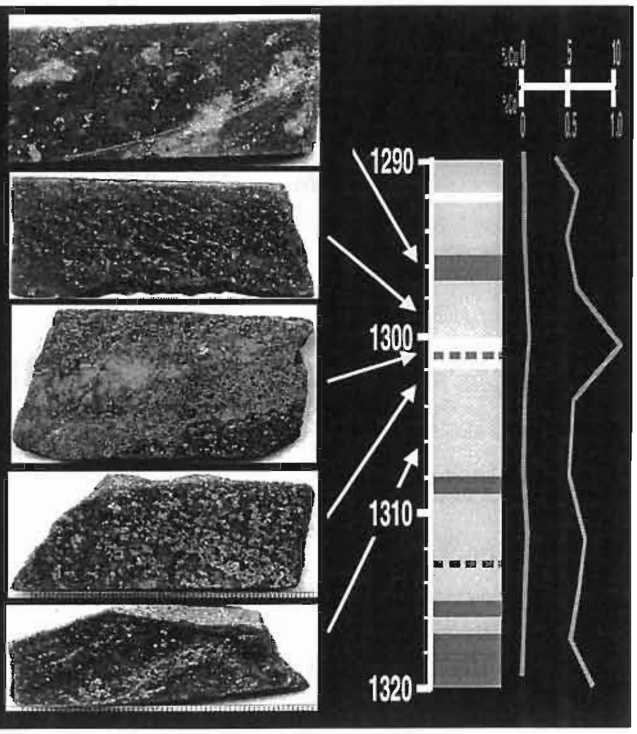

2nd Order Sulphide Zonation

- cm-scale rhythmic banding of sulfide phases
- Fe-rich sulfides partitioned into stratiform albitic domains
- Bornite +/- tremolite becoming dominant at peripheries

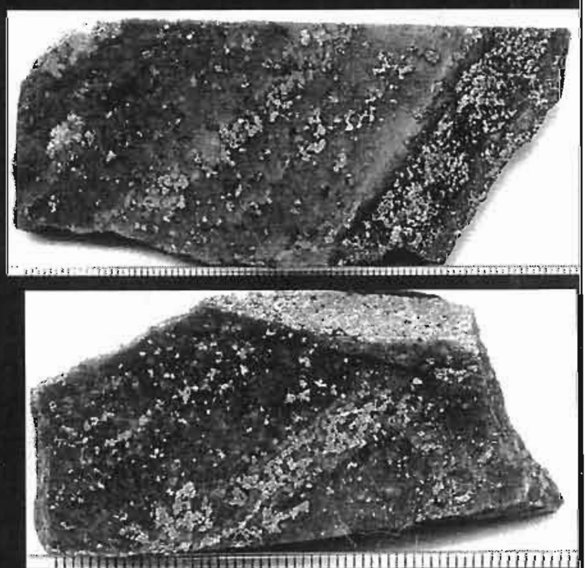

Albite-Sulfide-Heavy Mineral Association

zircon
monazite
tourmaline
huttonite
rutile

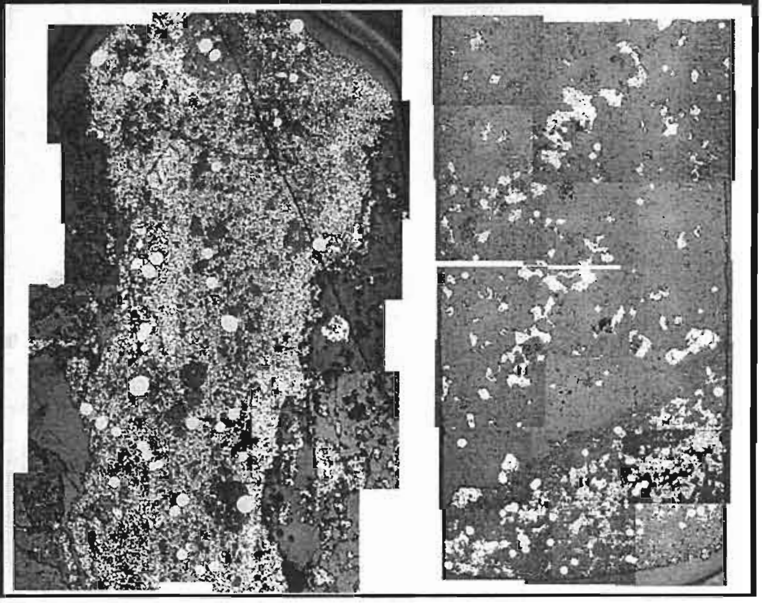

Albiltic Domains: Fluid Influx Zones

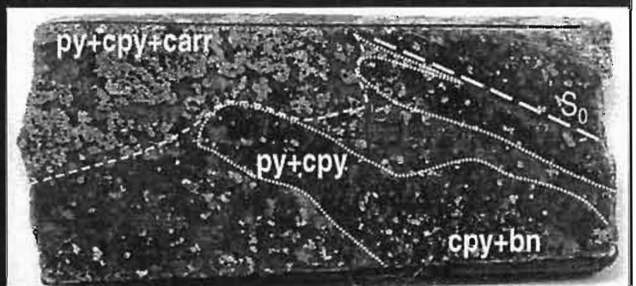

- Albitic zones locally cross-cut primary layering
- Albite and sulfides "bleed" into layer-parallel seams
- Metasomatic alteration products
- Sulphide zonation relates primarily to cross-cutting albitic zone: evidence for genetic association of various sulphide phases and textures

Albiltic Domains: Fluid Influx Zones

Peripheral domains
- spatial association of sulfides and albite

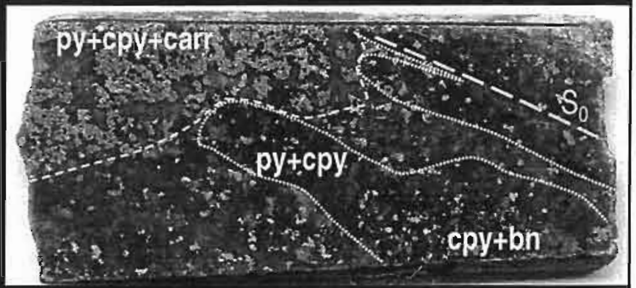

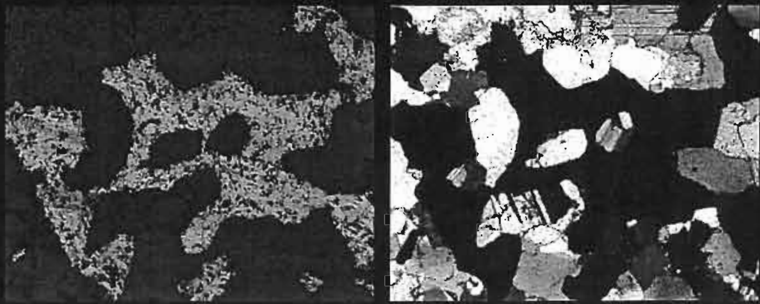

Sulphide Paragenesis

- Simple, consistent sulphide paragenesis

pyrite ⟶ carrollite ⟶ chalcopyrite - chalcopyrite + bornite

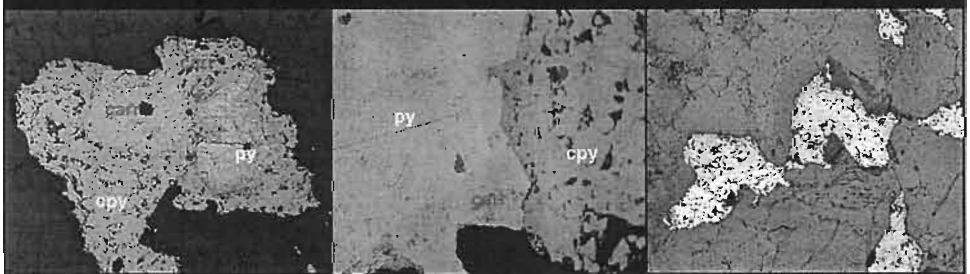

- Fe-rich phases partitioned within the cores of fluid influx zones
- Bornite concentrates at fringes of fluid pathways

Nature of fluid pathways

- Are fluid pathways controlled by primary porosity and permeability (syn-diagenetic) - or can we find evidence for strain-induced secondary permeability (late diagenetic - epigenetic)?

Heavy Mineral Bands: Ore Zone

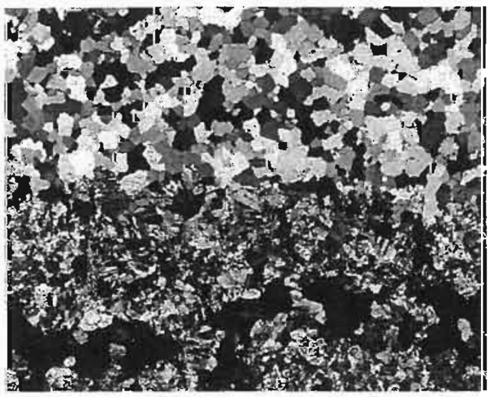

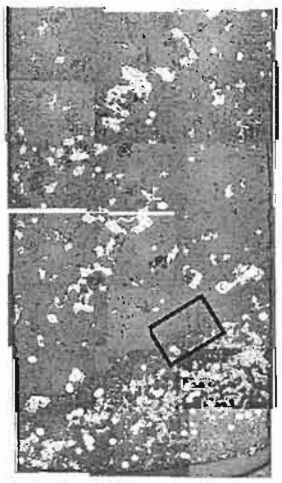

- Sharp margins of albitic domain
- Pervasive microfracturing
- Loss of detrital texture in quartz domain
- Healed microfractures in quartz at edge of albitic domain

Heavy Mineral Bands: Footwall

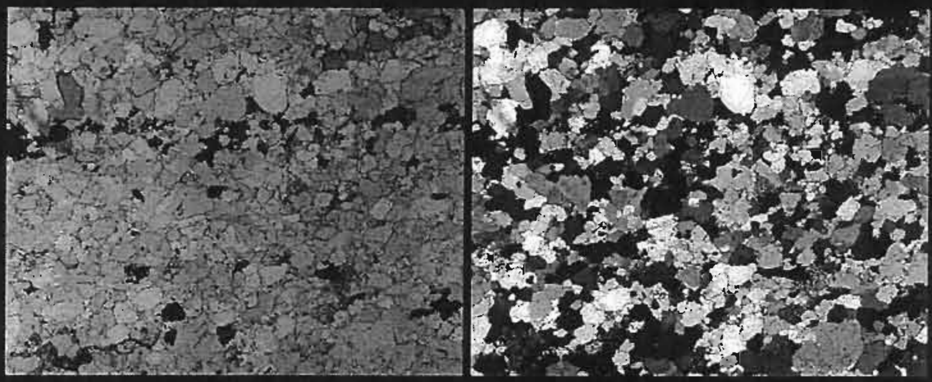

- reduced in grainsize in heavy mineral bands
- possible increased original clay content
- subtle permeability contrast with neighbouring siliciclastic domains

Fluid Pathways: Grain-scale deformation

- microfracture arrays concentrated within albitic cores
- healed microfractures at immediate peripheries
- minimal displacement
- loci of tourmaline growth
- post-date albitisation

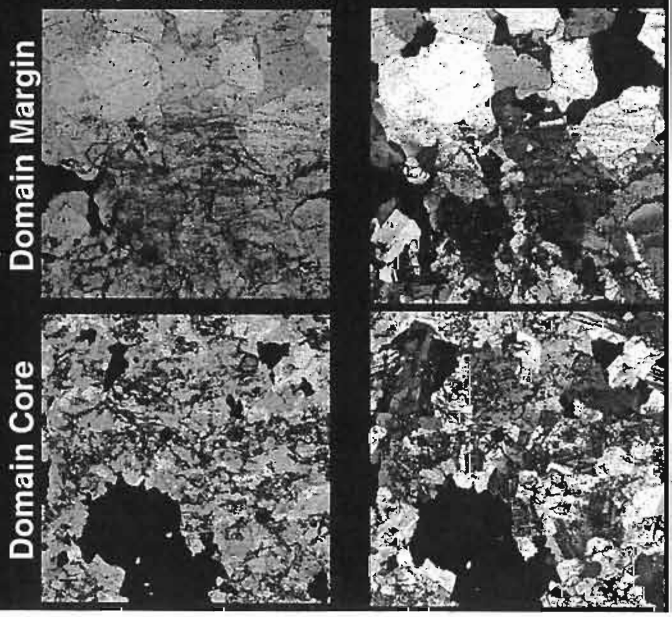

Fluid Pathways: Grain-scale deformation

- grain-size reduction via fracturing
- no displacement or rotation

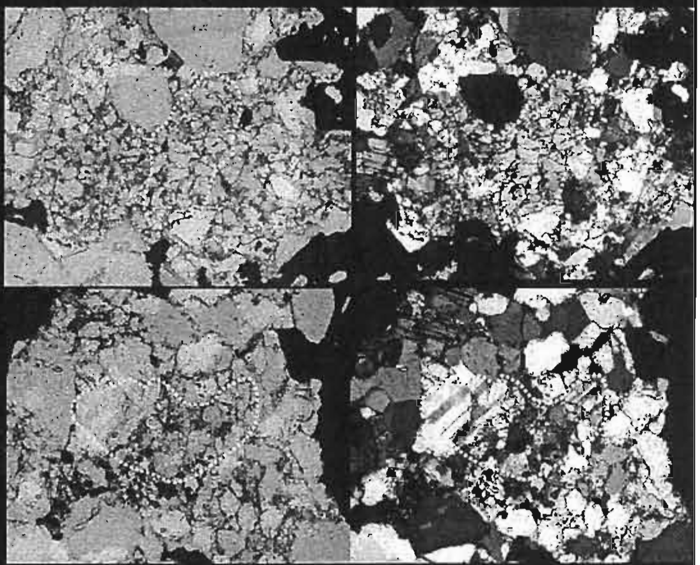

- shear fractures in albite
- overgrowth by quartz and tourmaline

Fluid Pathways: vein association

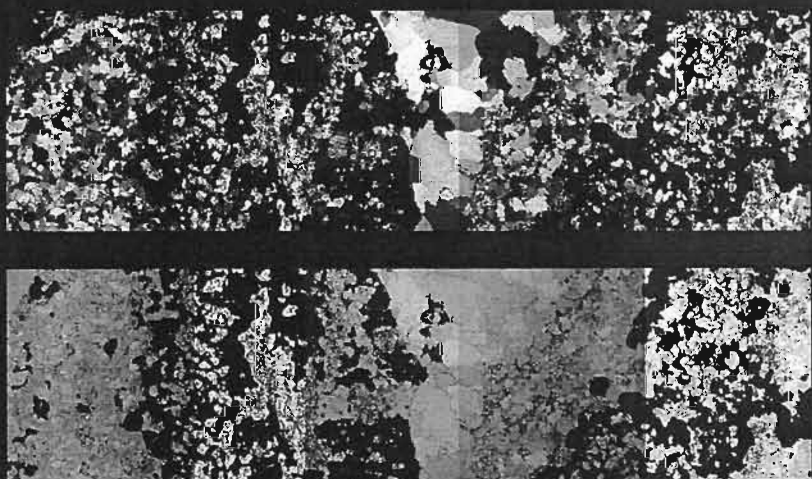

- Common spatial association of quartz veins with the cores of albite-sulfide domains
- in all cases, veins demonstrably post-date albitisation

Fracture-controlled albite-sulfide zones

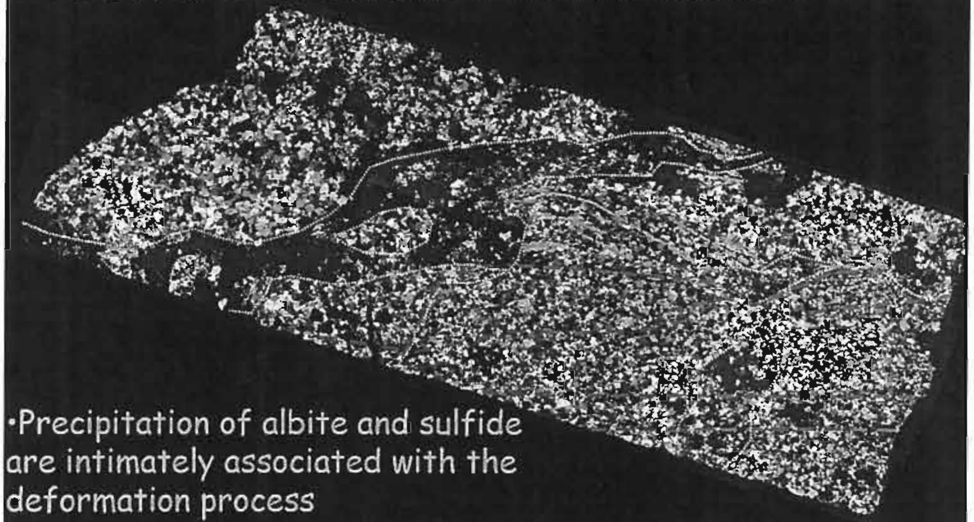

- Precipitation of albite and sulfide are intimately associated with the deformation process
- albite and sulfides concentrated within cross-cutting shear zones and fracture arrays

Fluid pathways: systematic fracture array

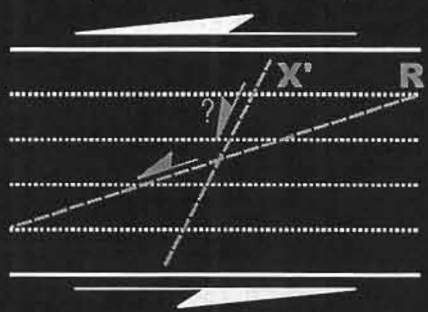

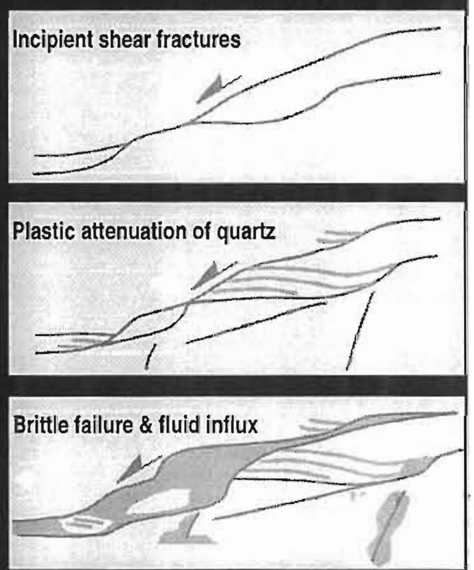

- fracture geometry developed during layer-parallel attenuation/shear
- partition of strain into dilational jogs
  - plastic deformation: attenuated quartz
  - brittle deformation: fluid influx

Chemical Dating of Monazites

Rationale

- monazite recrystallisation can occur at relatively low temperatures (<300°C) in the presence of a hydrothermal fluid
- fluid infiltration coincides with heavy mineral bands
- potential to constrain age(s) of hydrothermal fluid

Method

- electron microprobe U-Th-Pb chemical dating
- assumption that all lead is radiogenic: ie. inheritance of "common Pb" is insignificant
- knowledge of relative abundances of elements within the system, decay constants for Th and U, allows age calculation
- high spatial resolution: 1 micron spot size - reduces "mixing" effects

Results

- greatly increased abundance of monazite within ore zone compared to footwall (sample separated by 170')
  - 2 grains in footwall (1 sample) cf. Average 24 grains within ore zone (2 samples)
    1) change in provenance
    2) enhanced growth of non-detrital monazite within ore zone
  - data required from stratigraphically equivalent, unmineralised holes

- ore zone monazites have anomalously low Th
  - typical of hydrothermal monazite
  - Pb contents are consequently low (43% of 175 analyses at or below detection Pb: 120ppm)
  - very high error ranges within the ore zone
    - 4% of data from ore zone returned 1sigma errors <10% of calculated age (166 spots)
    - data from footwall returned 1sigma errors 3-9% of calculated age (9 spots)

Th* - Pb Abundances

Footwall
- 2 populations
- high initial Th contents

Ore Zone
- comparatively low initial Th
- outliers:
  - high Pb indicating older age
  - high Th anomalously young age

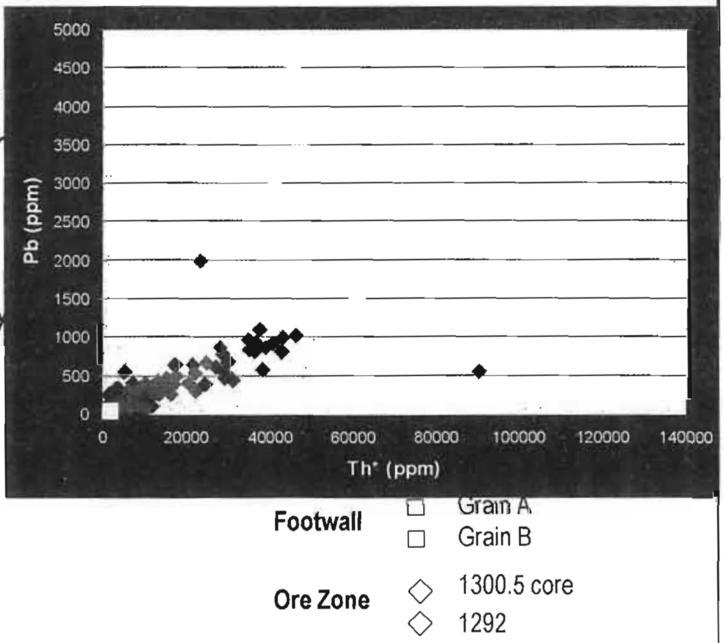

Footwall

Detrital Grain
- regular compositional zoning
- 3 age populations
  - 2045Ma
  - 1600Ma
  - 1162Ma
- ages do not correspond to compositional zones

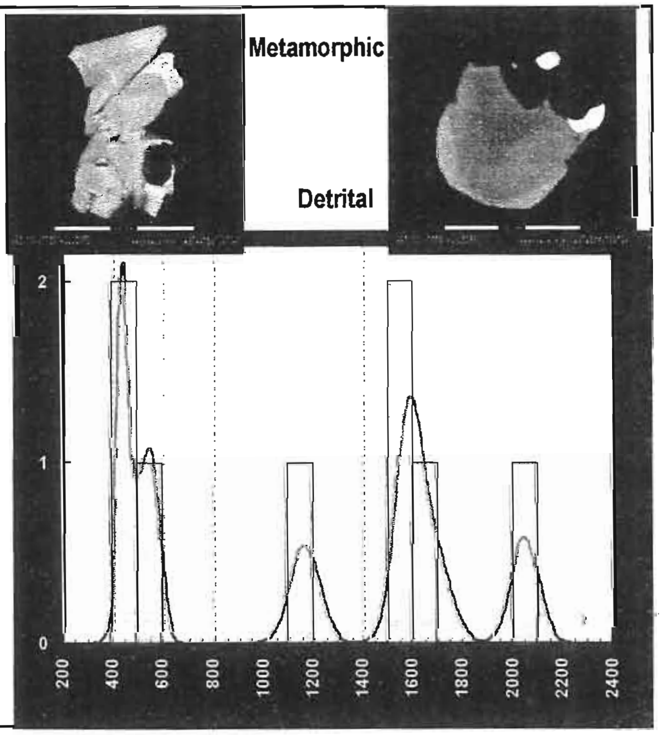

Footwall

Metamorphic Grain
- irregular habit
- subtle zonation at margins
- 2-sigma error - single age at 463+/-32Ma

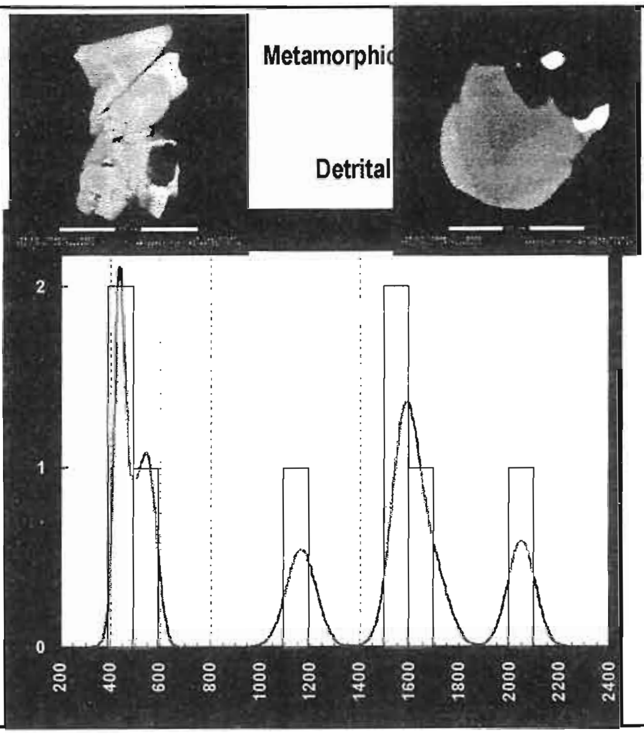

Ore Zone

- Very broad range of calculated ages
- 500Ma peak on probability curve

- 99% fit a single isochron:

  500 +/- 42 Ma

  - slope strongly biased towards data > 200ppm Pb

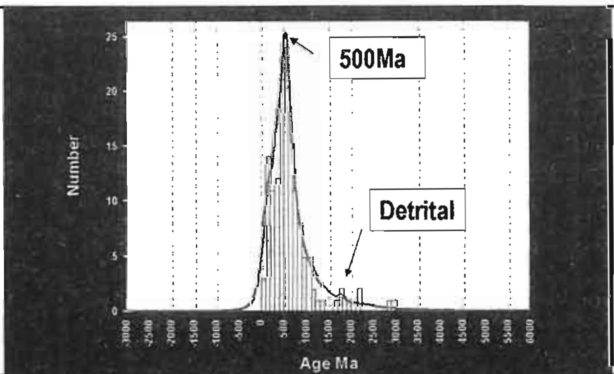

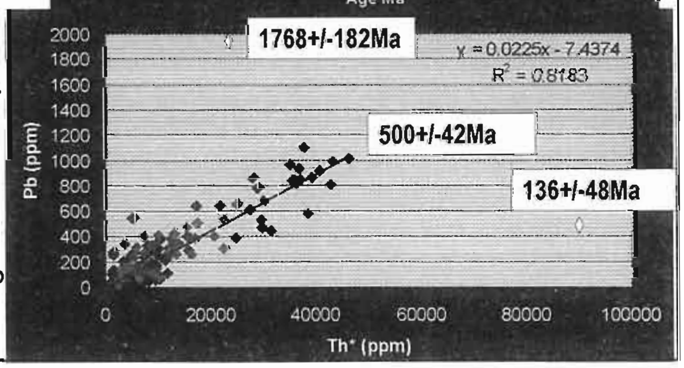

Internal Zonation of Monazites

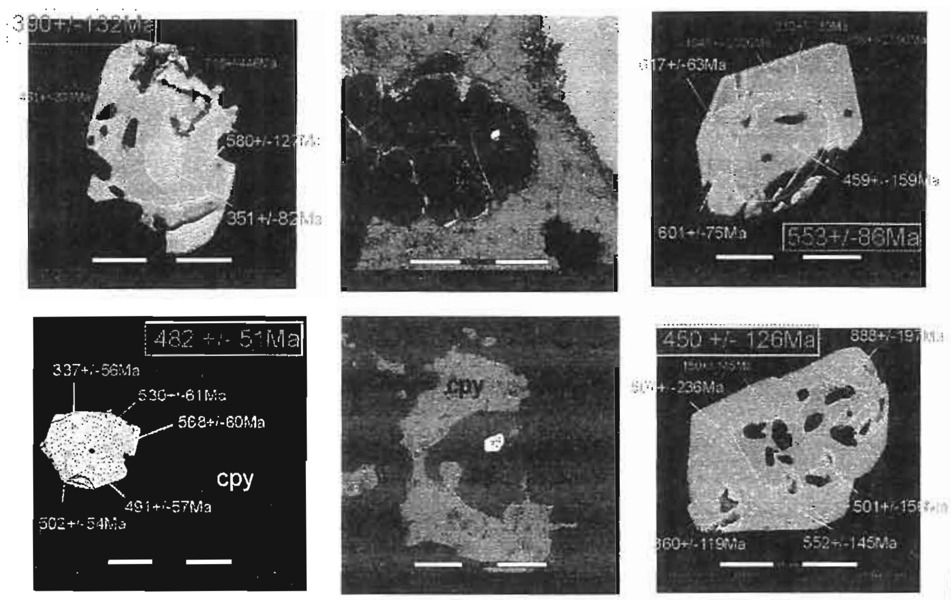

* spot ages quoted with 1 sigma error - weighted means with 2 sigma error

Summary

- Cu ore body situated at periphery of sub-basins; coincidence with major fault zones
- fluid infiltration was focussed mainly along layer-parallel seams (common association with heavy mineral bands)
- cores of fluid pathways: albite, pyrite, carrollite, chalcopyrite
- peripheries of fluid pathways: chalcopyrite, bornite, tremolite

Summary (cont.)

- fluid pathways form the loci for post-mineralisation strain
- syn-kinematic fluid infiltration is demonstrable rarely

- monazites within the ore zone are chemically distinct from those within the footwall
  - higher initial Th within footwall grains
  - low Th contents within ore zone are consistent with hydrothermal growth/recrystallisation
- 99% of ore zone grains conform to a 500Ma isochron
  - significant proportion have Th values to low to accurately constrain ages
  - textures indicate multiple recrystallisation phases
- textural relationships support Lufilian growth of albite and sulphides

Conclusion

Collectively, evidence from macro-scale ore/fault relations, grain-scale textural & geo-chronological studies favours a structurally controlled, epigenetic origin for at least part of the Chibuluma West deposit

- during folding, competency contrast between the matrix-poor *Orebody Quartzite* and matrix-rich *Hangingwall Sandstone*, led to strain accumulation along the contact

- shear and/or dilatancy was focussed along heavy mineral bands within the rigid lower unit, providing secondary permeability

- fluids were focussed along inverted basin-bounding growth faults (and possibly new footwall cut-out thrusts), and into a permeable (and potentially chemically favourable) horizon at the top of the *Orebody Quartzite*

Sulfur isotope systematics of the Chibuluma West Cu-Co deposit

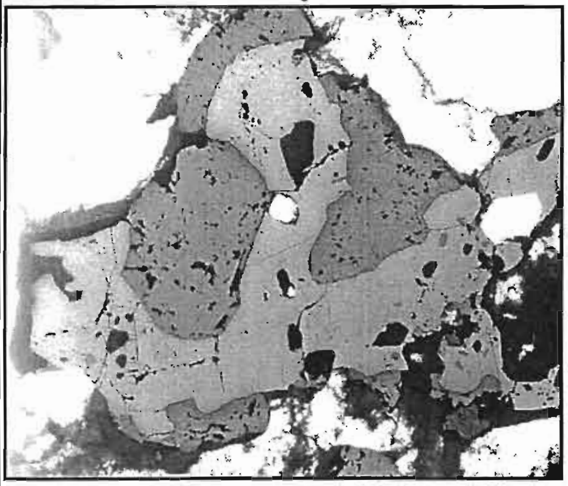

David Cooke
& David Selley

Centre for Ore Deposit Research

Fig. 17

Cp & py in quartzite - NS137 1300.5 ft

Rationale

- Test whether observed mineral zonation at Chibuluma is matched by S-isotope zonation
- Contrast results with other studies of sulfur isotope systematics in the copperbelt
- Implications for metal transport & deposition

Cp & py - NS137 1346 ft

Copperbelt - Sulfur Isotopes (D&J '65)

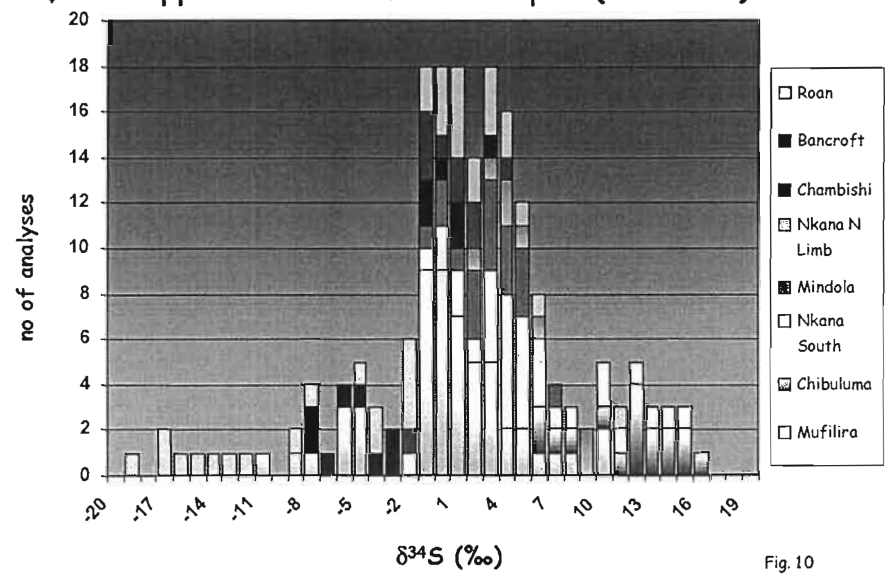

Fig. 10

Sweeney (1986)

- Konkola S-isotopes attributed to bacterial reduction of seawater sulfate (~17‰)
- Correlation between S-isotope compositions and stratigraphic position (transgressions & regressions)
- No evidence for metamorphic reequilibration
- Early diagenetic timing of sulfate reduction and metal deposition

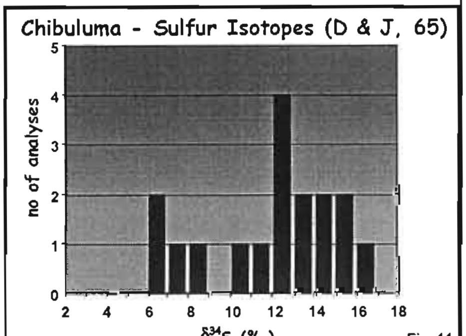

Fig. 11

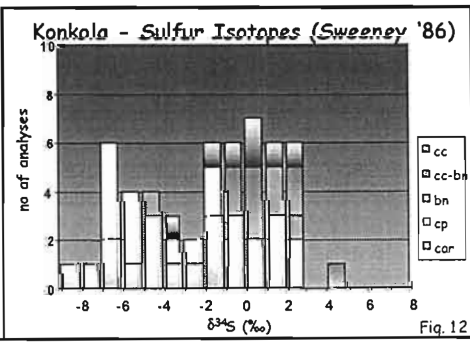

Fig. 12

Sweeney (1986) - Strat. Control

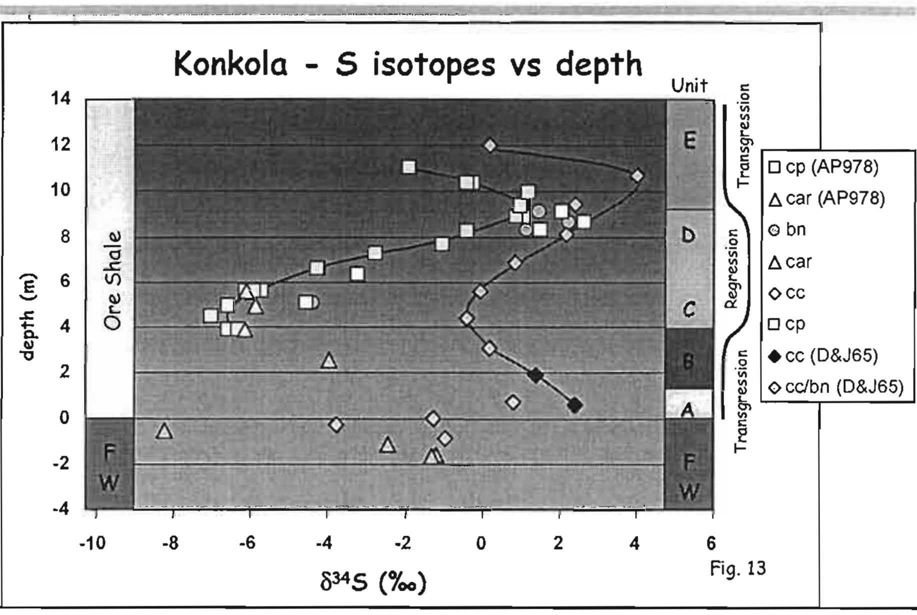

Fig. 13

Hitzman (2000) - Epigenetic Model

- Isotopic values at Chambishi are heaviest in fault zone (+4 to +5‰)
- Values decrease to -8‰ within 10m of fault zone
- Pyrite S-isotope values above mineralised ore shale are typically negative (-5 to -7‰)
- Sulfate $\delta^{34}S$ values at Chambishi are +20.5 to +22.6‰

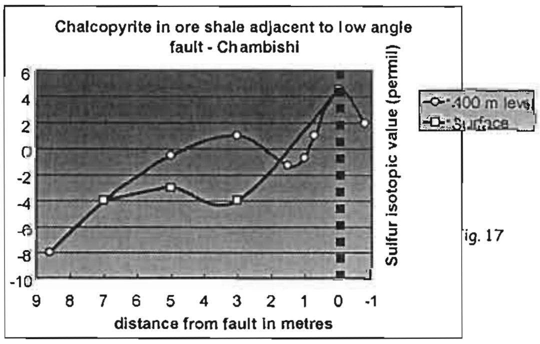

Fig. 17

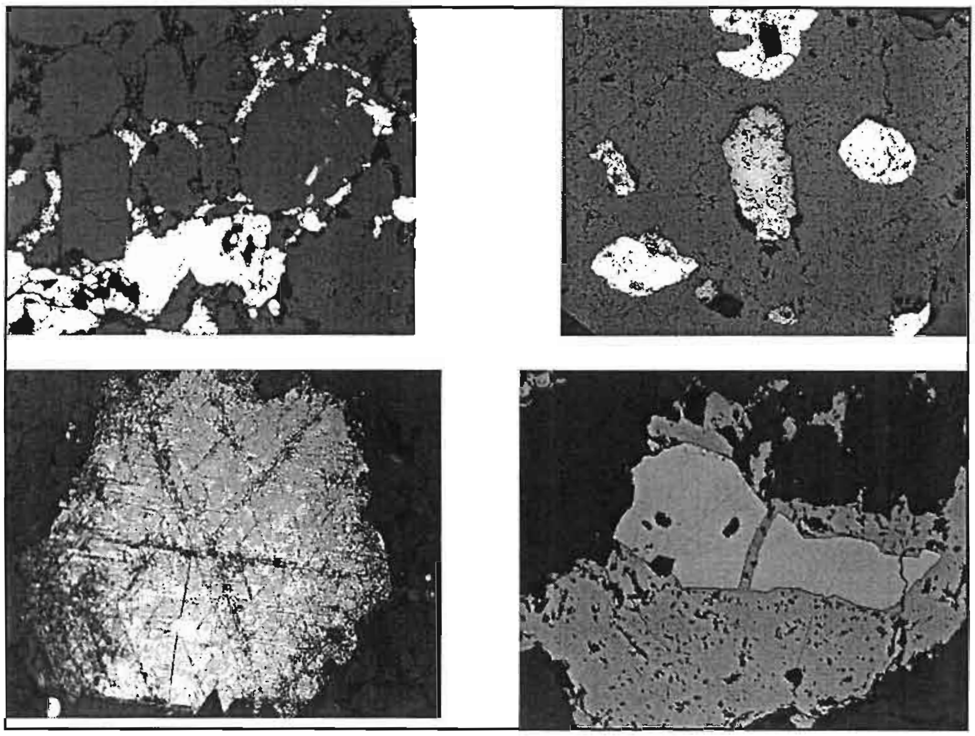

Chibuluma - Laser Ablation Results

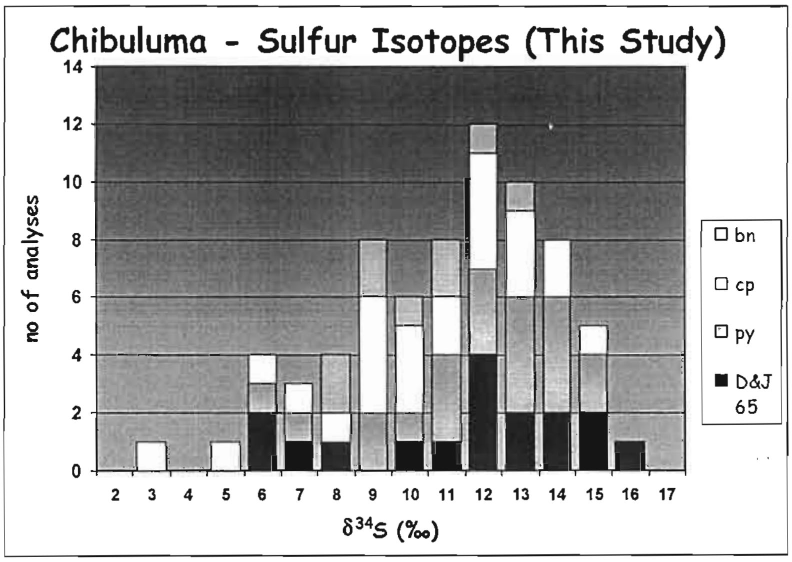

Chibuluma - Grade vs $\delta^{34}S$

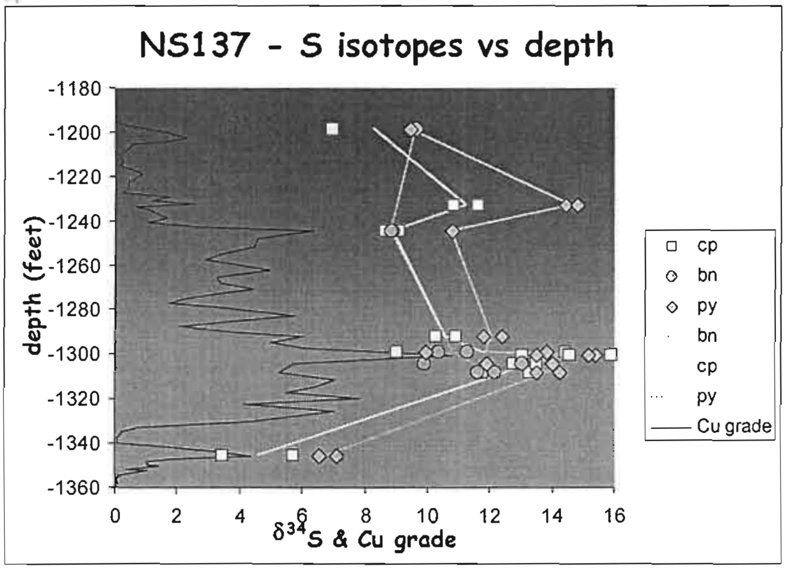

Chibuluma - Grade vs $\delta^{34}S$

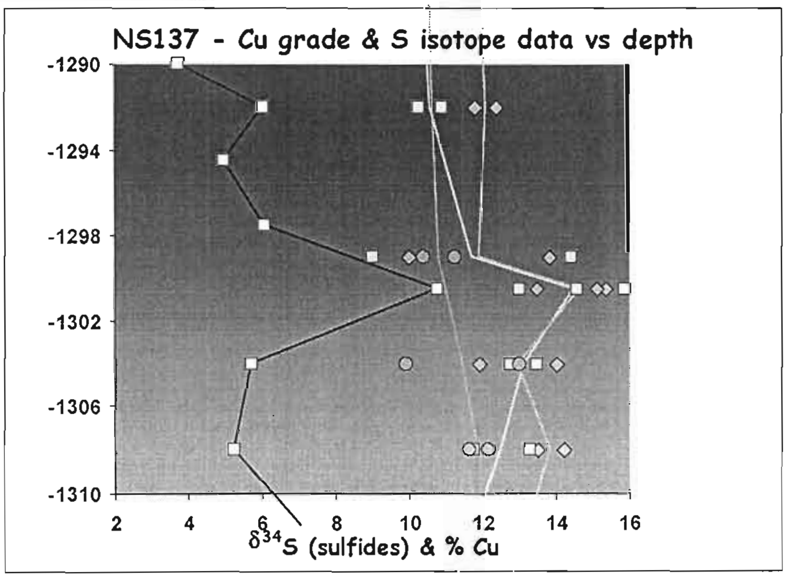

Summary

- Some correlation between observed mineral zonation and S-isotope zonation (structural control?)
- Thermochemical sulfate reduction or decomposition of organic matter to generate $H_2S_{(g)}$?
- Bacterial S-reduction not feasible at Chibuluma
- Different processes operating at different deposits?

Py with cp & car inclusions, & cc after bn - NS137 1198.5 ft

Sedimentology, mineral paragenesis and geochemistry of the Konkola North Copper deposit, Zambia

Nicky Pollington

Why Konkola North?

- Unaffected by strong penetrative deformation and lack of obvious hydrothermal alteration
- Hence primary sedimentary textures preserved throughout the host sequence

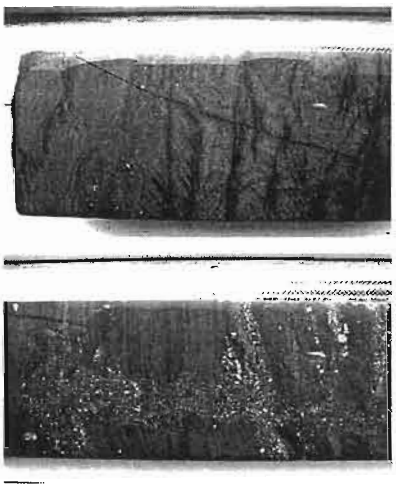

Why Konkola North?

- This provides the opportunity to study:
  - Environment of deposition of sediments and burial history
  - Primary sulphide textures and therefore paragenesis
  - Geochemistry of ore formation

Location

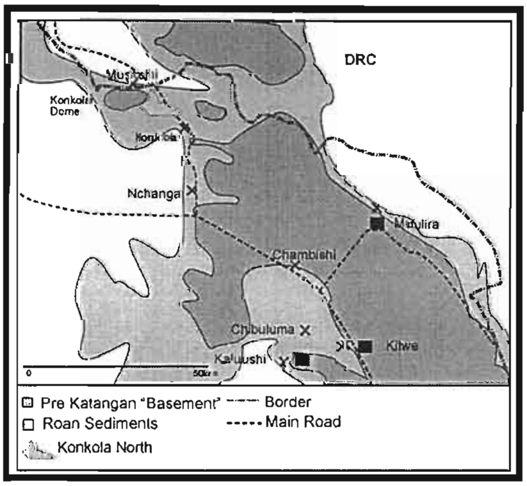

General Geology

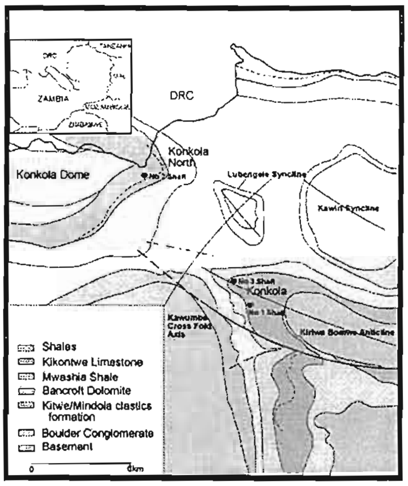

After Sweeney and Binda, 1989

Generalised Stratigraphy - Konkola North

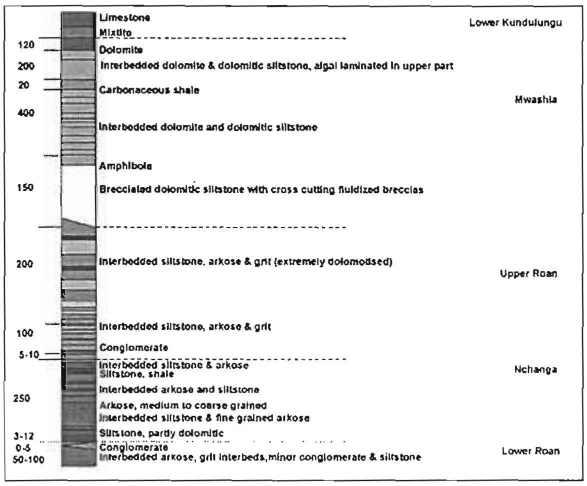

After AVMIN internal Report

What was the sedimentary environment for the different sedimentary packages? (Can we develop facies models to help guide exploration?)

- Method
  - Detailed logging and petrographic examination of the Konkola North drilling
  - Emphasis on host sequence - also correlating this with stratigraphic holes and others work to put into the broad picture
- Work to date follows

Konkola North drill holes

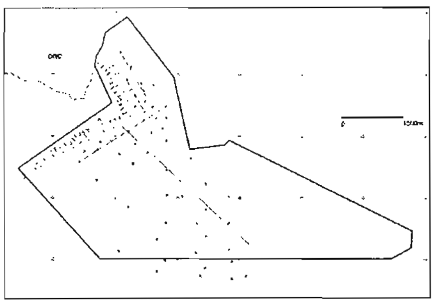

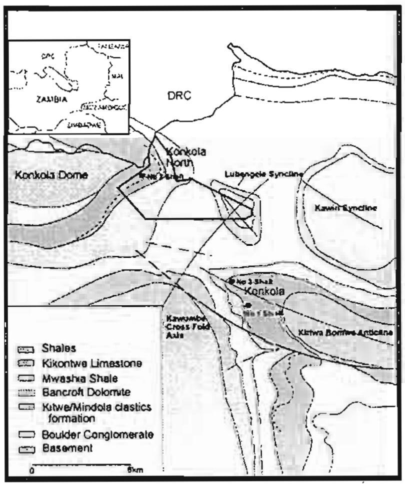

Detailed logging

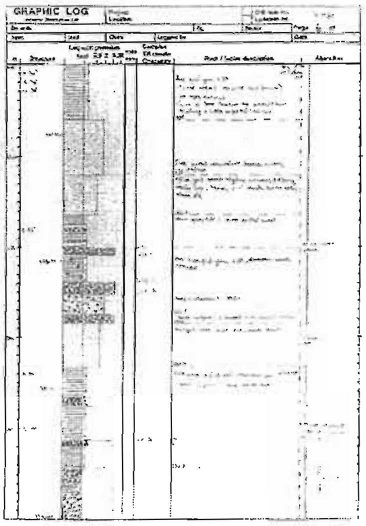

May 2002

AMIRA P544

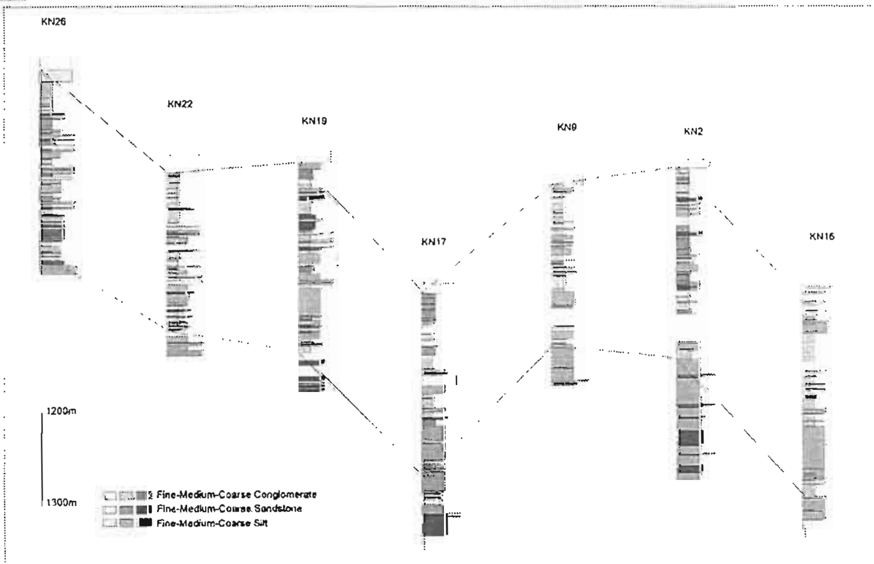

May 2002

AMIRA P544

Host sequence

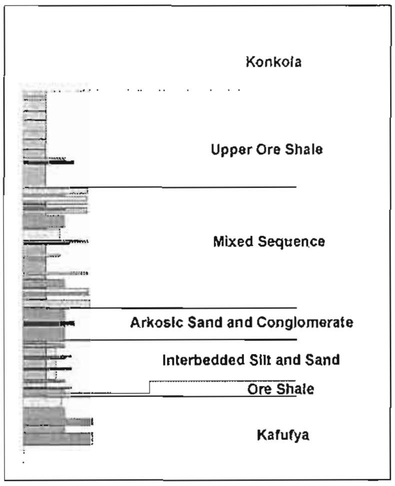

May 2002 AMIRA P544

Kafufya

- 50 - 100m
- Polymict conglomerate - med sand
- Qtz, fspar, sand, mud, qtzite
- Large scale cross bedding
- Leached and oxidised
- Abundant dissolution casts - Porous
- Majority of drilling finished 30m into this
- Coarser and more polymict in East
- Finer and more uniform in south

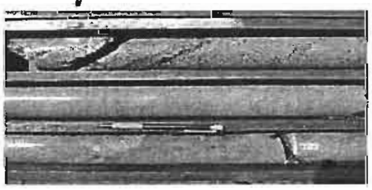

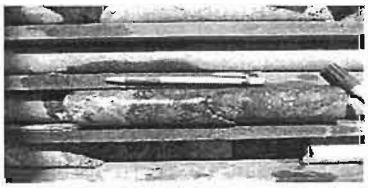

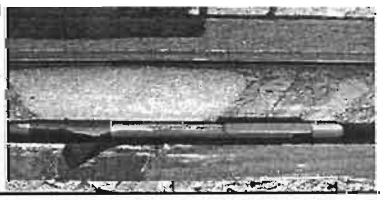

May 2002 AMIRA P544

Ore Shale

- 3-12m
- Abruptly overlies Kafufya
- Fine dark siltstone
- Microcline, kspar, qtz and dol
- Numerous fine upward fining sequences
- Predominantly very fine grained 65% <75microns

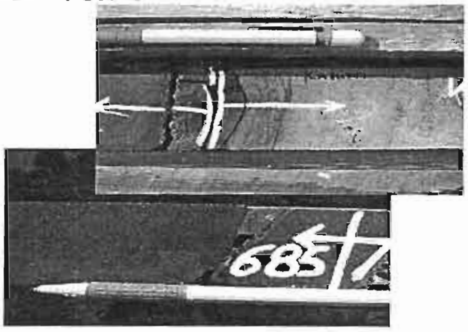

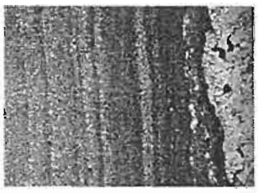

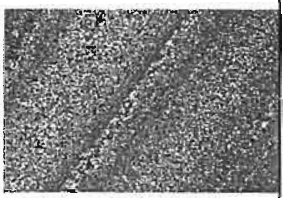

May 2002 AMIRA P544

Interbedded Silt and Sand

- 5-30m
- Interbedded med grey silts and med salmon sands
- Gradationally overlies Ore Shale
- Dewatering and load and flame structures common

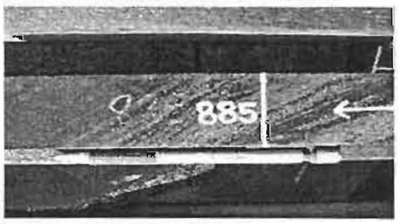

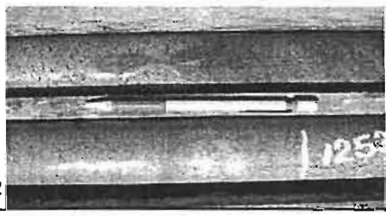

May 2002 AMIRA P544

Arkosic sand - Conglomerate

- 3-200m
- Med arkose - fine qtz fspar conglomerate
- No silt interbeds
- Extensive kspar alteration

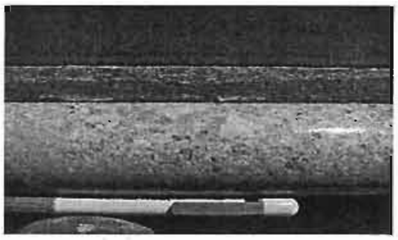

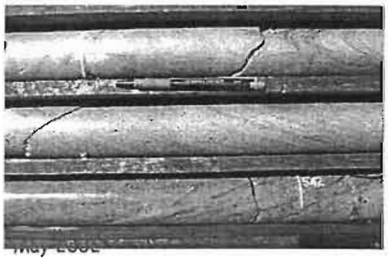

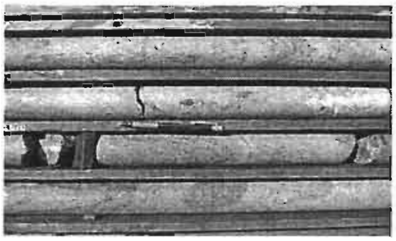

Mixed Sequence

- 80-300m
- Interbedded med conglomerate - med to coarse sands - subordinate siltstone - dolomite

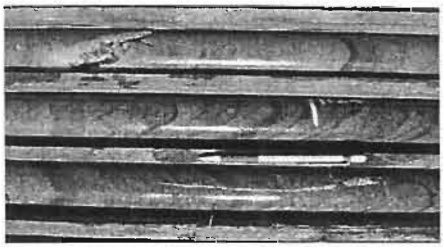

Upper Ore Shale

- 0-50m
- Fine dark siltstone
- Very similar appearance to OS1
- Soft sediment folding/crumpling at top and base
- Abundant pyrite and chalcopyrite
- Commonly intensely weathered

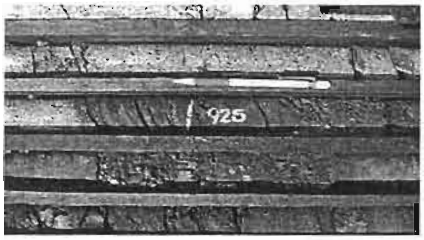

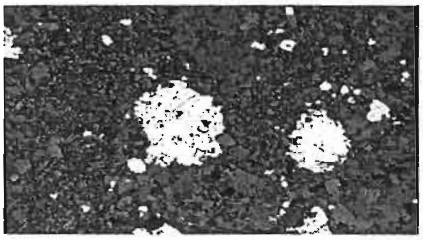

Konkola

- 0-25m
- Pebbly conglomerate
- Dominantly qtz and kspar clasts
- Med sand matrix

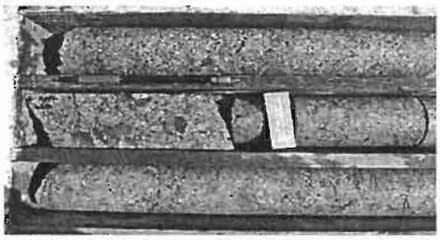

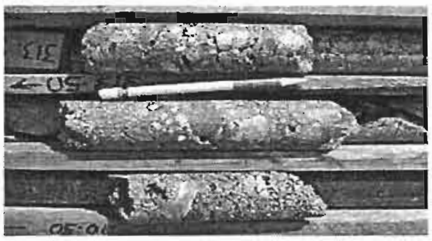

What does it all mean?

- Abrupt change of facies from the ore shale - sudden transgression but maintenance of clastic source
- Intermixing of mud and sand sequences indicates a possible mid fan delta position

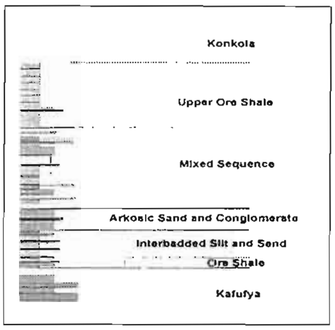

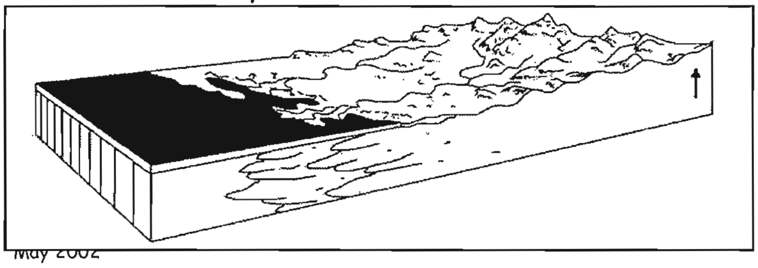

Mineral zoning within Konkola North Deposit

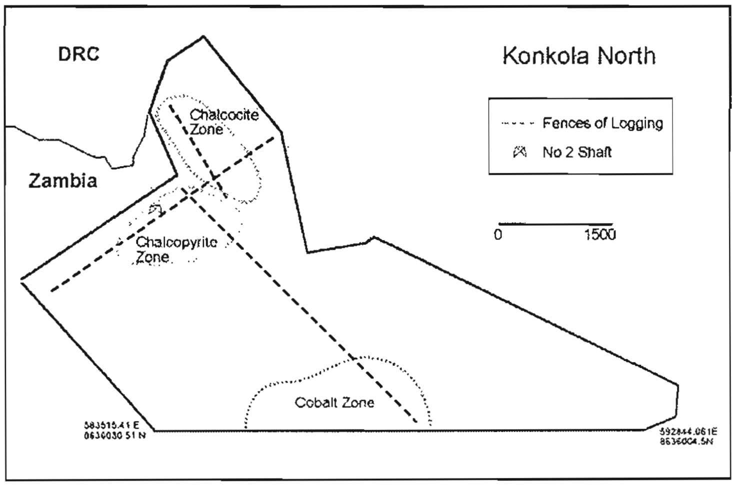

Ore Characteristics - East

- Cc and Bn dominant
- No iron oxides
- Specular Hm and red Hm stain throughout
- Mineralisation tends to start 1-2m above Kafufya/Ore Shale contact
- Primary Cc present
- Dark grey, fine silts

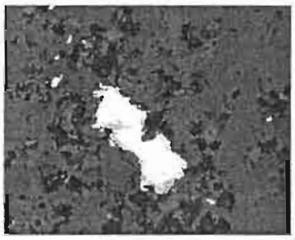

May 2002 AMIRA P544

Ore Characteristics - South

- Cpy and Py dominant, Bn common
- Secondary Cc
- Mineralisation starts on the contact
- Iron oxide concentrated on fractures and on the Kafufya/Ore shale contact
- Mod to intense leaching throughout

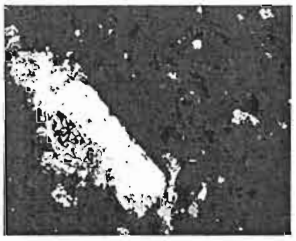

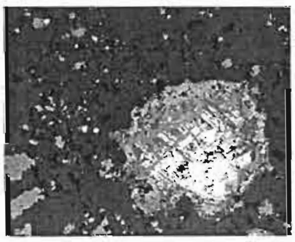

May 2002 AMIRA P544

Ore Characteristics - Far south

- Entire ore shale leached
- Common copper oxides below the Kafufya/Ore Shale contact
- "Wad" is common

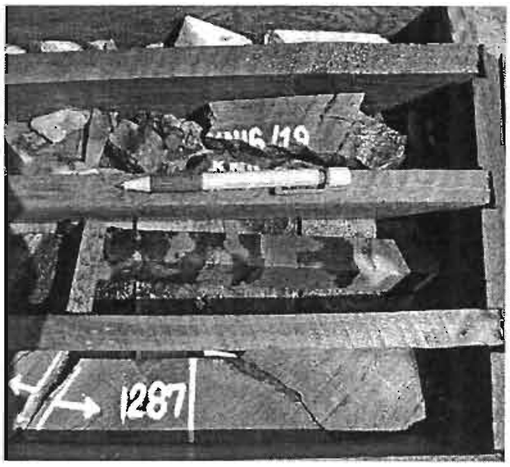

Future Work Plan 2002-2003

- Complete sedimentary logging including stratigraphic holes
- Document the various alteration types and their relative age relationships and stratigraphic distribution
- To use lithogeochemistry to discriminate barren from mineralised ore shale/siltstones
- LA ICP geochemistry to distinguish supergene from hypogene Cc based on textural observations already made
- Document the distribution of mineralisation vertically and horizontally within the ore shale
- Geochemically characterise different mineralised zones
- Isotope studies of sulphide minerals in ore shale and upper ore shale (Pilot study completed before return to field)

Timing, character and paragenesis of Konkola copper ores

Robert Scott & Nicky Pollington
Centre for Ore Deposit Research
University of Tasmania

Introduction

- Copper mineralisation at Konkola
  - hosted by ≤12m thick succession of thinly bedded-laminated arkosic meta-siltstone, shale and sandstone (Ore Shale)
  - Cu-sulfides:
    - extremely fine grained, disseminated throughout host rock
    - m.-c.g. sulfides within bedding-parallel dolomite bands, and massive or fibrous lenticular aggregates and veins (upper half of Ore Shale)
- high degree of textural preservation (e.g. fine lithologic layering and sedimentary structures) and fine-grained nature of host-rocks and sulfides, suggest primary character of ores not significantly modified by deformation and metamorphism (Sweeny and Binda, 1989)

Aims

- Assess extent and significance of deformation within the Ore Shale
  - structurally-controlled epigenetic mineralisation?
  - structural up-grading of existing ores?
- Textural character and distribution of ore minerals
- Paragenesis of the Cu-ores:-
  - primary zonation within Ore Shale and the "chalcocite problem"

Subdivision of the Ore Shale at Konkola (#1 and #3 Shafts)

Unit	Thickness	Host Rock	Mineralisation
Unit A	0.6 - 1m	Finely inter-laminated grey siltstone and pink/brown carbonate	Erratic oxide mineralisation and chalcocite in streaks or laminae parallel to bedding (~1.5% Cu).
Unit B	1.4 - 2m	Grey to yellow/brown, relatively massive sandy siltstone	Uniformly disseminated fine-grained chalcocite, chalcopyrite and bornite (~5.5% Cu).
Unit C	0.9 - 2m	Finely laminated grey siltstone with common calcareous horizons up to 4 cm thick	Chalcopyrite, bornite and chalcocite as fine disseminations, bedding parallel veins and lenticles (3-6% Cu).
Unit D	1 - 1.8m	Dark grey laminated siliceous siltstone, minor calcareous horizons	Similar to Unit C but more erratically distributed, sulfide lenticles more common (2.4% Cu).
Unit E	0.6 - 1.5m	Micaceous dark grey siltstone interbedded with brown feldspathic sandstone	Highly erratic chalcocite and minor oxide mineralisation (1.3% Cu).

Composition of the Ore Shale

- sandstone and siltstone layers:
  - (detrital) quartz + feldspar + white mica
  - interstitial sericite, biotite, carbonate, rutile (metasomatic or metamorphic origin)
- shale layers:
  - white mica, quartz, biotite, carbonate, rutile
- dolomite layers
  - grossly bedding parallel
  - carbonate "fronts" transect bedding locally
  - dolomite + quartz + feldspar ± mica

CODES / CSM AMIRA PROJECT P544 — MAY MEETING, 2002

Structural Setting

- Konkola in hinge region of WNW-plunging Kirila Bomwe anticline
- W-limb dips moderately to steeply W, N-limb dips <35-40°N at shallow levels, but steepens to >60° below 300 m

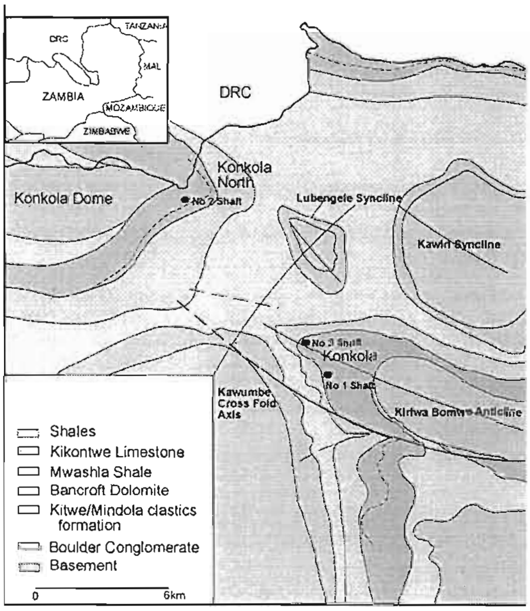

CODES / CSM AMIRA PROJECT P544 — MAY MEETING, 2002

Deformation within the Ore Shale

- rare asymmetric, open to isoclinal "intrafolial" folds (enveloped by ~planar bedding)
  - within or in association with dolomite bands
- late-stage disharmonic folds preferentially developed in Units A and E
  - slumping due to partial dissolution of the host rock?

Fabric development in Ore Shale

- grain-scale sedimentary textures modified by recrystallisation, dissolution at grain boundaries, and metamorphic/metasomatic mineral growth
  - detrital form of feldspar and muscovite grains generally well preserved
  - quartz extensively recrystallised in "clean" sandstone layers
- detrital muscovite
  - elongate grains, 1-3x diameter of qtz and feldspar grains in same layer
  - strong bedding-parallel alignment, esp. in sltst and shale layers

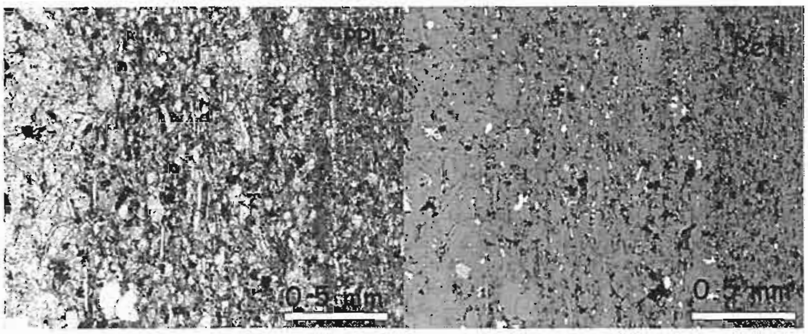

Sample K3-2, Ore Shale, Unit C

- bedding-parallel fabric principally defined by detrital mica
  - little or no associated alignment of metamorphic minerals
  - compaction, rather than tectonic fabric

Fabric development in Ore Shale

- (secondary) biotite
  - grains more equant and blocky than detrital muscovite
  - lacks preferred orientation except in carbonate-rich bands and fibrous veins where aligned *oblique to bedding*
- carbonate
  - equant to elongate grains in carbonate bands and fibrous bands
  - grain elongation *oblique to bedding*, but orientation variable over small distances

N.B. tectonic/metamorphic fabrics oblique to S_0 restricted to discrete layers or narrow bedding-parallel domains

Sulfide distribution and textural relations

- Disseminated sulfides
  - account for bulk of copper
  - interstitial to (?)replacive habit
  - grainsize similar to host sediments
    - not in hydrodynamic equilibrium with surrounding silicate grains ∴ not detrital
  - sulfides most abundant in coarser grained layers (up to 30% of thin layers)
    - grainsize (porosity) control on influx of Cu-fluids

Constraints on Cu introduction

- distribution of f.g. disseminated sulfides most consistent with
  - replacement of detrital or precursor diagenetic minerals, or
  - in-filling primary or secondary intergranular porosity
- present low apparent porosity of thin, commonly Cu-sulfide-rich sst layers suggests Cu introduced prior to recrystallisation (devel. of interlocking grain mosaics) under greenschist facies conditions

CODES / CSM AMIRA PROJECT P544 — MAY MEETING, 2002

blebby or lenticular sulfide aggregates and bedding parallel veins

- elongate m.-c.g. sulfide grains and aggregates within dolomitic bands or intergrown with qtz, carbonate, mica grains (relict fibres) in veins and lenticular aggregates
- grains aligned at moderate- to high-angle to bedding
- irregularly developed throughout Units C-E of Ore Shale
- f.g. disseminated sulfides may be depleted around "veins" and aggregates of coarser sulfides

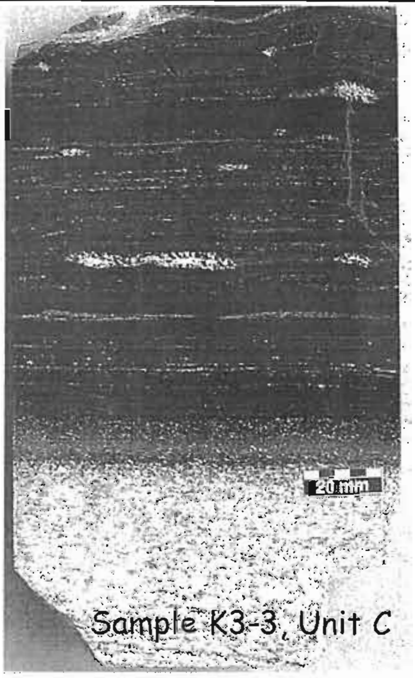

CODES / CSM AMIRA PROJECT P544 — MAY MEETING, 2002

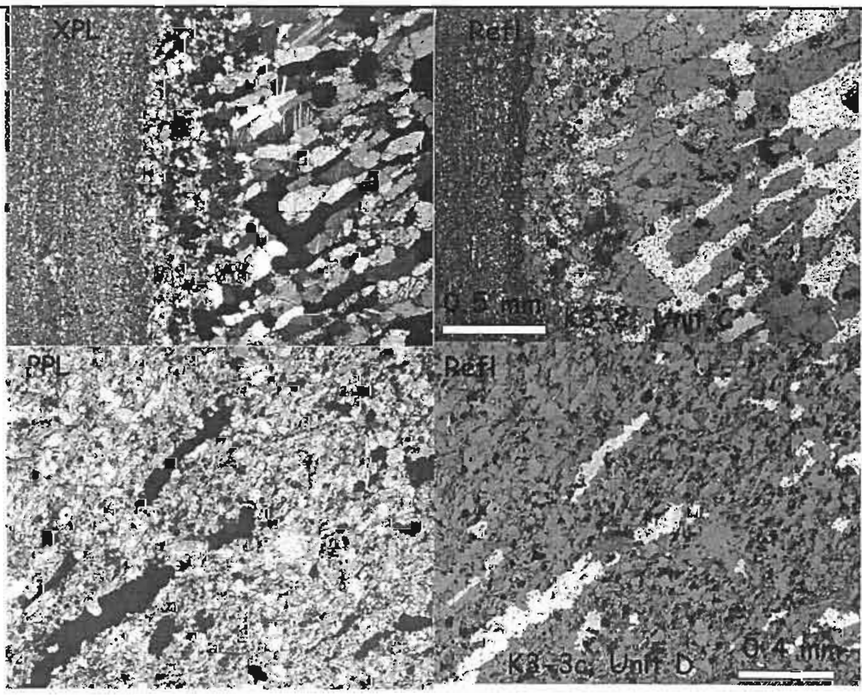

CODES / CSM AMIRA PROJECT P544 — MAY MEETING, 2002

elongate sulfide grains and aggregates

- orientation of sulfide fibres and elongate blebs ranges from ~90° to <20° to bedding, variable over small distances (e.g. cms)
- sulfides intergrown with similarly aligned carbonate±quartz±biotite±feldspar suggesting formation at peak (greenschist facies) metamorphic conditions

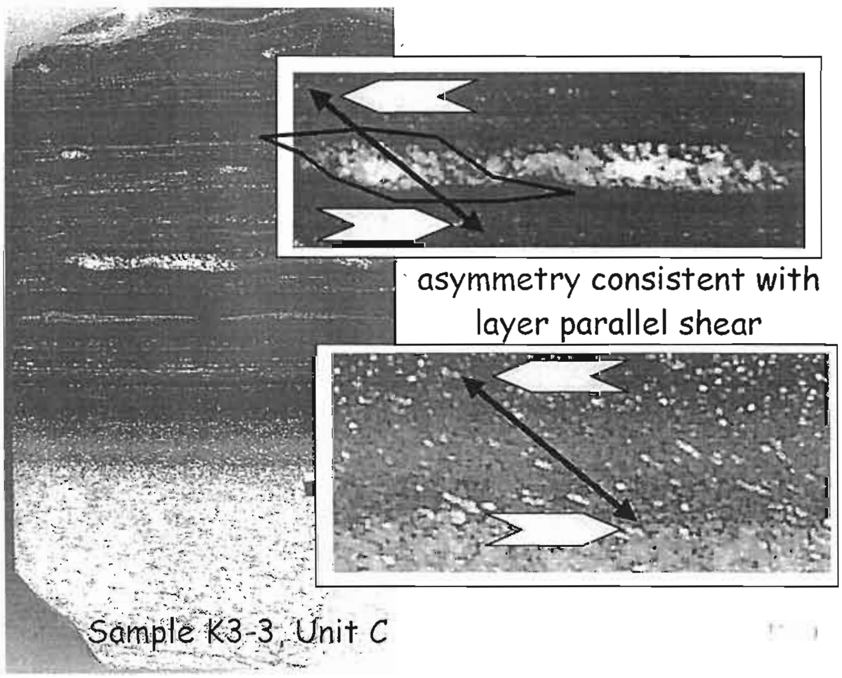

CODES / CSM AMIRA PROJECT P544 — MAY MEETING, 2002

Summary of textural relations

- Bedding-parallel compaction fabric only pervasive foliation developed
- Two-stage *textural* development of sulfide ores
- Elongate sulfide grains/aggregates oblique to bedding reflects minor remobilisation of original Cu-sulfides during layer-parallel shear (± minor dilation) at greenschist facies conditions (most likely during regional folding, e.g. Kirila Bomwe anticline)
- No evidence to support structurally-controlled, epigenetic mineralisation or significant structural upgrading of the Konkola ores

Copper Minerals Present in Konkola region

- Chalcopyrite $CuFeS_2$
- Bornite Cu_5FeS_4
- Chalcocite Cu_2S
- Covellite CuS
- Dominant assemblage
  - Konkola : Cpy + Bn with relative abundances varying greatly
  - Konkola North: Cpy + Py zone and Cc + Bn zone
- No systematic mineral zonation observed

Primary Chalcocite

- Appears in textural equilibrium with Bn
- Associated Bn tarnishes rapidly to purple/brown - visually distinct from orange tarnish on Bn associated with Cpy
- Best developed were Cpy is not present

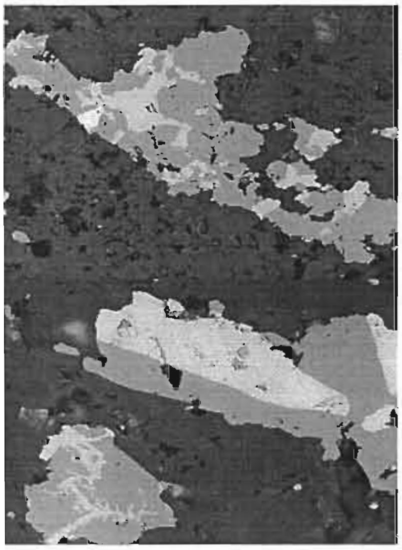

Primary Mineralisation

- Bn noted in textural equilibrium with both Cpy and Cc - however Cpy and Cc do not precipitate under same conditions
- Suggests two temporarily distinct assemblages deposited under different physiochemical conditions

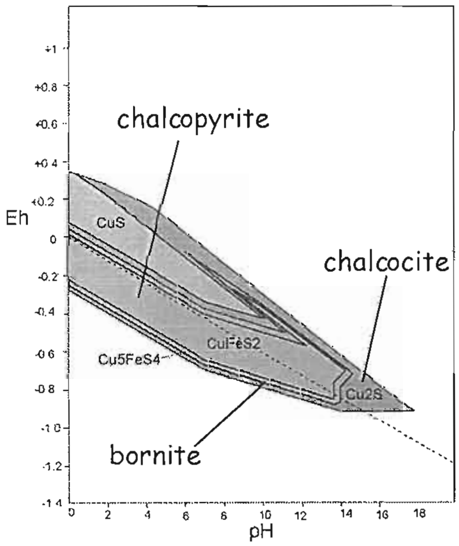

Secondary Chalcocite

- 2 occurrences both always associated with Haematite
  - Partial replacement of cpy and bn on grain boundaries and internal fractures
  - Entire grains - with chalcocite the only remaining Cu mineral

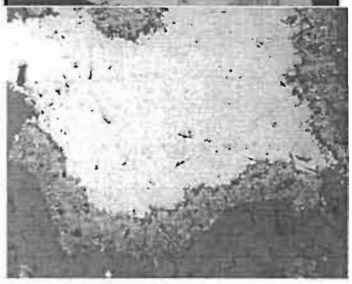

CODES / CSM AMIRA PROJECT P544 — MAY MEETING, 2002

Secondary Chalcocite

- Konkola - best developed at upper and lower portions of Ore Shale
- Konkola North - always associated with late iron oxide concentrations around fractures
- Replaces Cpy and Bn equally

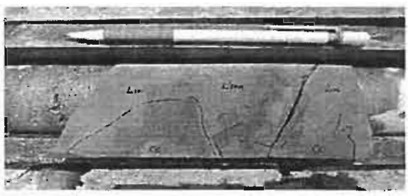

CODES / CSM AMIRA PROJECT P544 — MAY MEETING, 2002

Secondary Chalcocite

- Distribution, grain size and textural relations identical to hypogene sulfides
  - Suggests in situ replacement and limited mobility of Cu
  - Fe liberated during replacement largely immobile also
    - Large grains - rims of Hm
    - Fine grains - patchy Hm alteration of surrounding matrix

Secondary Chalcocite

- Conversion of Cpy and Bn to Cc is favoured by acidic waters however
  - low mobility of Fe
  - preservation of biotite and white mica
- Suggests supergene fluid was either near neutral or rapidly neutralised by reaction with Cu-sulfides

CODES / CSM AMIRA PROJECT P544 — MAY MEETING, 2002

Second phase of supergene alteration

- More oxidising conditions particularly developed at base and to lesser extent the top
- Cc partially or completely replaced by Malachite and lesser "Wad"

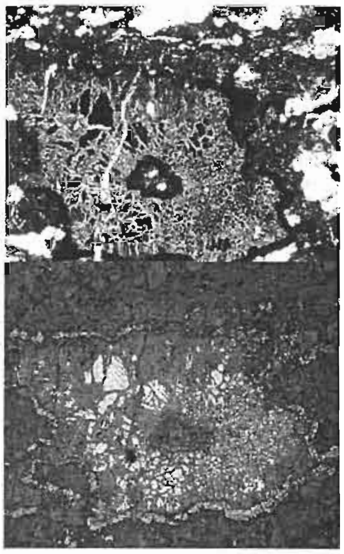

Summary

- Based on textural observations
  - Primary and Secondary Chalcocite present in Konkola region
  - Primary mineral observations include Bornite in apparent textural equilibrium with both Chalcocite and Chalcopyrite
    - Problematic as Chalcocite and Chalcopyrite precipitate under different conditions
  - Secondary Chalcocite always associated with Haematite
  - Secondary Chalcocite has similar textural characteristics to primary sulfides which suggests limited mobility of Cu
  - Second stage of supergene alteration converted secondary Chalcocite to Mal
- Test with LA-ICPMS to determine compositional differences

Comparative Study of Drill Cores from the Konkola North Orebody and Barren Gap

David Broughton, Colorado School of Mines

Introduction

The Konkola area lies at the northwestern end of the Zambian Copperbelt, and consists of two ore bodies continuous at depth, the South or No. 1 ore body and the North or No. 3 ore body (Figure 1). The ore bodies are separated by an unmineralized "barren gap" nearly 1.5 km wide at surface, that extends to a depth of approximately 600 metres. Below this the ore bodies merge, such that on a longitudinal section the gap forms a U-shaped zone. The gap was encountered early in the drilling delineation of the deposit, and not surprisingly was tested by few surface holes. The Konkola barren gap presents an opportunity to compare stratigraphically equivalent mineralized and unmineralized rock units, in a part of the Copperbelt that generally appears relatively undeformed.

Little is documented about the geology of the barren gap, or of the nature of its boundaries with the ore bodies. Fleischer et al. (1976) describe it as follows: "approaching the gap from the north orebody, ore is restricted to the C unit [note – the mine geologists subdivide the Ore Shale into five units, from base to top A through E, see Table 1] and lenticles of sandy dolomite increase in frequency and the shale layers between the thickening dolomites are crumpled and folded... cherty quartz lenses become more abundant in the dolomite bed and in the weathered formation form "quartz rubble" ... it may be suspected that an algal bioherm occupies part of the unexplored barren gap...". Sweeney and Binda (1989) mention it only in passing as a "presumed bioherm", and the current mine geologists also regard it as such.

A review of logs and preserved cores from the early surface holes through the barren gap indicated that the shallower intersections were in weathered ground unsuitable for study, and that the deeper intersections contain no significant carbonate. There is no "algal bioherm" at Konkola. A brief underground visit to the north ore body – barren gap transition area confirmed in general terms the above description of the transition: the abundance of carbonate increases southwards and mineralization (predominantly bornite) occurs selectively in the carbonate bands. Over a lateral distance of less than 25 metres the approximately 4 to 7 metre-thick combined C and D carbonate-banded units changed from 10 to 20 percent to approximately 50 percent carbonate. Individual bands commonly change in thickness across asymmetric NE trending folds (Figure 3a). Unfortunately, drift development had stalled and was soon afterwards terminated due to ground conditions, so that the transition from this high grade, bornite-carbonate zone to the unmineralized and carbonate-poor barren gap was not exposed.

This study compared drill cores through the Ore Shale in the North Orebody (KLB145) with unmineralized intersections from the barren gap (KLB67) and from a drill hole immediately east of the north ore body (KLB83) (Figure 1). The Konkola mine

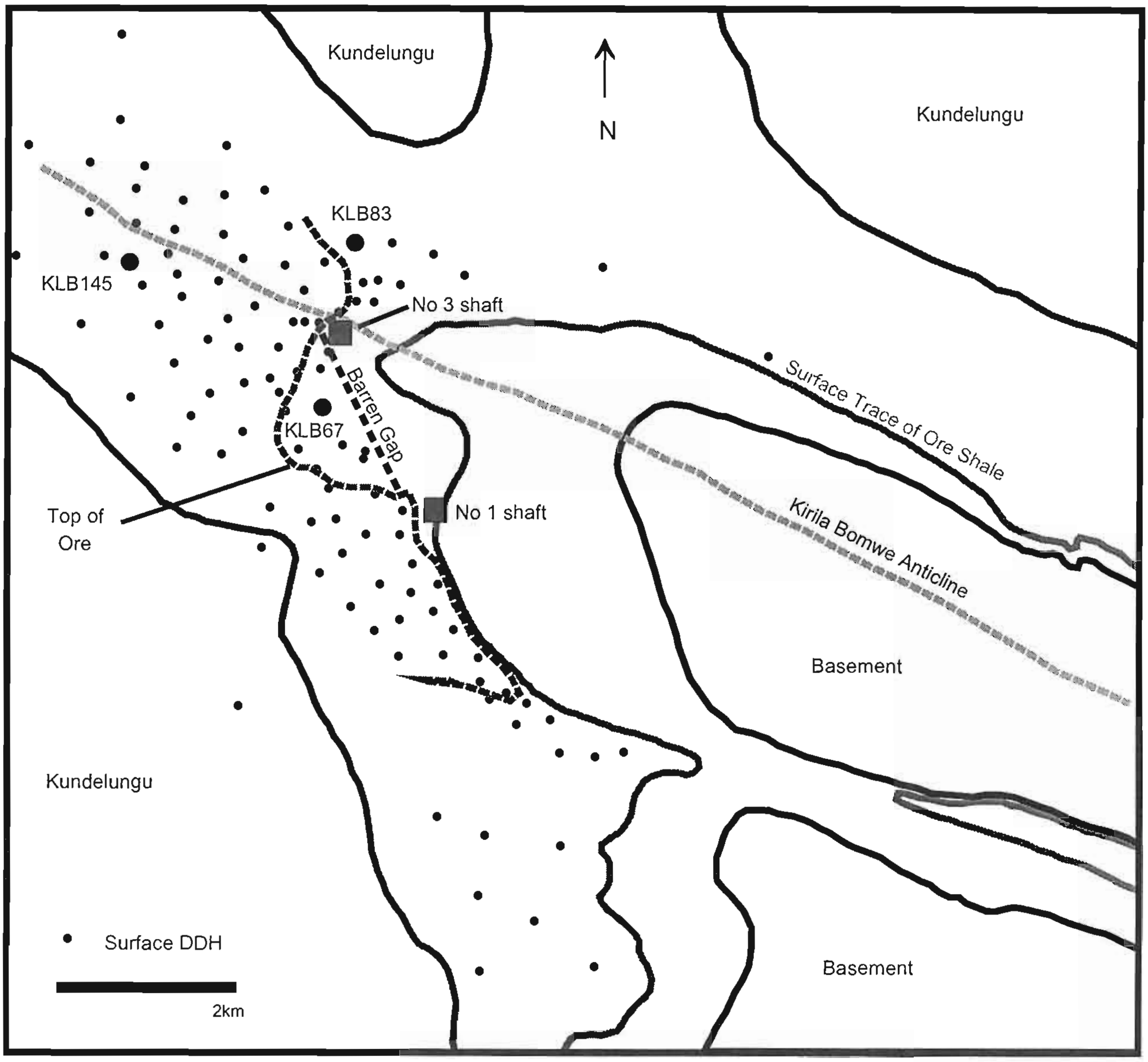

Figure 1. Simplified geology of the Konkola area, Northern Copperbelt, showing Konkola surface drill holes, location of the No. 1 (South Orebody) and number 2 (North Orebody) shafts, vertical projection of the orebdies, and position of the barren gap. Collar locations for the three holes used in the study are highlighted.

stratigraphic terminology is used for reference. Samples with secondary copper mineralization were excluded from the study, in order to focus on hypogene mineralization controls. Petrographic observations were augmented by cathodoluminescence (CL) and scanning electron microscope (SEM) studies.

Konkola North Ore Body, Drill Hole KLB145

Drill hole KLB145 intersected the north ore body on the south limb of the northwest-plunging Kirila Bomwe Anticline, approximately 2.6 km from drill hole KLB67 (Figure 1). In this area the rocks strike southeast and dip southwest at 25 to 30 degrees. The Ore Shale was intersected from 680.0 to 692.0 metres, and is underlain by 8 metres of Footwall Conglomerate, followed by 1 metre of Footwall Sandstone in which the hole was stopped at 701.0 metres depth. Mineralization above 1% Cu is confined to Ore Shale units A through D, and consists of hypogene sulfides (chalcopyrite, bornite, carrolite) throughout all of the zone but the lowermost 1.1 metres of unit A. This lower portion of the zone is weathered, and it contains predominantly secondary copper minerals. The underlying footwall conglomerate and sandstone are also weathered and contain sub-ore grade secondary copper mineralization. Sampling from this intersection was limited to six quartered cores, from which nine polished thin sections were prepared.

Figure 2 summarizes the geology, alteration, mineralization and assay results from the mineralized section of KLB145. The best mineralization coincides with a central zone of dolomite-biotite alteration and dolomite-veining in units C and D. Together these comprise 6.5 metres of the 11.5 metre intersection and have an average grade of 3.4% Cu, compared with 1.7% Cu for the remaining 5 metres. Cobalt values in the carbonate-rich units are approximately one-half that of the lower units B and A.

Table 1 Konkola Ore Shale Stratigraphy (modified from Sweeney and Binda, 1989)

Member, Unit	Thickness	Description
Hangingwall Quartzite (HWQ)	10 - 150m	Interbedded feldspathic arenite, greywacke, and minor siltstone
Ore Shale, Unit E (OSE)	0.6 - 1.5m	Interbedded siltstone and subordinate feldspathic arenite
Ore Shale, Unit D (OSD)	1 - 3m	Interbedded siltstone and dolomitic/calcareous feldspathic arenite, with bedding-parallel carb-qtz-Cu veinlets
Ore Shale, Unit C (OSC)	0.9 - 4m	Interbedded siltstone and dolomitic/calcareous feldspathic arenite, with bedding-parallel carb-qtz-Cu veinlets
Ore Shale, Unit B (OSB)	1.4 - 2m	Massive to laminated sandy siltstone
Ore Shale, Unit A (OSA)	0.6 - 1m	Finely laminated siltstone
Footwall Conglomerate (FWC)	0 -20m	Polylithic, poorly sorted conglomerate and interbedded coarse sandstone; usually leached.
Footwall Sandstone (FWS)	<40m	Poorly sorted feldspathic, lithic sandstone/greywacke; usually leached.
Porous Conglomerate (PC)	<40m	Polylithic, poorly sorted conglomerate, leached.

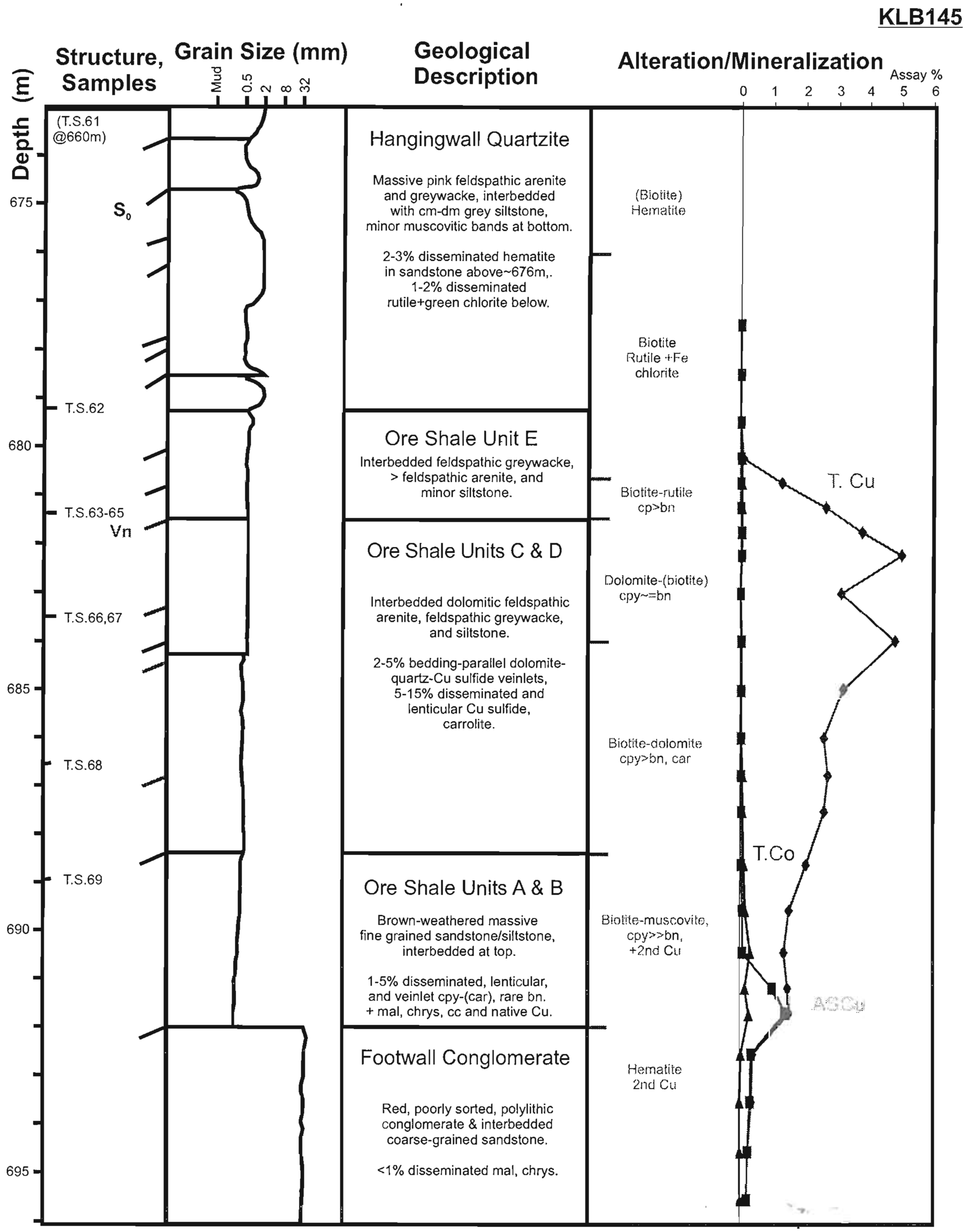

Figure 2. Summary graphical log of lower part of drill hole KLB145, Konkola North orebody. Note zoning of alteration-mineralization around central veined unit C+D. Upper contact of Cu +dolomite controlled by contact between veined arenite and overlying greywacke (unit E).

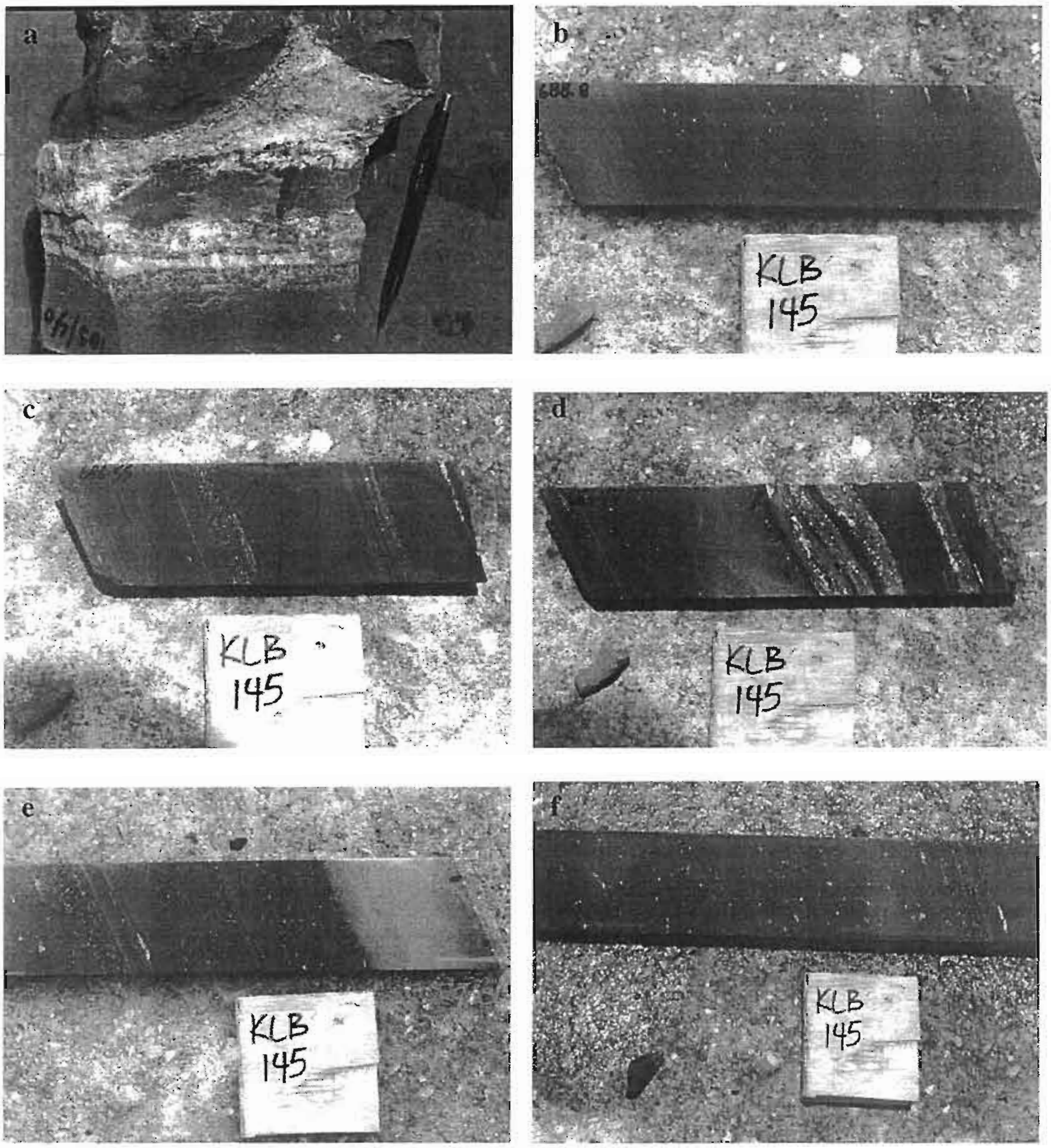

Figure 3. (a) Oriented sample from southern margin of Konkola North orebody, near barren gap, viewed to NE. Dolomite-bornite bands thicken SE (toward barren gap) across NE trending asymmetric fold structures. (b) sample of unit B, 688.8m, massive siltstone with disseminated sulfides. (c) sample of unit C, 686.55m, dolomitic sandstone-siltstone with banded/veinlet and disseminated sulfides. (d) sample of unit D, 683.45m, of bedding-parallel ferroan dolomite (stained) – sulfide veins. (e) contact between unit E (left) and unit D, dolomitized arenite. (f) sample of unit E at 681m, note disseminated sulfides, lack of carbonate. All core samples approximately 5cm across.

In the following section, a general description of the lithologies and mineralization will be followed by observations from petrographic study.

The footwall sandstone is a red to olive brown, massive to poorly bedded, coarse-grained greywacke or muddy sandstone, and may represent an interbed within the footwall conglomerate unit. The conglomerate is polylithic, massive bedded, unsorted, matrix- to locally clast-supported, with a coarse sandstone matrix and local cm to dm sandstone interbeds similar to that of the footwall sandstone. Both units are characterized by patches of red-weathered carbonate and hematite, and minor malachite-chrysocolla-chalcocite. The contact with the overlying Ore Shale (OS) is sharp and bedded.

The lowermost unit of the OS, from 692.0 to 688.4 m, consists of a massive-bedded, brownish (weathered), very fine-grained sandstone to siltstone that coarsens slightly upwards. It corresponds with the mine units A and B. The uppermost metre is finely laminated (Figure 3b) and is gradational to the overlying unit (C). Chalcopyrite occurs as disseminated grains, bedding-parallel lenticles and minor veinlets, along with malachite, chalcocite and local native copper below 689.0 m. Bornite is rare to absent. Carrolite is intergrown with chalcopyrite in the veinlets.

From 688.4 to 684.25 m the OS consists of cm to mm bedded, grey, fine- to coarse-grained dolomitized sandstone and siltstone. This unit occurs within the mine subunit C. Chalcopyrite and bornite occur as disseminated irregular grains, lenticles and veinlets, both parallel and oblique to bedding (Figure 3c). The veinlets contain fibrous quartz, ferroan dolomite and copper sulfides, which define a consistent down-dip (~WSW) lineation. In thin section some of the veinlets also possess a weak crenulation fabric. Ferroan dolomite is most intensely developed as halos to the veinlets.

From 684.25 to 681.5 (~units C and D) the OS consists of very fine to medium grained dark grey dolomitized sandstone interbedded on a cm to mm scale with pale grey dolomitized siltstone. The dolomite is associated with and forms haloes around bedding-parallel veinlets of ferroan dolomite-quartz-bornite-chalcopyrite (Figure 3d). Bornite and chalcopyrite are roughly equivalent in abundance. The upper contact of the dolomitic zone is sharp (Figure 3e), and coincides with a lithological change from arenite (dolomitized) to greywacke.

The uppermost unit of the OS extends from 681.5 to 678.5, and consists of a coarsening upwards sequence of interbedded sandstone and siltstone. Although the mine log placed the upper contact of unit E at 680.0 m, the contact between the OS and the HWQ is gradational and rather arbitrary, and here placed at the base of a prominent coarse-grained sandstone bed. Disseminated chalcopyrite and lesser bornite extend upwards from the dolomitic zone to 680.6 m (Figure 3f), above which the OS is barren of sulfides.

The HWQ consists of pink to grey, massive medium- to coarse-grained feldspathic sandstone and cm to dm thick bands of dark greenish to brownish grey siltstone. Hematite occurs above 676 m as disseminated grains and rare bedding-parallel concentrations, the latter associated with pinkish colouration.

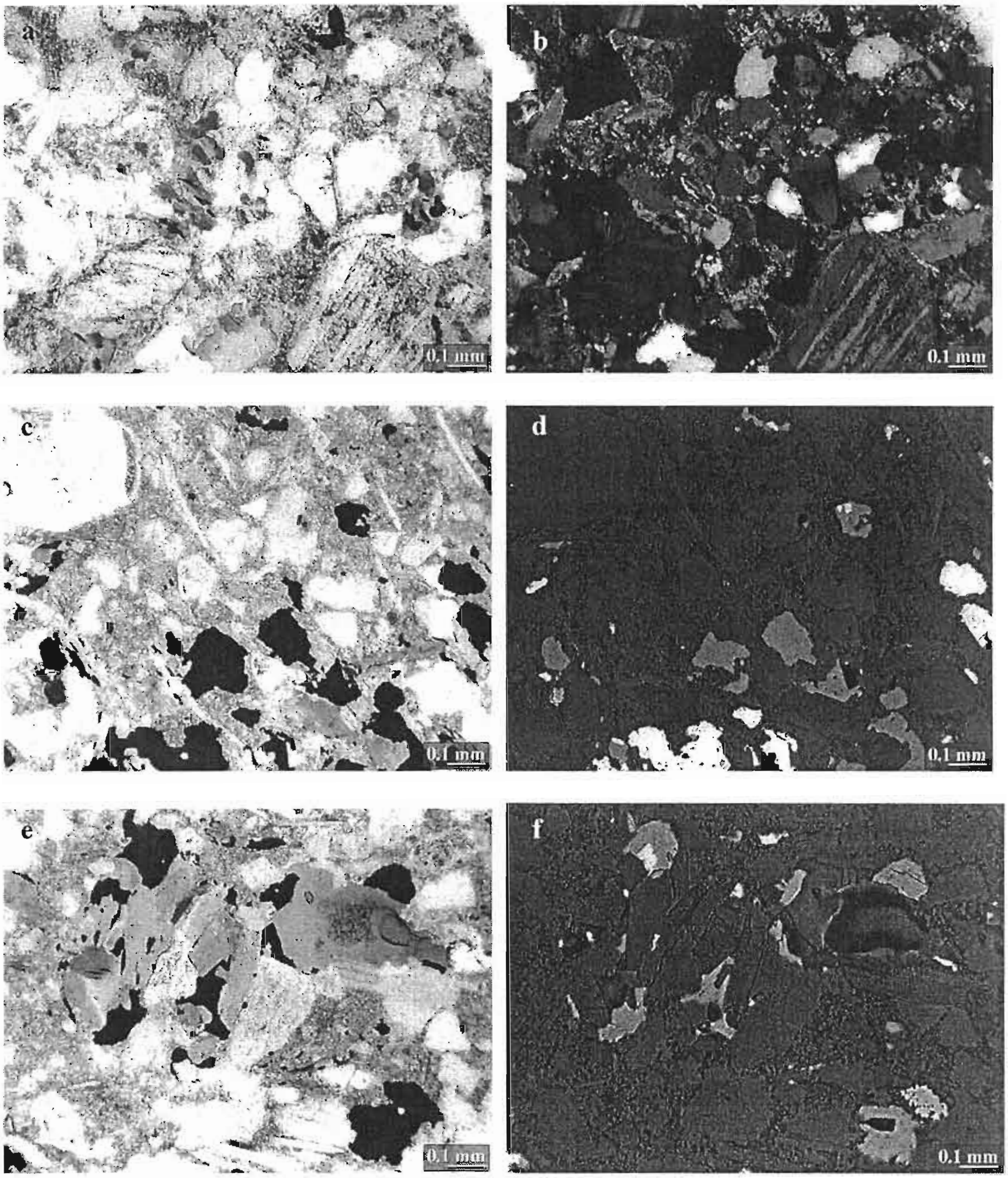

Figure 4, KLB145 photomicrographs, showing zoning and textures of alteration-mineralization across the OS. (a,b) TS62, feldspathic arenite with biotite+muscovite alteration, rutile. (c,d) TS63, above dolomitic zone, feldspathic greywacke with biotite alteration, chalcopyrite-bornite. (e,f) TS63, "nodule" of biotite-bornite around detrital k-feldspar; bornite is late, rutile (bright grey) is enclosed in biotite (left center) and early – also note rutile separate from bornite in lower right.

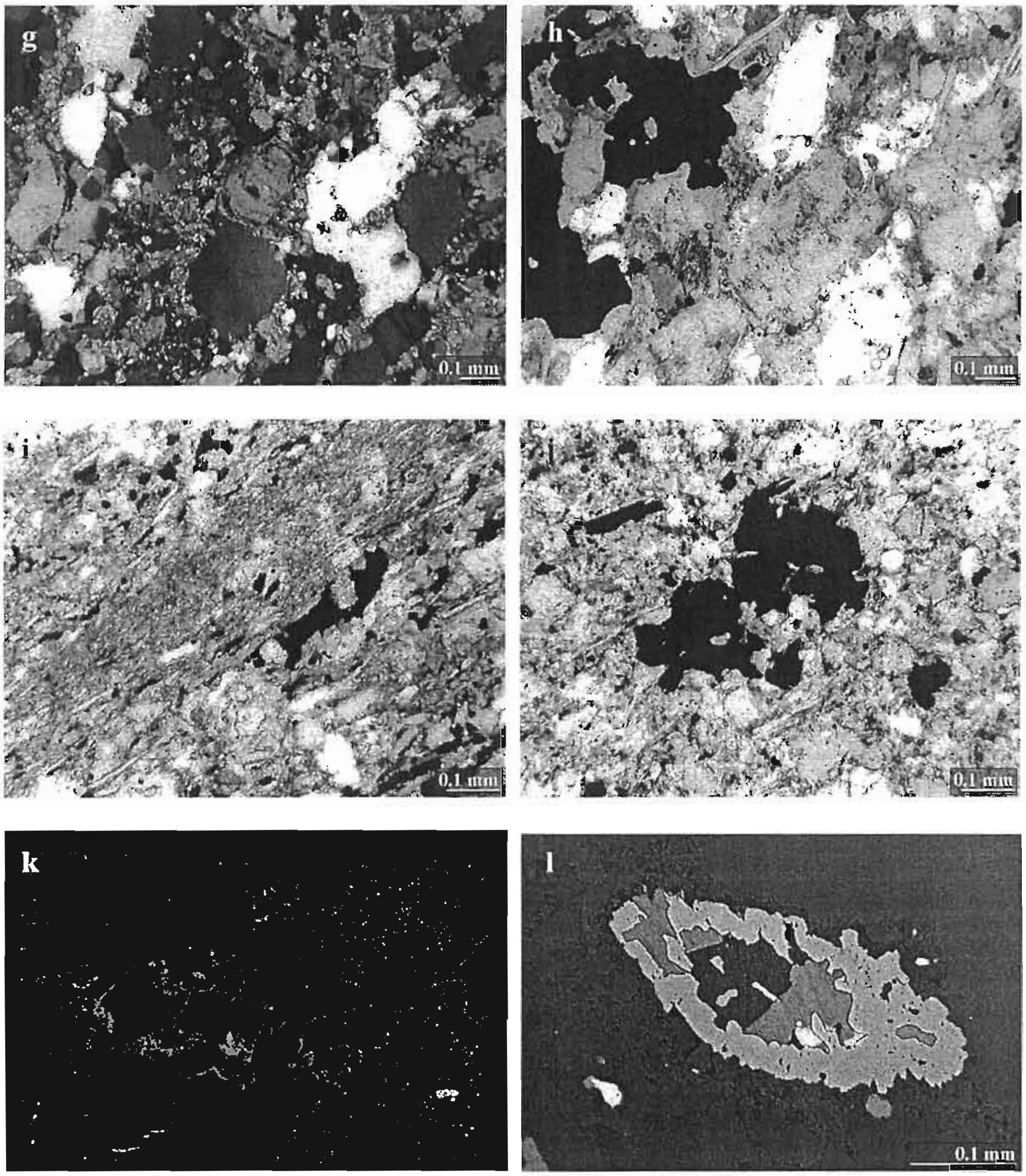

Figure 4 cont'd. (g). TS64, dolomite alteration replacing k-feldspar overgrowths in feldspathic arenite. (h) TS64, coarse chalcopyite-bornite and dolomite-biotite alteration in well-cemented feldspathic arenite. (i) TS67, bedded sandstone-siltstone, biotite-(dolomite) alteration and Cu sulfides predominantly in sandy layers. (j) TS69, coarse, irregular chalcopyrite in muscovite-(biotite) alteration at base of OS. (k) TS67, CL, dolomite-chalcopyrite veinlet, zoned from speckled ferroan to dark red ferroan to bright yellow-red (manganoan?) dolomite, and youngest chalcopyrite; field of view 2mm. (l) TS63, rutile (bluish) probably after sphene, filled with biotite (dark grey) and bornite-chalcopyrite.

In thin section, the sandstones and siltstones have well-preserved sedimentary and diagenetic textures, although tectonic fabrics are developed locally. The OS rocks are composed of subrounded to rounded detrital framework grains of quartz, k-feldspar, muscovite-altered feldspar, muscovite (large platy grains), minor granitic and cherty rock fragments, and accessory apatite and zircon. In most specimens these are poorly sorted, and occur within a matrix of fine silt to clay-sized k-feldspar, quartz and muscovite. The matrix, detrital muscovite and k-feldspar are variably overgrown by biotite and fine muscovite. Sulfide and oxide textures are described below.

The sandstones vary texturally between matrix-supported greywackes and matrix-poor feldspathic arenites. In the arenites, the grains are in mutual contact, may show evidence of pressure solution, and quartz and feldspar overgrowths and cement are common, often preserving dust rims of Fe-Ti oxides and mica after clay (Figure 4a, b, h, see also Figure 6c, k). Quartz cement is relatively common in the arenites, and locally has undulose extinction, suggesting it pre-dates Lufilian deformation. In the greywackes, detrital grains are less commonly in mutual contact, and overgrowths of quartz and feldspar are rare or absent (Figure 4c, d).

The distribution of matrix-rich and matrix-poor sandstones appears to be an important control on the distribution of carbonate and sulfide mineralization. The top of carbonate alteration at 681.5m is coincident with the contact between an overlying greywacke and the underlying feldspathic arenite (Figure 2, 3e). Dolomite in the altered arenite occurs as discrete grains overgrowing feldspar, biotite, matrix and possibly quartz (Figure 4g, h). In addition, mineralization is preferentially developed within sandstones rather than siltstones, as can be seen in its overall distribution (Figure 2) as well as on the thin section scale (Figure 4i).

A distinct zoning exists across the OS, both in alteration and sulfide mineralogy (Figure 2). The central zone (units C & D) is characterized by bedding-parallel dolomite-chalcopyrite-bornite-(quartz, biotite, k-feldspar, apatite) veinlets, ferroan dolomite-(biotite) alteration and approximately equivalent amounts of disseminated bornite and chalcopyrite (Figure 3d, 4g, h). Biotite is destroyed where dolomitization is most intense. This central zone contains the high grade mineralization and "carries" the entire interval . It is enveloped by a zone of less intense, biotite-dolomite alteration and fewer veinlets, where chalcopyrite is more abundant than bornite. This interval also contains visible carrolite in the footwall of the central zone. The outermost mineralized zone consists of biotite and generally fine-grained muscovite alteration, rare to absent veinlets, and, especially in the footwall, chalcopyrite much more abundant than bornite. The footwall zone also contains more abundant carrolite.

The Lower Roan hangingwall and footwall of the mineralized interval are characterized by minor biotite alteration and ubiquitous, widespread specular hematite, both as disseminated grains and in veinlets. The hematite facies is separated from the mineralized interval by a zone of biotite-(muscovite)-rutile-Fe chlorite (Figure 2, 4a,b).

Sulfide textures are distinctive, and in some instances similar to those of hematite in the stratigraphically equivalent barren intersections. Hematite is absent within the mineralized zone, however, clusters and individual minute grains of rutile are present in trace to accessory amounts, and are locally intergrown with biotite (Figure 4e,f) or mantled by Cu sulfide (Figure 4l). In most instances rutile appears to have formed prior to Cu sulfides, probably during diagenetic oxidation (dust rims). Chalcopyrite and bornite are mutually intergrown, or chalcopyrite occurs as rims and fracture-related infillings or replacements of bornite. Pyrite is absent. The Cu sulfide grains generally vary in grain size according to the grain size of their host rock, however a wide range exists and the largest sulfide grains are always much coarser than the detrital silicates. Chalcopyrite and bornite are most commonly found in direct association with biotite and dolomite, with which they form small grain aggregates, nodular structures and in the central zone, veins (Figure 4 c-f). Similar nodular structures containing anhydrite were described elsewhere at Konkola (Sweeney and Binda, 1989), and were interpreted as sulfide replacement features after diagenetic (evaporitic) anhydrite nodules. Anhydrite was not observed in any of the three holes examined, but where seen elsewhere in the district usually occurs in structurally late sites (veins).

Morphologically, the disseminated sulfide grains vary from subspherical but non-rounded (eg. very irregular at the grain boundary scale), to lenticular or platy (particularly where developed within biotite), to highly irregular (Figure 4). Copper sulfide grains are observed to mantle or partly replace detrital silicate grains and their overgrowths, apatite overgrowths, and dolomite. Within and adjacent to veins, Cu sulfides typically brecciate dolomite and quartz, and fill open space between the non-sulfide minerals (Figure 4k). This range of textures can be seen in both the dolomite-altered and non-dolomite-altered zones, although the altered zones generally contain a greater proportion of outsized and irregular grains. This suggests that all of the copper sulfides record the same mineralization event associated with the veins and the dolomite-biotite alteration. The overall impression is one of sulfide precipitated or remobilized late in the paragenetic history, as the final phase in vein filling, replacement of matrix, detrital grains and diagenetic overgrowths, and as grains nucleated on and replacing earlier oxides.

Sweeney and Binda (1989) described brown-luminescent feldspar overgrowths on normal, blue-luminescent k-feldspar within the OS, and documented elevated Cu contents (~0.25% Cu) within some of these overgrowths. They interpreted these features as a critical piece of evidence for Cu being present within the (diagenetic) fluid that caused the overgrowths. Both clear and cloudy k-feldspar and k-feldspar overgrowths were noted during the current study. In many clouded grains the clear feldspar persists along cleavage into the grain core, and in this type "dust rims" of Fe-Ti oxides and mica are absent. In contrast, some of the clear feldspar grains have oxide-mica dust rims that pre-date the cloudy overgrowths. The clear and clouded feldspar do not show any compositional variation with semi-quantitative SEM/EDS. There was no indication (SEM) of elevated Cu content in the overgrowths, and, in contrast, some of the overgrowths and detrital grains are clearly mantled and partly replaced by paragenetically later Cu sulfides. Sweeney and Binda noted malachite in their samples, and included it as part of the diagenetic sequence, and it is suspected that their samples were affected by relatively recent secondary copper formation, as is prevalent in many parts of the mine.

Cathodoluminescence study of the alteration and vein carbonates demonstrated a complex paragenetic history of changing Fe and Mn contents. The matrix carbonate grains are commonly cored with rhombs of ferroan dolomite, which is successively overgrown by dolomites of generally lower iron content. A distinctive yellow luminescent carbonate is commonly present roughly midway through the sequence, and is likely related to elevated Mn content. These overgrowths are preserved within coarse-grained, dark to bright red luminescent dolomite and/or calcite, that forms mosaics of interlocked grains whose overall morphology is unrelated to the earlier zoned carbonates. A similar progression is observed in veins, where early, finely zoned carbonates are enveloped within younger, texturally simple, dark to bright red luminescent dolomite (Figure 4k). This confirms a genetic link between the matrix and vein dolomites.

In summary, the mineralized intersection occurs within interbedded feldspathic arenites, feldspathic greywackes and siltstones, but is best developed within the sandstones. Mineralization displays a marked zoning from a central, high-grade, bornite-chalcopyrite zone of ferroan dolomite-(biotite) alteration and abundant veining, through a proximal, lower grade, biotite-muscovite zone with chalcopyrite prevalent over bornite, to a distal zone of biotite-muscovite with rutile but no sulfides. Cobalt is present throughout the sulfide zone but most abundant occur in the lower, dolomite-poor interval. The mineralized zone is enveloped within widespread specular hematite mineralization, of probable earlier age. Diagenetic overgrowths of quartz and feldspar are present in the arenites, and trap earlier diagenetic Fe-Ti oxides and micas.

Konkola Barren Gap, Drill Hole KLB67

Drill hole KLB67 intersected the Ore Shale midway between the North and South ore bodies, at a depth of 211.7 to 219.3 metres (Figures 1, 5, 6a). Core angles indicate a true thickness of 7.2 metres, about 4 metres less than in KLB145. Assay results for the intersection range from 0.03 to 0.06% TCu for all but the lowermost 1.3 metres, which averaged 0.11% TCu and 0.04% ASCu. Mineralization was not observed in the core, and it is suspected that the minor Cu values are related to fine-grained secondary copper.

The hole ended in 7.5 metres of interbedded pinkish to pale conglomerate and coarse-grained feldspathic sandstone (Porous Conglomerate, PC), overlain by 14.8 metres of red to grey to beige, massive bedded, and very coarse-grained feldspathic sandstone (Footwall Sandstone, FWS, Figure 5). Both of these units contain up to 3% disseminated and bedding-parallel specular hematite. The Footwall Conglomerate is missing in this hole, such that the OS lies directly upon the FWS. This suggests that the OS – FWS contact is an unconformable surface, correlative with the base of the OS and/or the base of the FWC. The distribution of the FWC is irregular on the scale of the deposit, and unrelated to the location of the barren gap.

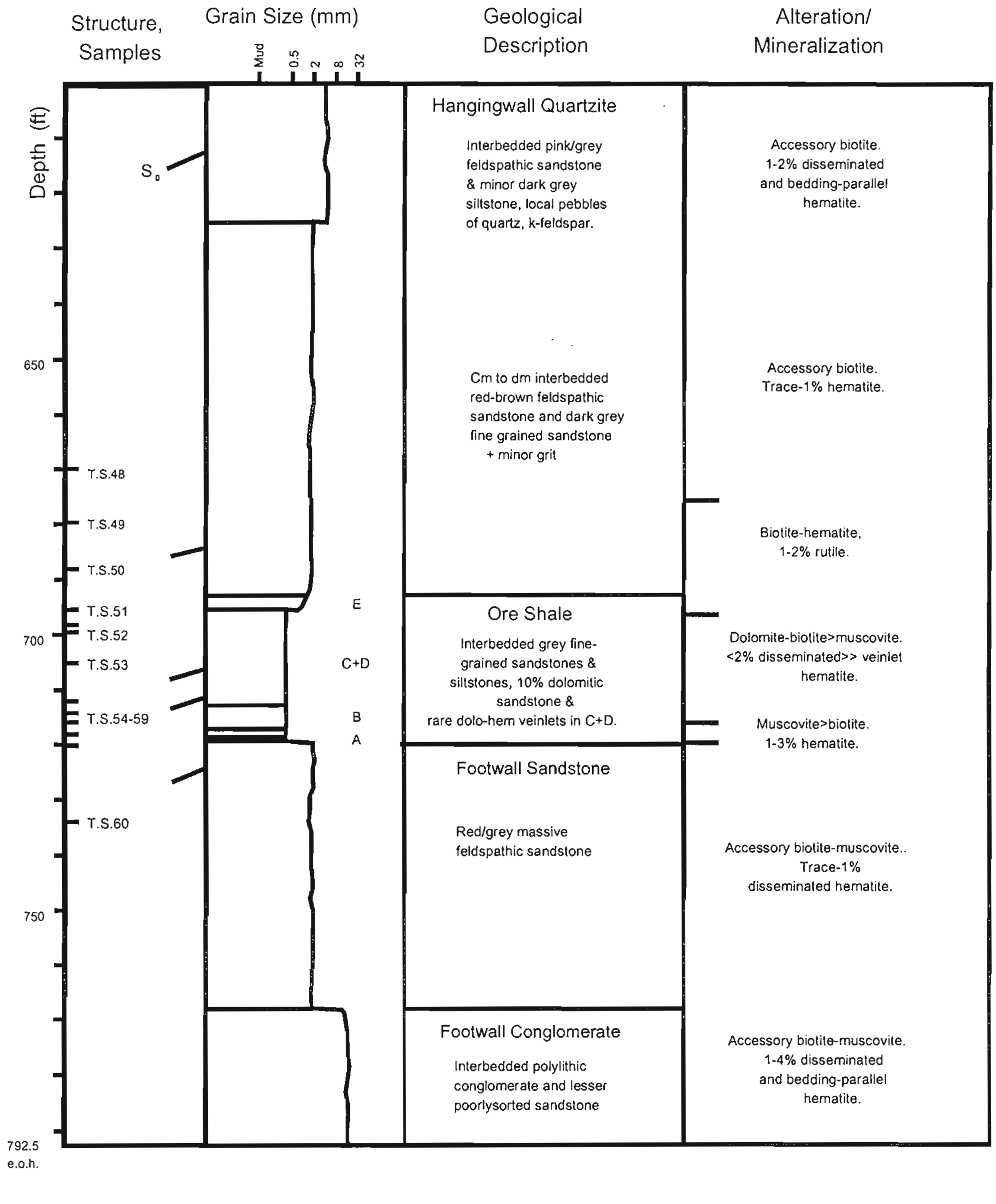

Figure 5. Summary graphical log of lower part of drill hole KLB67, in Konkola Barren Gap. Note zoning of dolomite-biotite-muscovite alteration.

Each of the five subunits of the OS are present in KLB67, which suggests depositional continuity between the mineralized and barren OS "stratigraphies" - placed in quotation marks because the OS stratigraphy is partly defined by the abundance of dolomite veinlets and alteration. The combined lowermost subunits, A and B, are 1.8 m thick and comprises a buff-weathered to dark grey-green very fine-grained sandstone/siltstone. They are overlain by 6.7 metres of dark green-grey fine to very fine-grained sandstone, interbedded with up to 10% discontinuous mm to cm bands of medium to coarse-grained dolomitic feldspathic arenite (subunits C and D). Bedding-parallel veinlets of dolomite-quartz-specular hematite and disseminated specular hematite are almost exclusively confined to the lowermost 1.4 metres of this zone. The OS is capped by 0.8 m of dark grey fine-grained sandstone interbedded with approximately 5% cm-thick beds of coarse-grained feldspathic sandstone, and up to 5% green-grey siltstone (subunit E).

The OS is overlain by a thick hangingwall sequence of cm- to dm-interbedded red-brown feldspathic greywackes and sandstones, and dark green-grey very fine-grained sandstone/siltstone, locally with "grit", that contain prominent disseminated specular hematite. Although quartz and feldspar overgrowths are present in the three thin sections made of these sandstones (Figure 6c, d), they are generally poorly cemented. The amount and distribution of cement affects permeability, and could play a role in controlling the subsequent movement of mineralizing fluids. For instance, well-cemented hangingwall or footwall rocks could form seals to cross-stratal fluid migration, and barren gaps could develop where cementation was poor, or dissolved prior to mineralization.

Thin sections were made of two samples from the FWS, 0.3 and 5 metres below the unconformable OS contact. Both consist of matrix-poor feldspathic lithic sandstones with rounded to subrounded detrital k-feldspar, quartz, granitic and chert rock fragments, cemented by quartz and k-feldspar overgrowths. Abundant porosity (up to 30%) exists in both samples, and is defined predominantly by mm-sized, generally rounded but irregular shaped holes. There is no Cu or Fe staining associated with the holes, as might be expected were they leached sulfide grains. Detrital feldspar and quartz grains show no signs of dissolution and are therefore unlikely to be the origin of the porosity. This texture is common throughout the OS footwall and, to a lesser degree, hangingwall rocks in the Konkola area, and may be caused by dissolution of carbonate or sulfate.

In thin section, the original sedimentary composition and morphology of the barren gap lithologies appear identical to those in KLB145. The sandstones are poorly sorted with up to 20% matrix, and contain detrital k-feldspar, quartz, muscovite and lithic fragments as described above (Figure 6b). The siltstones contain only rare lithic fragments, and a greater abundance of muscovite, but are otherwise similar to the sandstones.
The detrital quartz, feldspar and lithic grains in the sandstones are commonly coated with "dust rims" of biotite and muscovite (after clay), hematite and rutile, preserved by k-feldspar and quartz overgrowths (Figure 6c, d). The quartz is more abundant and locally forms a cement that post-dates the authigenic feldspar. The quartz cement often shows undulose extinction and recrystallization, and therefore pre-dates at least part of the Lufilian deformation.

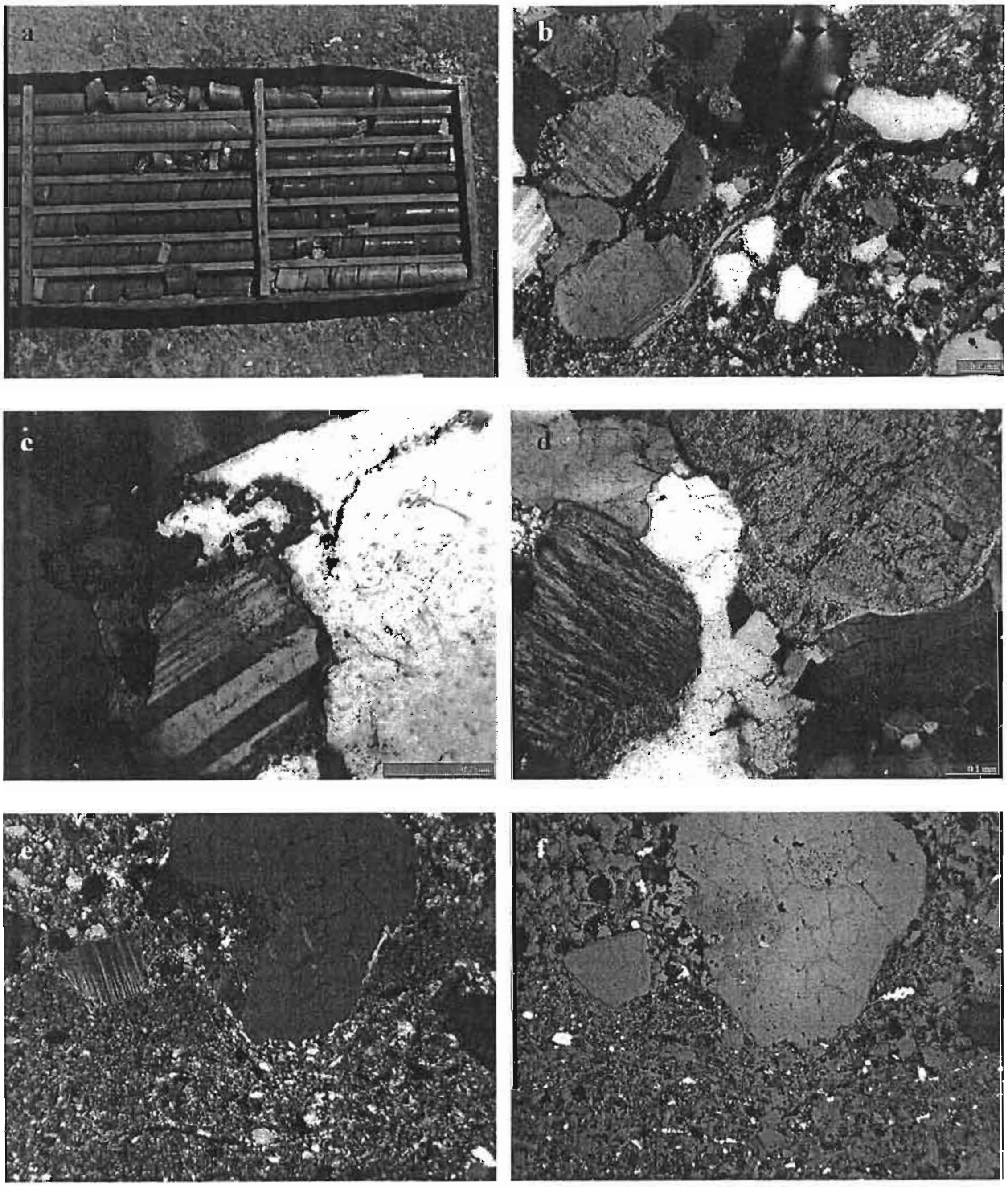

Figure 6, KLB67 and KLB83. (a) KLB67 barren gap intersection of Hangingwall Quartzite, Ore Shale, and Footwall Sandstone. (b) KLB67, TS48 (HWQ), contact between feldspathic arenite and feldspathic greywacke, note detrital (bent) muscovite. (c) KLB67, TS50 (HWQ), quartz overgrowths trap early dust rims of rutile-hematite-(mica)n and a rutile pseudomorph after sphene. (d) KLB67, TS50 (HWQ), quartz cement after earlier k-feldspar overgrowth. (e,f) KLB67, TS51, Ore Shale E – D transition zone, contact between siltstone and pebbly arenite, hematite (reflected light) is fine-grained, after ilmenite/amorphous Fe oxides, notable lack of coarse grained hematite at contact.

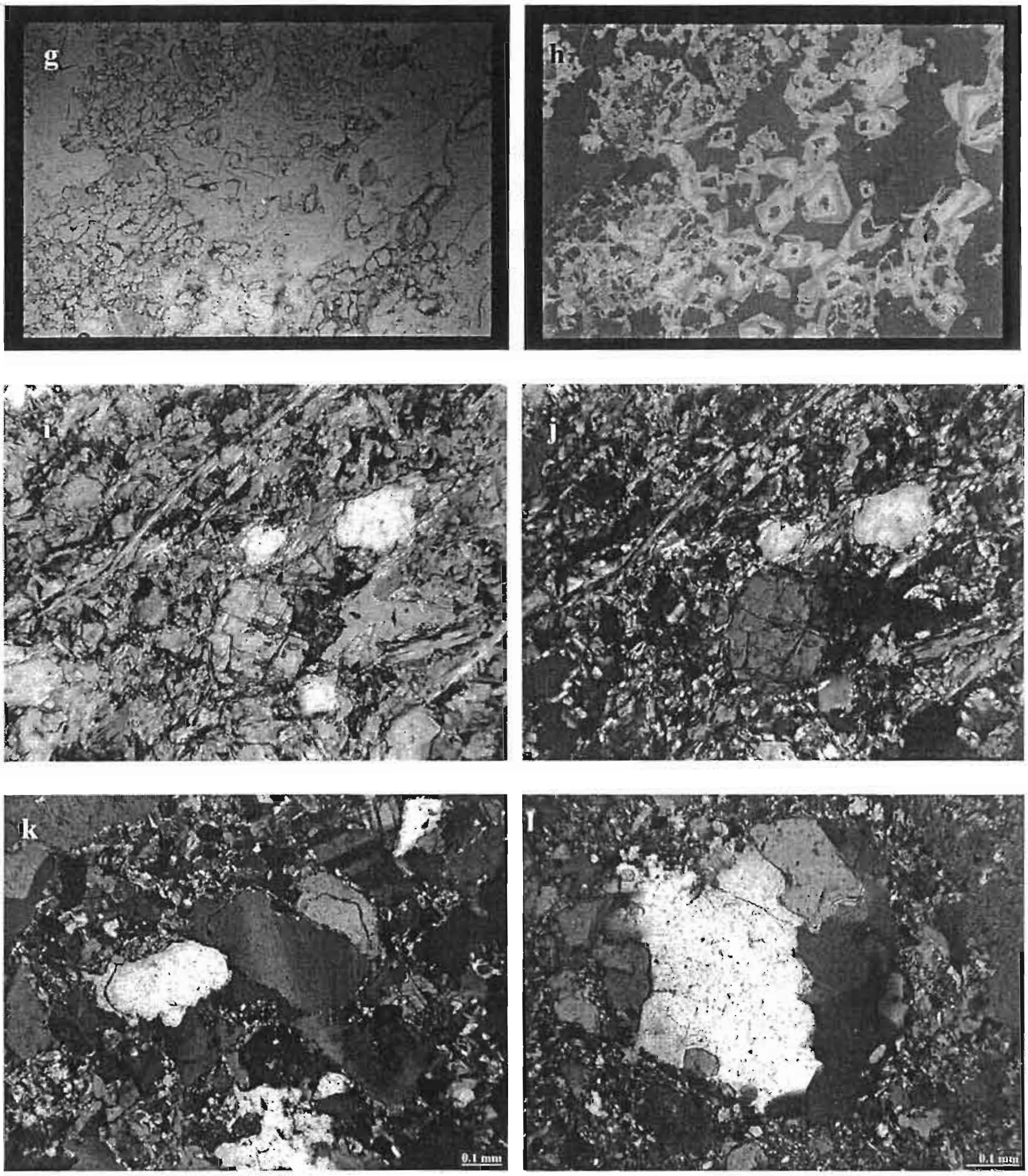

Figure 6, cont'd. (g,h) KLB67, TS52 (OSD), plane light and CL views of dolomite-(hematite) veinlet, with early zoned Fe/Mn rhombohedral dolomite and late, space-filling red-luminescent ferroan dolomite. (i,j) KLB67, TS53 (OSC), dolomite-biotite-muscovite (fine-grained) alteration and minor opaque hematite in feldspathic arenite. (k) KLB83, TS70 (HWQ), quartz overgrowths preserve diagenetic hematite-rutile-mica (clay) dust rims, hydrothermal/metamorphic biotite in groundmass. (l), KLB83, TS72 (FWS), ferroan dolomite alteration of groundmass and detrital quartz.

The matrix, detrital muscovite and to a minor extent the k-feldspar grains and overgrowths are variably overgrown by metamorphic/hydrothermal biotite. The biotite is commonly intergrown with, or partly replaced by dolomite, and also contains specular hematite and local rutile along cleavage planes.

Hematite most commonly occurs as disseminated platy and subangular to rounded, originally octahedral grains up to 1 cm in size (Figure 6e, f). The octahedral grains are composed of partly to completely martized magnetite and ilmenite, and locally preserve octahedral cleavage and skeletal habits. SEM/EDS study indicates that the hematite consistently contains minor amounts of Ti. The size of the hematite grains is roughly proportional to that of the surrounding detrital silicates. Unlike the Cu sulfides, disseminated hematite does not form overgrowths on authigenic quartz and feldspar, and is interpreted as the metamorphic product of diagenetic and detrital Fe-Ti oxides. Hematite abundance ranges between 0.5 and 3%, much lower than the sulfide content in KLB145.

The barren gap veinlets are composed predominantly of dolomite, with lesser quartz, orthoclase, biotite, and minor specular hematite. The carbonate shows multiple stages of growth under CL, from early dark Fe-rich dolomite rhombs through successive euhedral overgrowths of varying Fe content, to a pore space filling cement of dark red luminescent dolomite (Figure 6g, h). Hematite is found within the last stage of dolomite. The veinlets have dolomite–biotite alteration haloes similar to those in KLB145 (Figure 6i, j). This paragenetic sequence is similar to that of the mineralized veins, and suggests they were coeval.

In summary, the barren gap lithologies are identical to those in the mineralized zone and preclude the possibility that the gap is lithologically controlled. There is neither any evidence to support an origin by secondary leaching of Cu sulfides. The sandstones and siltstones in the barren gap appear to have undergone the same diagenetic history, with early oxidation and weathering recorded by dust rims of Fe-Ti oxides and micas (clays), followed by later diagenetic k-feldspar and quartz overgrowths. Bedding-parallel veinlets, predominantly composed of carbonate, are present in the intersection, but are much less abundant than in the mineralized zone. There is a corresponding reduction in the amount of dolomite alteration. Specular hematite occurs mainly as disseminated grains that are texturally consistent with an origin via metamorphism of detrital and diagenetic Fe-Ti oxides.

Konkola North Orebody Margin, Drill Hole KLB83

Drill hole KLB83 was collared on the northern limb of the Kirila Bomwe Anticline, approximately 200 m east of the edge of the North ore body (Figure 1). It intersected the OS at a depth of 715.2 to 731.2 metres, for a calculated true thickness of 11.7 m. Assays ranged from 0.02 to 0.09% TCu. Fleischer et al. (1976) describe the eastern margin of the North orebody as coincident with a gradual facies change from interbedded sandstones and siltstones to feldspathic arenites indistinguishable from the footwall sandstones. As in the barren gap transition, "approaching the margin of the orebody, the ore is confined to the top of the B unit and to the C unit", in other words to the carbonate-rich part of the section.

The core from KLB83 was examined briefly and three samples taken. The OS in KLB83 is underlain by 10.8 m of grey-pink, leached conglomerate (FWC) and 17.7 m of grey, medium-grained feldspathic sandstone (FWS). It is overlain by grey to pink feldspathic sandstones and minor interbedded siltstones of the HWQ. Up to 5% specular hematite occurs in both the hangingwall and footwall rocks, as angular to rounded detrital grains (probably after magnetite) and platy, often euhedral crystals (after ilmenite and diagenetic amorphous iron oxides)

In thin section, quartz overgrowths are present in the hangingwall sandstones and preserve diagenetic dust rims (Figure 6k). Hydrothermal/metamorphic biotite locally overgrows the groundmass. The footwall sandstone can be classified as a poorly sorted feldspathic greywacke, with local matrix-poor bands of feldspathic arenite. It is compositionally similar to the sandstones described from the other drill holes. Coarse-grained dolomite and biotite are intergrown and replace the detrital grains and matrix to varying degrees (Figure 6l). Under CL the dolomite shows alternate Fe-rich and Fe-poor growth zones. The presence of dolomite in the OS footwall is interesting, and may indicate migration of the altered (and mineralized?) interval - this is common elsewhere in the Copperbelt on the margins of ore bodies.

As in the barren gap, each of the subunits of the OS occurs in the KLB83 intersection, and, except for the presence of hematite, there are no apparent differences in original composition from the rocks of the mineralized intersection. The OS interval contains up to 5% mm to cm bands of dolomitic sandstone, and no significant veining. Two samples were collected, of a feldspathic greywacke at the upper contact of the OS, and of a siltstone from unit B. The feldspathic greywacke contains local quartz grains with authigenic overgrowths that preserve minute grains of hematite and rutile as "dust rims". Approximately 2% hematite also occurs as typical rounded (detrital) and platy (authigenic) grains. The siltstone contains 1 to 2% similarly textured but correspondingly smaller grains of hematite and rutile. As in KLB67, the Fe-(Ti) oxide content in the OS is much less than the Cu sulfide content in the equivalent interval. Biotite is fine-grained, and the coarse biotite associated with mineralization in KLB145 is absent.

In summary, the KLB83 intersection is similar to that of the barren gap, containing only minor amounts of carbonate alteration and veining, disseminated specular hematite after probable authigenic Fe oxides, and preserved early diagenetic dust rims on detrital grains. Additional sampling is required to more completely characterize the intersection.

Summary and Conclusions

The lithologies that host mineralization in KLB145 are indistinguishable from those in the barren holes, KLB67 and KLB83, thus there does not appear to be a lithological control on the lateral distribution of mineralization. The barren gap is not a carbonate bioherm, and in fact contains less carbonate (as alteration) than the mineralized interval. Also, the barren holes do not consistently have a different footwall or hangingwall lithology that might control mineralization.

Diagenetic features are readily observable in the cores, and are again relatively consistent between the barren and mineralized intersections. They consist of early hematite, rutile and mica (after clay) dust rims on detrital silicate grains, which are preserved by later overgrowths of k–feldspar and quartz. No evidence was found of Cu mineralization associated with these features. Hematite present within the barren holes is identical to that in the hangingwall and footwall of the mineralized zone, but is volumetrically minor, usually less than 2%.

The Cu-Co mineralization in KLB145 is associated with hydrothermal / metamorphic ferroan dolomite, biotite and muscovite alteration and veins, in a sequence of roughly symmetric zones. The highest copper grades occur in a central, bornite-rich zone associated with abundant veins and dolomite-biotite alteration. Lower grades are found in proximal biotite-muscovite alteration where chalcopyrite dominates. Cobalt (carrolite, and possibly cobaltian chalcopyrite?) is highest where dolomite is poorly developed or absent. Coarse-grained and often irregular sulfides are most abundant in the dolomitic zone, but present throughout. Platy or bladed sulfides, likely after hematite/ilmenite, are also present throughout.

Dolomite veins and dolomite-biotite alteration also occur in the barren intersections, but lack sulfide, and are volumetrically less significant. The indication is that these holes are on the fringes of the hydrothermal system. It would be anticipated that within such a system any record of an earlier mineralization event would be destroyed, and the mineralized zone in KLB145 in fact lacks such a record. However, it might also be expected that any earlier event would be preserved on the margins of the hydrothermal system, and this is not the case. It is therefore difficult to argue for there being two superimposed mineralizing events at Konkola.

Future work will include completing a sulfur isotopic study on the mineralization to determine whether any variation exists amongst the texturally different sulfides, and SEM/EDS study of the biotite to determine whether metamorphic and hydrothermal phases can be distinguished.

References

Fleischer, V.D., Garlick, W.G., and Haldane, R., 1976, Geology of the Zambian Copperbelt, *in* Wolf, K.H., ed., Handbook of Strata-bound and Stratiform Ore Deposits, Volume 6: Elsevier, Amsterdam, p. 223-352.

Sweeney, M.A., and Binda, P.L., 1989, The role of diagenesis in the formation of the Konkola Cu-Co orebody of the Zambian Copperbelt, *in* Boyle, R.W. et al., eds, Sediment-hosted Stratiform Copper Deposits, Geol. Assoc. Canada Sp. P. 36, p. 499-518.

Character, Distribution, Timing and Origin of Copper Mineralisation at Mufulira

Robert Scott

Centre for Ore Deposit Research
University of Tasmania

Introduction

- Mufulira largest Copper belt deposit NE of the Kafue anticline (Remaining total resource, 30/11/00: 41.5 Mt @ 3% Cu)
- 30—80m thick Ore Formation consists of variably argillaceous quartzite and arkose interbedded with lesser shale and dolomite within the Lower Roan
- Thickness of the Lower Roan below the Ore Formation is highly variable (0—180m) apparently reflecting original basin topography (Brandt et al., 1961)

Copper mineralisation at Mufulira

- describe composition, textural relations, paragenesis and mineralogical zonation associated with copper ores at Mufulira
- composition and character of host rocks
- evidence for timing and origin of copper mineralisation

CODES SRC

CODES / CSM AMIRA PROJECT P544 — MAY MEETING, 2002

Location

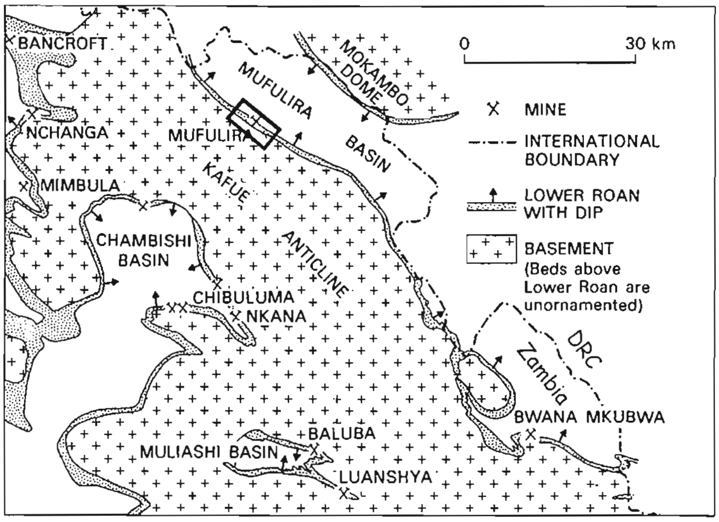

CODES SRC

CODES / CSM AMIRA PROJECT P544 — MAY MEETING, 2002

Regional Geology & Stratigraphy

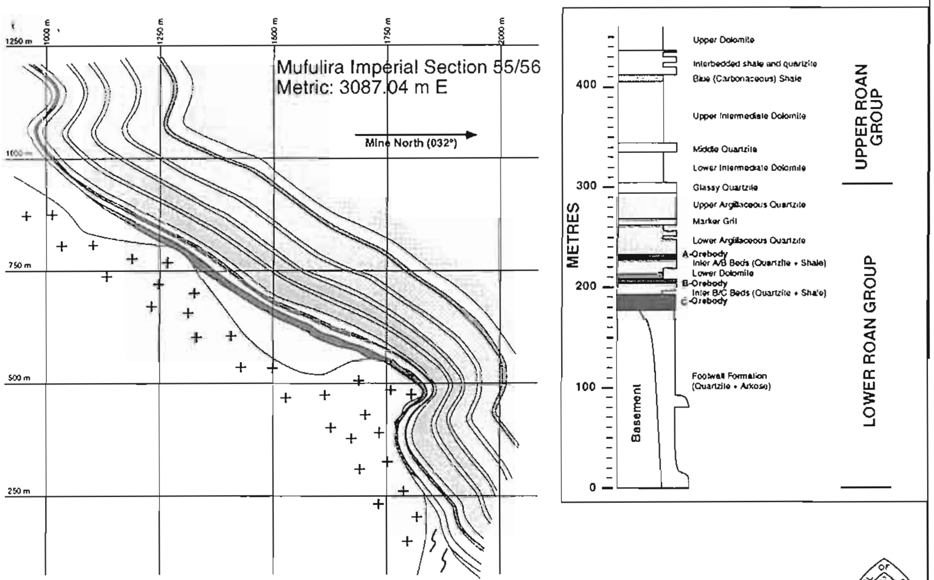

CODES SRC

CODES / CSM AMIRA PROJECT P544 — MAY MEETING, 2002

SCHOOL OF MINES 1874 COLORADO

Approach

- petrographic, microstructural (and geochemical*) analysis of samples collected underground on 1140' and 1240' Levels

*results to reported at a later date

CODES SRC

CODES / CSM AMIRA PROJECT P544 — MAY MEETING, 2002

SCHOOL OF MINES 1874 COLORADO

Ore Formation

- 3 main strata-bound horizons (A-, B- and C-Orebodies, generally 5 —10 m thick)
- smaller and higher grade up-section (i.e. from C-OB to A-OB)
- C-OB lateral dimensions 8 x 8 km
- inter-ore beds 10-20 m thick, also contain economic Cu locally (Eastern (sub-) Basin)
- Cobalt is negligible at Mufulira

Mufulira Orebodies

Unit	Lithology	Thickness	Mineralisation
A-Orebody	Argillaceous feldspathic quartzite, black carbonaceous quartzite ("greywacke"). Minor pebble to boulder conglomerate locally.	Av.: 6.1 m Max.: 13.7 m	4.5-5.5% Cu, disseminated Cc and Bn at upper levels, Cpy + Bn ± (?)Cc at depth
B-Orebody	Argillaceous and locally feldspathic quartzite, black carbonaceous quartzite ("greywacke")	Av.: 7.6 m Max.: 15.2 m	3.5-4.5% Cu, dominantly disseminated Bn, Cpy increases towards the fringes
C-Orebody	Argillaceous (sericitic) and locally feldspathic fine to medium grained quartzite, black carbonaceous quartzite ("greywacke")	Av.: 13.7 m Max.: 22.7 m	2.5-3.5% Cu, disseminated and lesser quartz + carbonate vein-hosted Cpy >> Bn, except at fringes

Mufulira long-section

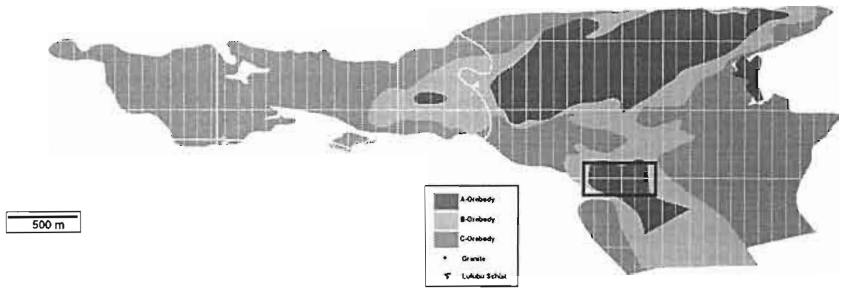

Basement highs (not shown) define 3 sub-basins
Area of underground mapping and sampling outlined

Previous studies

- syngenetic, diagenetic models for Cu-mineralisation (van Eden, 1974; Fleischer et al., 1976 Annels, 1979)
  - ppt of Cu-sulfides result of sulfate reduction (early diagenetic anhydrite) during diagenesis
- detrital component (Binda, 1975; Fleischer et al., 1976)

Zonation

- economic fringes of the orebodies do not reflect underlying basement topography or limits of the host rocks (Brandt et al., 1961)
- thickness variations and mineralogical zonation within ore lenses reflects basement topography to some extent (Brandt et al., 1961; Fleischer et al., 1976; cf. Annels, 1979)
  - C-OB lower grade and pyritic where it straddles basement highs
  - richest C-OB Cu-mineralisation often developed on immediate flanks of basement highs
  - A-OB thicker and higher grade directly above basement highs

CODES SRC

Host-rock textures

MUF-1, FW to A-OB

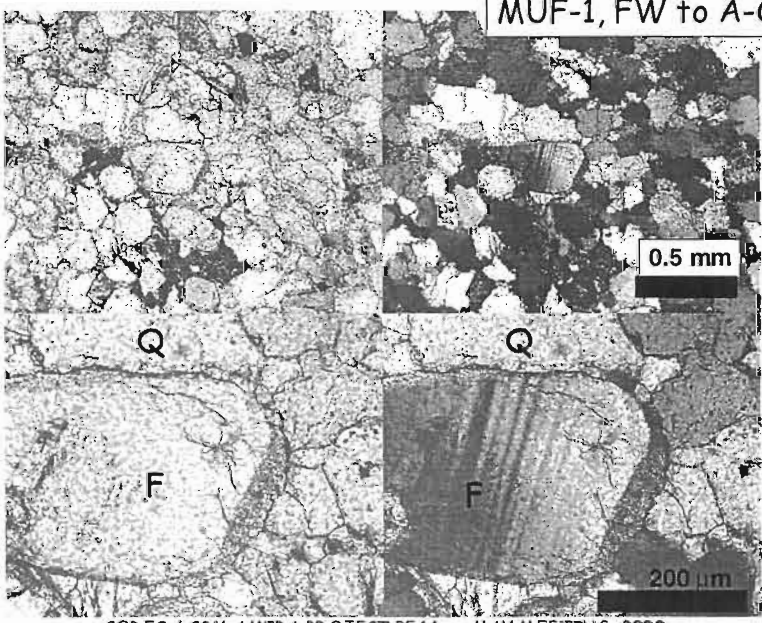

CODES SRC

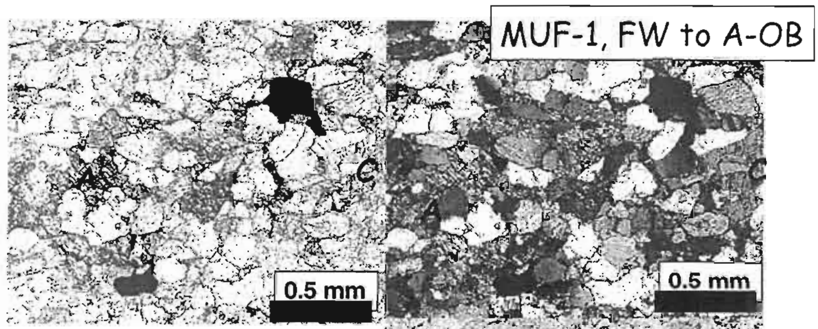

- anhydrite, carbonate
  - variable distribution throughout Ore Formation
  - habit and distribution reflect degree of compaction in host rock

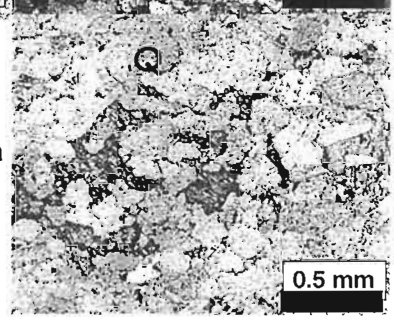

Host-rock textures

- Early diagenetic(?) overgrowths on detrital quartz and feldspar grains
- Advanced grain-scale dissolution and recrystallisation of detrital quartz grains in "clean" quartzite and arkosic sst
  - *Low porosity* interlocking grain mosaics
  - Anhydrite, carbonate distribution indicate significant mobility of these phases during development of present rock fabric

Distribution of Cu-sulfides

- interstitial to replacive habit
- habit and distribution reflects degree of compaction in host layers

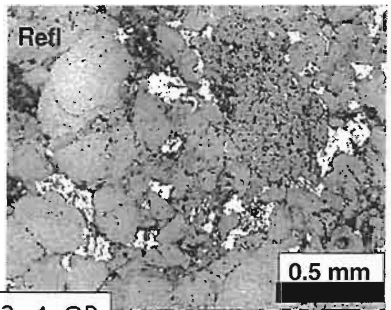

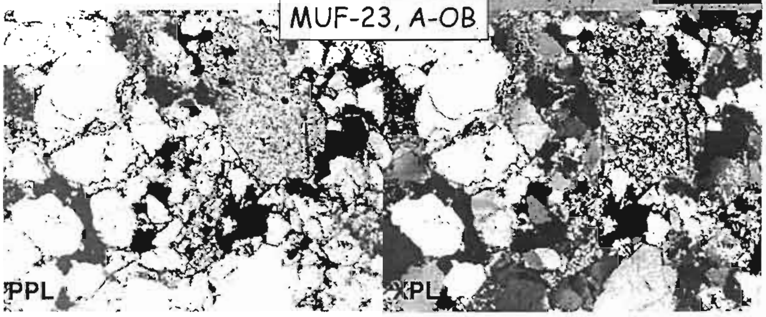

Distribution of Cu-sulfides

- (?)Carbonaceous material (after hydrocarbons?) coats detrital grains and early diagenetic overgrowths
- Cu-sulfides post-date early qtz + fsp diagenetic(?) overgrowths

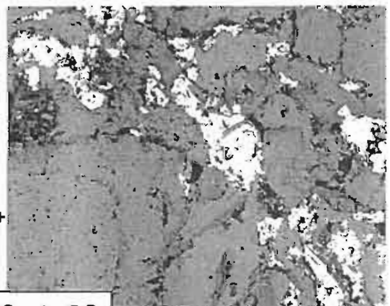

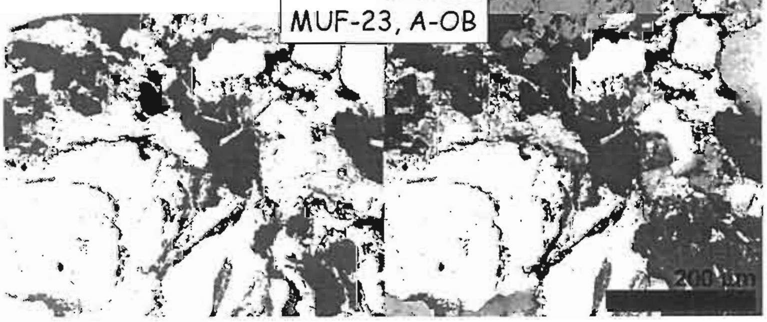

high-grade A-OB (MUF-23) barren fringes A-OB (MUF-21)

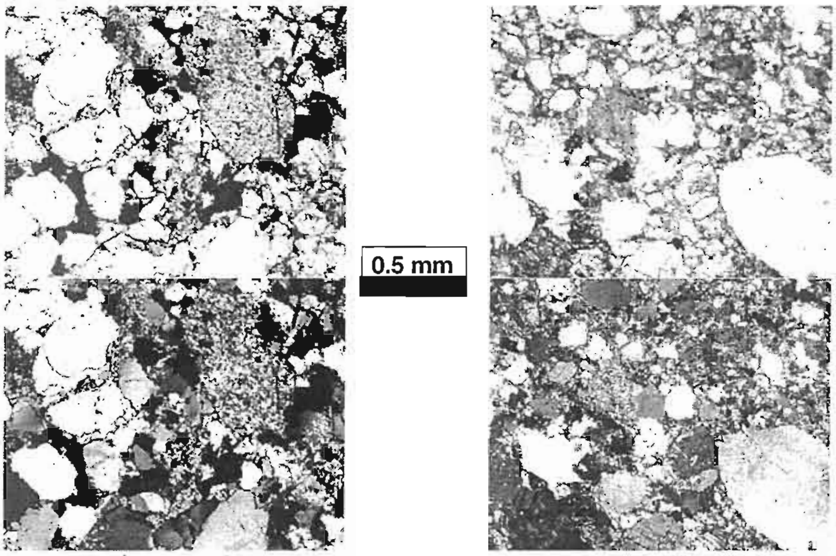

carbonaceous?
less argillaceous
no anhydride, carbonate

abundant biotite,
anhydride, carbonate

Pyritic C-OB

- Cpy largely post-dates Py
- Cpy as non-replacive (illus.) to replacive overgrowths on euhedral Py

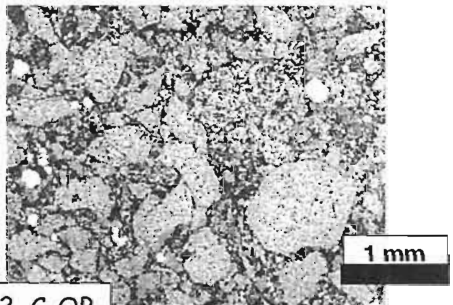

MUF-22, C-OB

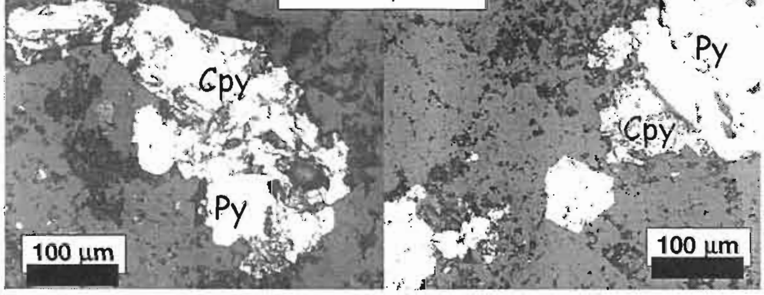

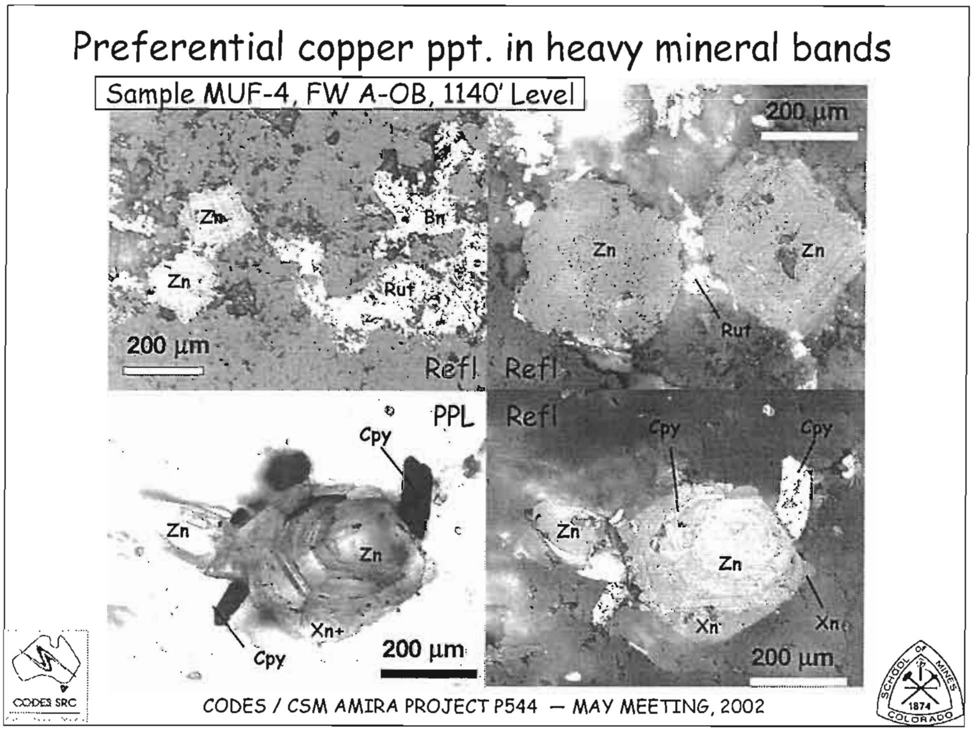
Preferential copper ppt. in heavy mineral bands
Sample MUF-4, FW A-OB, 1140' Level
Zn
Zn
Bn
Ruf
200 µm
Refl
Refl
Zn
Zn
Rut
200 µm
PPL
Cpy
Zn
Zn
Xn+
Cpy
200 µm
Refl
Cpy
Cpy
Zn
Zn
Xn
Xn
200 µm
CODES SRC
CODES / CSM AMIRA PROJECT P544 — MAY MEETING, 2002
SCHOOL OF MINES
1874
COLORADO

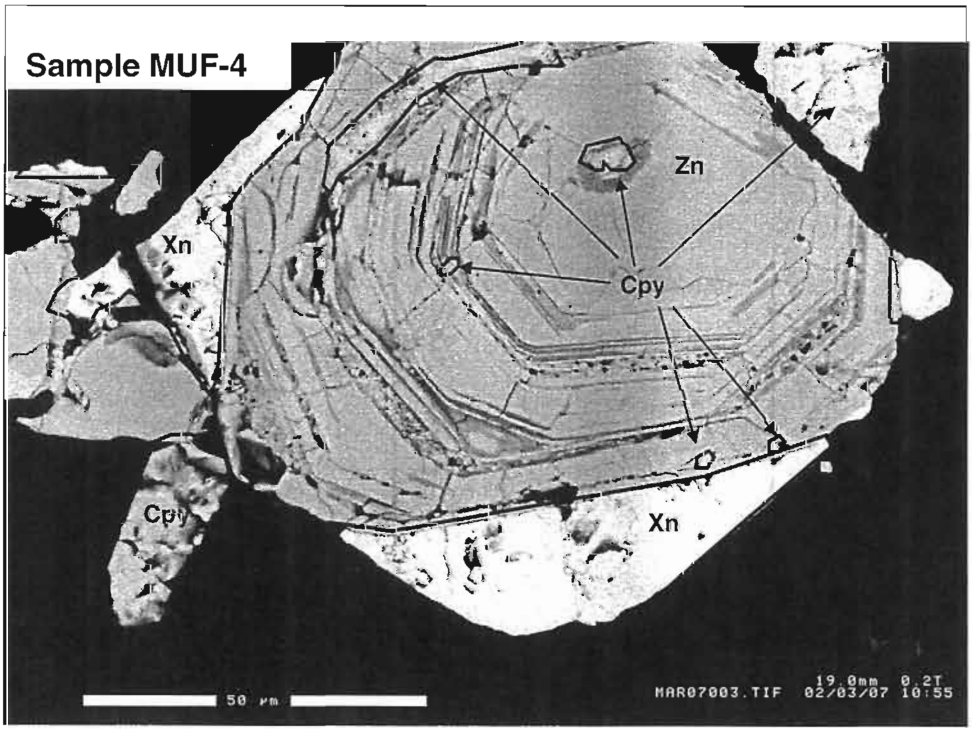
Sample MUF-4
Zn
Xn
Cpy
Cpy
Xn
50 µm
MAR07003.TIF
19.0mm 0.2T
02/03/07 10:55

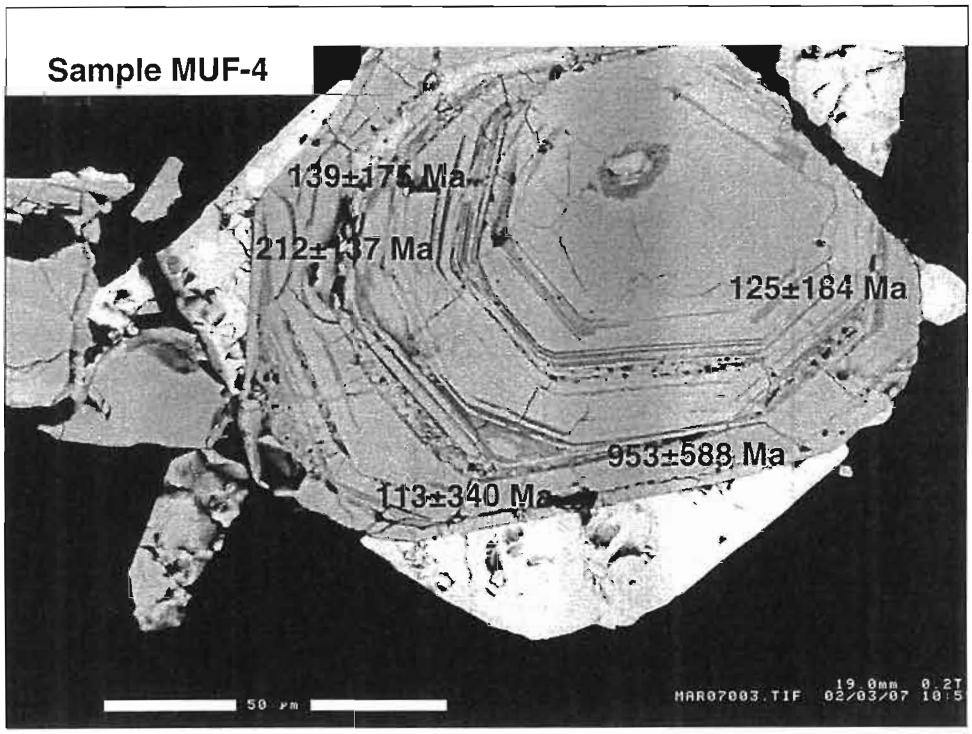
Sample MUF-4
139±175 Ma
212±137 Ma
125±184 Ma
953±588 Ma
113±340 Ma
50 µm
19.0mm 0.2T
MAR07003.TIF 02/03/07 10:5


50 µm
20.kV 700x BSED
CSL, Uni. of Tasmania
MAR07004.TIF 02/03/07 11:25
19.7mm 0.2T
CODES SRC

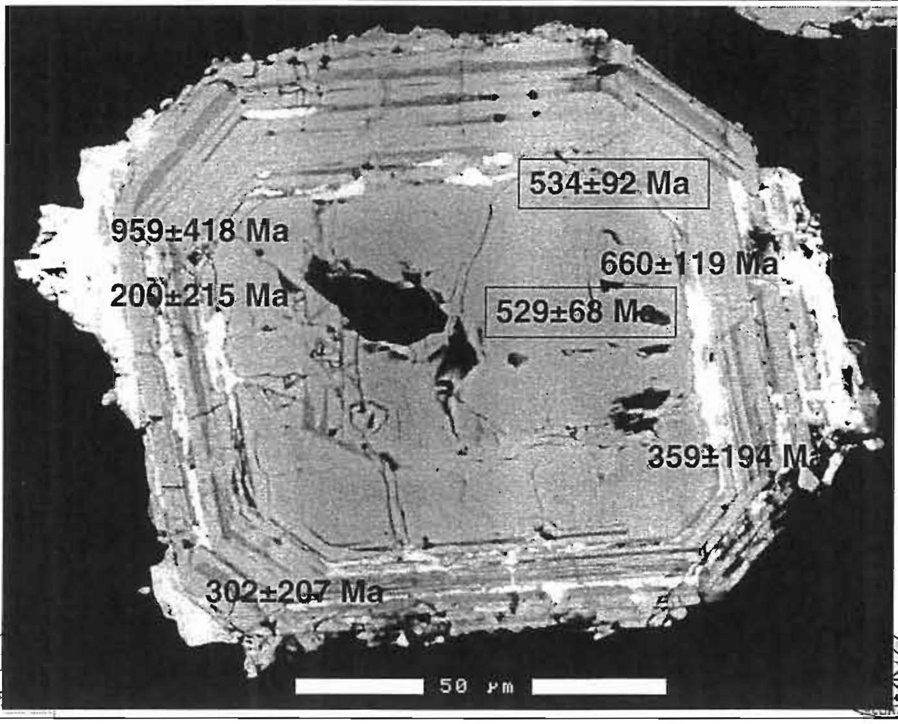

Summary

- Introduction of Cu-ores after early diagenetic overgrowths on detrital quartz and feldspar, but prior to the development of low porosity interlocking grain mosaics
- Ore Formation marks transition from relatively clean quartzite and arkose to more argillaceous (± calcareous) sediments and position of individual ore bodies appears to reflect similar (cyclic) transitions
- Facies changes reflect change in basin geometry/structural architecture

Summary cont......

- Other potentially important factors influencing Cu ppt
  - anhydrite, residual hydrocarbons, heavy minerals
- Although pre-Lufilian (?)diagenetic origin for Cu-ores is inferred on textural grounds, what is the significance of 530 Ma U-Th-Pb ages for xenotime/chalcopyrite intergrowths?
  - Question of precision? U-Th-Pb contents of close to detection for the electron microprobe.
  - Resetting during the Lufilian Orogeny?

CODES SRC

CODES / CSM AMIRA PROJECT P544 — MAY MEETING, 2002

SCHOOL OF MINES 1874 COLORADO

Style and stratigraphic context of copper mineralisation: Ndola West

Robert Scott

Centre for Ore Deposit Research
University of Tasmania

CODES SRC

SCHOOL OF MINES 1874 COLORADO

Introduction

- Ndola West Prospect 3-6 km WNW of Ndola township
- NE flank of the Kafue anticline
- In 2000, ZamAnglo drilled a series of diamond holes to test for copper mineralisation in the Lower Roan

CODES / CSM AMIRA PROJECT P544 — MAY MEETING, 2002

Location & Regional Geology

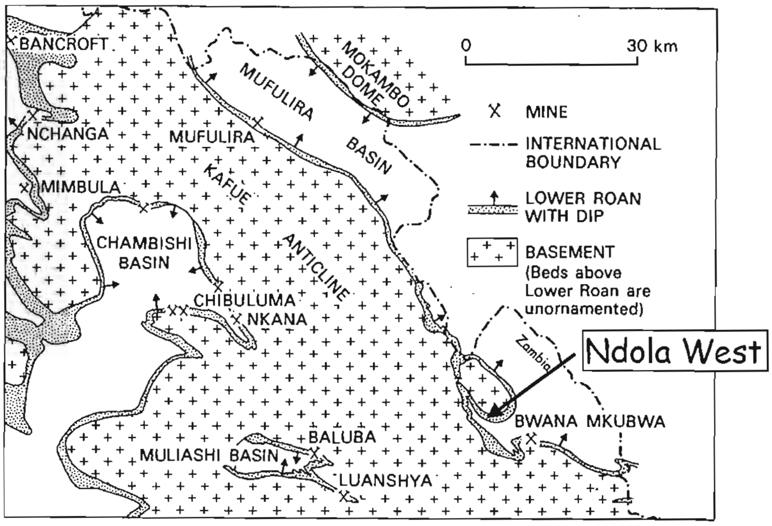

CODES / CSM AMIRA PROJECT P544 — MAY MEETING, 2002

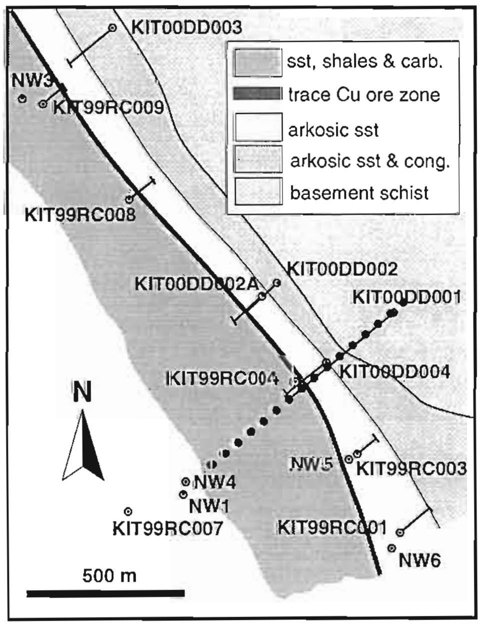

Location of drill holes - surface geology

Detailed stratigraphic and structural logging of Ndola West drillholes:

KIT00DD001 (730 m)
KIT00DD004 (300 m)
DD004 Def 1 (56 m)
DD004 Def 2 (58.5 m)

CODES / CSM AMIRA PROJECT P544 — MAY MEETING, 2002

Style and stratigraphic context of copper mineralisation at Ndola West

- Aims of this presentation:
  - Stratigraphy and chemo-stratigraphy of Lower Roan: (ZamAnglo multi-element geochemistry for KIT00DD001 and DD004, presented with permission)
  - distribution, style and origin of copper mineralisation

CODES / CSM AMIRA PROJECT P544 — MAY MEETING, 2002

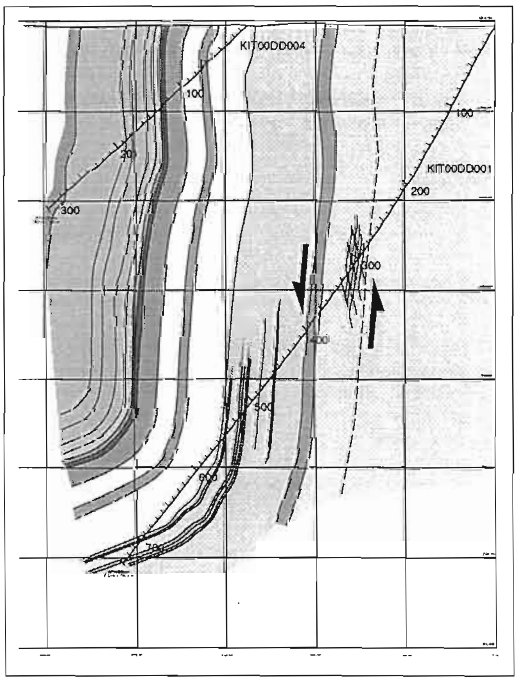

Geological section

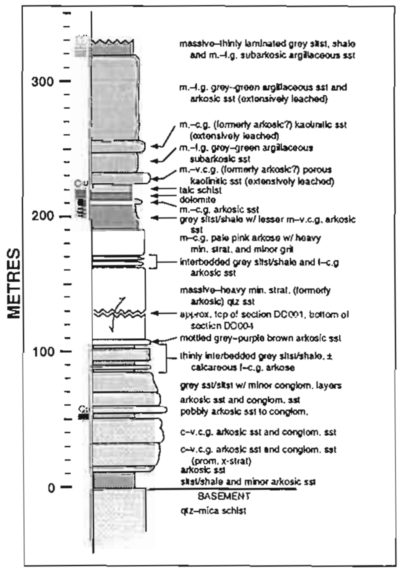

CODES / CSM AMIRA PROJECT P544 — MAY MEETING, 2002

Lower Roan Stratigraphy

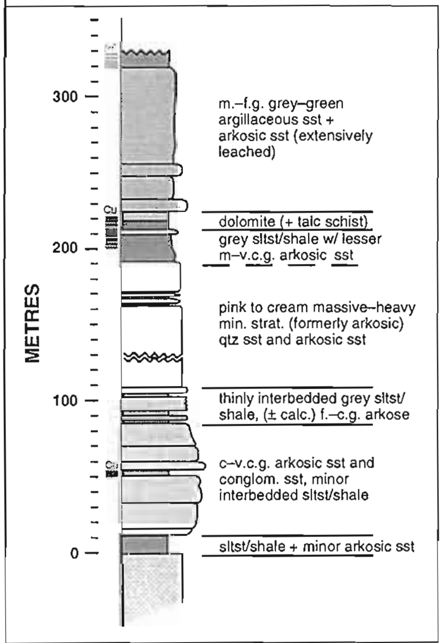

CODES / CSM AMIRA PROJECT P544 — MAY MEETING, 2002

Lower Roan Stratigraphy

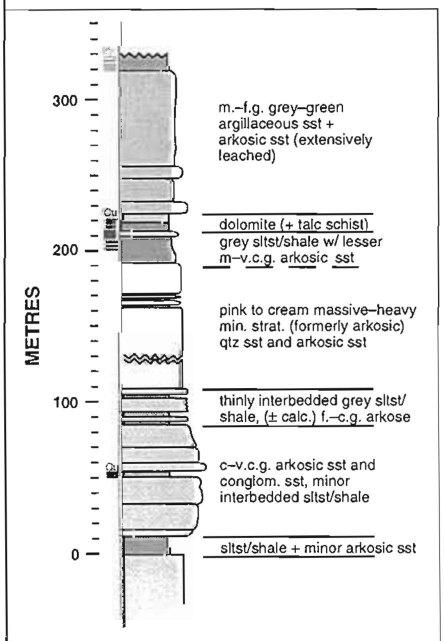

CODES / CSM AMIRA PROJECT P544 — MAY MEETING, 2002

Lower Roan Stratigraphy

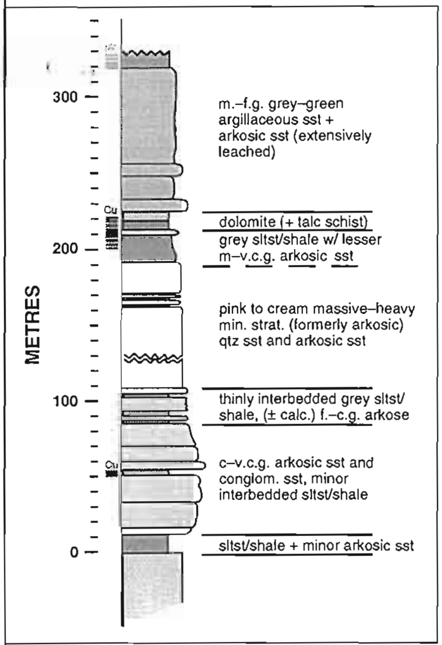

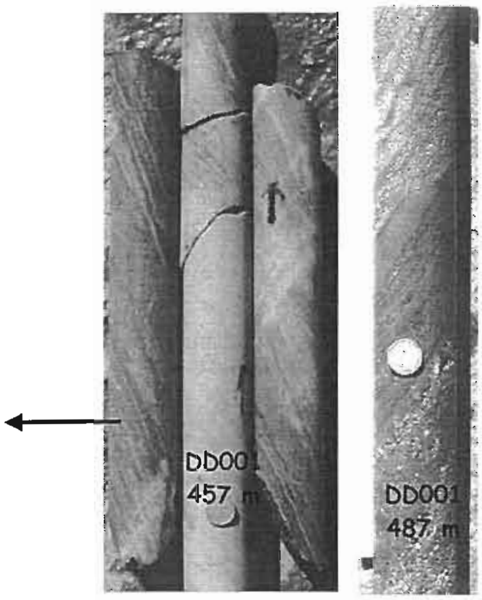

CODES / CSM AMIRA PROJECT P544 — MAY MEETING, 2002

Lower Roan Stratigraphy

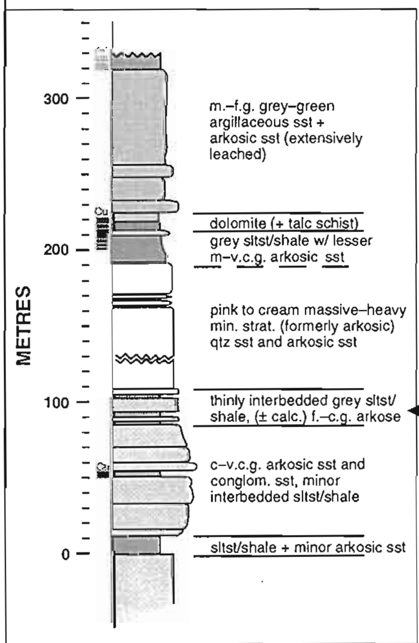

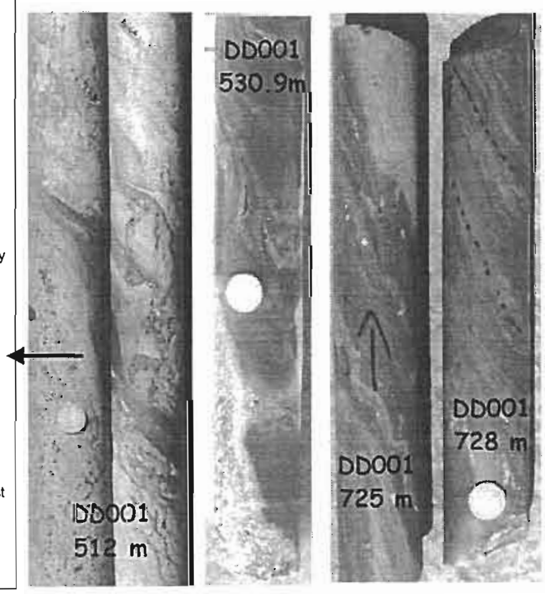

CODES / CSM AMIRA PROJECT P544 — MAY MEETING, 2002

Lower Roan Stratigraphy

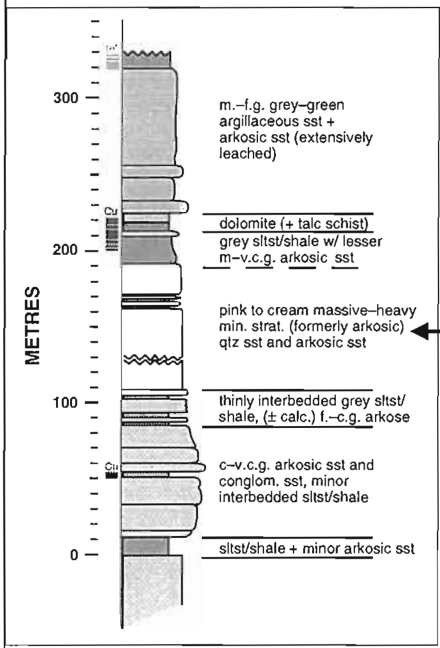

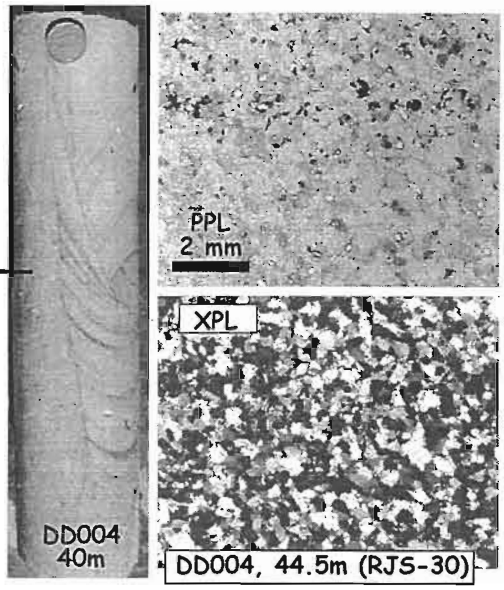

CODES / CSM AMIRA PROJECT P544 – MAY MEETING, 2002

Lower Roan Stratigraphy

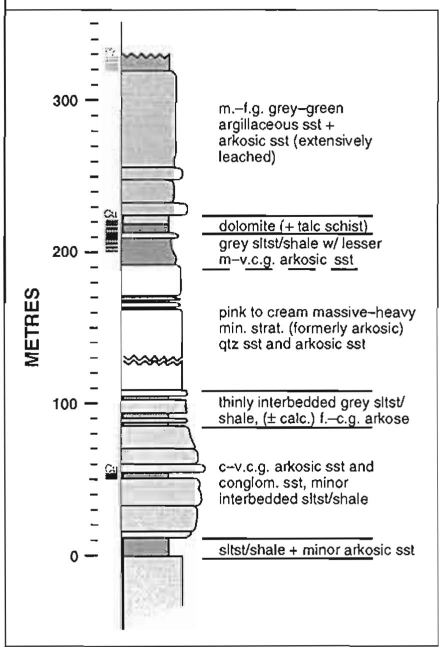

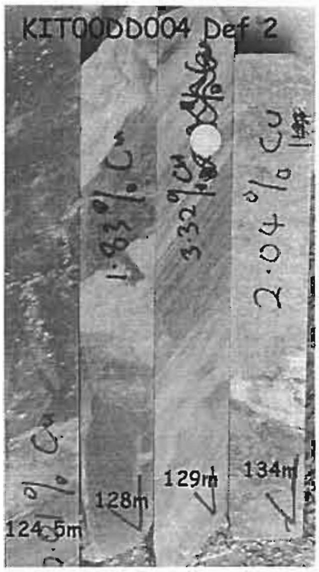

CODES / CSM AMIRA PROJECT P544 – MAY MEETING, 2002

Lower Roan Stratigraphy

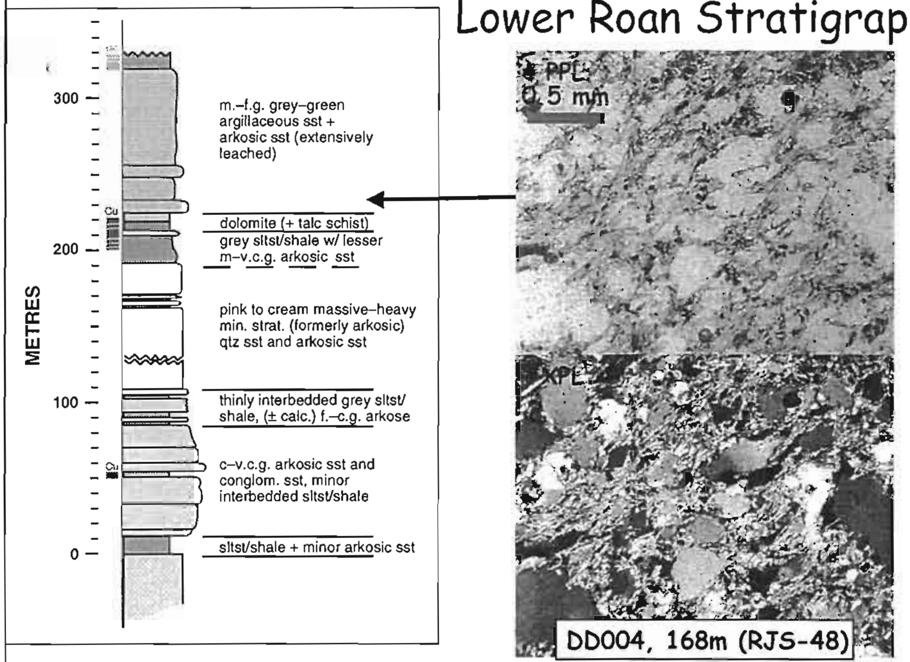

CODES / CSM AMIRA PROJECT P544 — MAY MEETING, 2002

above "ore horizon" below "ore horizon"

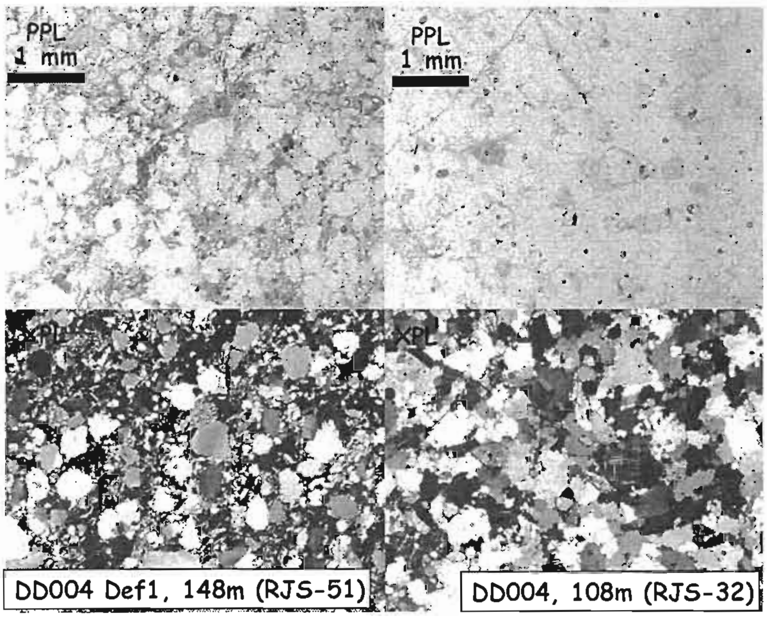

CODES / CSM AMIRA PROJECT P544 — MAY MEETING, 2002

Lower Roan Stratigraphy

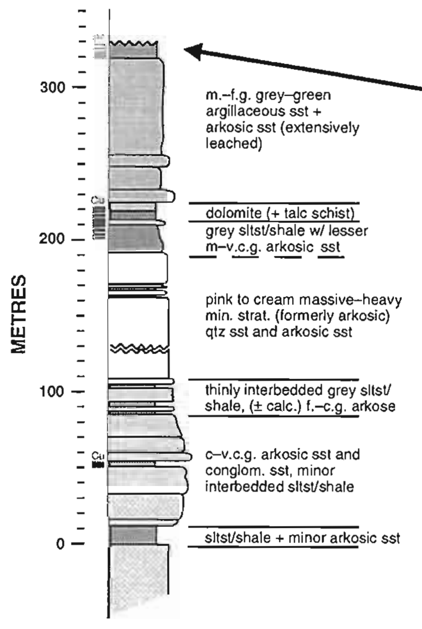

CODES / CSM AMIRA PROJECT P544 — MAY MEETING, 2002

Comparison with Mufulira

Ndola West

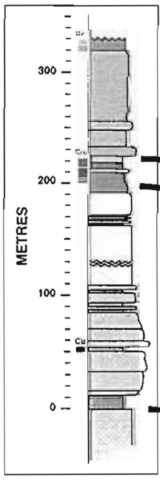

Mufulira

Argillaceous (±arkosic) sst

Ore Horizon

Footwall arkosic sst and conglomerate (± minor sltst/shale)

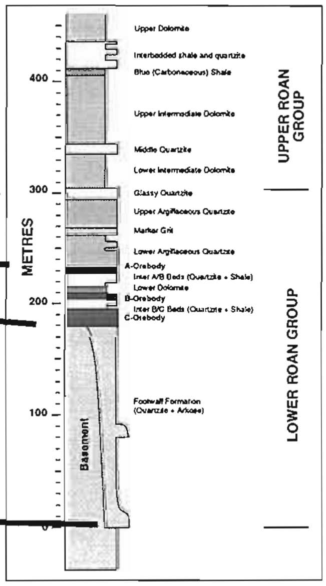

CODES / CSM AMIRA PROJECT P544 — MAY MEETING, 2002

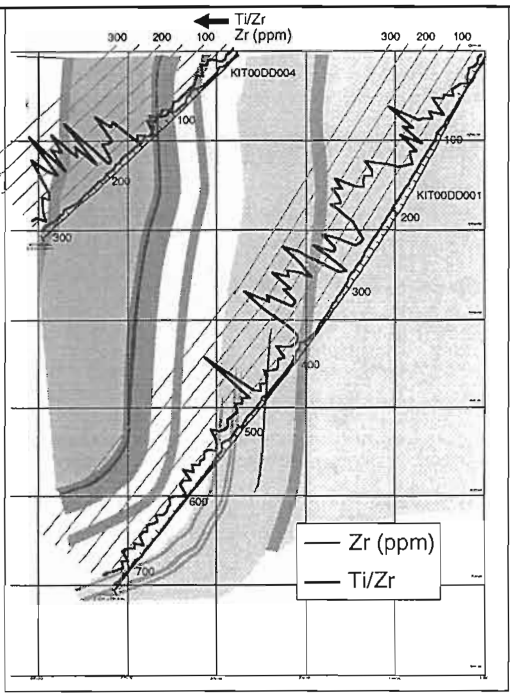

Chemo-stratigraphy: Ti/Zr

- Ti/Zr
  - generally <50, in "footwall" succession
  - highly variable (50-200) in argillaceous sst above "Ore Horizon"
- Zr
  - slightly elevated through "ore horizon", below dolomite

CODES / CSM AMIRA PROJECT P544 — MAY MEETING, 2002

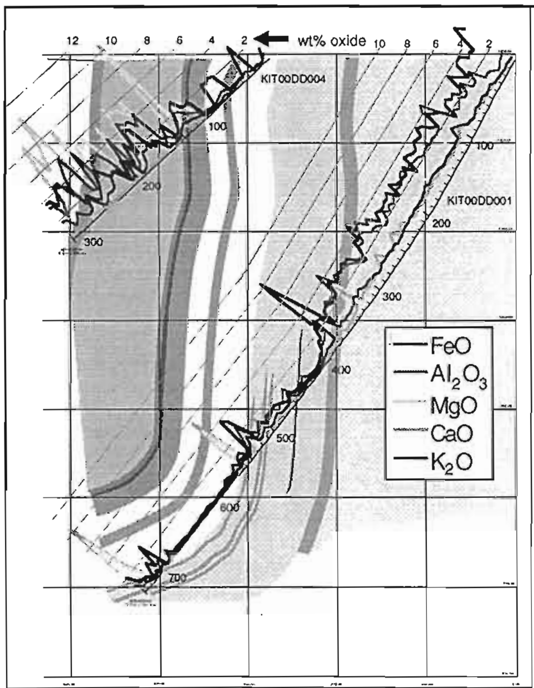

Chemo-stratigraphy: majors

- "dead" zone below ore horizon
- argillaceous sst higher, more variable Al, Mg & K than units below ore horizon, reflecting increased mica (Mg-biotite to phlogopite) content

CODES / CSM AMIRA PROJECT P544 — MAY MEETING, 2002

Cu, Zn, Pb,Co distribution: DD004

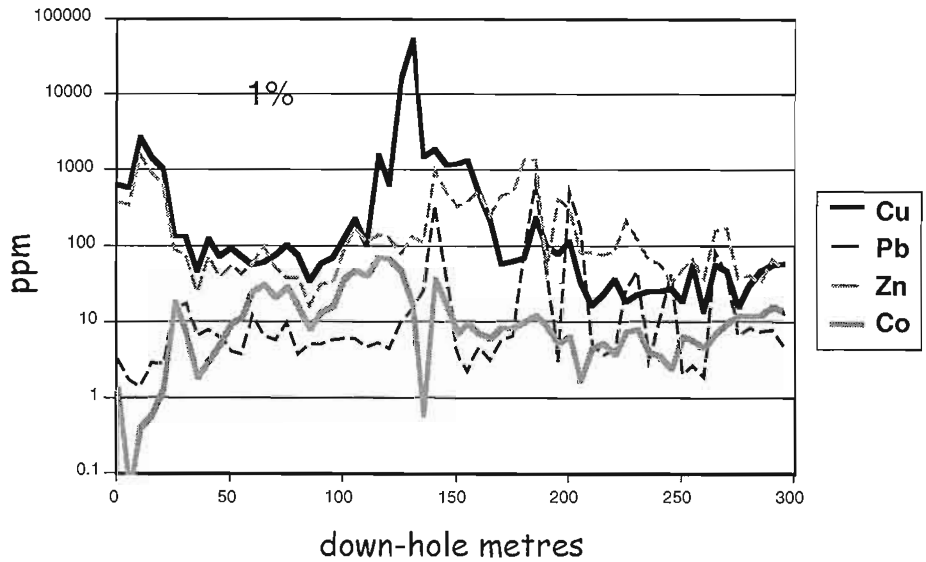

CODES / CSM AMIRA PROJECT P544 – MAY MEETING, 2002

Copper ores

- Main "ore zone" 15-25 m wide
- host-rocks:
  - silicified m.g. arkose - qtz sst w/ patchy carbonate alteration
  - underlain by dk grey bio-rich carb. altered sltst and shale; overlain by dolomite
- f.g. disseminated cc, bn > cpy in arkose - qtz sst
- md.-c.g. bn>cpy within qtz veins and dolomite

CODES / CSM AMIRA PROJECT P544 – MAY MEETING, 2002

- "Ore zone" host-rocks moderately to strongly deformed
- 8-10 m wide zone of strong fabric development ($//S_0$) in siltstone/shale at base of "Ore zone"
- 8 m wide zone of talc schist caps "Ore zone"
- foliation overprints patchy carbonate alteration + Cu-sulfides

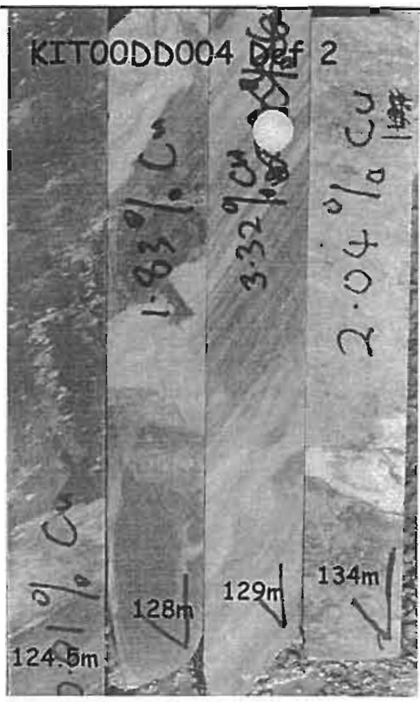

textural relations:
disseminated ore

sulfides
interstitial-replacive
habit

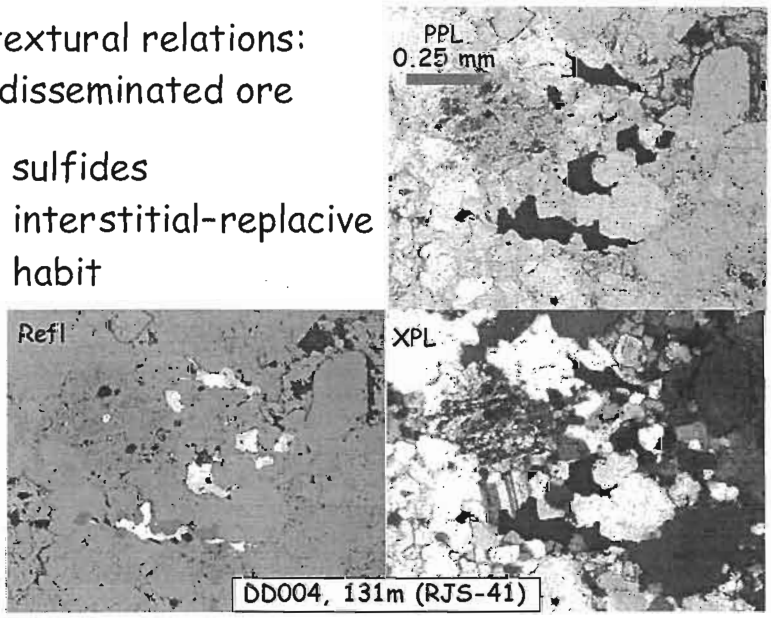

textural relations: carbonate-hosted ore

m.-c.g. sulfides overprinted by thin anastamosing talc schist bands

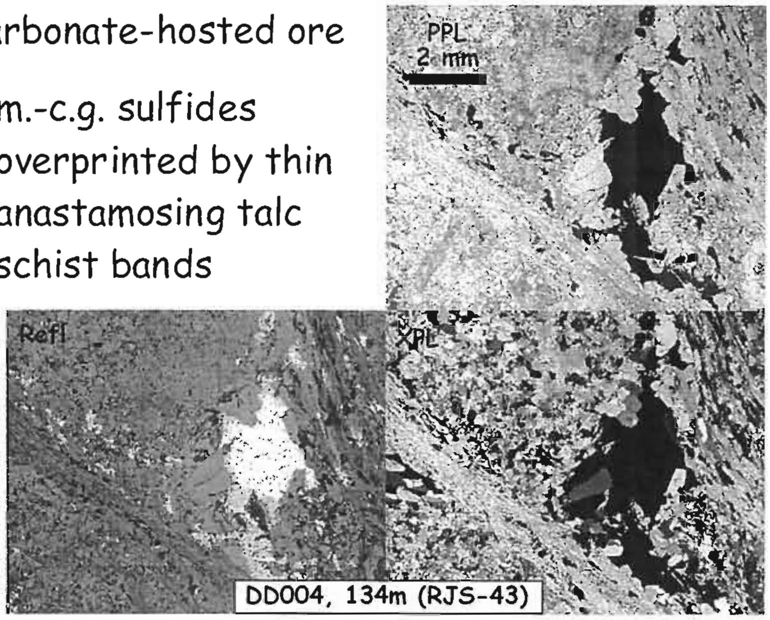

CODES / CSM AMIRA PROJECT P544 — MAY MEETING, 2002

Cu timing: lower mineralised horizon

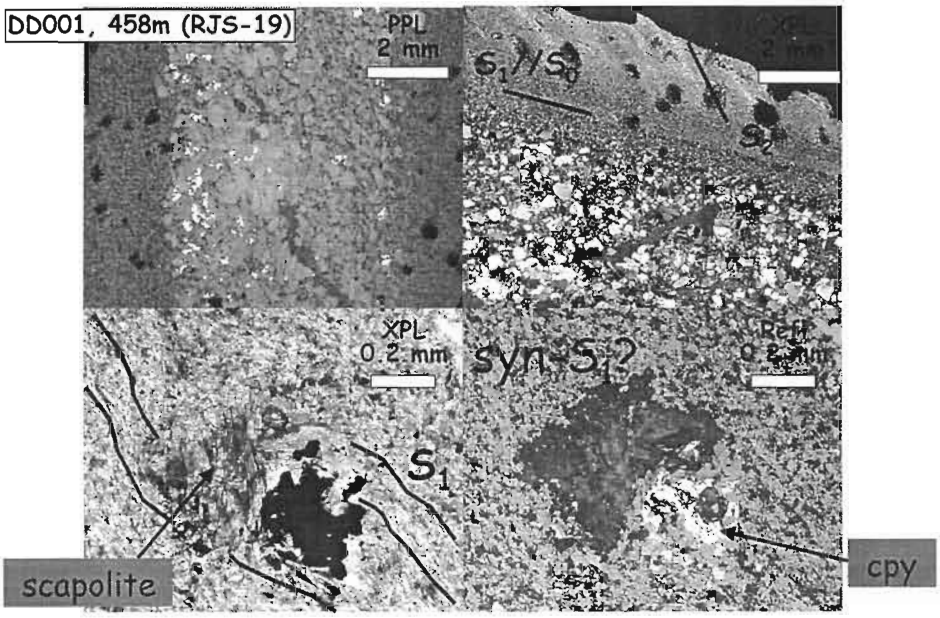

CODES / CSM AMIRA PROJECT P544 — MAY MEETING, 2002

Summary

- Lower Roan stratigraphy and position of mineralisation broadly comparable to Mufulira
- Lower part of sequence (below main ore horizon) dominated by arkosic to sub-arkosic sst and conglomeratic sst (NB. extensive feldspar destruction locally)
- Main ore horizon capped by dolomite, and thick sequence of Mg-biotite-rich argillaceous sandstone
- Introduction of Cu-sulfides predates variably developed layer parallel foliation (S_1)

Zambia: Lithogeochemistry Update

Kalulushi Archive

•4 filing cabinets of monthly metallurgical assays !

•Limited suite of elements

•Small amount of multi-element data; quality control?

hence NO USE TO P544

Present Strategy

•Opportunistic (e.g., mill feed samples) & directed

Zambia: Lithogeochemistry Update

RULE NUMBER ONE

•Geochemical studies will be undertaken with context provided by our other geological investigstions

Techniques

•XRF major & trace elements

•Some trace elements by ICP and/or INAA

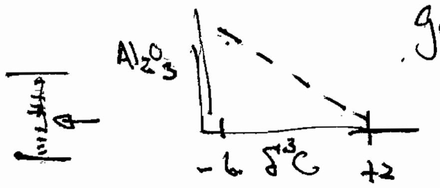

Get set with a variable silt/carb ratio to check effect of metamorphism.

Zambia: Lithogeochemistry Update

Chambishi Basin

C/O isotopes set.

•78 samples from RCB~~2~~1 & RCB2 provide a reference chemostratigraphic section for the Roan — XRF analyses now complete

Include some for C/O.

•Nkana: 47 samples from underground exploration hole SOB (Croaker PhD); production samples from SOB, Central, Mindola North and Mindola shafts — XRF analyses now complete

•Future Chambishi Basin work will involve additional samples as part of Mawson Croakers PhD (incl. Barren gaps?); subsets of samples for Corg and C/O isotopes)

AMIRA P544 May 2002 ppt01.mcgoldrick

Zambia: Lithogeochemistry Update

Konkola Dome - Kirilabomwe Area

•XRF analyses are complete for 6 underground samples collected from No3 shaft workings in June 2001 by RS & PMcG

•XRF analyses are complete for 11 samples from DDH KLB67 ('barren gap' drill hole) —DB & PMcG

•Future focus will be on samples collected as part of Nicky Pollington's PhD; Konkola North drilling provides a unique opportunity to examine the geochemical variability in shaley facies vertically and laterally in the Lower Roan in some detail

AMIRA P544 May 2002 ppt01.mcgoldrick

Zambia: Key Questions (con)

Mufulira Basin

- Limited sampling to date
- 5 underground grab samples & 2 mill feed samples collected in June 2001—XRF analyses are complete
- Zamanglo have made available an excellent ICP multi-element data set for Ndola West

AMIRA P544 status report: *In situ* xenotime and monazite U-Th-Pb geochronology

Neal McNaughton

Centre for Global Metallogeny
University of Western Australia

Bibliography: xenotime & monazite

McNaughton, N.J., Rasmussen, B. and Fletcher, I.R., 1999. SHRIMP U-Pb dating of diagenetic xenotime in siliciclastic sedimentary rocks. *Science 285*, 78-80.

Fletcher, I.R., Rasmussen, B. and McNaughton, N.J., 2000. High-precision SHRIMP U-Pb geochronology of authigenic xenotime. *Aust. J. Earth Sci. 47*, 845-859.

Rasmussen, B., Fletcher, I. R. and McNaughton, N. J., 2001. Dating low-grade metamorphism by SHRIMP U-Pb analysis of monazite in shales. *Geology 29*, 963-966.

Rasmussen, B., Bengtson, S., Fletcher, I.R. and McNaughton, N.J., 2002. Discoidal impressions and trace-like fossils more than 1,200 million years old. *Science.*

Vallini, D., Rasmussen, B., Krapez, B., Fletcher, I.R. and McNaughton, N.J., submitted. Obtaining diagenetic ages from metamorphosed sedimentary rocks: U-Pb geochronology of unusually coarse xenotime cement in phosphatic sandstone. *Geology.*

Kositcin, N., McNaughton, N.J., Griffin, B.J., Fletcher, I.R., Groves, D.I. and Rasmussen, B., submitted. Textural and geochemical discrimination between xenotime of different origin in the Archaean Witwatersrand Basin, South Africa. *Geochim. Cosmochim. Acta.*

Dawson, G.C., Fletcher, I.R., Krapez, B., McNaughton, N.J. and Rasmussen, B., submitted. 1.2 Ga thermal metamorphism in the Albany-Fraser Orogen of Western Australia: consequence of collision or regional heating by dyke swarms? *J. Geol. Soc., London.*

Phosphate chemistry

Xenotime (Y,M-HREE)PO4

Monazite (LREE,Th)PO4

For geochronology:
U-Th substitute &
radiogenic Pb retained;
high "blocking temperature"

Origin of xenotime-monazite

	Xenotime	Monazite
Diagenesis:		
- early	x	-
- late	x	?
Metamorphism:		
- very low grade	x	x
- low to medium	x	x
- high grade	x	x

Origin of xenotime-monazite (cont.)

	Xenotime	Monazite
Alteration	x	x
Veins	x	x
Igneous:		
- granites	x	x
- pegmatites	x	x
- carbonatites	x	?

In situ ion microprobe (SHRIMP) geochronology of xenotime-monazite

U-Pb and Th-Pb geochronology using O_2- ion beam with spot size of ~10 microns

Archaean to Palaeoproterozoic:
use 207Pb/206Pb age → +/- 0.2% to 0.5%

Neoproterozoic to Palaeozoic (to younger):
use U-Pb or Th-Pb age → +/- 1% to 2%

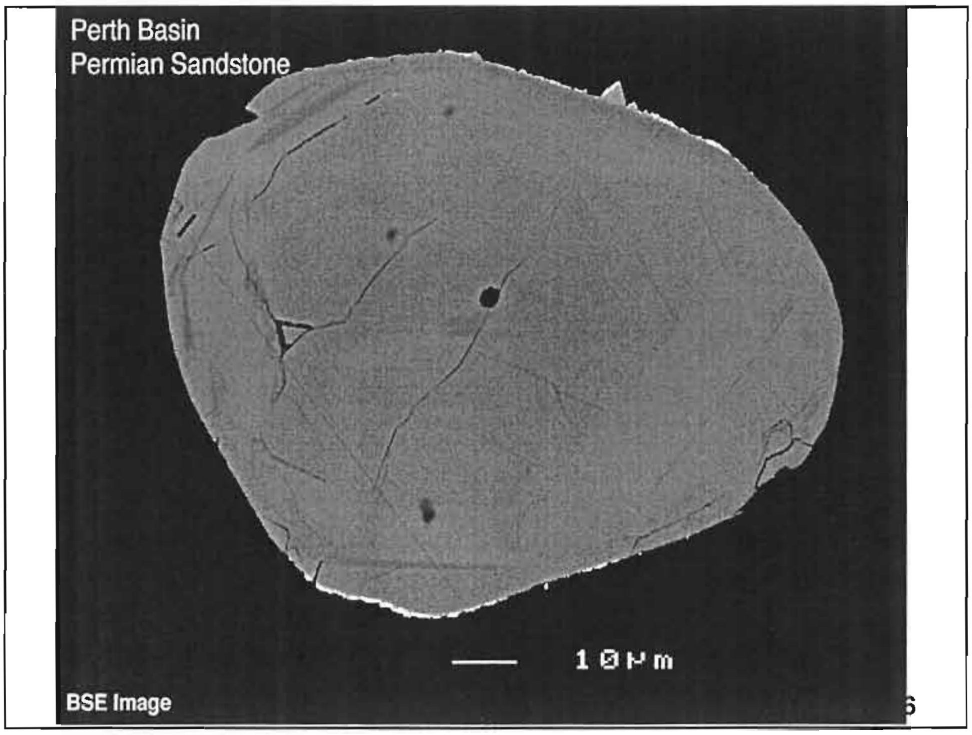
Perth Basin
Permian Sandstone
10µm
BSE Image
6

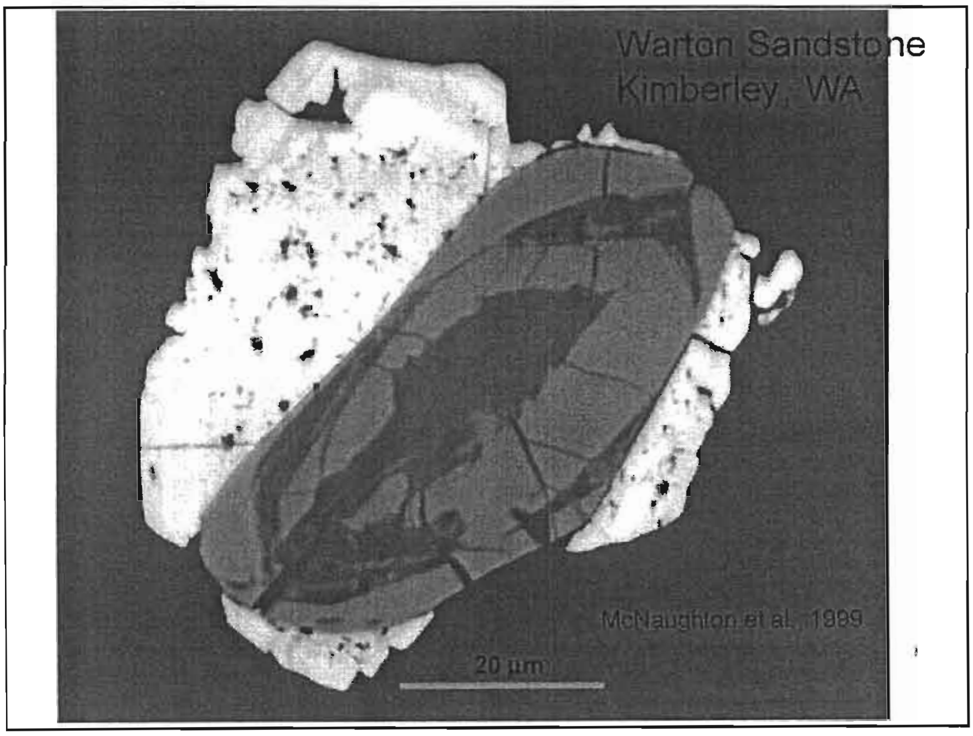
Warton Sandstone
Kimberley, WA
McNaughton et al., 1999
20 µm

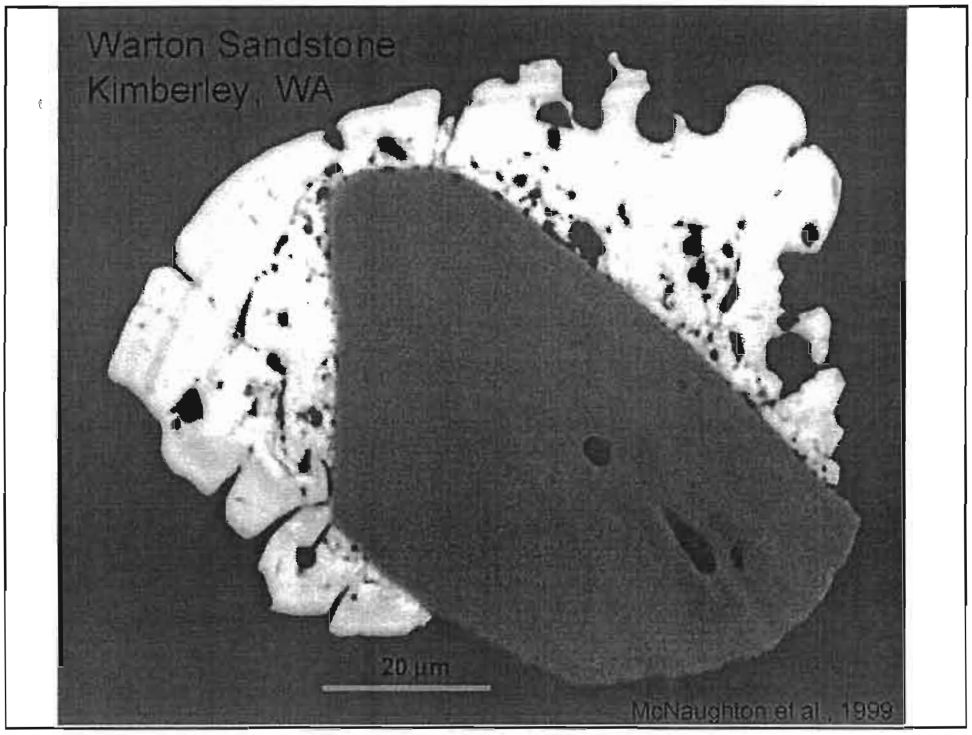
Warton Sandstone
Kimberley, WA
20 µm
McNaughton et al., 1999

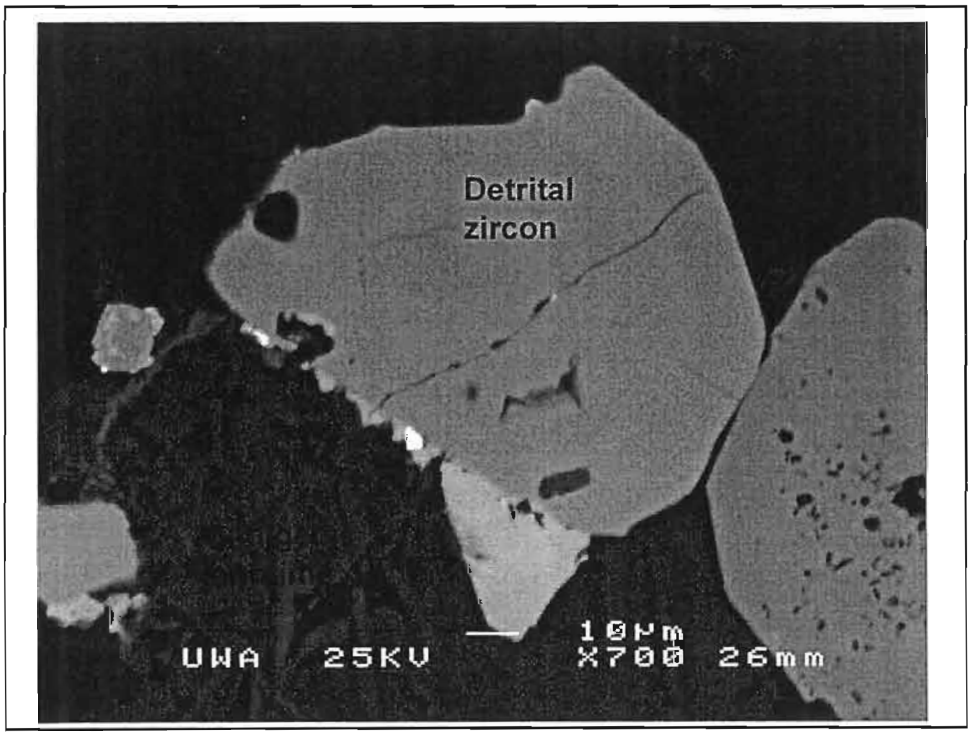
Detrital
zircon
UWA 25KV
10µm
X700 26mm

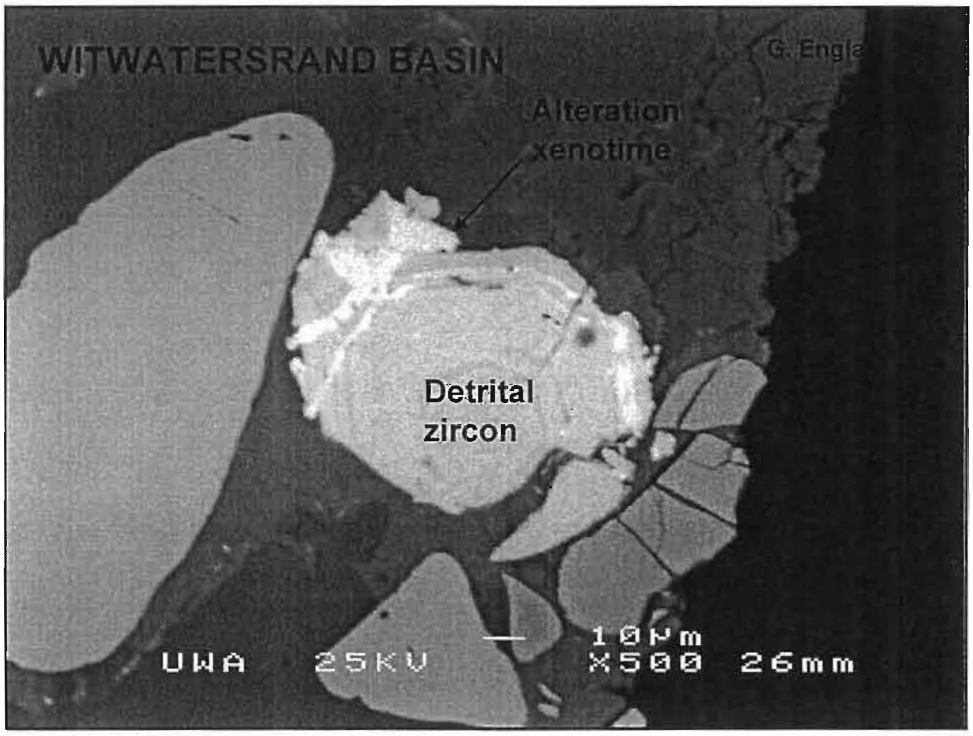
WITWATERSRAND BASIN
G. Engla
Alteration
xenotime
Detrital
zircon
10µm
UWA 25KV X500 26mm

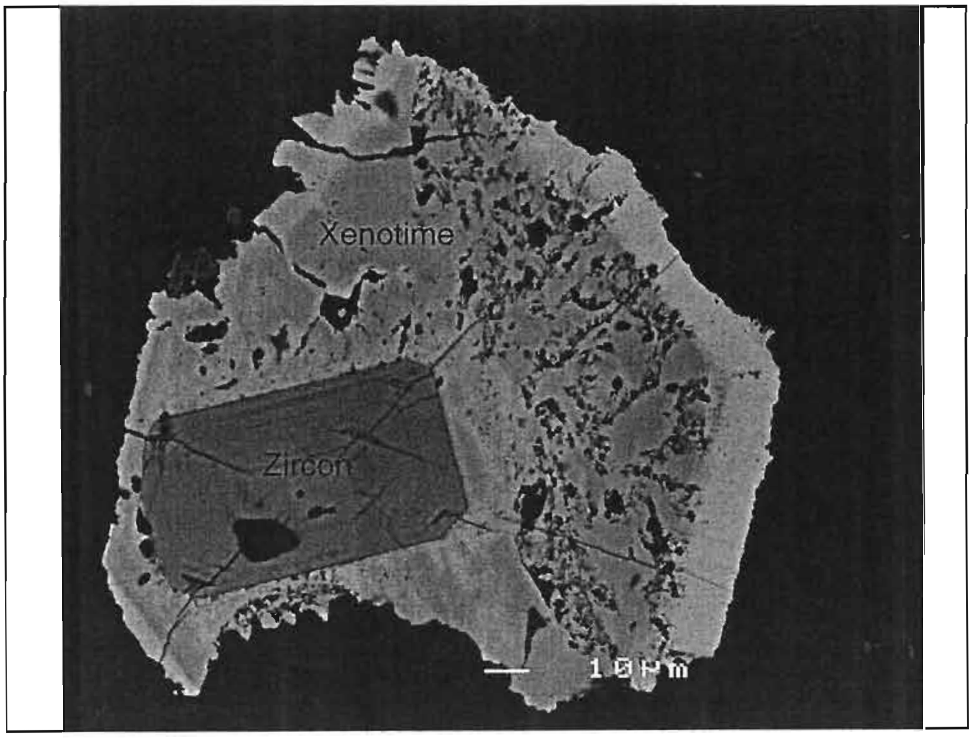
Xenotime
Zircon
10µm

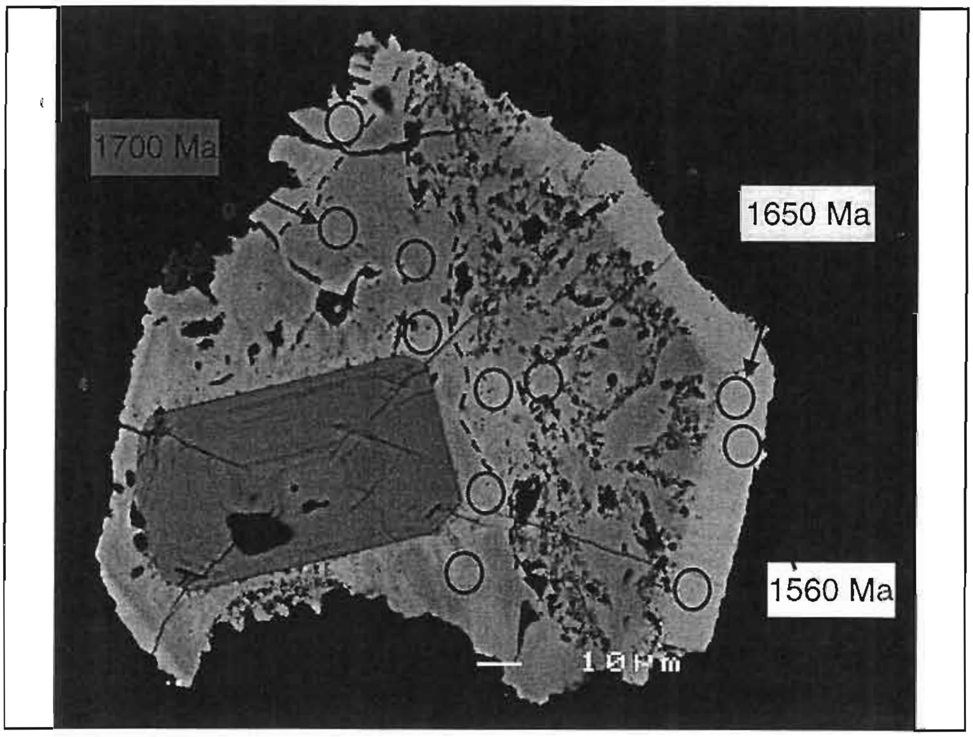

Recent example: xenotime

Diagenetic age from xenotime of 1704 +/- 7 Ma for sandstone previously constrained to ~1750 - ~700 Ma

(McNaughton et al., 1999: *Science 285*, 78-80)

AGE SPECTRA FOR DIAGENETIC XENOTIME FROM WARTON SST, KIMBERLEY, WA

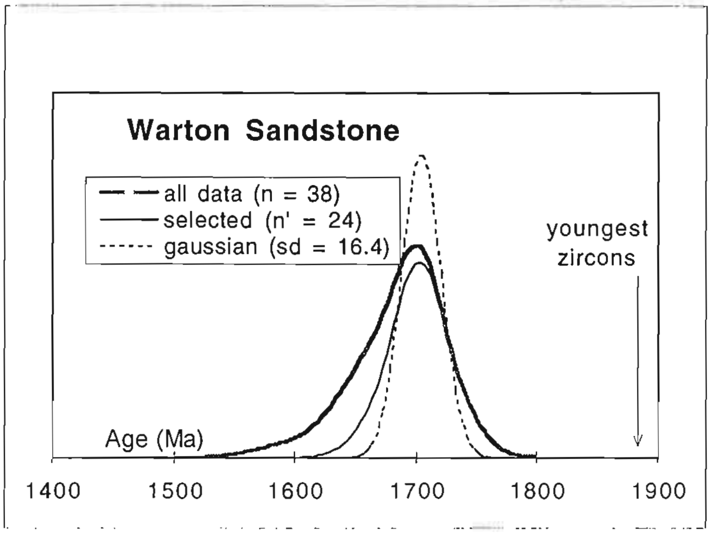

McNaughton et al., 1999

Recent example: monazite

Metamorphic age from monazite of 2196 +/- 6 Ma for very low grade metamorphism (prehnite-pumpellyite facies)

(Rasmussen et al., 2001: *Geology 29*, 963-966)

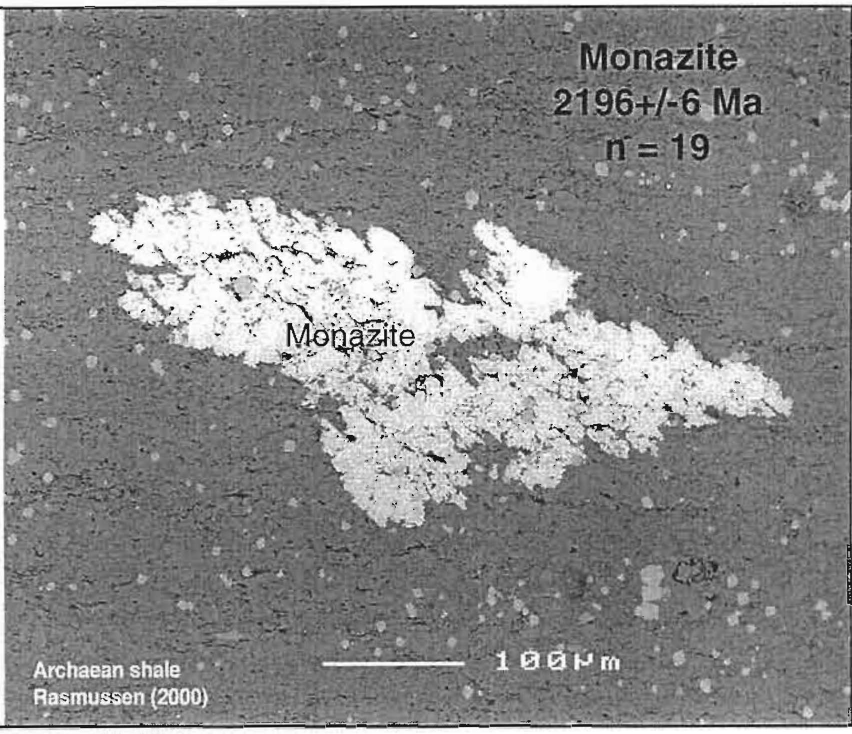

Recent example: multiple xenotime events

Witwatersrand basin

Xenotime forms in sandstones during fluid flow events: → xenotime dates events which affect basin, such as diagenesis, alteration and metamorphism

(England et al., 2001. *Terra Nova*)

AGE SPECTRA FOR WITWATERSRAND (CENTRAL RAND) XENOTIME FROM MINERALISED SAMPLES

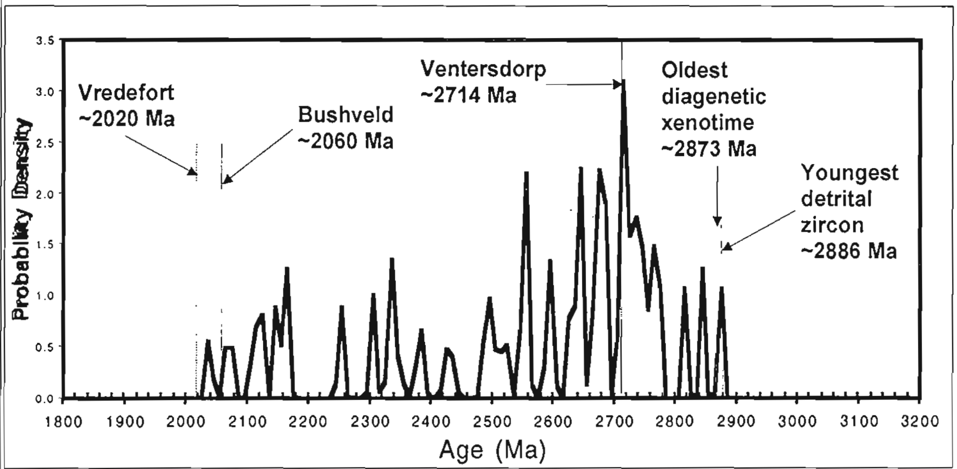

G.England, 1999

Recent examples (cont.)

Diagenetic and three hydrothermal alteration event ages from xenotime in sandstones of the Witwatersrand Basin (Kositcin et al., submitted)

Diagenesis	~2780 Ma
Alteration associated with:	
- Ventersdorp lavas	~2720 Ma
- unknown event	~2200 Ma
- Bushveld intrusion	~2060 Ma

The keys to successful *in situ* geochronology

- **Petrography:**
  know the textural timing of the xenotime you are dating

2. ***In situ* analysis methods:**
   - ion probe,
   - electron probe,
   - laser ICP-MS.

In situ U-Th-Pb geochronology

Method	Size (µm)	Age precision
SHRIMP	~10	best
Electron probe	~3	worst (xt) better (mon)
Laser ICP-MS	~30	intermediate

Xenotime geochemistry: to discriminate origin

Robust discriminators

- U, Eu, Gd/Yb discriminate magmatic from diagenetic-hydrothermal-metamorphic

Less robust discriminators

- Diagenetic from hydrothermal

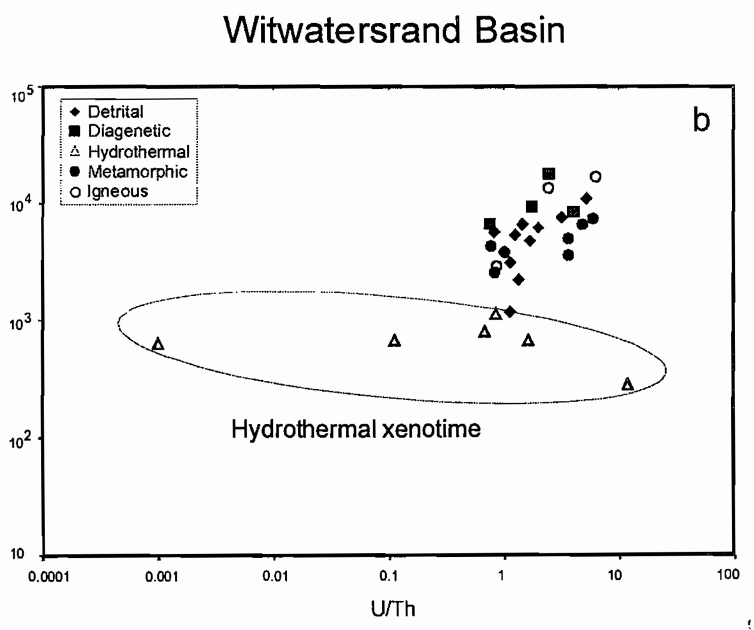

(from Kositcin et al., submitted)

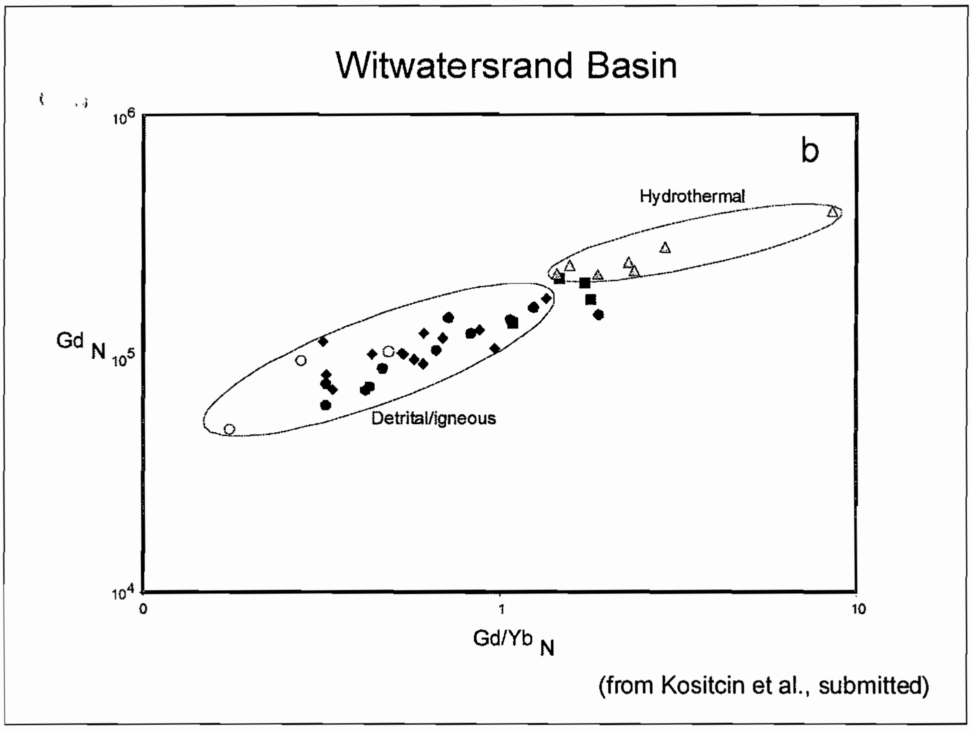
Witwatersrand Basin
b
Hydrothermal
Detrital/igneous
Gd N
Gd/Yb N
(from Kositcin et al., submitted)

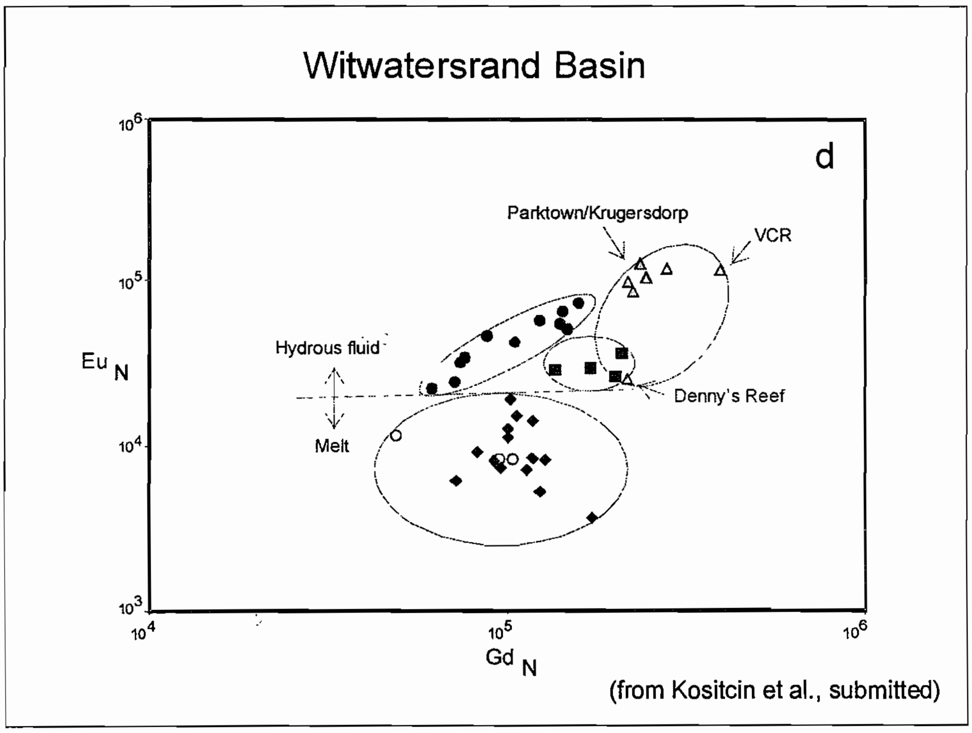
Witwatersrand Basin
d
Parktown/Krugersdorp
VCR
Hydrous fluid
Melt
Denny's Reef
Eu N
Gd N
(from Kositcin et al., submitted)

Xenotime geochemistry combined with age and texture allow discrimination of xenotime origin

What about monazite geochemistry?
..............currently being studied

The End

"CHIME"
CHEMICAL ISOCHRON METHOD

MEASURE U-Th-Pb CONTENTS BY IN SITU WDS ELECTRON PROBE ANALYSIS --> CALCULATE AGE

CHEMICAL ISOCHRON METHOD

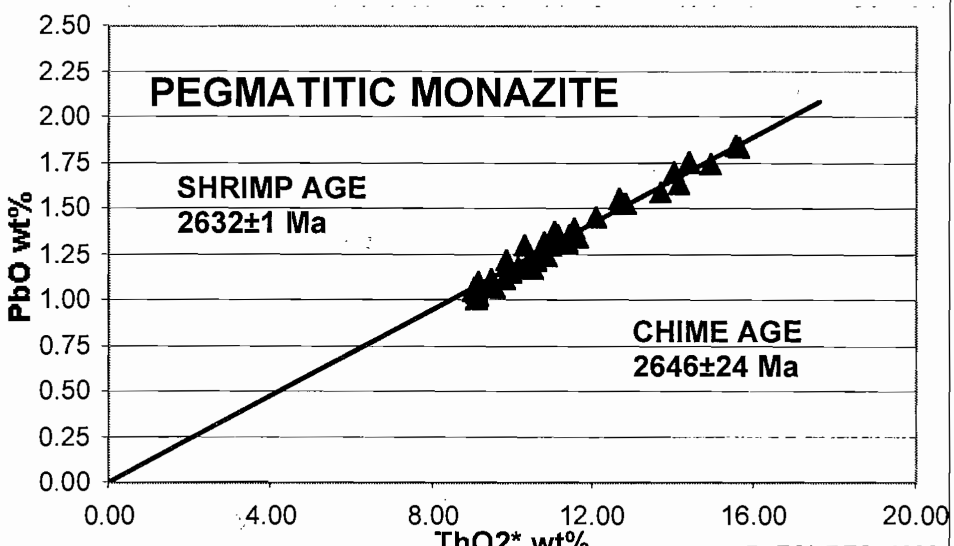

D. FORBES, 1999

CHEMICAL ISOCHRON METHOD

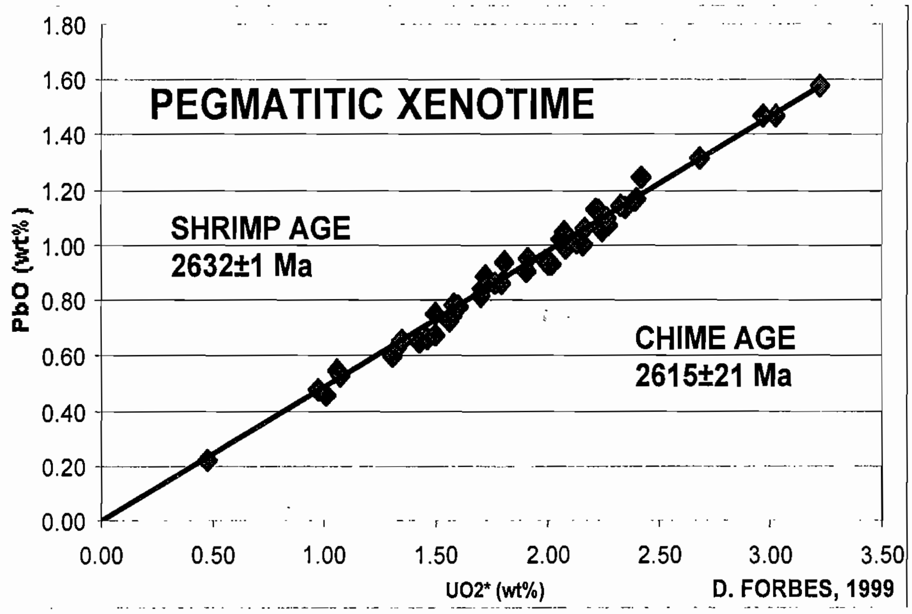

ADVANTAGES OF CHIME

BY WDS:

- AREA OF ANALYSIS ~3 microns
- FAST AND AUTOMATIC
- CHEAP

DISADVANTAGES OF CHIME

BY WDS:

- ASSUMES CONCORDANCE
- ASSUMES NO COMMON Pb
- LESS PRECISE FOR YOUNG GRAINS WITH LOW U-Th CONTENTS
- RESTRICT APPLICATIONS TO ARCHEAN (PRECAMBRIAN?)
- XENOTIME LESS VIABLE THAN MONAZITE

Towards a better understanding of the temporal evolution of the Zambian Copperbelt: geochronology and geochemistry of xenotime

Presented by Galvin Dawson

(PhD student)
Centre for Global Metallogeny,
University of Western Australia

Outline

- Aim and approach
- Known age constraints of basin
- Xenotime
  - textural classification
  - geochronology
- Correlation of xenotime ages to these events
- REE geochemistry and element mapping
- Discussion
- Conclusions and further work

Aim

To determine the temporal evolution of the Zambian Copperbelt using trace phosphate and zircon geochronology

Possible events: Xenotime/Monazite

Diagenesis

Alteration

Metamorphism/Deformation

Mineralisation

Other tectonic events: Zircon

basin extensional events

- Gabbro sills and other dykes sampled

Approach

- Regional sampling from both highly mineralised and less-mineralised zones
  - Less mineralised/altered zones (distal)
    - Age of the Katangan host rocks (diagenetic xt)

    (IT27, NE6B, KN18, RCB2 drill holes)
  - More mineralised/altered zones (proximal)
    - Age of peak metamorphism, deformation, alteration and *mineralisation

    (Mufulira, Nkana, Nchanga, Konkola underground mines)
- Identify various phases of xenotime growth to distinguish these important geological events
  - by integrating petrography, geochemistry and geochronology

Known age constraints of basin

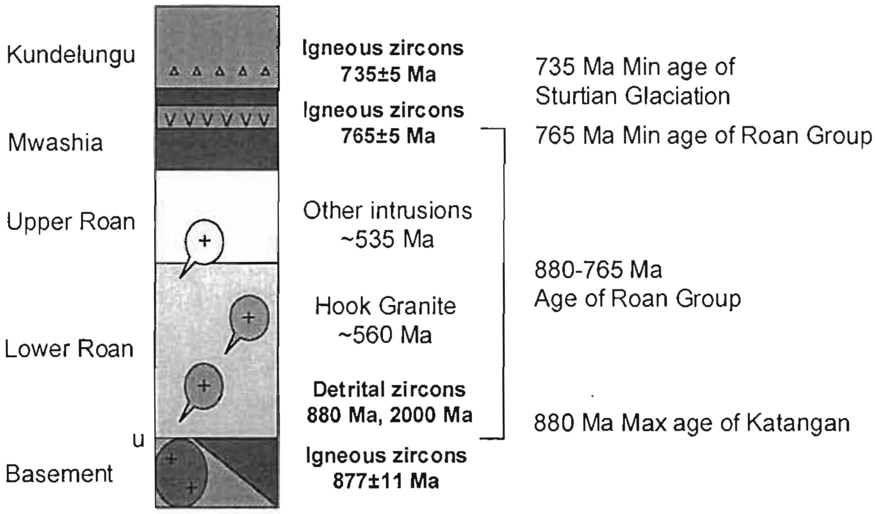

Xenotime textures

- *Least diagnostic feature of xenotime to be used for determining origin and timing
  - Different growth zones aren't always visible
  - Difficult to interpret textural relationships
- Firstly look at…'Diagenetic' looking xenotime?

Back-scattered
SEM image

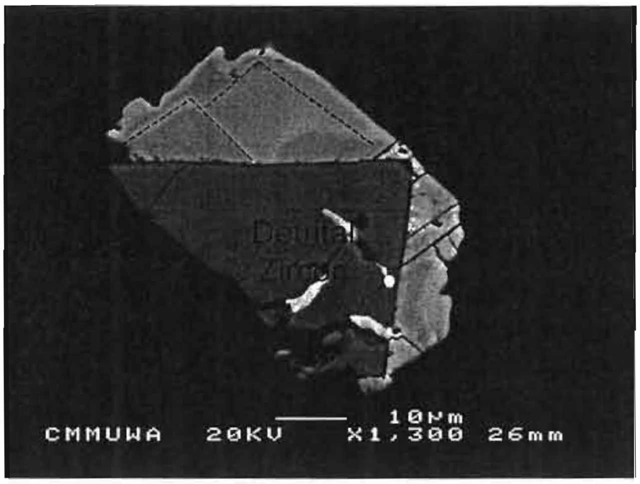

Back-scattered
SEM images

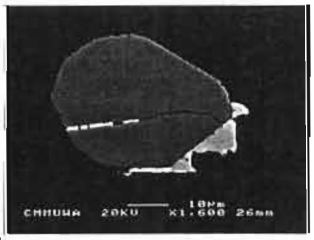

Authigenic
Xenotime

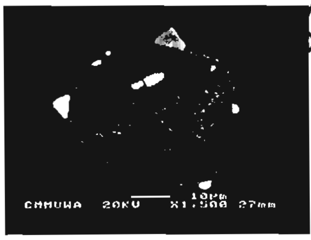

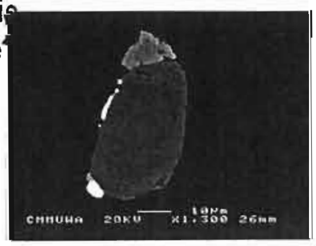

Xenotime textures

- 'Hydrothermal' and 'metamorphic' looking xenotime

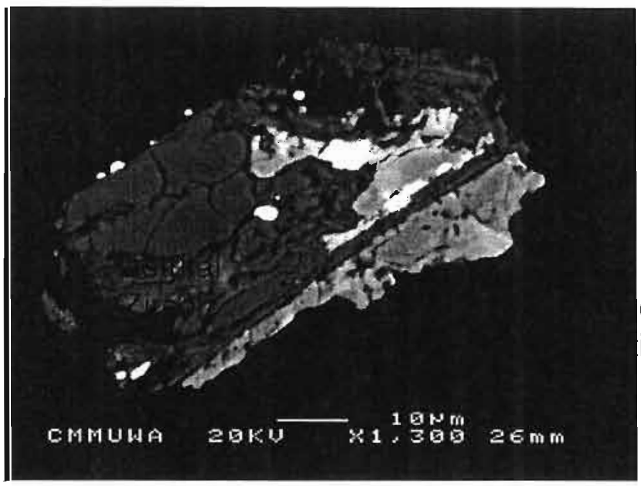

ermal
ime

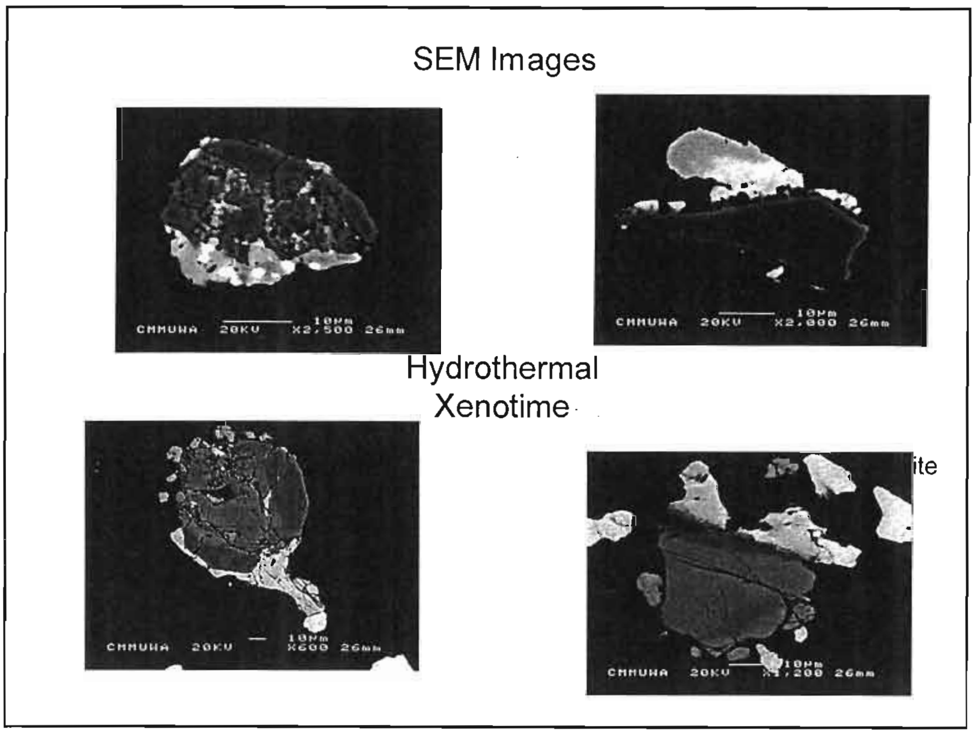
SEM Images
Hydrothermal
Xenotime

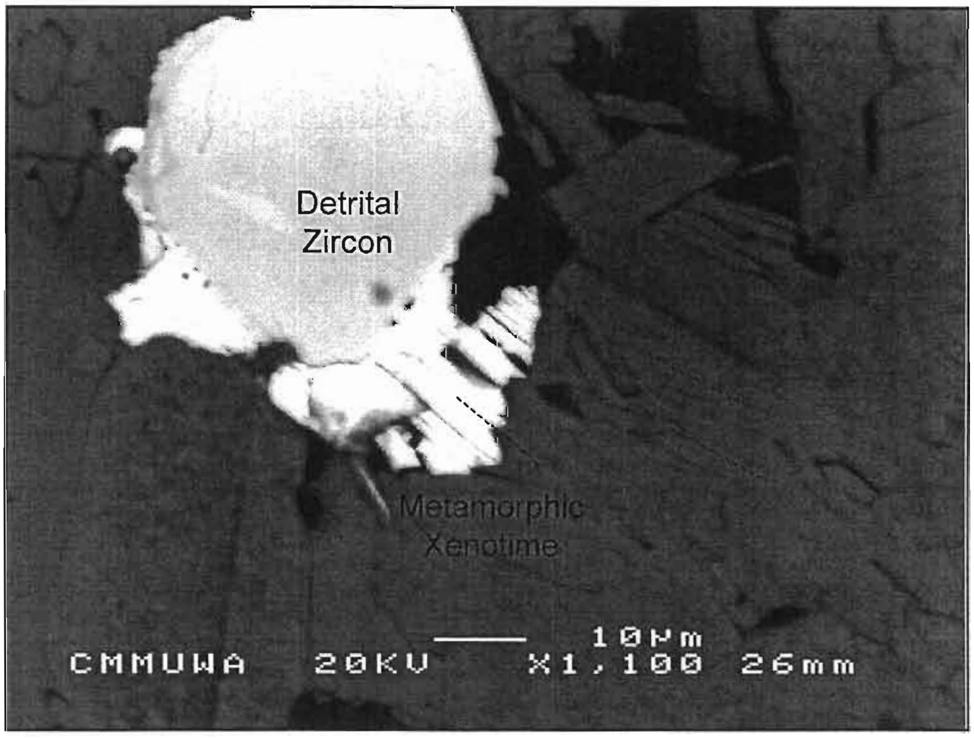
Detrital
Zircon
Metamorphic
Xenotime
10µm
CMMUWA 20KV X1,100 26mm

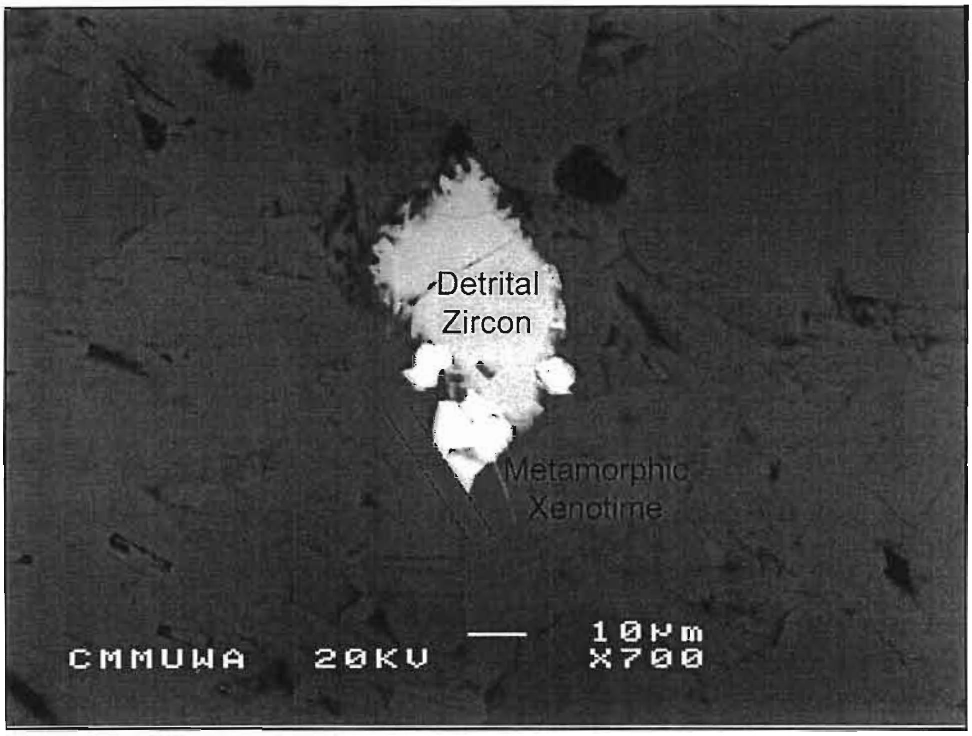

Detrital Zircon
Metamorphic Xenotime
CMMUWA 20KV
10μm X700

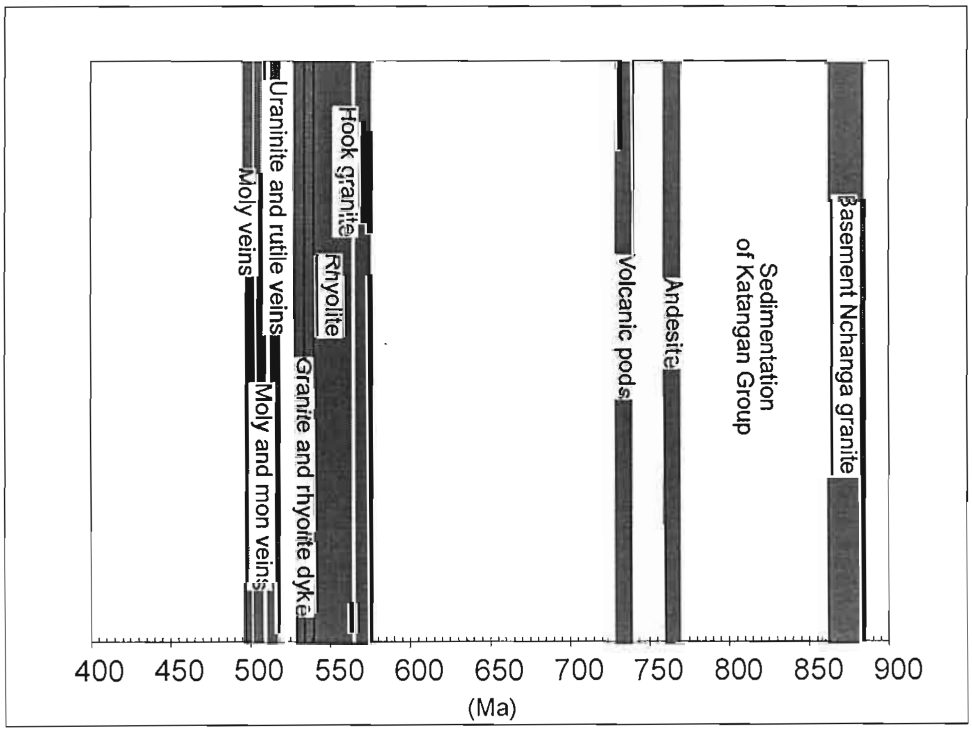

Moly veins
Uraninite and rutile veins
Moly and mon veins
Granite and rhyolite dyke
Hook granite
Rhyolite
Volcanic pods
Andesite
Sedimentation of Katangan Group
Basement Nchanga granite
400 450 500 550 600 650 700 750 800 850 900
(Ma)

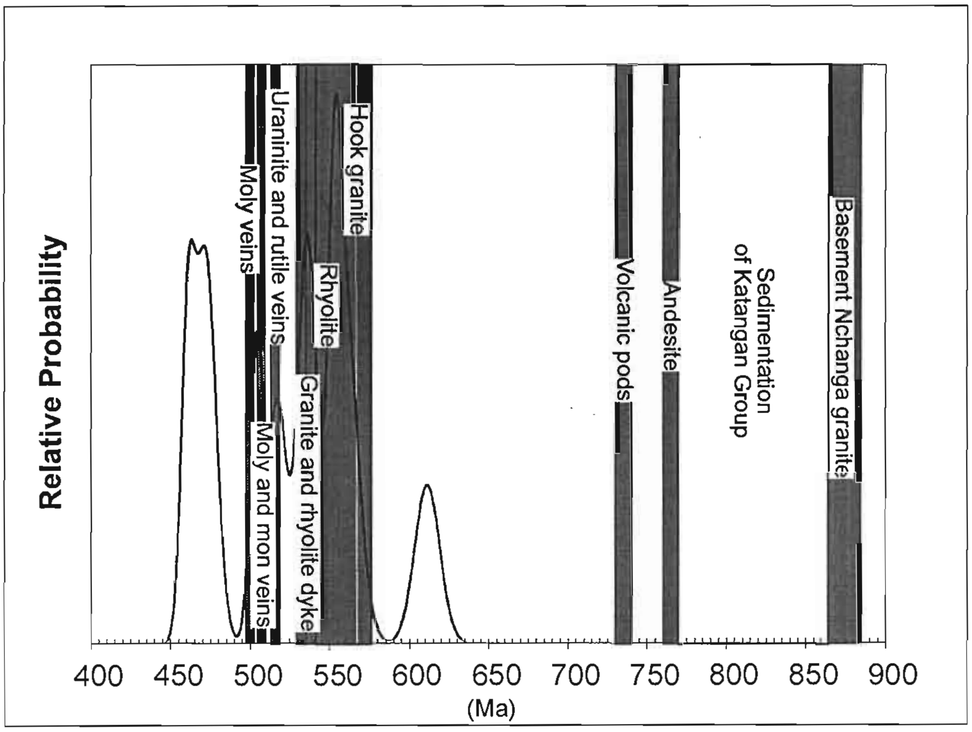
Relative Probability
Moly veins
Uraninite and rutile veins
Moly and mon veins
Rhyolite
Granite and rhyolite dyke
Hook granite
Volcanic pods
Andesite
Sedimentation of Katangan Group
Basement Nchanga granite
400 450 500 550 600 650 700 750 800 850 900
(Ma)

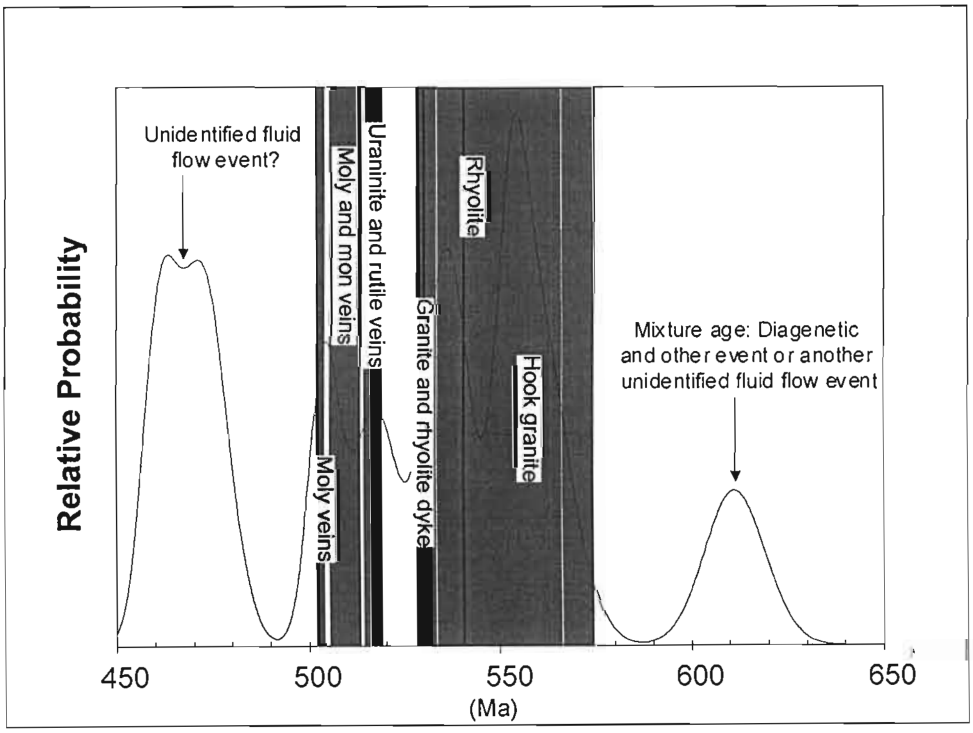
Relative Probability
Unidentified fluid flow event?
Moly and mon veins
Moly veins
Uraninite and rutile veins
Granite and rhyolite dyke
Rhyolite
Hook granite
Mixture age: Diagenetic and other event or another unidentified fluid flow event
450 500 550 600 650
(Ma)

REEgeochemistry

- WDS REE data
  - Use REE patterns to 'potentially' distinguish various geologic events

REE geochemistry

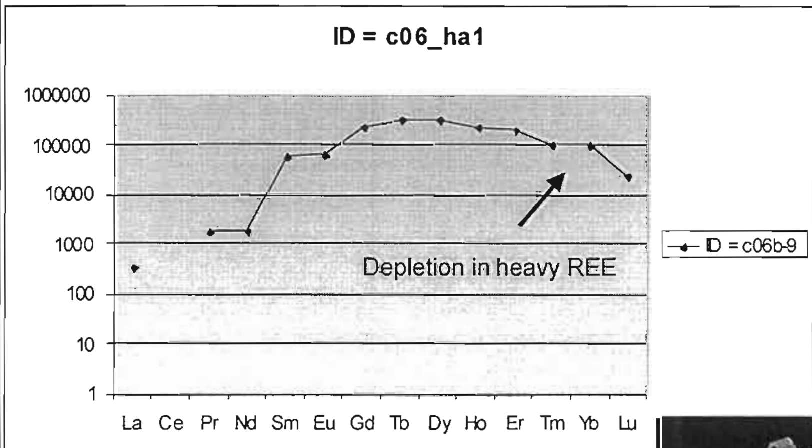

Youngest event
(~470 Ma)

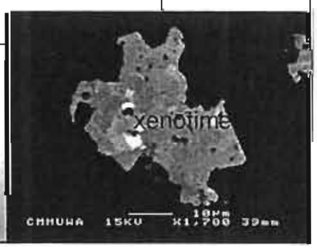

REE geochemistry

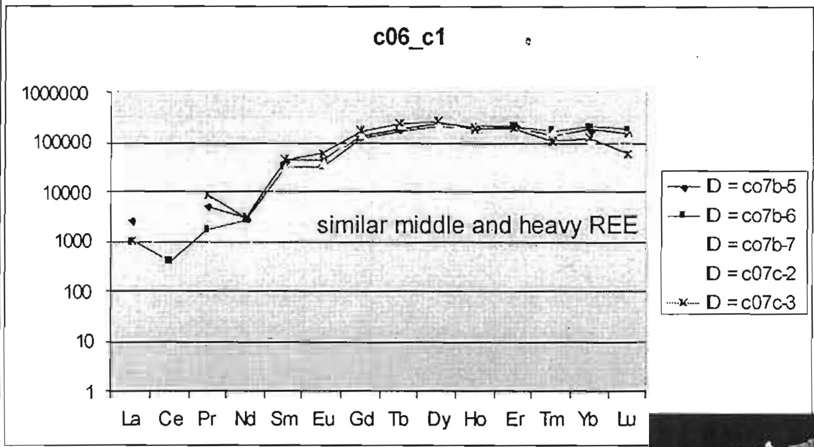

Pan-African event?
(~530-570 Ma)

REE geochemistry

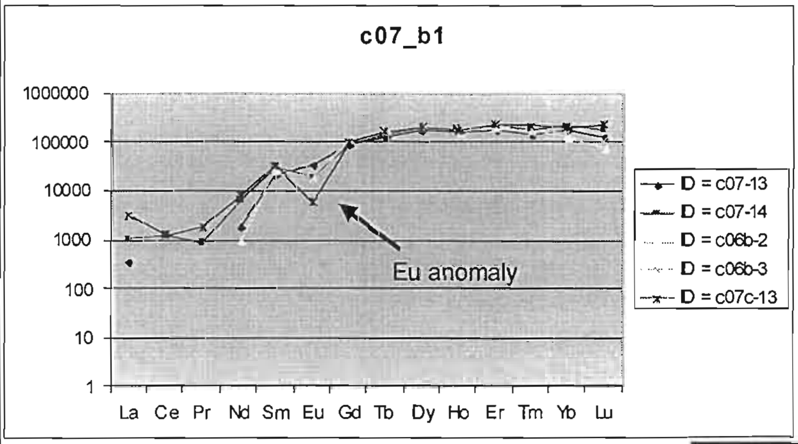

Detrital grain
(~1300 Ma)

Discussion

- All (or most) xenotime is hydrothermal/metamorphic
  - 'Diagenetic looking' grains give hydrothermal/MM ages
- Geochemistry is useful, but not conclusive, yet…
  - Small data set
  - Other complications such as source of fluid, detection limits?
- Interpreting the petrographic relationship between xenotime and the ore minerals is essential for understanding the mineralisation process.
- If xenotime and ore minerals are coeval, then…
- Cu mineralisation probably *Later* than diagenesis
- Mineralisation assoc. with Pan African Orogeny?

Conclusions

- No authigenic xenotime found…Yet!
- Xenotime formed during other fluid flow and heating events in the basin
- Ages correspond to known events in basin
  - Hook granite, other granites and rhyolites, veining
- Possible fluid flow event identified ~470 Ma?
- Determining the age of mineralisation is looking promising…Further textural and geochemical work required
- Using xenotime textures alone is not reliable enough to determine origin
  - Combining geochemistry and trace element mapping with the geochronology is essential

Further work

- Detailed petrography of selected samples
- Increase xenotime data set for ore and non-ore samples
- Assess monazite alteration(?) ages: SHRIMP & probe
- Other alteration minerals?? = rutile ages??
- Date gabbro sill (Upper Roan), albitic dolerite from DDH IT-27
- Further phosphate geochemistry: discriminate origin?
- Syntheses with ore deposit-regional data

THE END